HIGH FREQUENCY THERMIONIC TUBES

HIGH FREQUENCY THERMIONIC TUBES

By

A. F. HARVEY

B.Sc., D. PHIL., A.M.I.E.E.

With a foreword by

E. B. MOULLIN

M.A., Sc.D., M.I.E.E.

SECOND EDITION
(REPRINTED)

LONDON

CHAPMAN & HALL LTD.

37 ESSEX STREET W.C.2

1946

FIRST PUBLISHED, 1942
REPRINTED, 1943
SECOND EDITION, 1944
REPRINTED, 1946

THIS BOOK IS REPRINTED FROM STANDING TYPE. THE PAPER AND BINDING CONFORM TO THE AUTHORIZED ECONOMY STANDARDS

Catalogue No. 81/4

Printed in Great Britain by The Whitefriars Press Ltd., London and Tonbridge
Bound by G. & J. Kitcat Ltd., London. *Flexiback Binding.*

FOREWORD

THE recent developments in television have called for the use of ultra high radio frequencies, and the result has produced revolutionary changes in tube and circuit technique. Up to a point the new requirements have been met by improved construction of the familiar multi-electrode thermionic tube. Dr. Harvey devotes the first two chapters of his book to describing such new tubes, and the effect of their residual parameters : it will be welcomed by all as a gathering together of new results and values not otherwise readily accessible.

The third chapter is a preliminary account of the work, initiated by Mr. J. A. Ratcliffe, on the use of positive ion tubes as a means of studying conveniently effects which are appreciable with electrons only at frequencies so high as to preclude accurate measurement.

The need for the use of short wavelengths has stimulated interest in methods of producing them which do not depend on the conventional use of a three-electrode tube : a study which has been in progress for many years, in physical laboratories of Universities.

Much of Dr. Harvey's book is devoted to the magnetron, and a collected account of the work on this puzzling piece of apparatus is most welcome. The magnetron would seem to offer an ideal problem of classical mechanics : doubtless the solution will require difficult feats of mathematical analysis, but once this is achieved, and in the main it has been by the brilliant work of Dr. F. B. Pidduck, the analyst might well be forgiven for feeling that it was almost redundant to test his solution in the laboratory. But once he was persuaded to do so he would receive a severe shock. For there is some violent conflict between the problem of the real magnetron and the problem of mechanics which it appears to present. So far no on ehas been able to suggest what idealisation has unwittingly been introduced into the mathematical statement of a seemingly

elementary problem. The three-electrode tube has always behaved quantitatively as calculated : once add a magnetic field and chaos seems to reign. Dr. Harvey has done great service in presenting his long study of magnetron characteristics and the reader will be wise to remember always that in the simplest problem of all, the cut-off, behaviour approaches the expected only in conditions which are widely removed from those postulated in the classical analysis. He will then realise that all the important oscillatory properties occur when the field is so strong that no anode current should be possible ; thus they are mathematically untouchable. Is it then any wonder that many of the papers published on the magnetron generator seem only a record of an isolated experiment behind which there is little to be seen of general principles ?

I have had the pleasure of watching, in my Laboratory at Oxford, Dr. Harvey's exceptional experimental skill and in assisting with some of the measurements he describes and of urging him to produce this book. The ordered sequence of his methodical work places him among the half-dozen workers who can be said with truth to have contributed appreciably to our quantitative knowledge of the behaviour of the magnetron. Their work will stand : some day a prophet will arise who will tell us why things happen so. Meanwhile we are grateful to Dr. Harvey, both for his extensive original contribution and for sifting and collecting the best from a welter of inconclusive publications.

The last chapter gives an outline of velocity modulation tubes, Klystrons, etc., and of wave guides and horn radiators. It forms a very useful introduction and survey of a subject which is in its infancy and about which comparatively little is known at present.

E. B. MOULLIN.

Magdalen College,
Oxford.

PREFACE TO THE SECOND EDITION

THE extensive and increasing use of very high-frequency electrical energy in radio communication, television, medicine and specialised fields requires that the performance of electrical components and apparatus at such frequencies be known with accuracy. The almost universal use of thermionic tubes in such apparatus, operating under a large variety of conditions, renders a thorough knowledge of their properties and behaviour very necessary.

This book gives an account of these properties of thermionic tubes and their relation to those of the associated electric circuits. The influence of frequency of operation is discussed and the limitations of normal type tubes at very high frequencies are pointed out. Much space is devoted to consideration of special thermionic tubes which are of particular value at these frequencies. Apart from the modern trend towards this end of the spectrum, it is at these very high frequencies that the tube properties become more predominant and where the greatest theoretical and practical difficulties are encountered. Emphasis is mostly laid on the electrical properties of the thermionic tubes themselves, but the methods of measurement are described in detail with the intention of indicating the practical application of these tubes to high frequency problems. To make the book as complete as possible extensive recent references to other published work are given.

Chapter I is mainly of an introductory nature and deals with the properties of thermionic tubes at frequencies low enough to make electron transit time effects negligible. Chapter II shows how at very high frequencies the performance of normal thermionic tubes is, in general, adversely affected and includes some experimental results obtained at these frequencies. Chapter III describes the retarding field generator, which is especially suited for very high-frequency operation and includes some experimental results using positive ion tubes. Chapter IV introduces the magnetron, which is examined in detail, since, apart from its present pre-eminent position as a powerful generator of very high frequency, its

comparatively simple electrode structure enables the comparison of theory and experiment to be made more readily. Chapter V gives an account of the properties of the magnetron in the resonance and electronic régimes at very high frequencies, and here again the experimental details are described. Chapter VI describes the Klystron and allied thermionic tubes for use at very high frequencies, and a section is included on wave guides and allied subjects, since at very high frequencies the thermionic tube and its circuit tend to be indistinguishable.

The major portion of this book is due to results of the author's experimental work carried out in the Engineering Laboratory of Oxford University, and later in the Cavendish Laboratory of Cambridge University. The author takes this opportunity of thanking Dr. A. C. Bartlett, M.A., for helpful advice during the writing of Chapters I and II, Mr. J. A. Ratcliffe, M.A., for much instruction in the technique of positive ion tubes described in Chapter III, Dr. F. B. Pidduck, for helpful discussion on the theory of the magnetron given in Chapter IV, the authors of the published articles which have been abstracted and the many others who have been of assistance. The author also wishes to express his thanks to the Institution of Electrical Engineers, the Cambridge Philosophical Society, The Cambridge University Press, "The Wireless Engineer," and "Journal of Applied Physics," for the loan of illustrations and blocks and to these and other journals for permission to abstract articles published by them. He is also indebted to Standard Telephones and Cables Ltd., General Electric Co. Ltd. and the Mullard Valve Co. Ltd. for photographs and descriptions of their high frequency tubes, and to the Sperry Gyroscope Co. Inc. for the use of their trade marks "Klystron" and "Rhumbatron." He is grateful to the publishers, Messrs. Chapman & Hall, and to their Technical Managing Director, Mr. John L. Bale, for their assistance during difficult times. Finally, the author wishes to express his deep gratitude to Dr. E. B. Moullin, M.A., for writing his kind and interesting foreword and for his continued help, advice and encouragement throughout the progress of the work and the writing of this book.

Jesus College, Oxford, and
Trinity College, Cambridge.

A. F. HARVEY.

CONTENTS

CHAPTER IV

CHAPTER V

CHAPTER VI

ABBREVIATED TITLES FOR BIBLIOGRAPHY

ALTA FREQ.	Alta Frequenza.
ANN. PHYS.	Annalen der Physik.
BELL SYS. TECH. J.	The Bell System Technical Journal.
BULL. ASSOC. SUISSE ELÉC.	Bulletin de l'Association des Suisse Eléctriciens.
BULL. SOC. DES ELÉC.	Bulletin de la Société des Eléctriciens.
COMPTES REND.	Comptes Rendus.
ELEC. COMM.	Electrical Communication.
ELEC. ENG.	Electrical Engineering.
ELECTROT. J. TOKYO.	Electrotechnical Journal, Tokyo.
E.N.T.	Elektrische Nachrichten Technik.
E.T.Z.	Elektrotechnische Zeitschrift.
FUNKTECH. MONAT.	Funktechnische Monatshefte.
G.E.C.J.	G.E.C. Journal.
GEN. ELEC. REV.	General Electric Review.
HELVET. PHYS. ACTA	Helvetica Physica Acta.
HOCHF. TECH. U. ELEK. AKUS.	Hochfrequenz-technik und Electro-akustik.
INDIAN J. PHYS.	Indian Journal of Physics.
J. APPL. PHYS.	Journal of Applied Physics.
J. EXP. AND THEOR. PHYS.	Journal of Experimental and Theoretical Physics (Russian).
J. FRANKLIN INST.	Journal of the Franklin Institute.
J. INST. ELEC. ENG.	Journal of the Institution of Electrical Engineers.
J. PHYS. ET RAD.	Journal de Physique et le Radium.
J. SCIENT. INSTR.	Journal of Scientific Instruments.
J. TECH. PHYS.	Journal of Technical Physics (Russian).
LA RIC. SCIENT.	La Ricerca Scientia.
LINCEI REND.	Lincei Rendus.
L'ONDE ELÉC.	L'Onde Eléctrique.
NIPPON ELEC. COMM. ENG.	Nippon Electrical Communication Engineering.

NUOVO CIM. . .	Il Nuovo Cimento.
PHIL. MAG. . .	Philosophical Magazine.
PHILIPS TECH. REV. .	Philips Technical Review.
PHILIPS TRANS. NEWS	Philips Transmitting News.
PHYS. BER. . .	Physikalische Berichten.
PHYS. REV. . .	The Physical Review.
PHYS. Z. . . .	Physikalische Zeitschrift.
PHYS. Z. SOWJET. .	Physikalische Zeitschrift der Sowjetunion.
PROC. CAMB. PHIL. SOC.	Proceedings of the Cambridge Philosophical Society.
PROC. INST. RAD. ENG.	Proceedings of the Institute of Radio Engineers.
PROC. PHYS. SOC. .	Proceedings of the Physical Society.
PROC. ROY. SOC. .	Proceedings of the Royal Society.
Q. JOURN. MATH. .	Quarterly Journal of Mathematics.
R.C.A. REV. . .	R.C.A. Review.
REP. RAD. RES. JAPAN	Report of the Radio Research in Japan.
REV. GÉN. D'ELÉC. .	Revue Générale de l'Eléctricité.
SCI. NEWS LETTER .	Science News Letter.
SCIENT. AMERICAN .	Scientific American.
TECH. PHYS. U.S.S.R.	Technical Physics of the U.S.S.R.
T.F.T. . . .	Telegraphen und Fernsprech Technik.
TELEFUNKEN ZEIT. .	Telefunken Zeitschrift.
WIRELESS ENG. .	Wireless Engineer.
Z. F. PHYS. . .	Zeitschrift für Physik.
Z. F. HOCHF. TECH. .	Zeitschrift für Hochfrequenztechnik.
Z. F. TECH. PHYS. .	Zeitschrift für Technische Physik.

HIGH FREQUENCY THERMIONIC TUBES

CHAPTER I

GENERAL PROPERTIES OF THERMIONIC TUBES

(*a*) RECTIFICATION AND AMPLIFICATION

Tube Construction. The usual construction of a thermionic tube takes the form of a cathode, thermally or otherwise emitting charged particles, together with other electrodes, to which are applied suitable electrical potentials. The electrode on which the emitted particles, invariably electrons, finally impinge is known as the anode and the intermediate electrodes, generally of open mesh construction, are known as grids. The whole system is enclosed in a vessel which is normally highly evacuated, but occasionally may contain a suitable gas at low pressure to give particular properties to the tube.

It is common to mount the electrodes on a glass pinch through which the leads are taken and this is sealed to a glass envelope. Some tubes employ a metal envelope or shell and the electrode leads are brought through glass eyelets. The size, material, and design of the electrodes depend, of course, on the purpose to which the tube will be put. After assembly the electrodes and glass envelope are heated thoroughly to remove occluded gas and then the tube is evacuated to as high a degree as possible. Finally a small quantity of some substance called a getter is volatilised inside the tube to remove the last traces of gas. Further details on the manufacture of thermionic tubes are given in other works, but the construction of more specialised tubes will be referred to later.

The Diode. The simplest form of thermionic tube is the diode, and when the anode potential is sufficiently high all the emitted particles travel to the anode and the tube is said to be

saturated. In this case the anode current depends on the emissive properties of the cathode and also on the heating power (or temperature), as shown in Fig. 1 for a pure tungsten emitter. The change in filament resistance is also shown,

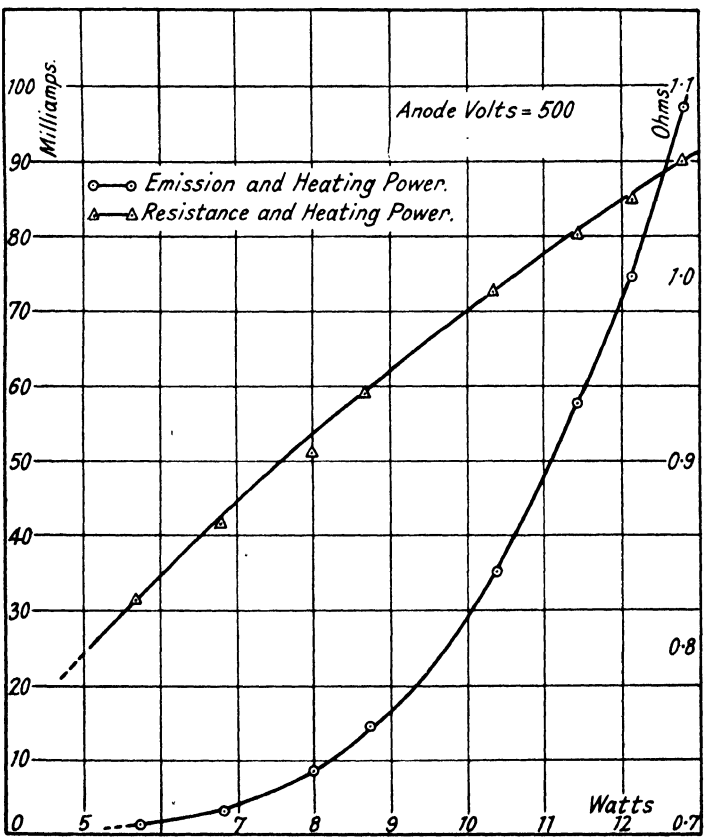

Fig. 1. Filament characteristics of diode type CW10.

since both these curves will be required later. In general, the distribution of field between the electrodes is modified by the space charge of the travelling particles, and when this is large enough the field at the cathode becomes zero, and finally slightly negative, when the tube is said to be space charge limited. For planar electrodes, neglecting the initial velocities

of emission, C. D. Child (8) gives the space charge limited current as

$$i = \frac{\sqrt{2}}{9\pi}\sqrt{\frac{e}{m}}\frac{V^{3/2}}{d^2} \quad . \quad . \quad . \quad . \quad . \quad . \quad (1)$$

where V is the anode voltage and d the interelectrode distance. This relation follows directly from integration of Poisson's equation, but more recently E. B. Moullin (27) has given an alternative derivation. Thus in the plane where the electric field is zero a barrier is formed and the force at a plane distant x from it is equal to 4π times the charge between unit areas of these planes. If an electron takes a time t in transit between these planes and i is the current per unit area, then

$$\text{Force} = 4\pi \times \text{charge}.$$

$$\therefore \frac{d^2x}{dt^2} = \frac{4\pi e}{m}it$$

and

$$\frac{dx}{dt} = \frac{4\pi e}{m}\frac{it^2}{2} = \sqrt{\frac{2eV}{m}}$$

assuming the electrons cross the barrier with zero velocity and that V is the potential at x. Further integration and substitution give

$$x = \frac{2\pi e i t^3}{3m}$$

$$= \frac{2\pi e i}{3m} \cdot \frac{1}{\pi^{3/2} i^{3/2}} \cdot \left(\frac{mV}{2e}\right)^{3/4} \quad . \quad . \quad . \quad . \quad (2)$$

For planar electrodes distance d apart this gives equation (1) above.

For cylindrical electrodes the analysis is much more complex and I. Langmuir (22) gives the space charge limited current as

$$i = \frac{2\sqrt{2}}{9}\sqrt{\frac{e}{m}}\frac{V^{3/2}}{r\beta^2} \quad . \quad . \quad . \quad . \quad . \quad (3)$$

where r is the anode radius and a that of the cathode and

$$\beta = \log\frac{r}{a} - \frac{2}{5}\left(\log\frac{r}{a}\right)^2 + \frac{11}{120}\left(\log\frac{r}{a}\right)^3 - \frac{47}{3300}\left(\log\frac{r}{a}\right)^4 + \ldots \quad (4)$$

which for $r \gg a$ is nearly unity. It is also shown that for any shape of electrode the $V^{3/2}$ law still holds.

An important parameter of the thermionic tube is its impedance, and under space charge limited conditions it will be seen that the diode has the properties of a positive resistance. The

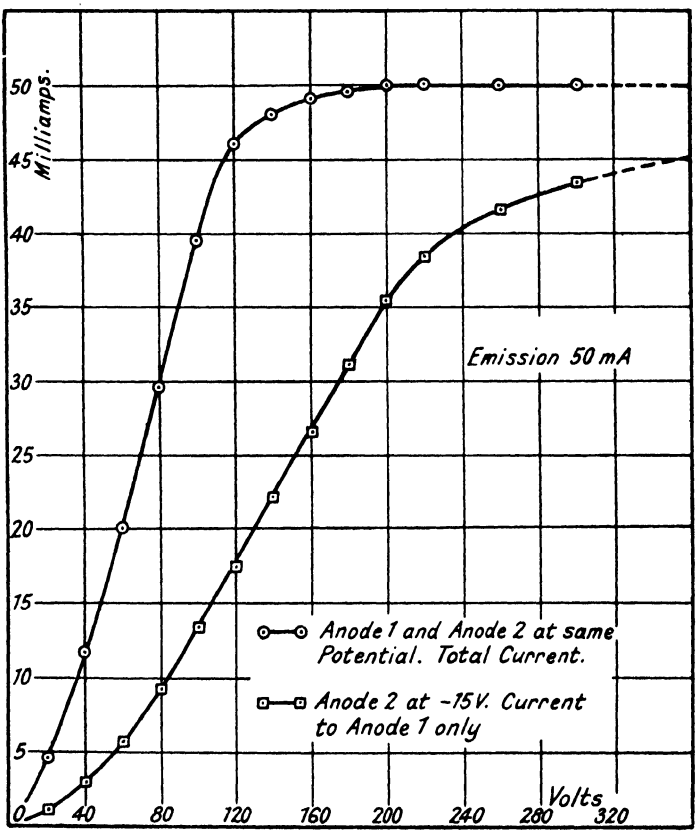

FIG. 2. Anode current characteristics of diode type CW10.

value for steady potentials is given by V/i, whereas that for small superimposed alternating potentials, termed the dynamic or slope resistance, is given by $\frac{dV}{di}$. It is this latter quantity which is of fundamental importance in tube and circuit calculations. Fig. 2 gives the anode current for a special diode, to be

described later, with the anode in two segments. When one of these is held at a lower potential the anode current is much diminished, due to the change in electrostatic field at the cathode. This control of the anode current by a third electrode will be dealt with more fully when the triode is discussed.

Another important characteristic of thermionic tubes is the transit time of the electrons between the electrodes, and this can be calculated from the voltage distribution, which has been given for cylindrical electrodes by I. Langmuir (23) for the case where space charge is negligible and by A. Scheibe (34) when space charge is sufficient to reduce the cathode field to zero. When the space charge has an intermediate value the transit time in the cylindrical diode becomes difficult to work out, but the solution for the planar case has been examined theoretically and experimentally by R. Cockburn (9, 10), who also works out the voltage distribution between the electrodes. It is shown that space charge increases the transit time, but most of this increase occurs just before the cathode field becomes zero.

For electrodes of separation d, the transit time is given to within a factor 2, for planar or cylindrical electrodes, and for all conditions of space charge and magnetic field (for example, the magnetron) by

$$T = \frac{3d}{2}\sqrt{\frac{2m}{eV}} \quad . \quad . \quad . \quad . \quad (5)$$

For slowly moving electrons

$$e = 1{\cdot}602 \times 10^{-19} \text{ coulombs.}$$
$$m = 9{\cdot}107 \times 10^{-28} \text{ gm.}$$

and thus with V in volts, d in cms., the transit time becomes

$$T = \frac{5{\cdot}04d}{10^2\sqrt{V}} \mu\text{secs.} \quad . \quad . \quad . \quad (5a)$$

The velocity of an electron with energy V volts is given by

$$u = 5{\cdot}94 \times 10^7 \sqrt{V} \text{ cm./sec.}$$

and as V increases from 100 to 20,000 volts the velocity increases from about 0·02 to 0·3 times the velocity of light. The effective

mass of an electron moving with speed u is increased to a value m' such that

$$\frac{m'}{m} = \frac{1}{\sqrt{\left(1 - \frac{u^2}{c^2}\right)}}$$

where c is the velocity of light. Since 20,000 volts is the maximum anode voltage usually employed, even in high power transmitting tubes, this effect can be neglected when dealing with transit time and other effects in thermionic tubes.

Rectification. An inherent property of the diode is that it can rectify alternating signals and in the high vacuum form it is capable of handling very high voltages, but the current output is comparatively low due mainly to the large voltage drop across the tube. This can be much reduced by filling the tube with a suitable gas or vapour at low pressure, since the ions which are formed neutralise the large negative space charge of the electron stream. Further information on the properties of high vacuum rectifiers is given, for example, by E. B. Moullin (29), and on mercury vapour high-power rectifiers by C. R. Dunham (12). Rectification of small amplitude waves is employed extensively in measuring apparatus such as thermionic voltmeters and in radio receivers such as detectors and frequency changers. The non-linear anode current characteristics of thermionic tubes are made use of in modulation, demodulation and heterodyne circuits in various kinds of transmitting and receiving apparatus where complex frequency waves are formed.

The Triode. When a third electrode in the form of an open mesh grid is added the total current is a function of the potentials of the grid and anode and is given by the previous formula for the equivalent diode of anode potential

$$V = V_g + \frac{1}{\mu} V_a \quad . \quad . \quad . \quad . \quad . \quad (6)$$

where V_g is the grid and V_a the anode potential acting at a position approximating to that of the grid. The constant $1/\mu$ is known as the durchgriff of the two electrodes and is related to their geometry. The variation of this characteristic with

space current, etc., has been dealt with by W. E. Benham (2). A similar relation can be obtained for tubes of four or more electrodes, and, as in the case of the diode, the tube impedances and electron transit times can be calculated. If ρ is the anode resistance then μ/ρ has the dimensions of a conductance. This important parameter or factor of merit of thermionic tubes is known as the mutual or trans-conductance. Its value is approximately the same for most types of tubes and lies between 1 and 12 mA/volt, the larger values being obtained by the employment of large cathode areas and emissions and close grid to cathode clearances. For triodes the values of μ (amplification factor) vary between 5 and 50. In the screen grid tetrode and pentode the fluctuating anode potential has little effect on the space current and the values of μ and ρ are correspondingly much larger.

Amplification. This third electrode, by its greater control, endows thermionic tubes with the ability to amplify signals applied to it, and these amplifiers are classified according to the conditions under which the tubes operate. When the range of operation lies on the straight portion of the anode current characteristic the tube is said to work in Class A, and this is the normal condition especially when minimum distortion is required. Fig. 3*a* shows the circuit of a two-stage audio-frequency amplifier constructed to give uniform gain over a wide range of frequencies, as can be seen from the output voltage curve in Fig. 4*a*. Fig. 3*c* gives the circuit of another amplifier which is capable of giving high power outputs with little distortion of wave form. Since the control grid is never at a positive potential, Class A amplifiers require little input or driving power. A disadvantage is that the tube is taking its normal anode current even if the applied signal amplitude is zero, and when delivering power the anode dissipation falls, and hence both efficiency and output of the tube are limited.

Since iron-cored transformers are commonly used in conjunction with thermionic tubes it will be helpful to briefly discuss their design. If A is the area of the core, T_P the primary turns, ω_0 the pulsatance at the lowest frequency desired, then the voltage is given by

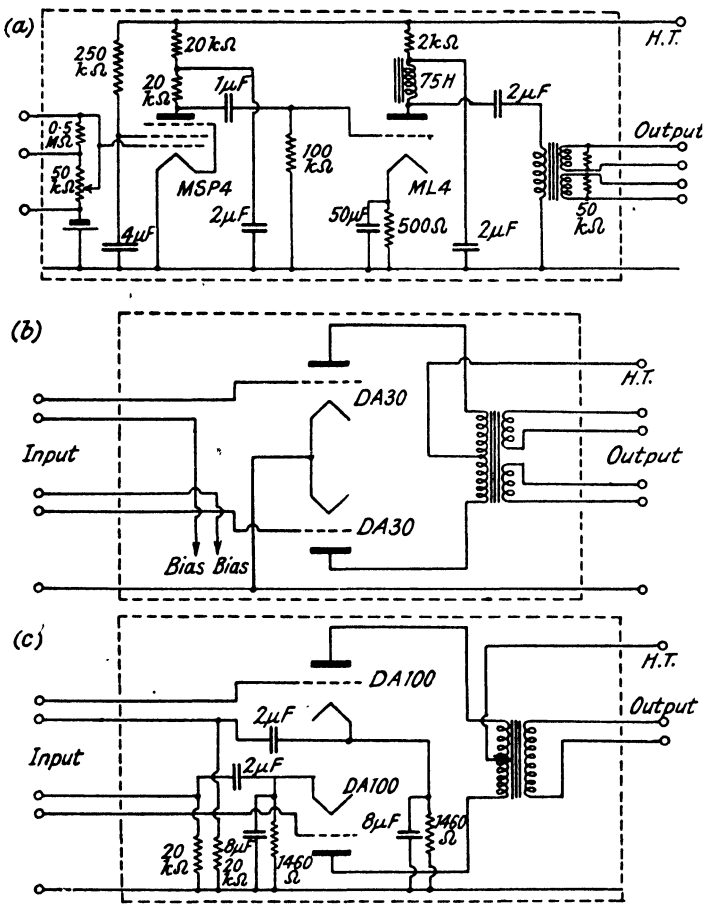

FIG. 3. Audio-frequency amplifier circuits.

$$E = \frac{2{\cdot}22\,\omega_0\,ATB_{\max}\,10^{-8}}{\pi} \text{ volts} \quad . \quad . \quad . \quad (7)$$

and the current by

$$I = \frac{10\,B_{\max}\,l}{4\pi T\mu\sqrt{2}} \text{ amps.} \quad . \quad . \quad . \quad . \quad . \quad (8)$$

where l is the core length and μ the permeability. If λ is the reactance factor $\left(\text{defined as } \frac{\omega_0 L}{R}\right)$ where R is the generator resistance, then

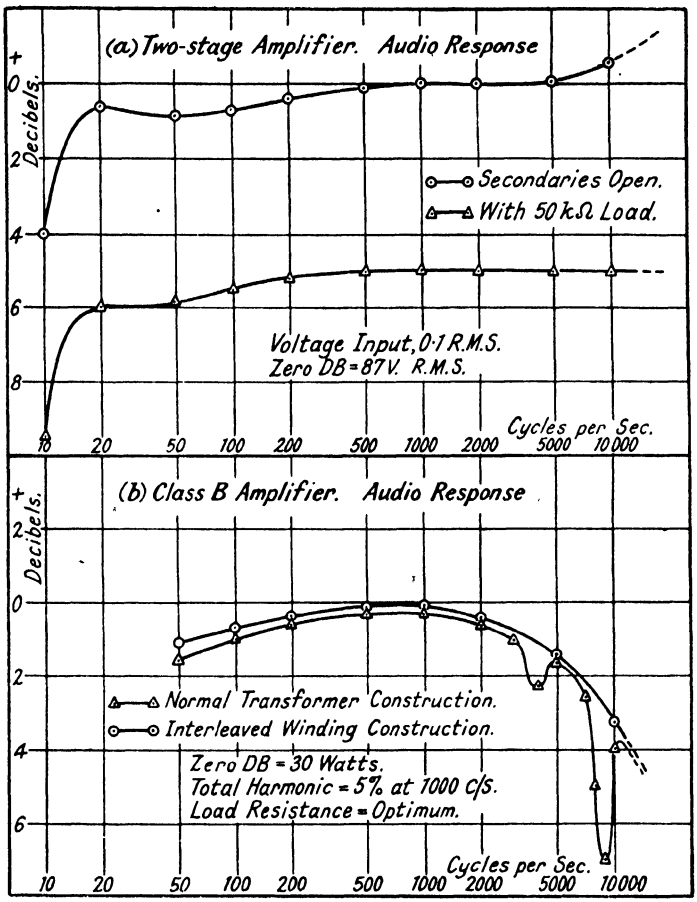

FIG. 4. Audio-frequency amplifier response curves.

$$R = \frac{\omega_0 L}{\lambda} = \frac{4\pi T^2 \mu A \omega_0 10^{-8}}{10 l \mu}$$

and the power output is given by

$$P = \frac{E^2}{R} = \frac{\omega_0 l A}{8\pi} \cdot \frac{B^2_{\max}}{\mu} \cdot 10^{-7} \lambda \text{ watts} \quad . \quad . \quad . \quad (9)$$

Thus the "volume" of the iron given by

$$lA = \frac{8\pi P 10^7 \mu}{B^2_{\max} \lambda \omega_0} \quad . \quad . \quad . \quad . \quad . \quad . \quad (10)$$

gives the size of core required. B_{max} is chosen from the available magnetisation curves to give reasonable distortion (5–10%) at ω_0 due to saturation. The reactance factor is chosen to give reasonable attenuation at ω_0 (0·5 dB when $\lambda = 3$ and the load and generator resistances are equal). Now

$$PR = E^2 = \frac{\omega_0{}^2 A^2 T^2 B^2 10^{-16} \pi}{2}$$

and so

$$T_P = \frac{10^8 \sqrt{2PR}}{A \,.\, B_{max}\, \omega_0}$$

while the secondary turns are given by

$$T_S = T_P \sqrt{\frac{Z}{R}}$$

where Z is the load resistance. From these the wire sizes can be determined and to avoid resonance effects the number of turns should not exceed 10,000. In this respect special cores such as radio metal are advantageous.

When the mean grid potential is not less than the cut-off value, and when the instantaneous grid potential may become positive the tube is said to work in Class B, and if minimum distortion is required it is necessary to operate with two tubes in push-pull. Such an arrangement is generally employed in the output stage of powerful audio-frequency amplifiers and also in amplifiers of modulated radio-frequency signals when it results in high efficiency and power output. A typical amplifier of the former kind is shown in Fig. 3*b*, and since the mean anode current fluctuates with the input it is necessary to supply the negative grid bias from a separate source. Since current flows to either anode only during alternate half-cycles, the effective generator impedance is four times the value for one tube alone. The performance figures are given in Fig. 4*b*, from which it will be seen that for best performance this amplifier requires a transformer with interleaved windings, the result being to reduce self-capacity and leakage inductance so that self-oscillation is not easily induced by the shock effect caused by grid current flowing on the wave peaks.

When the mean grid potential is such that current cut off

occurs the tube acts as a Class C amplifier, and this results in very high efficiencies and good power output, although the wave-form distortion is excessive. As a result these amplifiers are generally employed for radio-frequency unmodulated waves where suitable tuned circuits can be used, since it can be shown that when these are of reasonably high Q the output voltage is very nearly sinusoidal, although the anode current of the tube may contain large harmonic components. Thus if V_1, V_3, V_5, etc., are the voltage components due to currents I_1, I_3, I_5, etc., flowing through the circuit tuned to I_1 and having a magnification Q, then it is well known that

$$\frac{V_3}{V_1} = \frac{3}{8Q} \cdot \frac{I_3}{I_1}, \frac{V_5}{V_1} = \frac{5}{24Q} \cdot \frac{I_5}{I_1}, \text{ etc. . . . .} \quad (11)$$

Thus, even if I_3/I_1 is 0·3 and I_5/I_1 is 0·15, then if Q is 10, which is typical for a loaded transmitter circuit, no harmonic component of voltage is as great as 1%, and in general the amplitude of the nth harmonic decreases as the ratio $1/n$. Thus in the analysis of the operating conditions of an oscillator or amplifier with a tuned circuit it is a very close approximation to assume a simple harmonic voltage fluctuation, and it will be helpful to bear this in mind during the later work.

W. L. Everitt (15) has examined analytically the operating conditions in Class B and C radio-frequency amplifiers and the influence of the angle of current flow on the output, impedance and efficiency is discussed. When the angle of flow is constant the amplifier is linear, and in the particular case when it is 90° it is termed Class B operation as described above. Some experimental checks were described which were made at a frequency of 60 c/s using tuned circuits.

In screen grid tubes, pentodes and high μ triodes the anode current is substantially independent of plate voltage within limits, and F. E. Terman and J. H. Ferns (36) make an analysis of such tubes operating as amplifiers and harmonic generators. The latter are of importance in high-frequency work, since by tuning the anode load circuit to a harmonic of the anode current wave-form frequency multiplication can be obtained, and by successive use of such multipliers very high-frequency sources of great stability can be obtained. The optimum

angles of flow for maximum harmonic frequency output can be determined, and it is found that this best angle is almost exactly inversely proportional to the order of the harmonic.

W. H. Doherty (11) describes a new type of modulated wave high-frequency amplifier in which the anode supply is varied in conjunction with an impedance inverting network. I. E. Mouromtseff and H. N. Kozanowski (30) analyse the operating conditions of thermionic tubes as modulated and continuous wave Class C amplifiers and the effect of grid dissipation on the available power output. Further analysis and information on the various types of amplifiers described above are given by K. A. Macfadyen (25), F. E. Terman (35), L. E. Barton (1), B. F. Miller (26) and others.

Secondary emission. It is possible for certain thermionic tubes, known in operation as the dynatron type, to exhibit the properties of a negative resistance to small changes in electrode potentials. In general, as shown in the case of the triode and tetrode dynatrons with low anode potentials, this is due to the primary electrons striking the anode and causing the emission of secondary electrons which travel to the high potential electrode. It will be shown later that this property of negative resistance enables the tube, in conjunction with suitable parallel tuned circuits, to supply power and act as a self-contained generator of high-frequency energy. These dynatron oscillators, while usually of only low power, have advantages of simplicity and frequency stability which make their use common in measuring technique, for example, as wave meters and impedance measuring devices.

In screen grid tubes secondary emission current from the anode can be greatly reduced by a suppresser grid (*i.e.*, the pentode) or "beam" construction. If more secondary electrons than primary are emitted, as can happen over a certain range of anode potential, then special secondary emission tubes can act as amplifiers. Examples are the Mullard EE50, which has a very high value of mutual conductance and certain amplifier tubes for use with photo-cells. In transmitting tubes secondary emission is a disadvantage since the current to the control grid when its potential is positive may reverse, and with the usual grid leak bias resistor a large anode

current would flow. These effects can be minimised by employing special materials and coatings for the electrodes.

Noise Voltages. It is well known that a resistance R gives rise to a noise voltage given by Nyquist's expression $\overline{e^2} = 4KTRdf$, where df is the frequency bandwidth, T the absolute temperature, and K is Boltzmann's constant of $1{\cdot}380 \times 10^{-16}$ erg/degree. In thermionic tubes a kindred effect occurs in which similar voltages are developed due to the random rate of electron emission. This is generally known as " shot effect " and is of practical importance in the design of high gain amplifiers and receivers since the noise voltage in the first tube places a lower limit to the useful input signal. The fluctuation in a diode current I is expressed by

$$\overline{i^2} = F^2 . 2eIdf$$

where F^2 is the space charge smoothing factor. In addition noise voltages are generated by cathode surface variations termed flicker effect, ionisation, secondary emission, and in multigrid tubes by division noise.

(*b*) POSITIVE FEED BACK

Negative Resistance. The effective properties of a thermionic tube are changed under dynamic conditions when a fraction of the fluctuating anode potential is fed back to the grid circuit. When this is such that the two voltages are half a cycle out of phase positive feed back is obtained. This amount of feed back may be sufficient to cause the effective tube resistance to become negative, and when this is less than the positive resistance of the tuned anode load circuit the tube is capable of generating sustained oscillations. This positive feed back can be carried out in a variety of ways, and a full account is given by H. A. Thomas (38) of the various equivalent networks. Fig. 5*a* shows the circuit and Fig. 5*b* the performance curves of a generator which consists of a tetrode and a circuit incorporating a quartz crystal, a suitable coil and condenser being placed in the anode lead and adjusted so that the resonant frequency is slightly higher than the crystal frequency. Modulation of the carrier output is obtained by simultaneous variation of the anode and screen voltages.

This circuit oscillates by virtue of the piezo-electric effect of the quartz plate which in mechanical vibration develops an electric potential. The plate is electrically equivalent to a series

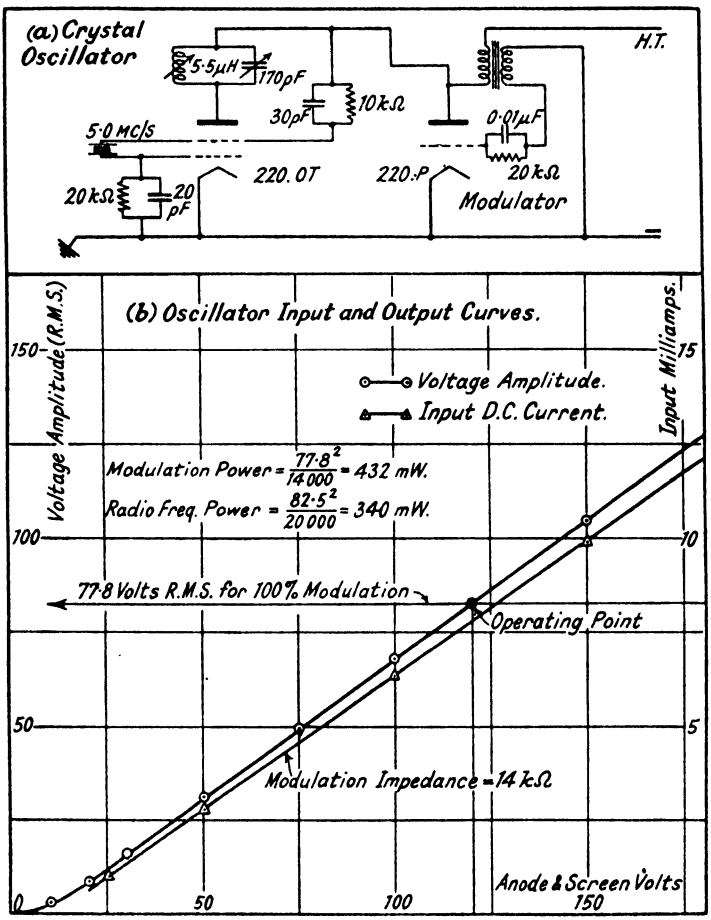

FIG. 5. Crystal controlled oscillator

resonant circuit with components of large reactance and small resistance and in practice frequencies between 1 and 10 Mc/s can very conveniently be obtained.

Oscillator conditions. The general conditions obtaining in a high-frequency oscillator (and also in a Class C amplifier)

can be approximately considered from Fig. 6, which shows the variation of the electrode voltages and currents with respect to time. For good efficiency and output the anode voltage should fall to only about 20% of its mean value, in order that

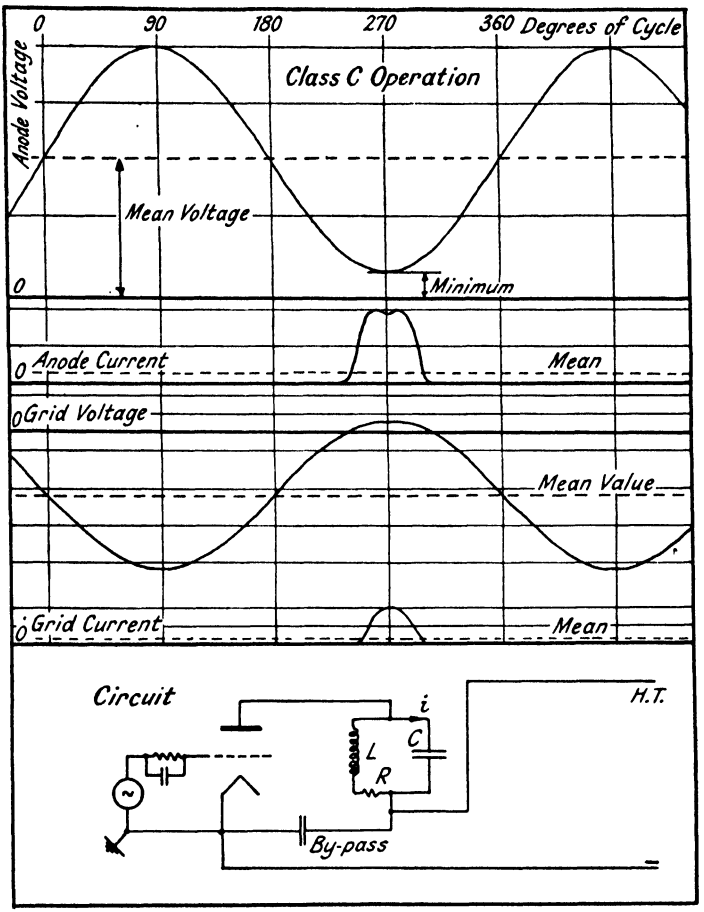

FIG. 6. Characteristics of a tube in Class C operation.

the anode dissipation may be small. Then

$$\sqrt{2}\,\omega L i = 0{\cdot}8V \quad . \quad . \quad . \quad . \quad . \quad (12)$$

where ω is the pulsatance and L the inductance, and i is the R.M.S. oscillatory current in the tuned circuit. Now if R

is the series radio-frequency resistance and W the power output (which is generally known approximately for a tube of given anode dissipation), then

$$W = i^2R \quad . \quad . \quad . \quad . \quad . \quad . \quad . \quad . \quad (13)$$

Since the anode current flows for only a small portion of a cycle (the grid voltage being for the most part greater than the cut-off value by virtue of its large negative bias), it is important that the circuit decrement be low, otherwise the anode voltage will not swing down low enough when current flows. A suitable value for this is $\frac{\pi}{10}$, so that the ratio of amplitude of successive cycles is about 70%. This gives

$$Q = \omega L/R = 10 \quad . \quad . \quad . \quad . \quad . \quad . \quad . \quad (14)$$

and these three equations enable the unknowns R, i, L to be calculated to give optimum results for any particular tube. Thus for a pentode type PT6 rated to give 150 watts with an anode voltage of 1,250, if the frequency be chosen as 1 Mc/s,

$$\left.\begin{aligned} \omega Li &= 0{\cdot}56 \times 1250 = 710 \quad . \quad . \quad . \\ i^2R &= 150 \quad . \quad . \quad . \quad . \quad . \quad . \quad . \quad . \\ \omega L/R &= 10 \quad . \quad . \quad . \quad . \quad . \quad . \quad . \end{aligned}\right\} \quad (15)$$

which give $i = 2{\cdot}11$ amps, $R = 33{\cdot}7$ ohms, and $L = 53{\cdot}7$ μH, the necessary tuning capacitance being 472 $\mu\mu$F. More accurate and elaborate methods of estimating the performance of thermionic tubes are described by D. C. Prince (31) and others.

Frequency Stability. It is generally essential that the frequency of oscillation shall remain accurately constant under conditions of variation of load and electrode voltages, and this problem of frequency stability has received much attention by many workers, as, for example, E. B. Moullin (28) and H. A. Thomas (38). When a great degree of constancy is required special circuits and temperature control are necessary. In this respect the quartz crystal oscillator is of advantage since its high ratio of reactance to resistance enables a nearly steady frequency to be obtained. Changes in tube impedances due to operation conditions can be minimised by arranging the circuit so that only a fraction of these are effectively across the tuned circuit while changes in the linear dimensions of the

inductors and condensers due to temperature can be minimised by partly using materials of negative temperature coefficient and special mechanical design. In short wave transmitters the stability requirements are stringent, particularly when selective receivers are used. Here the thickness of a quartz crystal is too small for reliability and it is usual to generate a submultiple frequency. By means of Class C amplifier stages this is doubled or trebled up to the required frequency. A good degree of control is also obtained by properly adjusted and terminated concentric lines in the grid circuit.

(c) NEGATIVE FEED BACK

Voltage Feed Back. When the fraction of the fluctuating anode potential is in phase with that of the grid, negative feed back is obtained. The principle of this was first explained by H. S. Black (3), who showed that many advantages could

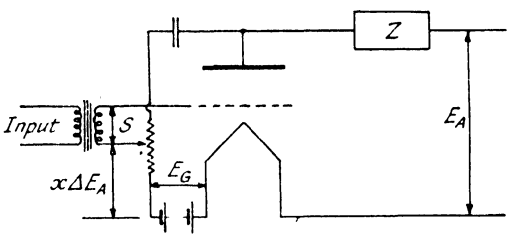

FIG. 7*a*. Voltage feed back.

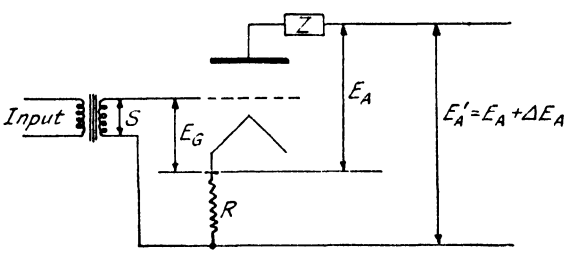

FIG. 7*b*. Current feed back.

be so obtained and its use has lately become prominent, especially in the output stages of audio-frequency amplifiers and in telephone line repeaters handling a large number of separate channels simultaneously. As with positive feed back,

the effective tube properties are modified and an analysis with some experimental results is given below.

If a certain fraction x of the anode potential is fed back we have voltage feed back, and if the anode load impedance is Z then if ΔE_A is the change in anode potential due to a signal change ΔS, a certain voltage $x\Delta E_A$ is fed back to the grid. Thus if ΔE_G is the grid potential we have, from Fig. 7*a*,

$$\Delta E_G = \Delta S + x\Delta E_A \quad . \quad . \quad . \quad . \quad . \quad (16)$$

and if μ is the amplification factor of the tube and ρ its anode resistance, then the anode current change is given by

$$\Delta I_A = \frac{\mu \Delta E_G}{\rho + Z} = \frac{\mu(\Delta S + x\Delta E_A)}{\rho + Z} \quad . \quad . \quad . \quad (17)$$

Now since $\Delta E_A = -Z\Delta I_A$ substitution in (17) gives

$$\Delta I_A = \frac{\mu \Delta S}{\rho + Z(1 + \mu x)} = \frac{\dfrac{\mu}{(1 + \mu x)} \cdot \Delta S}{\dfrac{\rho}{1 + \mu x} + Z}$$

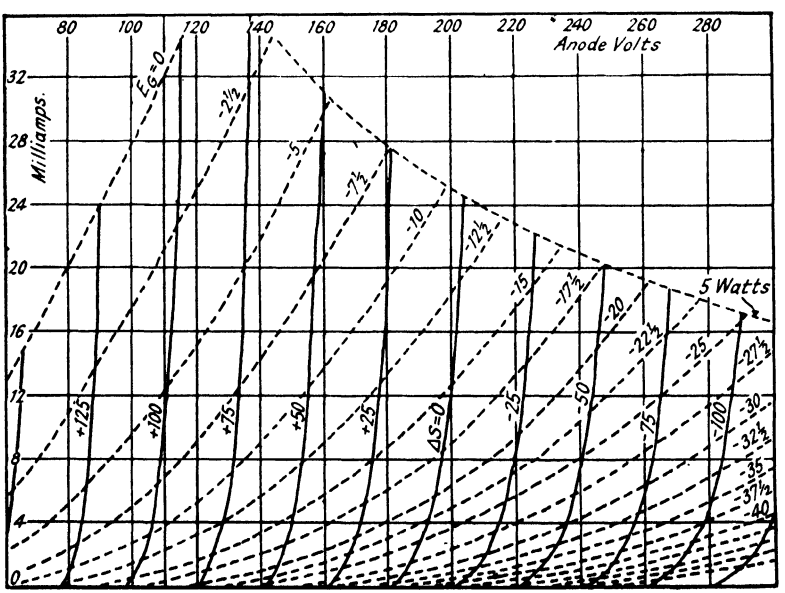

FIG. 8. Triode ML4. Anode characteristics with 100% negative feed back.

which is the current change given by a tube of amplification factor $\frac{\mu}{1+\mu x}$ and resistance $\frac{\rho}{1+\mu x}$, both quantities being less than the values with no feed back.

Experimental Curves. These changes are illustrated in the characteristic curves shown in Fig. 8 for the output triode ML4 and Fig. 9 for the output pentode N43, which are derived

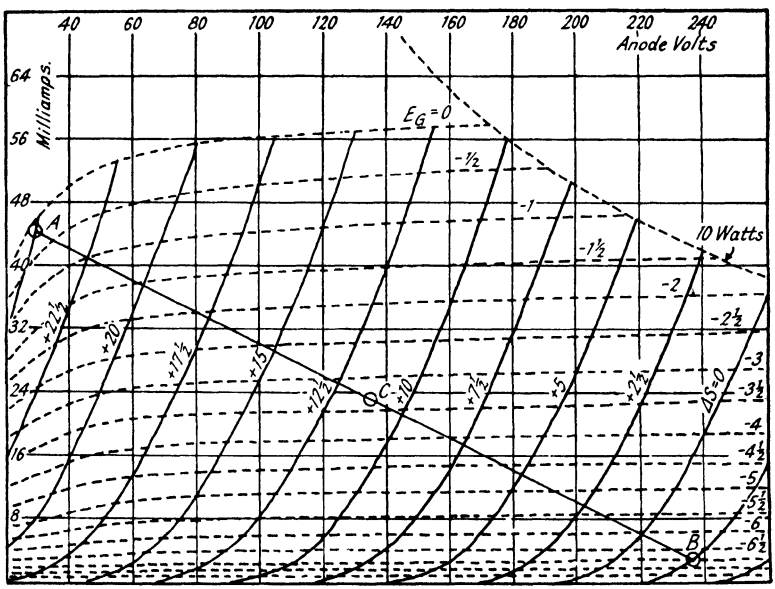

FIG. 9. Pentode N43. Anode characteristics with 10% negative feed back. Screen voltage 250.

from the normal characteristics (obtained in the usual manner by direct measurement) using equation (16). Thus for the triode, if the datum point for $S = 0$ be taken at $E_A = 200$, $E_G = -15$, a complete series of curves can be constructed for various values of ΔS and fractions of feed back. The starting-point for the pentode was $E_A = 250$, $E_G = -3$, although, as with the triode, the same results are obtained for any starting-point.

It will be observed that in the case of 100% feed back the amplification factor is slightly less than unity, as was indicated

from the simple theory given above. The internal resistance of both the tubes is much decreased, and it will be seen from the curves how negative feed back reduces the distortion due to curvature and irregularity of the original characteristics. It is possible to use these curves in the normal way, and if, for example, Z is a resistance of 5,000 Ω and the anode supply voltage is 250, then the load line can be drawn as is done for the pentode with 10% feed back. Avoiding distortion due to grid current and also curvature at small anode currents, it will be seen that a reasonable swing would be from A to B or a change in S of 27½ volts peak to peak, giving an R.M.S. value of 9·8 volts. The mean value of S is marked at C, and this is chosen as the operating point, *i.e.*, a value of $E_G = -3{\cdot}3$ volts for the anode voltage chosen. Similar load lines can be drawn for other cases or when the anode impedance consists of a choke or transformer.

Apart from reducing distortion, the low effective anode resistance is a great advantage when the tube is supplying power to a variable load, such as that, for example, of the input of a Class B amplifier which takes heavy grid current on the peaks of one half-cycle only. The use of negative feed back under such circumstances is preferable to a stepdown transformer, since the voltage swing available is not decreased, but rather increased by the distortion correcting properties. In practice the feed back can be obtained in several ways, one method being to take it from a tapping on a potentiometer connected across the anode load impedance, a suitable blocking condenser being inserted as shown in Fig. 7*a*.

Current Feed Back. Another method of feed back is to cause a voltage in series with the input signal which is proportional to the anode current flowing, and this is usually termed current feed back. The simplest way in which to achieve this is to place a resistance R in the cathode lead, so that it is common to both anode and grid circuits. Then as before, from Fig. 7*b*

$$\Delta I_A = \frac{\mu \Delta E_G}{\rho + Z + R} = \frac{\mu \Delta S}{\rho + R(1 + \mu) + Z} \quad . \quad . \quad (18)$$

since $\Delta E_G = \Delta S - R\Delta I_A$. Equation (18) shows that the

apparent tube resistance is now $\rho + R\ (1 + \mu)$, and thus has been increased by current feed back. Provided μ is large, the tube current $\Delta I_A = \Delta S/R$, and is thus sensibly constant. Various combinations of voltage and current feed back can be made which give the tube a number of useful properties, and an account of these is given by L. I. Farren (16), together with the methods of carrying it out. Negative feed back can also be made to correct distortion in output transformers as well as in the tubes by feeding back voltage from, say, the loud speaker coil, as described by V. C. Henriquer and B. D. H. Tellegen (18).

BIBLIOGRAPHY

1. Barton, L. E. "Recent Developments of Class B Audio and Radio Frequency Amplifiers." *Proc. Inst. Rad. Eng.*, 1936, **24**, 985.
2. Benham, W. E. "A Contribution to Tube and Amplifier Theory." *Proc. Inst. Rad. Eng.*, 1938, **28**, 1093.
3. Black, H. S. "Stabilised Feed Back Amplifiers." *Bell. Sys. Tech. J.*, 1934, **13**, 1.
4. Brainerd, J. G. "Mathematical Theory of the Four Electrode Tube." *Proc. Inst. Rad. Eng.*, 1929, **17**, 1006.
5. Carson, J. R. "A Theoretical Study of the Three Element Vacuum Tube." *Proc. Inst. Rad. Eng.*, 1919, **7**, 187.
6. Chaffee, E. L. "Theory of Thermionic Vacuum Tubes." 1933.
7. Chaffee, E. L. "Equivalent Circuits of an Electron Triode and the Equivalent Input and Output Admittances." *Proc. Inst Rad. Eng.*, 1929, **17**, 1683.
8. Child, C. D. "Motion of Positive Ions." *Phys. Rev.*, 1911, **32**, 498.
9. Cockburn, R. "Variation of Voltage Distribution and Transit Time with Current in the Planar Diode." *Proc. Phys. Soc.*, 1935, **47**, 810.
10. Cockburn, R. "Variation of Voltage Distribution and Transit Time in the Space Charge Limited Planar Diode." *Proc. Phys. Soc.*, 1938, **50**, 298.
11. Doherty, W. H. "A New High Efficiency Power Amplifier for Modulated Waves." *Proc. Inst. Rad. Eng.*, 1936, **24**, 1163.
12. Dunham, C. R. "Hot Cathode Mercury Vapour Rectifier Circuits." *J. Inst. Elec. Eng.*, 1934, **75**, 278.
13. Eastman, A. V. "Fundamentals of Vacuum Tubes." 1937.
14. Everitt, W. L. "Optimum Operating Conditions for Class C Amplifiers." *Proc. Inst. Rad. Eng.*, 1934, **22**, 152.
15. Everitt, W. L. "Optimum operating Conditions for Class B Radio Frequency Amplifiers." *Proc. Inst. Rad. Eng.*, 1936, **24**, 305.

16. FARREN, L. I. "Some Properties of Negative Feed Back Amplifiers." *Wireless Eng.*, 1938, **15**, 23.
17. FAY, C. E. "The Operation of Vacuum Tubes as Class B and Class C Amplifiers." *Proc. Inst. Rad. Eng.*, 1932, **20**, 548.
18. HENRIQUER, V. C. and TELLEGEN, B. D. H. "Inverse Feed Back —Its Application to Receivers and Amplifiers." *Wireless Eng.*, 1937, **14**, 409.
19. HEROLD, E. W. "Negative Resistance and Devices for obtaining it." *Proc. Inst. Rad. Eng.*, 1935, **23**, 1201.
20. JEN, C. K. "A New Treatment of Electron Tube Oscillations with Feed Back Coupling." *Proc. Inst. Rad. Eng.*, 1931, **19**, 2109.
21. KUSUNOSE, Y. "Calculation of Characteristics and the Design of Triodes." *Proc. Inst. Rad. Eng.*, 1929, **17**, 1706.
22. LANGMUIR, I. "The Effect of Space Charge and Residual Gases on Thermionic Currents in High Vacuum." *Phys. Rev.* 1913, **2**, 450.
23. LANGMUIR, I. *Phys. Rev.*, 1923, **21**, 419.
24. LEVAN, J. D. and WEEKS, P. T. "A New Type of Gas-filled Amplifier Tube." *Proc. Inst. Rad. Eng.*, 1936, **24**, 180.
25. MACFADYEN, K. A. "Modifications of the Push Pull Output Stage." *Wireless Eng.*, 1935, **12**, 528 and 639.
26. MILLER, B. F. "An Analysis of Class B and Class C Amplifiers." *Proc. Inst. Rad. Eng.*, 1935, **23**, 496.
27. MOULLIN, E. B. "Time of Flight of Electrons." *Wireless Eng.*, 1935, **12**, 371.
28. MOULLIN, E. B. "Effect of Curvature of the Characteristic on the Frequency of the Dynatron Generator." *J. Inst. Elec. Eng.*, 1933, **73**, 186.
29. MOULLIN, E. B. "An Analysis of the Diode Rectifier." *J. Inst. Elec. Eng.*, 1937, **81**, 667.
30. MOUROMTSEFF, I. E. and KOZANOWSKI, H. N. "Analysis of the Operation of Vacuum Tubes as Class C Amplifiers." *Proc. Inst. Rad. Eng.*, 1933, **23**, 752.
31. PRINCE, D. C. "Vacuum Tubes as Power Oscillators." *Proc. Inst. Rad. Eng.*, 1923, **11**, 275, 405 and 527.
32. SALZBERG, B. "Notes on the Theory of the Single Stage Amplifier." *Proc. Inst. Rad. Eng.*, 1936, **24**, 879.
33. SCHADE, O. H. "Beam Power Tubes." *Proc. Inst. Rad. Eng.*, 1938, **26**, 137.
34. SCHEIBE, A. "The Generation of Ultra-short Waves with Hot-Cathode Tubes." *Ann Phys.*, 1924, **73**, 54.
35. TERMAN, F. E. *Radio Engineering*, 1937.
36. TERMAN, F. E., and FERNS, J. H. "The Calculation of Class C Amplifiers and Harmonic Generator Performance of Screen Grid and Similar Tubes." *Proc. Inst. Rad. Eng.*, 1934, **22**, 359.
37. TERMAN, F. E. and ROAKE, W. C. "Calculation and Design of Class C Amplifiers." *Proc. Inst. Rad. Eng.*, 1936, **24**, 620.
38. THOMAS, H. A. "Theory and Design of Valve Oscillators." 1939.
39. WAGENER, W. G. "Simplified Methods for computing the Performance of Transmitting Tubes." *Proc. Inst. Rad. Eng.*, 1937, **25**, 47.

CHAPTER II

THE INFLUENCE OF FREQUENCY OF OPERATION

(a) EFFECT ON TUBE PROPERTIES

Circuit Changes. Up till now the impedance and general properties of thermionic tubes have been assumed to depend only on the electrode voltages and the circuit connections and that they were independent of the frequency of operation.

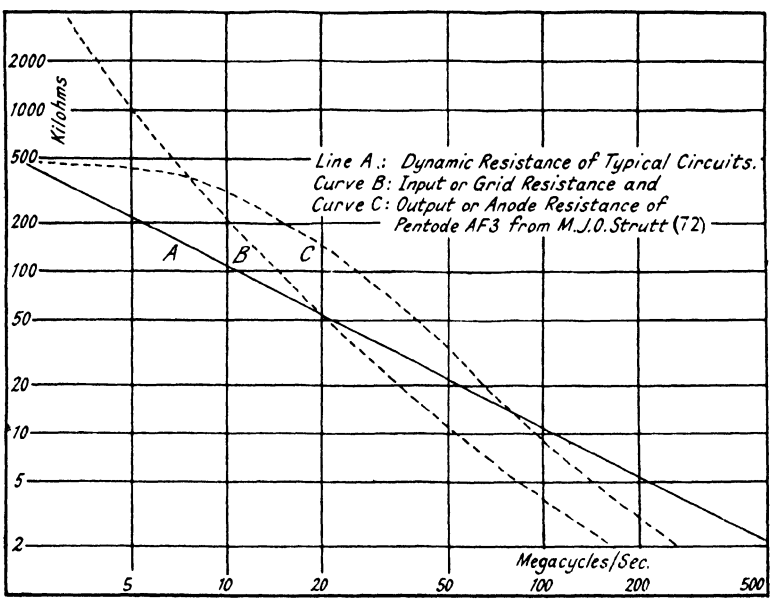

FIG. 10. Influence of frequency of operation on tube properties.

While this is true provided the frequency is sufficiently low it is found that as this is raised the tube properties are profoundly modified.

The performance of thermionic tubes may be modified at high frequencies, due, in part, to circuit properties. Thus

N. E. Lindenblad (38) shows that the decreasing capacitive reactance of the tube necessitates increased tube lead currents, and consequently losses, in order to maintain the proper electrode potentials, although in well-designed circuits this effect is not serious. Further, the stray capacitances place a minimum on the value of tuning capacitance, and thus beyond a certain frequency the dynamic resistance of the tuned circuit commences to fall. The dynamic resistance becomes

$$Z = \frac{\omega^2 L^2}{R} = \frac{\omega L}{R} \cdot \frac{1}{\omega C} = \frac{Q}{2\pi C} \cdot \frac{1}{f} \quad . \quad . \quad . \quad (19)$$

where ω is the pulsatance, f the frequency, L the inductance and C the capacitance. In general, the magnification factor Q ($= \omega L/R$) of the circuit is not critical to frequency and thus Z falls inversely as the frequency, and if Q is 100 while the minimum capacitance is 15 $\mu\mu$F, the dynamic resistance has the value shown by the full line in Fig. 10. With this decreased dynamic resistance of the tuned circuit alone the tube is only capable of supplying a reduced useful output. It is possible to minimise this fall in dynamic resistance by employing circuits in the form of parallel or concentric lines, since the dynamic resistance and magnification factor of these are large at very high frequencies, and at wavelengths of the order of 1 metre their size become quite practicable.

Tube Characteristics. It has been shown by M. J. O. Strutt (72) that for the determination of tube performance at very high frequencies the constants which require to be known are the input impedance, output impedance, mutual conductance and feed back impedance. Thus for any given tube the performance, say, as an amplifier or frequency changer can be predicted by the experimental determination of these constants. Of these, the grid or input impedance requires the most careful determination since it falls to very low values at high frequencies, thus leading to low efficiency in transmitting tubes and low stage gains in receiving tubes. For comparison some results given for the high-frequency pentode type AF3 are shown by two curves in Fig. 10. It will be seen that above 20 Mc/s the input grid resistance is lower than the dynamic

resistance of the typical tuned circuit mentioned earlier. The anode or output resistance does not fall to quite such low values, due to the higher operating voltages, and consequently smaller transit times, and also because the lead inductances do not have a great effect. For this particular pentode the mutual conductance was found to be unchanged at frequencies up to 300 Mc/s, and this is in agreement with theory. The feed back impedance falls with increasing frequency and it may be considered as a small capacitance between the anode and control grid with a value depending on the frequency. When the frequency becomes high enough the input resistance falls to such low values that excessive damping occurs and the gain of the preceding stage may become less than unity.

Electron Inertia. In general the greater portion of this loss of performance is due to modifications in the tube properties due to the finite transit time of the electrons, with the result that they no longer follow instantly changes in electrode potentials. One result of this is that when electrons impinge on an electrode their velocity of arrival can be greater or less than the value corresponding to the instantaneous potential. They are thus apt to fall on the anode or cathode with increased energy, and in the case of the latter an increase of emission occurs as observed by R. L. Narasimhaiya (47), who found a triode to oscillate after its filament supply had been disconnected

The influence of frequency on the tube impedance and other properties has been examined theoretically by F. B. Llewellyn (39–44) and W. E. Benham (2–4) and others, who show that the resistance is altered at very high frequencies and may become negative at certain values. The trans-conductance (or slope) of the tube becomes complex at very high frequencies, the phase angle increasing with frequency, but decreasing with increase of electrode voltages as would be expected.

Although finite electron transit time would be expected to impose an upper limit on the frequency of operation of a given tube with certain operating potentials, W. R. Ferris (12) and D. O. North (49) have shown that an earlier limit is reached due to the effect of transit time on the grid input resistance. Thus from consideration of the displacement currents to the

control grid of a triode caused by the transit of the electrons it follows that during a small portion of the cycle when the grid potential is increasing in a positive direction there is a net current flowing into the grid, and when the grid potential is decreasing in a positive direction there is a net current flowing out of the grid. This current is given by

$$I_{g_1} = KS_K E_{g_1} fT \quad . \quad . \quad . \quad . \quad . \quad (20)$$

where K is a constant depending on the electrode geometry and potentials, T is the transit time to an arbitrary point and S_K is the cathode slope (change of cathode current with respect to grid potential). Hence the input admittance is

$$Y = KS_K fT \quad . \quad . \quad . \quad . \quad . \quad . \quad (21)$$

It can be shown that there is a phase displacement represented by θ between the grid potential maximum and zero instantaneous current depending on T and the frequency f, and this gives rise to a conductive component

$$G' = Y \sin \theta \simeq Y\theta = KS_K f^2 T^2 \quad . \quad . \quad . \quad (22)$$

Thus energy is fed into the grid and this appears as heat dissipated at the collector electrode. Hence the input resistance due to this cause is inversely proportional to the frequency squared and in any given tube, inversely proportional to the cathode current slope.

Residual Reactances. The inevitable small inductances of the leads to the electrodes and the respective interelectrode capacitances also cause changes in the phases of the electrode currents, and it is shown theoretically by M. J. O. Strutt and A. Van der Ziel (75) that in the case of normal receiving type triodes and pentodes this effect is large. This has also been demonstrated by R. L. Freeman (16). Thus from Fig. 19 the pulsating component of cathode current I_K produces a voltage drop across the cathode lead inductance L_K given by

$$E_K = \omega L_K I_K \quad . \quad . \quad . \quad . \quad . \quad (23)$$

which lags the input signal by 90°. This voltage drop causes a current through the grid cathode capacitance C_{g_1K} which leads E_K by 90°, and is hence in phase with the input signal representing an input conductance

$$G = \omega^2 C_{g_1K} L_K S_K \quad . \quad . \quad . \quad . \quad . \quad (24)$$

Thus if S_K is 8 mA/v, C_{g_1K} is 5 $\mu\mu$F and L_K is 0·03 μH the input resistance would be about 8,300 Ω at 50 Mc/s due to this cause alone. This relation is modified, as shown by B. J. Thompson (80) and F. Preisach and I. Zakariás (53), by the inductance of the screen (or in a triode, the anode) lead and the associated grid capacitance, but this will be dealt with later. It will be seen that both conductances G' and G obey the same law as regards frequency and slope, and it is not easily possible to separate the two effects experimentally.

Receiving Tubes. In normal types of tubes these disadvantages have been partially overcome by careful design and construction, such as the employment in receiving or low-power tubes of very small electrode sizes and short leads to them. D. G. Burnside and B. Salzberg (7) have described the development and manufacture of such "acorn" type tubes and show that the electrical characteristics are about the same as larger tubes, but the input impedance is much higher and is about 80,000 ohms at 50 Mc/s for the "acorn" pentode as against 30,000 ohms for the larger 6C6 pentode. Fig. 11 shows photographs about full size of the Marconi-Osram "acorn" triode HA1 and pentode ZA1. Another receiving tube developed for very high-frequency operation is the "all glass" tube described by M. J. O. Strutt, in which the electrode leads are arranged to be as short as possible and are taken through the glass envelope by separate seals. Fig. 12 shows the Mullard EF50, which is of this type of construction

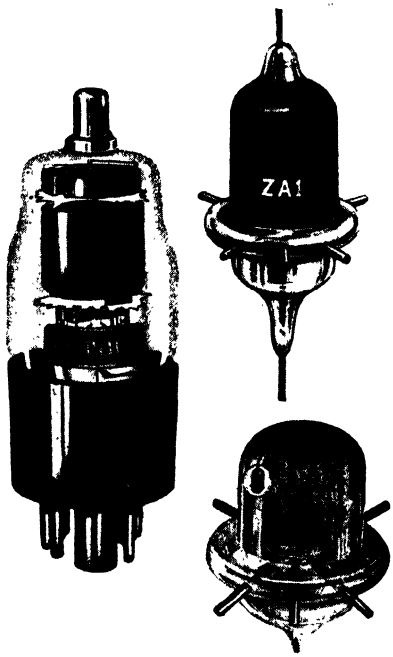

FIG. 11. The Osram ZA1 "acorn" pentode HA1 "acorn" triode, and Z62 pentode.

and the layout of the inside of the tube can be clearly seen. A modified form of this pentode, the EFF50, has two electrode assemblies in one envelope and is intended for push-pull working, so that the cathode lead carries no high-frequency current. Fig. 11 also shows the Osram Z62 high-frequency pentode. The properties of these and other tubes will be discussed later when the experimental results are described.

In screen-grid tetrodes and pentodes the inductance of the

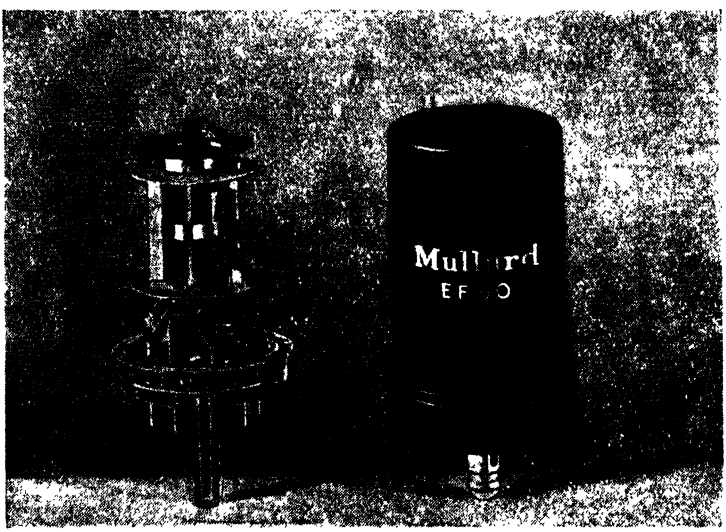

FIG. 12. Construction of Mullard EF50 pentode.

screen lead causes an apparent change in the anode to control grid capacitance, and this may be sufficient to result in instability. By considering the control grid, screen grid, earth and anode as a star network with the screen grid at the centre, then by transformation to the equivalent delta network the effective change in anode to control grid capacitance becomes

$$C = \frac{\omega^2 C_{g_2 a}\, C_{g_1 g_2}\, L_{g_2}}{\omega^2 L_{g_2}(C_{g_1 g_2} + C_{g_2 a}) - 1} \quad . \quad . \quad . \quad (25)$$

If the screen is returned to earth *via* a small capacitance C_2, then L_{g_2} and C_2 can be made to form a series resonant circuit

at a given frequency, and for other frequencies the apparent capacitance becomes

$$C = \frac{(\omega^2 L_{g_1} C_2 - 1)\, C_{g_2 a} C_{g_1 g_2}}{(\omega^2 L_{g_1} C_2 - 1)\,(C_{g_1 g_2} + C_{g_2 a}) - C_2} \quad . \quad . \quad (26)$$

It can be shown that under some circumstances an improvement is obtained by placing the small condenser C_2 inside the tube envelope, a well-known example being the RCA832.

The decrease of coil resistances at very high frequencies makes it difficult to obtain a satisfactory signal to noise ratio in the first stage of amplification in a receiver. In order that the signal to noise ratio in the aerial shall not be unduly decreased the equivalent noise resistance (assumed to be in series with the grid) of the tube must be as small as possible compared with the dynamic resistance of the grid circuit, which, at very high frequencies, is governed partly by the grid damping. This resistance decreases with frequency, although the noise resistance remains sensibly constant. Thus receiving tubes for very high frequencies must have a low noise resistance in order to make stages before the frequency changer beneficial.

Transmitting Tubes. In the case of transmitting tubes the lead effects are not so serious due to the lower interelectrode capacitances, but transit time effects cause limitations due to the electrode dimensions. These can be minimised by employing high operating voltages. A. V. Haeff (23) has investigated experimentally the effect of electron transit time on the performance of power amplifiers. In a neutralised triode or screen-grid type tube the phase of the output voltage is independent of the input, and thus the efficiency of the tube as an amplifier was found experimentally to be higher than as an oscillator in which electron transit time causes phase changes. F. A. Kolster (35) discusses the various types of tuned circuits and describes a low-loss high-capacity self-contained tank circuit suitable for high-frequency operation, typical parameters being an inductance of 0·05 μH, a capacitance of 90 $\mu\mu$F and a magnification factor of 2,000 at 4 m. wavelength.

In a high-frequency oscillator the tuned circuit is effectively

between anode and control grid, and thus this total capacitance is shunted across it. When a transmission line is used, this capacitance is equivalent to a small length of it, and can impose a limit on the minimum wavelength. M. R. Gavin (20) shows that the impedance of a line of $Z_0\ \Omega$ and length l cm. is given, for a wavelength λ cm., by

$$Z = Z_0 \tan \frac{2\pi l}{\lambda}$$

and if C is the tube capacitance, then

$$\tan \frac{2\pi l}{\lambda} = \frac{\lambda}{6\pi . 10^{10} . CZ_0}$$

It is desirable for a given minimum C and l to use a line of low characteristic impedance, and in this respect a concentric line with special cylindrical electrodes is advantageous. By estimating the effect of transit time it is shown that the efficiency falls by 10% when

$$\lambda = \frac{2 \times 10^4 (3d_{gK} + d_{ga})}{\sqrt{E_A}}$$

where d_{gK} and d_{ga} are the grid cathode and grid anode distances and E_A is the mean anode voltage.

FIG. 13. Standard Telephones 4304B triode for frequencies up to 400 Mc/s.

C. E. Fay and A. L. Samuel (10) describe transmitting tubes for very high-frequency operation. One, similar to the Standard Telephones 4304B triode shown in Fig. 13, has a dissipation of 50 watts for an anode voltage of 1,250. In push-pull two tubes are capable of giving an output of 34 watts at 35% at 200 Mc/s, while the frequency limit is 400 Mc/s at a voltage of 750. In this tube the electrodes, particularly the

grid and cathode, are closely spaced and the dissipation of the small anode is increased by making it of graphite. The envelope is of hard glass to withstand high temperature and only a minimum of insulating material is employed in the electrode assembly. For use above 300 Mc/s a smaller tube has been developed with a dissipation of 30 watts at 400 volts.

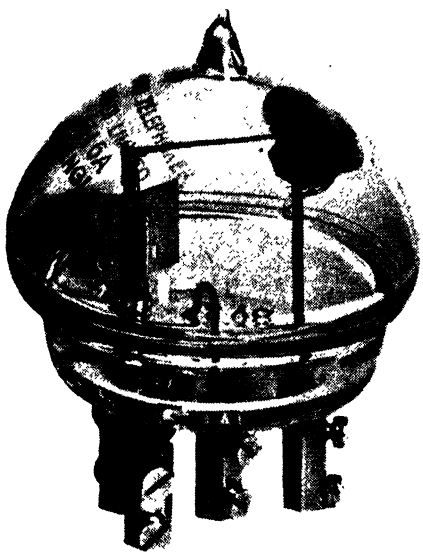

FIG. 14. Standard Telephones 4316A triode for frequencies up to 700 Mc/s.

Fig. 14 shows the Standard Telephones 4316A triode, which is capable of giving an output of 8·5 watts at 300 Mc/s and 4·0 watts at 600 Mc/s with an oscillation limit of 750 Mc/s.

Similar principles apply to transmitting tubes designed for much larger power outputs. Fig. 15*a* shows a Mullard PY2-250, which is a 2,000-volt, 250-watt pentode, with a thoriated tungsten filament. The anode connection, and also an extra suppressor grid connection, are brought out at the top of the bulb, and the base is of a new type having very short contacts

instead of pins in order to reduce the inductance of the leads. This tube will give an output of 550 watts at 15 metres and is useful down to a wavelength of about 5 metres. Fig. 15*b* shows a Mullard PX12-15, which is a 12 kV, 12 kW, water-cooled pentode with a pure tungsten filament. On long wavelengths

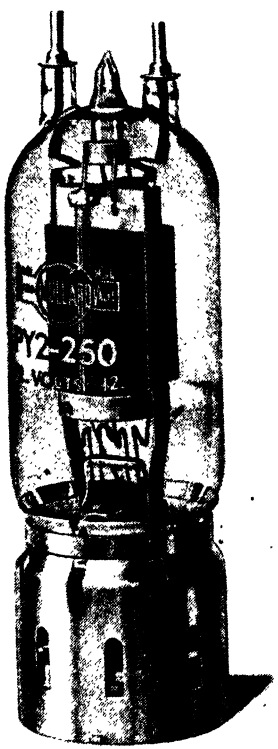

FIG. 15*a*. Mullard PY2-250 transmitting pentode.

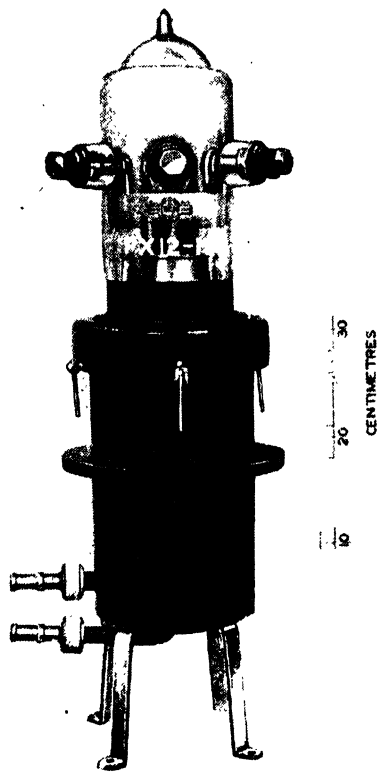

FIG. 15*b*. Mullard PX12-15 water-cooled pentode.

an output of 14·4 kW is obtainable, and at 6 metres a pair of these tubes would give about 14·5 kW. W. G. Wagener (81) describes the RCA888, which is a small water-cooled triode of 1 kW anode dissipation giving 550 watts output at 100 Mc/s and 300 watts at 200 Mc/s.

A. K. Wing (83) describes a double tetrode similar to the

RCA type 832, designed to give 10 watts at 250 Mc/s with 400 volts. This tube is primarily designed as a radio-frequency amplifier driven by a crystal-controlled oscillator and frequency multiplier or by a stable high-frequency master oscillator. The plate leads are brought out through the top of the bulb

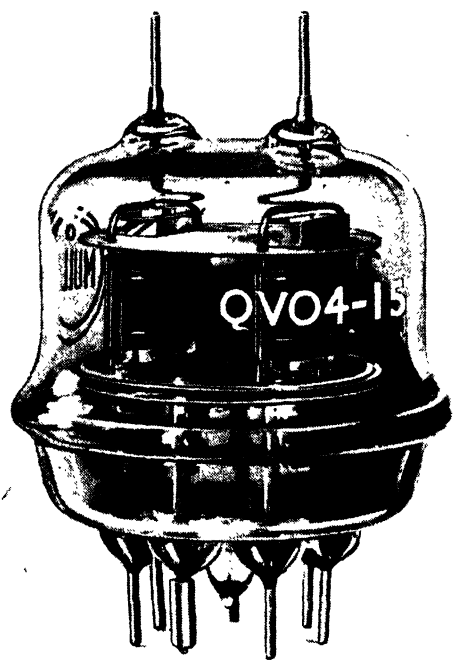

FIG. 16. Mullard QV04-15 double tetrode.

and the remainder through the base, an arrangement which lends itself well to parallel line circuits for the input and output. A description of a tube of similar construction is given by A. L. Samuel and N. E. Sowers (63) and the associated circuits and equipment for measuring the performance are examined in detail. Fig. 16 shows the Mullard QV04-15, which is again a double tetrode. This is mounted on an all-glass base and is

rated at 400 volts and 7·5 watts per unit, giving an output of 22 watts at 3 metres.

A. L. Samuel (61, 62) describes some special triodes and pentodes in which the inductance of the leads is reduced by bringing two from each electrode out from either end, and the outputs obtainable are about 60 watts at 300 Mc/s and 2 watts at 1,500 Mc/s. The latter is equivalent to the Standard Telephones 3B/250A triode shown in Fig. 17. When these

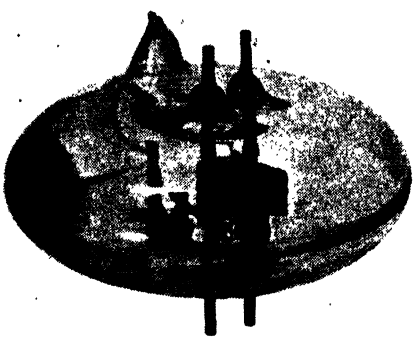

FIG. 17. Standard Telephones 3B/250A triode for frequencies up to 1,700 Mc/s.

tubes are used with a parallel wire circuit, as is usual for these very high frequencies, the wavelength possible is shorter when a half wave line is used than when a quarter wave line is used with single-ended operation. Further details of development work and properties of transmitting tubes for very high frequencies are given by D. H. Black (6), W. G. Wagener (81), and L. E. Lindenblad (38).

(*b*) MEASUREMENTS AT VERY HIGH FREQUENCIES

Method Used. As stated earlier the estimation of the performance of thermionic tubes at very high frequencies requires the knowledge of certain constants and these have been

determined experimentally for various kinds of tubes. The method adopted is generally that described by M. J. O. Strutt (72), the circuit of the measuring equipment being given in Fig. 18. In brief, the change in dynamic resistance of a tuned circuit is measured when the tube is connected in parallel with it. The tube resistance can be determined by the conductance variation method by comparing it with a known high-frequency standard resistance (Dubilier ½ watt metallised type), as described by W. R. Ferris (12) and the author (26),

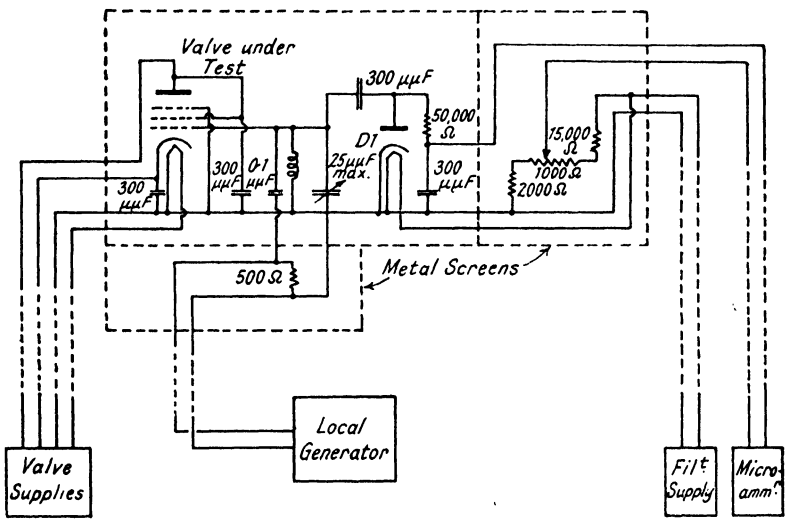

FIG. 18. Circuit for measuring tube constants by M. J. O. Strutt's method.

but in this case determination of the dynamic resistance is by the susceptance variation method of measuring the width of the resonance curve at a known point. Thus if the coupling or input condenser is so small that the current I through the tuned circuit is constant and Z is the dynamic resistance of the circuit, then the voltage V across the circuit is given by

$$V = \frac{I}{\frac{1}{Z} + j\left(\omega C_0 - \frac{1}{\omega L_0}\right)} \quad . \quad . \quad . \quad (27)$$

and if V_1 is the voltage at resonance and V_2 the voltage when the parallel capacitance is altered to C_0',

then $$V_1 = IZ \quad . \quad . \quad . \quad . \quad . \quad . \quad . \quad . \quad . \quad . \quad (27a)$$

and $$Z = \frac{1}{\omega(C_0' - C_0)} \sqrt{\left(\frac{V_1}{V_2}\right)^2 - 1} \quad . \quad . \quad (28)$$

giving the dynamic resistance in terms of a known susceptance difference and a known voltage ratio. If $\omega \Delta C$ is the susceptance difference at the voltage V_2 on either side of the resonance curve and f is the frequency, then

$$Z = \frac{1}{\pi f \Delta C} \sqrt{\frac{V_1^2 - V_2^2}{V_2^2}} = \frac{1}{\pi f \Delta C} \quad . \quad . \quad . \quad (29)$$

when $V_2 = 0{\cdot}707\ V_1$. This relation holds even when, as is usual at very high frequencies, there are comparatively large stray inductances and capacitances present, since these, with the coil inductance, can always be reduced, at a given frequency, to a fixed inductance and capacitance in parallel with the variable measuring condenser. The voltmeter may have neither a linear nor square law scale, and thus it is necessary to read the values of V_2 and V_1 for each measurement, although in the interests of accuracy the distuning should be such that V_2 is nearly $0{\cdot}7\ V_1$.

Diode Voltmeter. The voltage can be determined by a peak voltmeter employing a diode such as the Mazda D1 shown in Fig. 18. Standard condensers and resistors are employed and the arrangement must be compact to reduce errors due to stray inductance and capacitance. The errors in peak voltmeters of this pattern have been examined by C. L. Fortescue (14) and E. C. S. Megaw (45), while details on the performance of diode voltmeters at very high frequencies are given by L. S. Nergaard (48). The load condenser is charged up at the peak of every cycle of voltage and discharges through the D.C. voltmeter during the remainder of the cycle. It can be shown that if the error is not to exceed 0·1% the condenser must be at least $\frac{10^{15}}{2fR}$ $\mu\mu$F or 100 $\mu\mu$F when R is 50,000 Ω and f is 100 Mc/s. Actually a value of 300 $\mu\mu$F was used and, since the charging time is negligible, little time lag is introduced in the reading. During the peaks the diode

passes current, and if a linear characteristic is assumed equivalent to a resistance R_a (about 2,000 Ω) then the fractional error is $2{\cdot}2\left(\frac{R_a}{R}\right)^{2/3}$, which is appreciable. This and the error due to initial electron velocities, which can be considered as equivalent to a small constant voltage error, can be eliminated by calibration at 50 c/s, the reservoir condenser being increased to 8μF. Since the anode earth capacitance of this diode is

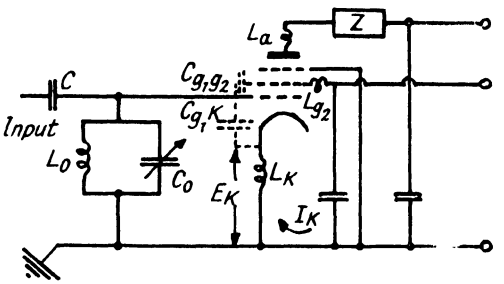

FIG. 19. Grid conductance due to lead inductance.

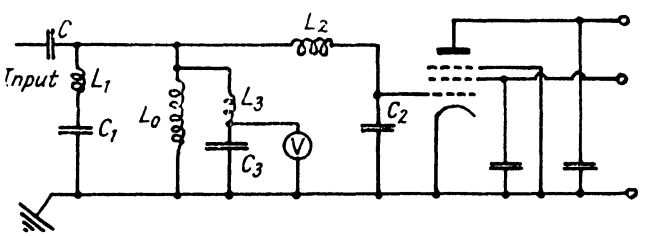

FIG. 20. Effect of lead and condenser inductance.

only 2·1 $\mu\mu$F, the error due to the potential dividing effect with the reservoir condenser of 300 $\mu\mu$F is small. The transit time of the diode given by

$$T \simeq 0{\cdot}15\,\frac{d \text{ cm.}}{\sqrt{V}}\,10^{-7} \text{ sec.} \quad . \quad . \quad . \quad . \quad (30)$$

is about one-tenth of a cycle at 100 Mc/s, the voltages V employed being not greater than 0·5 peak and the inter-electrode spacing d being 0·15 mm. approx. In general if the electron inertia error is not to exceed 1%, then $fd/\sqrt{V}$ must not exceed 0·1. From Fig. 20 if the inductance L_3 of the leads is

0·03 μH and the input capacitance C_3 (including strays) is 4·0 $\mu\mu$F, then the diode voltage given by

$$V_D = V \frac{1}{1 - \omega^2 L_3 C_3} \quad . \quad . \quad . \quad . \quad (31)$$

is within 5% of the circuit voltage V at 100 Mc/s, and this error is, of course, constant at all voltages. With these residuals the resonant frequency of the diode voltmeter is about 450 Mc/s (wavelength 67 cm.). The steady voltage developed by the diode across the reservoir condenser can be measured

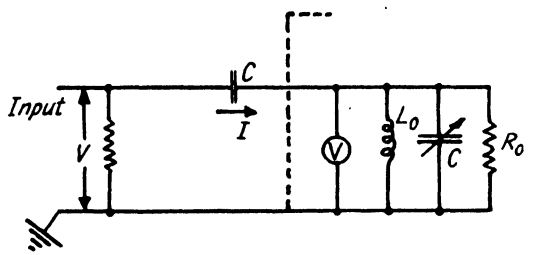

FIG. 21. Effect of finite coupling capacitance.

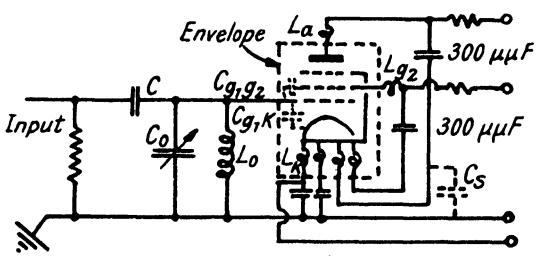

FIG. 22. Connections for tube with multiple cathode leads.

with a sensitive Cambridge Unipivot microammeter and a series resistance of 50,000 Ω. The hot damping at 100 Mc/s due to such a voltmeter can be shown, with the aid of a second tube voltmeter to be about 10,000 Ω. The standing current of the diode is usually backed off by a potentiometer across the filament supply to a fixed deflection and the relative voltage ratios read from the calibration curve which is assumed valid over the range of working frequencies.

Coil and Condenser. The tuned circuit consists of interchangeable inductance coils, the smallest being a single turn of

18 S.W.G. silvered copper wire 4 mm. diameter, and a variable condenser of range 3–28 $\mu\mu$F fitted with a slow motion dial so that variations of 0·01 $\mu\mu$F are readable. It is well known that variable condensers possess a residual inductance due to the finite size of the vanes and leads, and at high frequencies the effect of this inductance is appreciable. Thus for the highest accuracy compensation must be applied and this is done by calibrating the condenser at a low frequency when in position and determining the residual inductance by the method described by R. F. Field and D. B. Sinclair (13). In this, small fixed condensers are measured at high frequency at various settings of the variable condenser, different coils being used so that the frequency remains unaltered. To a good degree of approximation the variable condenser can be considered as a condenser in series with a small inductance, and thus if L_1 is the residual inductance and C_x the true value of the small fixed condenser which was measured, then if C_1 and C_2 are the dial readings

$$C_x \simeq \frac{C_1 - C_2}{1 - \omega^2 L_1(C_1 + C_2)} \quad . \quad . \quad . \quad . \quad (32)$$

By plotting $C_1 - C_2$ against $C_1 + C_2$ the intercept on the axis gives C_x and the inductance is given by

$$L_1 = \frac{\text{Slope of line}}{\omega^2 \times \text{intercept}} \quad . \quad . \quad . \quad . \quad . \quad (33)$$

A typical value for the residual inductance would be 0·012 μH, although in the case of measurements on such small condensers this cannot be determined with much accuracy.

It is also well known that a variable condenser possesses a finite conductance due to insulation leakage, eddy losses in the vanes, and power loss in the dielectric material supporting the plates. In general, for most well designed and constructed condensers these losses are only a small fraction of those in the rest of the circuit and the variation of effective condenser conductance over the tuning range can be neglected. The method of measuring this variation is also given by R. F. Field and D. B. Sinclair (*loc. cit.*).

In the arrangement employed by M. J. O. Strutt (72) the whole measuring set-up, including the tube to be measured,

was enclosed in an 18 S.W.G. copper box and the supply batteries and galvanometer were connected to it by screened cables. A sinusoidal current was caused in the tuned circuit by means of a 0·1 $\mu\mu$F input coupling condenser. From

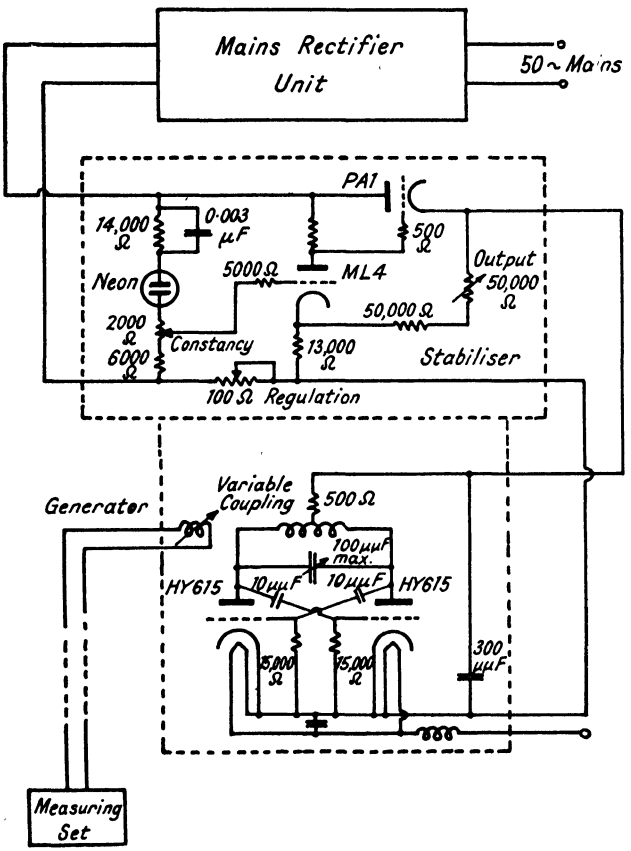

FIG. 23. Circuit of local generator and stabiliser.

equation (29) it will be seen that in order to determine the parallel resistance of the tube a knowledge of the frequency of the generator is necessary. In general, it will be sufficiently accurate if a normal wavemeter, preferably fitted with some form of detector, is employed.

Local Generator. Some care is necessary in designing a satisfactory local oscillator, since in order to use only very

loose coupling a reasonable power output was desirable, while since it is better to stabilise the high-voltage supply to counteract mains variations the voltage should not be very high. A common type of generator using a push-pull circuit is shown in Fig. 23, using type HY615 triodes. These tubes are of 5 watts anode dissipation with the anode and grid brought to caps on the top of the bulb, an arrangement which is very convenient for a self oscillator as opposed to a power amplifier. The output that can be obtained is about 1·5 watts at 150 volts up to 200 Mc/s. It would be possible to use acorn triodes, but the power of, say, 0·5 watt is hardly sufficient while tubes such as the Marconi-Osram DET12 require too large anode and filament supplies. The useful power from the oscillator to the measuring set can be controlled by varying the mutual inductance of the pickup coil and the oscillator coil. The stabiliser circuit shown is a frequently used one and can be relied on to keep the voltage within 1 volt for input variations of about 20 volts. The generator and stabiliser should be enclosed in separate compartments of a copper box which, with the supplies, must be kept several feet away from the measuring equipment. A signal generator or local oscillator for a similar purpose has been described by L. S. Nergaard (48), who used a split anode magnetron with a parallel wire circuit which could be continuously varied for wavelength changes. The stabiliser used gave an output of 2,000 volts and has been described by T. H. Johnson and J. C. Street (30).

Correction Factors. The tube socket in the measuring set is connected to the variable condenser by short lengths of copper strip and the circuit resistance determined with no tube in position and with the tube operating under different conditions. If Z_1 and Z_1' are the dynamic resistances without and with the tube then R_1, the tube resistance, is given by

$$R_1 = \frac{Z_1 Z_1'}{Z_1 - Z_1'} \quad . \quad . \quad . \quad . \quad . \quad (34)$$

and if C_0 and C_0' are the effective capacitances of the variable condenser at resonance, then the tube capacitance is given by

$$C = C_0 - C_0' \quad . \quad . \quad . \quad . \quad . \quad . \quad (35)$$

If the ends of the inductance coil are taken as a reference

point, the effective value C_0 of the variable condenser is given, from Fig. 20, as

$$C_0 = \frac{C_1}{1 - \omega^2 L_1 C_1} \quad . \quad . \quad . \quad . \quad . \quad (36)$$

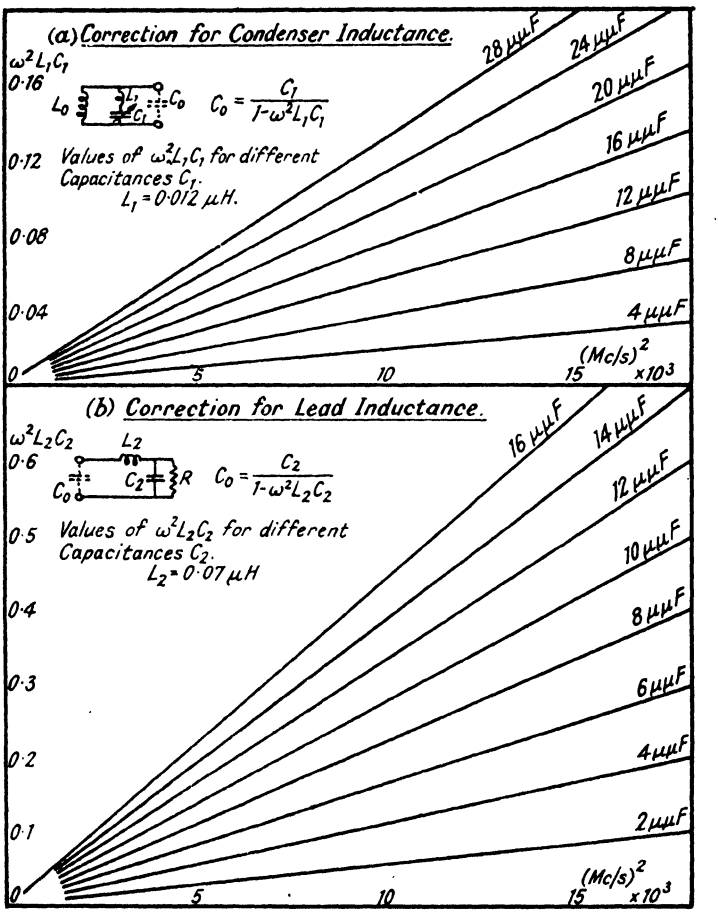

FIG. 24. Corrections for condenser and lead inductances.

where the residual L_1 is the previously mentioned typical value. Values of $\omega^2 L_1 C_1$ are plotted in Fig. 24*a* for different settings

of C_1. If the resonance curve is reasonably sharp and $\omega^2 L_1 C_1 \ll 1$, then the true dynamic resistance Z_0 is given by

$$Z_0 \simeq Z_1(1 - 2\omega^2 L_1 C_1) \quad . \quad . \quad . \quad . \quad (37)$$

and thus by inserting these values in equation (34) the tube resistance can be found.

A further correction for the tube resistance is necessary, due to the inductance of the input leads. This can be determined by measuring small fixed condensers (about 5, 10 and 15 $\mu\mu$F mica) placed in the tube socket, so that they approximate in position to the tube electrodes. If these capacitances are assumed unchanged at the frequency of measurement the effective values are given from Fig. 24*b* at the variable condenser terminals as

$$C_0 = \frac{C_2}{1 - \omega^2 L_2 C_2} \quad . \quad . \quad . \quad . \quad . \quad (38)$$

A typical value of lead inductance L_2 is 0·07 μH, and this represents the effective value including any mutual inductances that may be present. Values of $\omega^2 L_2 C_2$ are given in Fig. 24*b* for different tube capacitances, and by applying these corrections to the variable condenser effective values the input conductance of the tube under various conditions is known. Power considerations show that the true input tube resistance R_2, considered to act at the electrodes, is given by

$$R_2 = \frac{R_0}{(1 - \omega^2 L_2 C_2)^2} \quad . \quad . \quad . \quad . \quad (39)$$

the correction being obtained from the data of Fig. 24*b*, and for inputs of 10 $\mu\mu$F, say, the correction is very large. It is not possible to combine the corrections for condenser and lead inductance as suggested by E. C. Corke and J. L. Pawsey (10), nor to choose L_1 so that the corrections mutually cancel (since they act in opposite directions), as is done by F. Preisach and I. Zakariás (53), since it can only be done with one value of tube capacitance and due to the large corrections, errors would arise due to the input capacitance change with operating conditions as well as differences between one tube and another.

Although electromagnetic coupling with the usual electro-

static screen can be used, it is generally more convenient to use electrostatic coupling provided good screening is employed. With the circuit described and the coupling condenser removed the screening should be such that no measurable deflection of the galvanometer can be obtained. The conditions obtaining with finite coupling have been examined by D. B. Sinclair (67), and it is shown that even if this is enough to cause amplitude variation of the local generator no error is caused provided the impedance of an individual piece of apparatus is determined. The generator and small coupling capacitance can be replaced in theory by a small capacitance and high resistance in parallel with the tuned circuit. This will be seen from Fig. 21, and, provided the coupling is not altered during the measurements, these parameters remain constant. It is, however, desirable for the coupling condenser to be small in order to reduce the damping of the tuned circuit. Before making tube measurements and as a check on the above corrections, known resistors and condensers should be measured at the tube socket and directly across the variable condenser and the values obtained at high frequency should not differ much from the values measured on low-frequency bridges.

With these measurements on input damping and assuming normal tuned circuits, the magnification Q of the circuit is sufficiently high to ensure that the indicated voltages relate to the fundamental component only, and the harmonic currents induced from the generator present only negligible voltages across the tuned circuit.

Input Hot Resistance. The input hot resistance is defined as the equivalent parallel resistance due to damping at the grid of the tube when working under normal operating conditions. Similarly the cold resistance is a measure of the damping when the filament of the tube is unlit and the cathode emission zero. It is well known that the hot resistance alters with the space current flowing as shown for example by A. L. Sowers and N. E. Samuel (65). When the control grid is biassed sufficiently negative so that no current flows the input loss is that of the "cut off" resistance, a value which is usually slightly higher than the cold resistance, due mainly to the improvement in electrical conductivity of the cathode coating

material at its working temperature. It is convenient to separate the hot resistance into two parallel components, the first being the cut-off resistance due to dielectric and cathode losses, etc., and the second, termed the active resistance which represents the extra damping loss when current flows. M. J. O. Strutt (72) has given some figures for the input damping of typical receiving tubes and a curve for the AF3 pentode has been given in Fig. 10. Some results for other tubes are given in Table I.

TABLE I

Tube Type	Wavelength m.	Resistance in kΩ			
		Cold	Cut-off	Hot	Active
AF7	26·0	1,000	2,300	110	120
,,	21·2	690	1,400	70	74
,,	16·2	510	860	39	41
,,	12·4	350	540	23	24
,,	8·6	150	170	11	12
,,	5·6	110	120	4·5	4·6
VP4B	19·6	800	1,300	90	96
,,	9·8	380	250	21	23
SP4B	19·6	600	900	50	53
,,	9·8	280	310	11	11

As previously mentioned, many new types of tubes have been developed for use at very high frequencies and Fig. 25 shows some active input damping resistance figures given by F. Prakke, J. L. H. Jonker and M. J. O. Strutt (51) for a Mullard acorn pentode and for an all-glass (EF50 type) pentode. These resistances are much higher than for the tubes given in Table I and those for the acorn pentode are particularly high. This advantage of low damping is however minimised by the small mutual conductance and, of course, these small tubes have the disadvantage that they are difficult to manufacture and are more fragile than the larger types, particularly when fitted with many electrodes. From these results it will be seen that the damping increases rapidly with frequency, and that the " square law " damping predicted by theory is borne out

by the slope of these lines. These curves confirm what has been previously mentioned that at the higher frequencies particularly the input resistance is much less than the values of dynamic resistance of usual tuned circuits.

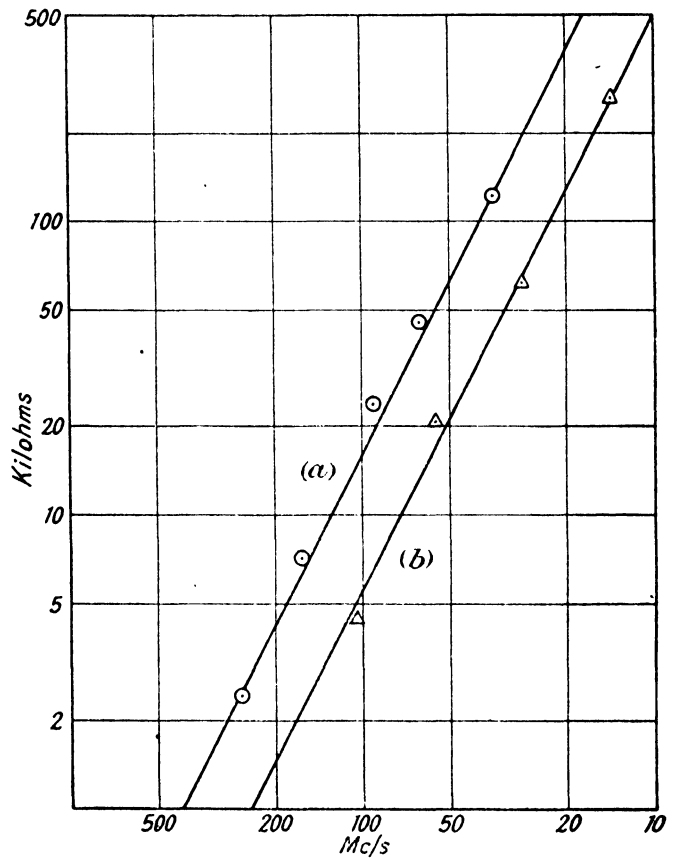

FIG. 25. Input resistance of Mullard (*a*) acorn pentode, and (*b*) pentode of all-glass construction.

Cathode Capacitance. Normally, the cathode pin of a thermionic tube is returned to earth by means of a bias resistor bypassed by a suitable capacitance. If this capacitance be removed then it is well known that feed back occurs between the anode and grid circuits. At low frequencies this feed back

is negative and reduces the amplification, but at very high frequencies an unbypassed cathode resistor reduces and stabilises the input conductance as demonstrated by F. E. Spaulding (69) and R. L. Freeman (17). The latter gives a detailed analysis of typical high frequency amplifying circuits and some results on typical receiving type pentodes. Other experimental results have been described by M. J. O. Strutt and A. van der Ziel (73, 78) who give curves showing the change in input conductance for different values of cathode resistor.

It is also shown in these papers that this cathode arrangement reduces variations of input capacitance due to space charge caused by shifting the grid bias as is normally done in automatic gain control systems. Due to the small total circuit capacitances obtaining at high frequencies this correction is a very desirable feature. Thus if C_f is the change in grid capacitance caused by feedback, C_S the increase caused by space charge, and R_K the value of the cathode resistor, then the input capacitance obtained by neglecting the effects due to anode impedance is given by

$$C_0 = \frac{C_{g_1K} + C_S + C_f}{1 + R_K S_K} \quad . \quad . \quad . \quad . \quad (40)$$

It is shown that for most tubes the optimum value of R_K is very near that for correct bias when the grid tuning condenser is connected to earth directly as in the conventional manner. The presence of the unbypassed cathode resistor reduces the effective mutual conductance of the tube by a factor $1/(1 + S_K R_K)$ which may be 0·7 or 0·8 in a typical case.

A reduction in damping may also be obtained by placing extra inductance in the cathode to earth lead, so that it produces a current to the grid out of phase with the input voltage signal, as suggested by R. L. Freeman (16).

Screen Inductance. It was stated earlier that the input resistance is modified by screen and anode lead inductances. From Fig. 19, for a pentode, the input resistance is modified by the voltage across L_{g_2}, due to the pulsating component of screen current and the grid to screen capacitance $C_{g_1g_2}$. Thus, taking into account the appropriate phases,

$$G = \omega^2(S_K C_{g_1K} L_K - S_{g_2} C_{g_1g_2} L_{g_2}) \quad . \quad . \quad . \quad . \quad (41)$$

where S_{g_2} is the screen current slope which in practice is about one-fifth the total or cathode current slope.

In the case of triodes the grid to anode capacitance C_{g_1a} causes a reaction due to the high frequency voltage on the anode lead inductance L_a and thus equation (24) must be modified to

$$G = \omega^2 S_K (L_K C_{g_1K} - L_a C_{g_1a}) \quad . \quad . \quad . \quad . \quad . \quad (42)$$

B. J. Thompson (79) has emphasised the possibility of reducing the grid damping of triodes by balancing the effects of the lead inductances of cathode and anode, as suggested by relation (42). Comparing formulæ (41) and (42), it is obvious that in the case of a triode the condition of balance $C_{g_1K} L_K - C_{g_1a} L_a = 0$ may be easily fulfilled, as the inductances and capacitances in question are nearly equal. In the case of screen grid tubes, however, the slope S_{g_2} is small and necessitates a large increase in L_{g_2}, and from relation (41) it is evident that an impracticably large value would be necessary. This modification is more suitable for frequency changers since the inductance in the screen lead reduces the screening effect of this electrode.

Mutual Conductance and Frequency. It has been previously stated that the input damping of a thermionic tube changes with the space current flowing, or more accurately, with the mutual conductance. F. Preisach and J. Zakariás (53) have measured these changes in the case of a number of tubes. Their method of measuremnt was similar to that of M. J. O. Strutt, described above, but in plotting their results they gave the total circuit conductance (inverse of the dynamic resistance). In their case the mutual conductance of the tubes were measured on an audio-frequency bridge. Typical of their results is Fig. 26, which shows the change in input conductance (increase of grid resistance) for five different high slope screen grid tubes. Curves 1–4 relate to tubes of conventional glass construction while curve 5 relates to a metal tube, the 1851, which is superior both in respect of electron loading and lead effects. The conductance of the tuned circuit alone was 65 micromhos (15,400Ω) and it will be observed that the relation between input and mutual conductances is sensibly linear.

Multiple Cathode Leads. It has been shown by F. Preisach

and I. Zakariás (*loc. cit.*) that separate cathode leads for the returns of the electrodes result in a reduction in input damping, a result to be expected from Fig. 19, since, in the ideal case no voltage drop would occur across the inductance of the cathode return lead. From their circuit, Fig. 22, if the anode and

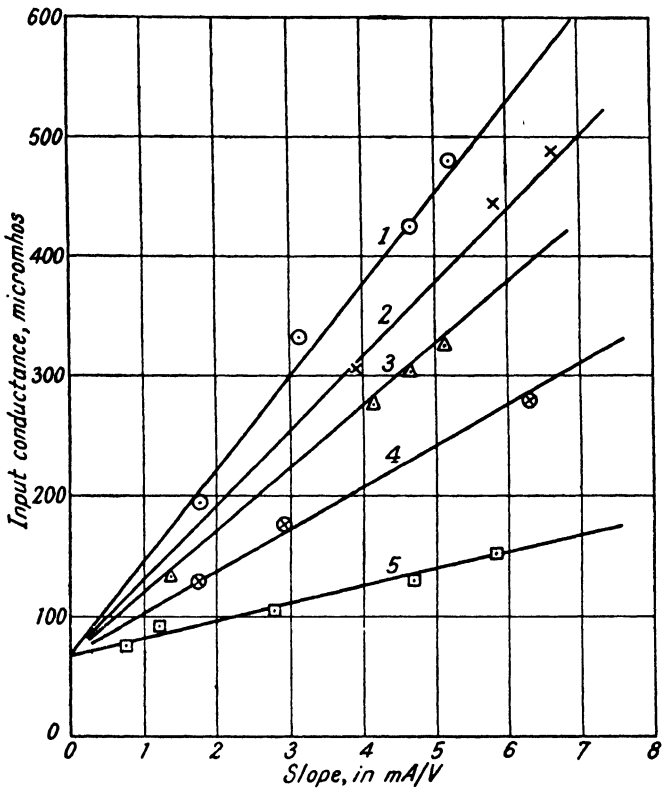

FIG. 26. Input conductance plotted against slope, for different high slope tubes, at a frequency of 37 Mc/s.

screen returns are made to different cathode leads as shown, then the input conductance due to this cause is given by

$$G = -\omega^2 S_{g_1} C_{g_1 g_2} (L_{g_2} + L_K) \quad . \quad . \quad . \quad . \quad (43)$$

and this negative value can be utilised for reducing the damping due to dielectric loss, etc., and electron inertia. If the anode

and screen returns are brought to a common cathode lead then the conductance is given by

$$G = -\omega^2 S_K C_{g_1 g_2} (L_{g_2} + L_K) \quad . \quad . \quad . \quad . \quad (44)$$

In practice, two, three or more cathode leads can be employed and these can be connected either in parallel to reduce

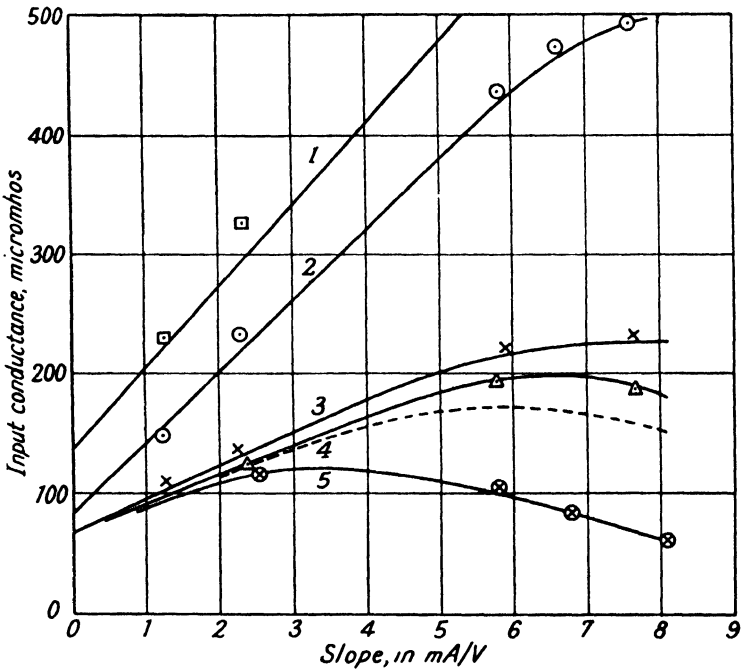

FIG. 27. Input conductance of tube with three cathode leads, the electrodes being returned to different ones in turn. The frequency was 37 Mc/s. Calculated electron loading is shown dotted.

the resulting inductance or separately to earth to generate a negative input conductance. Care should be taken in designing the lay-out of the cathode leads to avoid mutual inductance effects. In the anode circuit a capacitance C_{g_2} is present between the tuned circuit and earth as shown in Fig. 22, although the shunting effect of this would normally be negligible. F. Preisach and I. Zakariás (53) also describe a number of experiments on specially constructed multiple cathode lead tubes. Alternative connections were used for the cathode leads and electrode return connections and the changes in input damping

determined. The input conductance of a special multiple cathode lead tube is shown in Fig. 27 as a function of slope at a frequency of 37 Mc/s. These curves show the reduction of grid conductance when more than one lead is employed. In this particular tube there were two cathode leads brought out to the base, and another to the top cap of the tube. Curve 1 relates to an arrangement where only one cathode lead of the base was used in the usual manner, and Curve 2 when one base lead was connected to the control grid and screen grid, another base lead to the anode, the top lead not being used. Curve 3 is with one base lead and one top lead to the grids, the other base lead to the anode and the large reduction in damping observed would seem to indicate some mutual interaction between the base leads. Curve 4 is with the top lead to the control grid, and the two base leads to the anode and screen respectively, while Curve 5 is with the top lead and one base lead to the control grid, the second base lead to the screen grid and anode. It will be clearly seen that this latter curve provides over-correction as would be expected from the above formula, and for comparison the electron damping calculated according to the theory of D. O. North (49) has been included. Data for this tube is given in this paper as $C_{g_1K} = 9{\cdot}1\ \mu\mu F$, $C_{g_1g_2} = 3{\cdot}3\ \mu\mu F$, $S_{g_2}/S_K = 0{\cdot}26$, grid cathode distance 0·3 mm. and grid screen 1·3 mm. The base lead inductance was ·083 μH and that of the top lead was ·023μH.

Alternatively the leads may be connected in parallel and

TABLE II

Number of Cathode Leads	Leads employed	Input conductance, micromhos.		
		S_K = 1mA/V	S_K = 4mA/V	S_K = 7mA/V
Three	One base	20	110	210
,,	Two base	6	30	100
,,	Two base, one top	2	12	10
Four	One base	20	100	190
,,	Two base	0	10	40
,,	Three base	5	30	60
,,	One base, one top	− 2	10	45
,,	Three base, one top	− 2	10	45

used as one in the normal manner. Table II shows the advantage of doing this for two tubes described by F. Preisach and I. Zakariás (*loc. cit.*) fitted with three and four leads respectively, the electrodes in these tubes being smaller in dimensions than for the tube above. It was concluded that this type of construction is beneficial in the case of high slope tubes in

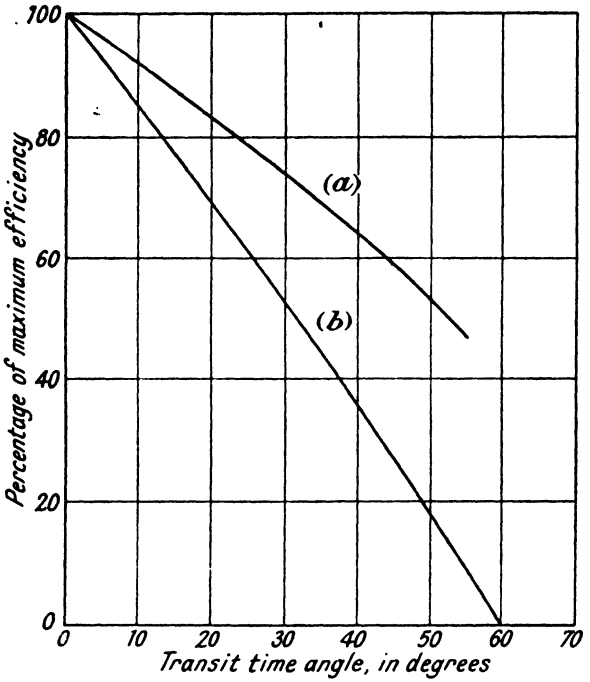

FIG. 28. The efficiency of a thermionic tube as (*a*) an amplifier, (*b*) an oscillator, when the transit time is a large fraction of the high frequency period.

which electrode lead effects are the predominant factor of input conductance.

Input Capacitance. The input capacitance of thermionic tubes has not been found to change appreciably with frequency, but it does alter quite noticeably with total space current as has been mentioned previously. Table III shows these changes as measured by F. Preisach and I. Zakariás (*loc. cit.*) at a frequency of 37 Mc/s as a function of cathode current slope.

TABLE III

Tube No.	Change in input capacitance, $\mu\mu$F		
	S_k = 1mA/V	S_k = 4mA/V	S_k = 7mA/V
1	1·0	3·3	—
2	0·4	1·4	2·1
3	0·3	1·1	1·9
4	0·5	1·7	2·7

Anode Resistance. It has been shown by M. J. O. Strutt (72) that the anode or output resistance of thermionic tubes also decreases with frequency and some results have already been given in Fig. 10 for the AF3 pentode. Table IV gives some anode resistance figures for other Mullard tubes.

TABLE IV

Tube type	Wavelength in metres	Anode resistance in kΩ			
		Cold	Cut-off	Hot	Active
AF7	20·4	490	450	250	580
,,	12·1	240	220	110	240
,,	8·0	81	78	45	110
,,	5·05	46	41	24	58
VP4B	10·3	114	—	72	—
,,	4·95	40	—	25	—
SP4B	10·3	123	—	72	—
,,	4·95	40	—	23	—

This damping should, of course, be considered as an extra loss in the anode tuned circuit, but it does not affect the generator impedance of the tube. As with the input circuit, no changes of output capacitance with frequency have been observed.

So far, only measurements on receiving type tubes have been described although, of course, many of the results apply to transmitting tubes. In general, these latter are employed in either amplifier or oscillator circuits and their performance, as mentioned earlier, is affected by lead effects and transit time.

A. V. Haeff (23) has given results, shown in Fig. 28, for the efficiency of amplifiers and oscillators at frequencies high enough to cause the transit time to be a large fraction of the high frequency period. As may be expected, the efficiency of an amplifier does not fall off quite so rapidly as an oscillator since to some extent the phase differences between the anode and grid potentials caused by transit time, do not have such a large effect.

General Conclusions. The above results have served to point out the changes in the properties of thermionic tubes at very high frequencies and have confirmed the statements made in the first section of the chapter. In receiving tubes a high transconductance is necessary in order to obtain reasonable voltage gains with the comparatively low dynamic resistances of circuits obtaining at these frequencies, but this necessitates a large cathode area and close spacing of the control grid resulting in a high input capacitance. This, in conjunction with the input lead inductance, leads to reduced values of input resistance. In a normal pentode the pulsating component of screen current causes extra input damping as shown earlier, so that the slope cannot be improved much by this method. There are also difficulties due to the equivalent noise resistance of the tube, especially when used as a frequency changer, and thus some signal frequency amplification is desirable.

In transmitting tubes the conflicting requirements of high operating voltages and small electrodes must lead to a compromise, and thus the power output at very high frequencies cannot be greatly increased with tubes of normal type. Nevertheless, triodes and pentodes are still useful in work at very high frequencies, due to their good modulation properties, frequency stability, and the fact that they can be driven as power amplifiers by suitable frequency multiplying systems from stable quartz crystal master oscillators.

Fortunately these changes in tube parameters, due to electron inertia, particularly make possible the working under entirely different conditions certain kinds of tubes the performance of which is inherently better at very high frequencies. These tubes which, while mainly of use in transmitters, can be used as local oscillators in receivers, include retarding field generators, the magnetron, and the recently developed Klystron

and allied tubes. In view of the unique properties of these tubes a considerable portion of this book is devoted to an examination of their properties and their mechanism of behaviour. The magnetron has been examined in greater detail since, apart from its present pre-eminent position as a self-contained ultra high-frequency generator of large power output, its comparatively simple electrode structure enables the comparison of theory and experiment to be made more readily and thus our knowledge of the mechanism of behaviour of thermionic tubes at very high frequencies can be extended.

BIBLIOGRAPHY

1. BARROW, W. L. "Measurement of Radio Frequency Impedance with Network Simulating Lines." *Proc. Inst. Rad. Eng.*, 1935, **23**, 807.
2. BENHAM, W. E. "Theory of the Internal Action of Thermionic Systems at Moderately High Frequencies." *Phil. Mag.*, 1928, **5**, 641, and 1931, **11**, 457.
3. BENHAM, W. E. "The Variation of Resistance and Capacitance of Thermionic Valves with Frequency." *Wireless Eng.*, 1931, **8**, 488.
4. BENHAM, W. E. "A Contribution to Tube and Amplifier Theory." *Proc. Inst. Rad. Eng.*, 1938, **26**, 1093.
5. BENNER, S. "Alteration of the Dielectric Constant of a Vacuum by Electrons." *Ann. Phys.*, 1929, **3**, 111.
6. BLACK, D. H. "Ultra Short Wave Oscillators." *Elec. Comm.*, 1939, **17**, 325.
7. BURNSIDE, D. G. and SALZBERG, B. "Recent Developments in Miniature Tubes." *Proc. Inst. Rad. Eng.*, 1935, **23**, 1142.
8. CANNAS, A. "Acorn Valves for Ultra Short Waves." *Alta Freq.*, 1935, **4**, 115.
9. CARRARA, N. "On the Detection of Micro-Waves." *Alta Freq.*, 1934, **3**, 661.
10. CORKE, E. C., and PAWSEY, J. L. *J. Inst. Elec. Eng.*, 1939, **84**, 448.
11. FAY, C. E. and SAMUEL, A. L. "Vacuum Tubes for Generating Frequencies above One Hundred Megacycles." *Proc. Inst. Rad. Eng.*, 1935, **23**, 199.
12. FERRIS, W. R. "Input Resistance of Vacuum Tubes as Ultra High Frequency Amplifiers." *Proc. Inst. Rad. Eng.*, 1936, **24**, 82.
13. FIELD, R. F. and SINCLAIR, D. B. "Determination of the Residual Inductance and Resistance of a Variable Air Condenser." *Proc. Inst. Rad. Eng.*, 1936, **24**, 255.
14. FORTESCUE, C. L. "Voltage Measurement at Very High Frequencies." *J. Inst. Elec. Eng.*, 1936, **79**, 179.
15. FRANKS, C. J. "Measured Input Losses of Vacuum Tubes." *Electronics*, 1935, July, p. 222.
16. FREEMAN, R. L. "Input Conductance Neutralisation." *Electronics*, 1939, Oct., p. 22.

17. FREEMAN, R. L. "Use of Feedback to Compensate for Input Capacitance Variations." *Proc. Inst. Rad. Eng.*, 1938, **26**, 1360.
18. FRITZ, K. "Push-pull Arrangement for the Amplification of Ultra Short Waves." *Hochf. tech. u. Elek. akus.*, 1941, **57**, 94.
19. GAVIN, M. R. "Electron Pump Effect at High Frequencies." *Wireless Engineer*, 1938, **15**, 81.
20. GAVIN, M. R. "Valves for Use at Ultra Short Wavelengths." *Wireless Engineer*, 1939, **16**, 287.
21. GEIGER, M. "Graphical Determination of Electron Transit Time Angles in Alternating Fields." *Hochf. Tech. u. Elek. akus.*, 1941, **57**, 157.
22. GÜTTINGER, P. "Behaviour of Space Charges in High Frequency Electric Fields." *Bull. Assoc. suisse Elec.*, 1940, **31**, 29.
23. HAEFF, A. V. "Effect of Electron Transit Time on the Efficiency of a Power Amplifier." *R. C. A. Rev.*, 1939, **4**, 114.
24. HAEFF, A. V. and SALZBERG, B. "Effect of Space Charge in the Grid Anode Region of Vacuum Tubes." *R. C. A. Rev.*, 1938, **2**, 336.
25. HARVARD, R. "Ceramics in Valve Construction." *Electronic Engineering*, 1941, **14**, 343 and 376.
26. HARVEY, A. F. "The Impedance of the Magnetron in Different Regions of the Frequency Spectrum." *J. Inst. Elec. Eng.*, 1940, **86**, 297.
27. HOLLMANN, H. E. "Investigation of Electron Motion in Alternating Fields with Ballistic Models." *Proc. Inst. Rad. Eng.*, 1941, **29**, 70.
28. JEN, C. K. "Induced Current and Energy Balance in Electronics." *Proc. Inst. Rad. Eng.*, 1941, **29**, 345.
29. JEN, C. K. "The Energy Equation in Electronics at Ultra High Frequencies." *Proc. Inst. Rad. Eng.*, 1941, **29**, 464.
30. JOHNSON, T. H. and STREET, J. C. "The Use of a Thermionic Tetrode for Voltage Control." *J. Franklin Inst.*, 1932, **412**, 155.
31. KELLY, M. J. and SAMUEL, A. L. "Vacuum Tubes as High Frequency Oscillators." *Elec. Eng.*, 1934, **53**, 1517.
32. KLEEN, W. "Position of Ultra Short Wave Valve Technique." *Zeitschr. f. Tech. Phys.*, 1940, **21**, 357.
33. KING, R. "Electrical Measurements at Ultra High Frequencies." *Proc. Inst. Rad. Enq.*, 1935, **23**, 885.
34. KING, R. "Beam Tubes as Ultra Frequency Generators." *J. Appl. Phys.*, 1939, **10**, 638.
35. KOLSTER, F. A. "Generation and Utilisation of Ultra Short Waves in Radio Communication." *Proc. Inst. Rad. Eng.*, 1934, **22**, 1335.
36. KÜHNHOLD, W. "The Upper Frequency Limit for Valve Generators with Reaction." *Hochf. Tech. u. Elek. akus.*, 1935, **46**, 78.
37. LANGMUIR, I. and BLODGETT, K. *Phys. Rev.*, 1923, **22**, 347.
38. LINDENBLAD, N. E. "Development of Transmitters for Frequencies above 300 megacycles." *Proc. Inst. Rad. Eng.*, 1935, **23**, 1013.
39. LLEWELLYN, F. B. "Vacuum Tube Electronics at Ultra High Frequencies." *Proc. Inst. Rad. Eng.*, 1933, **21**, 1532.

40. LLEWELLYN, F. B. "Phase Angle of Vacuum Tube Transconductance at very High Frequencies." *Proc. Inst. Rad. Eng.*, 1934, **22**, 947.
41. LLEWELLYN, F. B. "Note on Vacuum Tube Electronics at Ultra High Frequencies." *Proc. Inst. Rad. Eng.*, 1935, **23**, 112.
42. LLEWELLYN, F. B. "Operation of Ultra High Frequency Vacuum Tubes." *Bell. Sys. Tech. J.*, 1935, **14**, 632.
43. LLEWELLYN, F. B. "Equivalent Networks of Negative Grid Vacuum Tubes at Ultra High Frequency." *Bell. Sys. Tech. J.*, 1936, **15**, 575.
44. LLEWELLYN, F. B. "Electron Inertia Effects." 1941.
45. MEGAW, E. C. S. "Voltage Measurement at Very High Frequencies." *Wireless Eng.*, 1936, **65**, 135 and 201.
46. MOULLIN, E. B. "Radio Frequency Measurements," 1931.
47. NARASIMHAIYA, R. L. "Maintenance of Electron Emission after the Low Tension Supply is Disconnected." *Proc. Inst. Rad. Eng.*, 1935, **23**, 249.
48. NERGAARD, L. S. "Electrical Measurements at Wavelengths less than 2 Metres." *Proc. Inst. Rad. Eng.*, 1936, **24**, 1207.
49. NORTH, D. O. "Analysis of the Effects of Space Charge on Grid Impedance." *Proc. Inst. Rad. Eng.*, 1936, **24**, 108.
50. PETERSON, L. C. "The Impedance Properties of Electron Streams." *Bell. Sys. Tech. J.*, 1939, **18**, 465.
51. PRAKKE, F., JONKER, J. L. H., and STRUTT, M. J. O. "A New All-glass Valve Construction." *Wireless Engineer*, 1939, **16**, 224.
52. PICKEN, W. J. "Development of Wireless Transmitting Valves." *J. Inst. Elec. Eng.*, 1941, **88**, 2.
53. PREISACH, F. and ZAKARIÁS, I. "Input Conductance," *Wireless Engineer*, 1940, **17**, 147.
54. POSTHUMOUS, K. "Water-cooled Pentodes at Ultra Short Wavelengths." *Philips Trans. News.*, 1937, **4**, 1.
55. PRITSCH, J. "Generation of Ultra Short Waves." *Hochf. Tech. u. Elek. akus.*, 1941, **57**, 139.
56. RAO, M. K. "High-frequency Measurements of the Amplification Factor and Internal Resistance of a Thermionic Valve." *Indian J. of Phys.*, 1940, **14**, 247.
57. ROTHE, H. "Input and Output Resistance of Thermionic Valves at Very High Frequencies." *Telefunken Röhre*, 1936, July, p. 101.
58. ROTHE, H. "The Operation of Electron Tubes at High Frequencies." *Proc. Inst. Rad. Eng.*, 1940, **28**, 324.
59. RUNGE, I. "Transit Time Effects in Electronic Valves." *Z. f. Tech. Phys.*, 1937, **18**, 438.
60. SABAROFF, S. "An Ultra High Frequency Measuring Assembly." *Proc. Inst. Rad. Eng.*, 1939.
61. SAMUEL, A. L. "Extending the Frequency Range of the Negative Grid Tube." *J. Appl. Phys.*, 1937, **8**, 677.
62. SAMUEL, A. L. "A Negative Grid Triode Oscillator and Amplifier for Ultra High Frequencies." *Proc. Inst. Rad. Eng.*, 1937, **25**, 1243.
63. SAMUEL, A. L. and SOWERS, N. E. "A Power Pentode for Ultra High Frequencies." *Proc. Inst. Rad. Eng.*, 1936, **24**, 1464.

64. SAMUEL, A. L., FAY, C. E. and SHOCKLEY, W. "The Theory of Space Charge between Parallel Plane Electrodes." *Bell. Sys. Tech. J.*, 1938, **17**, 49.
65. SAMUEL, A. L. and SOWERS, N. E. "An Ultra-high Frequency Power Amplifier." *Bell. Sys. Tech. J.*, 1937, **16**, 11.
66. SIL, B. C. "The Variation of Inter Electrode Capacitance of a Triode at High Frequencies." *Phil. Mag.*, 1933, **16**, 1114.
67. SINCLAIR, D. B. "Series and Parallel Resonance Measurements at Radio Frequencies." *Proc. Inst. Rad. Eng.*, 1938, **26**, 1466.
68. SLOANE, R. W. and JAMES, E. G. "Transit Time Effects in Diodes in Pictorial Form." *J. Inst. Elec. Eng.*, 1936, **79**, 291.
69. SPAULDING, F. E. "Design of Superheterodyne Intermediate Frequency Circuits." *R. C. A. Rev.*, 1939, **4**, 485.
70. STRUTT, M. J. O. "The Characteristic Admittances of Mixing Valves for Frequencies up to 70 megacycles." *E. N. T.*, 1938, **15**, 10.
71. STRUTT, M. J. O. "Electron Transit Time Effects in Multigrid Valves." *Wireless Eng.*, 1938, **15**, 315.
72. STRUTT, M. J. O. "Characteristic Constants of High Frequency Pentodes." *Wireless Eng.*, 1937, **14**, 478.
73. STRUTT, M. J. O. British Patent No. 415,009.
74. STRUTT, M. J. O., and KNOL, K. S. "Measurements of Currents and Voltages Down to 20 cm." *Proc. Inst. Rad. Eng.*, 1939, **27**, 783.
75. STRUTT, M. J. O. and VAN DER ZIEL, A. "Causes for the Increase of Admittance of Modern High Frequency Amplifier Tubes on Short Waves." *Proc. Inst. Rad. Eng.*, 1938, **26**, 1011.
76. STRUTT, M. J. O. and ZIEL, A. VAN DER. "Some Dynamic Measurements of Electron Motion in Multi-grid Tubes." *Proc. Inst. Rad. Eng.*, 1939, **27**, 218.
77. STRUTT, M. J. O. and ZIEL, A. VAN DER. "An Amplifier Valve for Decimetre Waves." *Alta Freq.*, 1941, **10**, 187.
78. STRUTT, M. J. O. and ZIEL, A. VAN DER. "Simple Circuit Arrangement for Improving the Performance of High Frequency Amplifier Tubes." *E. N. T.*, 1936, **13**, 260.
79. THOMPSON, B. J. *R. C. A. Rev.*, 1938, **3**, 151.
80. THOMPSON, B. J. and ROSE, G. M. "Vacuum Tubes of Small Dimensions for Use at Extremely High Frequencies." *Proc. Inst. Rad. Eng.*, 1933, **21**, 1707.
81. WAGENER, W. G. "Development Problems and Operating Characteristics of Two New Ultra High Frequency Triodes." *Proc. Inst. Rad. Eng.*, 1938, **26**, 401.
82. WANG, C. C. "Large Signal High Frequency Electronics of Thermionic Vacuum Tubes." *Proc. Inst. Rad. Eng.*, 1941, **29**, 200.
83. WING, A. K. "A Push-Pull Ultra High Frequency Beam Tetrode." *R. C. A. Rev.*, 1939, **4**, 62.
84. WILLSHAW, W. E. "Some Impedance Characteristics of Tapped Resonant Lines." *Phil. Mag.*, 1940, **29**, 572.
85. ——— "An Ultra-high Frequency Transmitting Triode—the Hytron 75." *Q. S. T.*, 1940, **24**, 27.
86. ——— "Ultra-high-frequency Push-pull Transmitting Pentode." *Electronics and Television*," 1940, **13**, 272 and 381.

CHAPTER III

RETARDING FIELD GENERATORS

(*a*) GENERAL PROPERTIES

Barkhausen-Kurz Oscillations. The types of high-frequency generators described in the preceding chapter are known as reaction oscillators, since a necessary condition is that feed back shall be present between the anode and grid circuits. It is now proposed to deal with electronic generators in which the oscillations are produced by virtue of electron inertia in thermionic tubes, and it will be evident that such generators are inherently better at very high frequencies. The first known of these thermionic tubes which utilise electron inertia to advantage is the retarding field or positive grid generator, its discovery being made by H. Barkhausen and K. Kurz (2) during some tests on transmitting tubes when the grid was at a high positive potential and the anode at a slight negative potential. It was found that very high-frequency oscillations could be maintained in a circuit connected between grid and anode, grid and filament, or anode and filament, and the explanation given was that electrons are accelerated from the filament to the positive grid through which some of them pass. These are retarded in the grid-anode space and turn back to the grid. Those which pass through the grid again reach the neighbourhood of the filament and the process is repeated, and it is this to-and-fro motion of the electrons which results in the oscillations. For a tube with planar electrodes, neglecting space charge forces and initial electron velocities, and assuming the fluctuating electrode potentials are negligibly small, the wavelength corresponding to the electron vibration frequency is given by

$$\lambda = \frac{2000\, d_a}{\sqrt{E_g}} = \frac{4000\, d_g}{\sqrt{E_g}}. \quad . \quad . \quad . \quad . \quad . \quad (45)$$

where d_a and d_g are respectively the anode-cathode and grid-cathode distances and when the anode is at cathode potential. For any anode potential E_a, grid potential E_g and with the grid not necessarily midway between anode and cathode, the wavelength becomes

$$\lambda = \frac{2000}{\sqrt{E_g}} \cdot \frac{d_a E_g - d_g E_a}{E_g - E_a} \quad . \quad . \quad . \quad . \quad (45a)$$

It is considered that these B-K (Barkhausen-Kurz) oscillations are always present in the tube when operated under the above conditions and that an external circuit is only necessary when external power is required. Thus when the external impedance is zero at the frequency concerned the electrodes have no fluctuating component of potential.

For tubes with cylindrical electrodes, again neglecting the effects of space charge, the wavelength has been given by A. Scheibe (50) as follows :—

$$\lambda = \frac{4cr_g}{\sqrt{2\frac{e}{m}E_g}}\left[f\left\{\sqrt{\log_e \frac{r_g}{r_c}}\right\} + g\left\{\sqrt{\frac{E_g}{E - E_a} \cdot \log_e \frac{r_a}{r_g}}\right\}\right] =$$

$$\frac{4cr_g}{\sqrt{2\frac{e}{m}E_g}} K \quad . \quad (46)$$

where K is a constant depending only on the electrode geometry when the anode potential E_a is zero and

$$f(x) = x \cdot e^{-x^2} \int_0^x e^{u^2} du \quad . \quad . \quad . \quad . \quad . \quad . \quad (47)$$

$$g(x) = x \cdot e^{-x^2} \int_0^x e^{-u^2} du \quad . \quad . \quad . \quad . \quad . \quad . \quad (48)$$

where $x = \sqrt{\log_e \frac{r_g}{r_c}} = 1{\cdot}52 \sqrt{\log_{10} \frac{r_g}{r_c}}$ in $f(x)$

and $x = \sqrt{\frac{E_g}{E_g - E_a} \cdot \log_e \frac{r_a}{r_g}} = 1{\cdot}52 \sqrt{\frac{E_g}{E_g - E_a} \cdot \log_{10} \frac{r_a}{r_g}}$ in $g(x)$

These values have been given as follows by W. H. Moore (40), who also describes experiments on these oscillations without tuned circuits.

TABLE V

x	$f(x)$	$g(x)$	x	$f(x)$	$g(x)$
0·0	0	0	1·8	0·62419	40·360
0·1	0·00993	0·010	2·0	0·60268	98·010
0·5	0·21228	0·289	3·0	0·534	—
0·8	0·42568	0·998	4·0	0·516	—
1·0	0·53808	2·030	5·0	0·510	—
1·2	0·60872	4·088	7·0	0·504	—
1·5	0·64237	12·190	∞	0·500	—

The conditions obtaining when the grid potential has a fluctuating component has been analysed for the plane electrode triode by H. E. Hollmann (23), who assumes that the current flowing is sufficiently small so that space charge effects can be neglected and that the anode potential is that of the cathode and contains no alternating component. Thus, if the grid is midway between anode and cathode of distance $2d$ apart and E_0 is its fluctuating potential, then the electric force E acting on an electron is

$$E = \frac{E_g + E_0 \sin(\omega t + \phi)}{d} \quad . \quad . \quad . \quad . \quad (49)$$

and thus, if the electron is distance x from the grid,

$$-e \cdot \frac{E_g + E_0 \sin(\omega t + \phi)}{d} = m \frac{d^2x}{dt^2} \quad . \quad . \quad (50)$$

If at $t = 0$ the velocity is v_0 at $x = 0$, double integration of equation (50) gives

$$x = \frac{-e}{md} \cdot E_g \cdot \frac{t^2}{2} + v_0 t + \frac{e}{md} E_0 \left(\frac{\sin \omega t + \phi}{\omega^2} - \frac{t \cos \phi}{\omega} - \frac{\sin \phi}{\omega^2} \right) . \quad (51)$$

and if the frequency of the alternating grid potential is that of the electron

$$\omega t = \frac{\omega T}{2} = \pi$$

by putting $x = 0$ in (51), where T is the period of oscillation.

Now E_0 has a maximum negative value at $t = 0$, etc., as the electrons pass through the grid making $\phi = -\frac{\pi}{2}$.

$$\therefore \frac{T}{2} = \frac{v_0}{\frac{e}{md}\left(\frac{E_g}{2} - \frac{2E_0}{\pi^2}\right)}$$

where $v_0 = \sqrt{\frac{e}{m}} . 2(E_g - E_0)$ and since $\lambda = cT$

$$\lambda = \frac{4000 \sqrt{E_g - E_0} . d}{E_g - \frac{4E_0}{\pi^2}} \quad . \quad . \quad . \quad . \quad (52)$$

which agrees with the simple Barkhausen-Kurz formulæ given previously when $E_0 = 0$. If, say, $E_g = 500$ volts and d is 5 mm., then the B—K wavelength of 89·5 cm. becomes 86·9 when E_0 is 100 volts, and 82·5 when it is 200 volts. These values of E_0 are much greater than obtain in normal B—K operation, and so the wavelength change is negligible.

Gill-Morrell Oscillations. It has been shown by E. W. B. Gill and J. H. Morrell (19) that a different type of oscillation can occur which requires the presence of a suitable external circuit and also sufficient emission current to cause space charge limitation. In this case the voltage amplitude E_0 is large and the power outputs available are correspondingly increased. In these G—M (Gill-Morrell) oscillations the amplitude and frequency adjust themselves to suit the tuned circuit. The calculation of the wavelength of oscillation is complex with cylindrical electrodes due to the presence of considerable space charge, but a graphical method of determining the transit time has been given by J. S. McPetrie (34). It has been suggested by H. Alfven (1) that this electron motion gives the tube negative resistance properties, which increase with the emission current, and that when this reaches a value depending on the external load resistance, continuous oscillations occur. E. W. B. Gill and J. H. Morrell (19) point out that if there is an alternating component of p.d. between grid and anode, positive work is done on the moving electrons in this space during the half cycle in which they are accelerated

towards the anode, and negative work during the retarding half cycle. In the first case the electrons go to the anode, and in the second case to the grid, and the amount of negative work done determines the amplitude of oscillation with a given load resistance. E. W. B. Gill (15) suggests another mechanism of maintenance of these electronic oscillations which is possible when the anode diameter is considerably greater than the grid diameter, so that space charge limitation exists in the grid anode space, but not in the grid cathode space. In this case successive "rarefactions" and "compressions" of space charge traverse the grid anode space, so that oscillations can be maintained in a circuit whose oscillation period is twice the electron time of transit from grid to anode. Theory and experiment agree in showing that oscillations can be maintained over a band of wavelengths whose long-wave limit is given by equation (45), and that in this band the more general law

$$\frac{\lambda^2 I_g}{\sqrt{E_g}} = \text{constant} \quad . \quad . \quad . \quad . \quad . \quad (53)$$

holds, where I_g is the grid current.

The dependence of oscillation amplitude on emission current is usually quite critical, and the optimum filament emission is that representing transition from space charge to emission saturation. The optimum grid current usually follows a $E_g^{3/2}/d_g$ law, and it is found that the oscillation frequency depends to some extent on the degree of space charge.

Mechanism of Oscillation. Attempts have been made to correlate the measured wavelengths of oscillation with the various inter-electrode transit times by R. A. Chipman (6, 7) and R. Cockburn (10). The latter has shown that in general the retarding-field triode (positive grid generator) can maintain both G-M oscillations in which the wavelengths are determined completely by the external circuit and B-K oscillations in which the wavelengths are completely independent of the external circuit, provided the latter does not approach resonance with them. The B-K oscillations are shown to be of two distinct types: one due to the periodic to-and-fro motion of the electrons about the grid of the tube, and the other to a

resonant circuit formed by the grid-anode capacitance in parallel with the equivalent inductance of the electron cloud between these electrodes. The type actually obtained depends mainly on the degree of saturation of the grid-cathode space. A. Rostagni (48) infers, from observations on the G-M oscillations, the existence within the tube of a resonant circuit formed by the electron cloud between the grid and anode. It is shown that a system of electrons in statistical equilibrium between a pair of electrodes will, owing to its inertia, behave like an inductance when an alternating potential is applied to the electrodes. For a uniform distribution of electrons between plane parallel electrodes, the natural pulsatance ω of this resonant circuit is given by

$$\omega = \sqrt{\frac{4\pi e N^2}{m}}$$

where N is the number of electrons per cm.^{3} Although this relation agrees with experimental results, the theory has been attacked by many workers.

It is found that the effect of a constant magnetic field, applied in the direction of the electrode axis, on these electronic oscillations results in a decrease in oscillation wavelength, an increase in output, and maintenance of oscillation with positive anode voltages. A similar improvement in performance with normal reaction oscillators has been observed with the application of an organising magnetic field.

The Diode. These types of electronic oscillation are usually found only when there is an open mesh electrode, about which to-and-fro motion of the electrons can take place, and they are not found in the ordinary simple diode. When, however, the cathode is placed externally with the anode inside and concentric with it, then electron oscillations are found, as described by J. S. McPetrie (36), who suggests that this is due to the ease with which the electrons leaving the cathode can miss the small filamentary anode and therefore execute to and fro motion about it. It has been shown by W. E. Benham (4) and others that the conductance and capacitance of a diode are modified at very high frequencies and at certain particular values the conductance may be negative, although, as

mentioned above, the resulting oscillations appear to be difficult to create or detect. From the laws of motion of charged particles in an electric field the conductance and susceptance of the condenser-resistance circuit representing the diode can be calculated, and if ω is the pulsatance and T the transit time, then negative maxima of conductance occur at $\omega T = \frac{5}{2}\pi, \frac{9}{2}\pi$, etc. For the parallel plane diode, in a practicable case, the circuit would have to be tuned to a wavelength of only 7 cm. to detect these oscillations.

Although oscillations have not been produced in normal gas-free cylindrical diodes, some success has been obtained with perforated anodes by E. W. B. Gill and J. H. Morrell (19), and H. E. Hollmann (23). The case of the diode with applied magnetic field, known generally as the magnetron, will be dealt with in later chapters.

Practical Details. Summaries of the development of positive grid triodes as high frequency generators have been given by E. C. S. Megaw (39) and H. E. Hollman (23). The available power output of these oscillations increases rapidly with frequency, since the required positive grid potential increases and also the optimum value of space current. A limit is, however, soon reached by the allowable dissipation of the control grid, more especially as this intermediate electrode is difficult to cool satisfactorily. For triodes of normal dimensions the wavelengths of these electronic oscillations are generally less than 1 metre, while the power output and efficiency are both very low, the latter rarely exceeding a few per cent.

F. Hamburger (21) describes a triple grid tube with which B—K and G—M oscillations similar to those of a triode have been produced. Normally, electronic oscillations only occur with cylindrical electrodes, since a necessary condition of operation is the formation of a virtual cathode near the anode, which is made possible by the space charge of the electrons at the turning point near the anode. B. J. Thompson and P. D. Zottu (52) describe a planar tube fitted with a backing plate which provides a virtual cathode. The planar tube has the advantage that the close electrode spacing necessary for very high frequency operation can be obtained without the small

grid area and dissipation required in the cylindrical tube. C. E. Fay and A. L. Samuel (14) describe various kinds of *B—K* oscillations, and one example is fitted with a squirrel cage grid capable of dissipating 150 watts and oscillates between 450 and 600 Mc/s, giving a power output at the optimum frequency of 8 watts with 5% efficiency.

For the satisfactory production of oscillations in a triode, theory and experiment show that the optimum ratio of anode to grid diameter is of the order of 2·5 to 3·0. The filament should consist of a single straight wire with a low terminal voltage, the grid should preferably be a close-wound spiral, and in order to increase its heat dissipation an open-mesh anode construction is desirable. If W' is the maximum permissible dissipation per unit area of the grid, then E. C. S. Megaw (39) shows that from consideration of the B-K law and the optimum grid current the wavelength is given by

$$W' = \frac{4 \times 10^{11} . d_g^3}{\pi \lambda^5} \text{ watts per cm.}^2$$

where d_g is the grid diameter, l_g its length and

$$W' = \frac{\text{grid input power}}{\pi l_g d_g}$$

For satisfactory life W' should not exceed about 5 watts per cm.^{2} for a close molybdenum grid.

As an ultra-short wave transmitter the retarding field generator is usually used with a Lecher wire circuit connected to the grid and anode, and the effective length of this circuit is altered by varying the position of a shorting condenser along the line. The steady grid and anode potentials are applied at nodal points by means of high-frequency chokes. The onset of oscillations is detected by the accompanying increase of anode current which is roughly proportional to the amplitude of oscillation. The tuned circuit can then be coupled to a non-resonant feeder leading to the radiating system. Modulation of the output is usually effected by varying the anode voltage and in general a comparatively small variation results in nearly 100% modulation without serious distortion. The frequency stability of electron oscillators is not good, particularly under modulation conditions, although

they are perhaps no worse than reaction type self-oscillators at the same frequencies.

The problem of reception of waves below 1 metre presents difficulties even more severe than those with transmitters. Electron oscillators have been used for receiving purposes, and this is made possible by the rectifying action of these tubes. In some cases a distinct improvement can be obtained by employing super-regeneration.

Spiral Grid Tubes. Above 600 Mc/s the normal type of *B—K* oscillator is unsatisfactory, since the grid dissipation is excessive and optimum operation cannot be employed. H. G. Clavier (8) describes an alternative construction in which the grid takes the form of an unshorted spiral. This "spiral grid" electronic oscillator generates wavelengths much less than that calculated from the formulæ given above. C. E. Fay and A. L. Samuel (14) describe such tubes, and although the efficiencies are only 0·5–1·0%, outputs of 1·5 watts are possible at 24 cm. In the spiral grid tube the parallel wire external circuit is connected to the grid terminals, joined to either end of the grid, while the grid potential has a high positive value and the anode a comparatively high negative value with respect to the cathode. From the design point of view of these tubes, it is found that the expanded length of the grid wire is about 1·24 times the optimum wavelength. The spiral grid Barkhausen tube has also been described by J. Müller (41) and by W. D. Hershberger (22), who shows that different modes of oscillation, termed normal and dwarf waves, are possible so that $\lambda^2 E_g$ can have quite different values. A special spiral grid tube is described in which the anode is in three parts, the centre cylinder being maintained at a different potential to the outer.

A spiral grid or "Clavier" tube for use at 17·4 cm. has been described by E. H. Ullrich and W. L. McPherson (55). In operation the tube had 275 volts (D.C.) on the grid or oscillating electrode and 95 volts negative on the anode or reflecting electrode measured with respect to the cathode. The length of wire in the grid helix was 19 cm., the number of turns 17, the diameter of the helix 3·5 mm., the length of the glowing part of the filament 20 mm., and the length of

the cylindrical anode 13·5 mm. The filament took 3 amps. at about 4 volts and the grid and anode currents were 7·0 and zero mA (D.C.) respectively. Oscillations occurred for certain electrode voltages only and the tube was then saturated.

The transmission line output circuit can maintain oscillations provided its leakance per unit length is negative. A. G. Clavier (8) explains such a negative leakance by the variation of space charge density produced by the speeding up of electrons caused by any momentary increase of grid potential. The electron which leaves the filament an instant after this extra grid potential has been applied will be subjected to a greater accelerating force at any point of its " filament-grid " passage than were its fellow electrons which traversed this space before the grid potential was raised. It will therefore take less time to cover any distance. The grid potential does not, however, remain constant and the electron considered may gain on its fellows for part of the cycle and lose on them for the rest. It may thus reach the grid in less time than its immediate predecessors but with smaller final velocity. Thus the electron stream, which at the filament constitutes a constant current, reaches the grid with a superposed alternating current whose power is derived from the reduction of the average kinetic energy of the electrons at the grid. If the latter is tuned, so that a voltage shock produces a series of oscillations, and if the time taken by the electrons to traverse the " filament-grid " space is so adjusted that the superposed alternating current is out of phase with the alternating voltage, the negative leakance so produced will sustain the oscillations, provided that the load and losses are not too great.

It is found by experiment that with any given transmission line and load the same frequency can be generated by the spiral grid tube for different pairs of values of anode and grid potentials, the output being different for each pair. Thus amplitude modulation of a substantially constant carrier frequency is obtained by the simultaneous variation of grid and plate potentials, and this can easily be arranged with suitable potentiometers. With a mean grid voltage of 270, variations of $\pm$ 30 gave a linear 30% modulation. The spiral grid tube, when used as a receiver, is adjusted to a non-

oscillating condition, the signal being applied to the grid. Now consider an electron which leaves the filament and is reflected back before it reaches the anode. If its initial velocity at the filament was zero and if the applied voltages are constant, it will come to rest at a point between the grid and anode where the potential is zero. The electron may, during its journey between the filament and the anode, pick up an appreciable amount of energy from the signal applied to the grid. If the voltage applied to the anode is such that in the non-receiving condition those electrons that leave the filament with maximum velocity just fail to reach the anode, an increase in the grid potential will increase the number of electrons reaching the anode while a decrease of grid potential will not reduce the number. The average current in the anode circuit will therefore vary according to the amplitude of the signal applied to the grid. An amplifying effect can also be obtained, the operating conditions being usually different from those for detection. In both cases the filament emission is voltage saturated, and reaction is controlled by a quenching oscillator of, say, 500 kc. In communication on such short wavelengths the comparatively small powers available are compensated by the large gain radiation systems which can be used. These include wire aerial arrays of a large number of elements, lenses made of ebonite, etc., which can be 70 cm. diameter, say, for 19 cm. wavelength, and zone plates, which, however, tend to be wasteful of energy. A very efficient and satisfactory method is to use parabolic or paraboloidal mirrors, and these can give highly directional beams.

(*b*) EXPERIMENTAL RESULTS

Positive Ion Theory. It is difficult to make accurate measurements on the impedances, phase angles and other properties of thermionic tubes under the conditions obtaining for these oscillations since, as seen above, the frequency is normally so high that ordinary measuring instruments are inaccurate and the technique is complicated. It has been suggested by J. A. Ratcliffe and S. Kownacki (45) that these disadvantages can be considerably reduced by the use of

special thermionic tubes with positive ions instead of electrons as the travelling charged particles. Thus, if ϕ is the potential at any point measured from the cathode (source of ions), v is the velocity at a distance x, and v_0 the initial velocity of emission, then for planar-electrodes,

$$\frac{1}{2} mv^2 = \frac{1}{2} mv_0^2 + \phi e \quad . \quad . \quad . \quad . \quad (54)$$

and if n is the number of charged particles per unit volume Poisson's equation gives

$$\frac{d^2\phi}{dx^2} = -4\pi ne \quad . \quad . \quad . \quad . \quad . \quad (55)$$

while the conditions for continuity (or zero divergence) require that

$$\frac{dn}{dt} = -n \cdot \frac{dv}{dx} \quad . \quad . \quad . \quad . \quad . \quad (56)$$

Now if m is replaced by M, the mass of the positive ion, and the other quantities are kept constant, it is seen that from (54) both v and v_0 must be reduced in the ratio $\sqrt{m/M}$, or alternatively, the time scale is increased by a factor $\sqrt{M/m}$. Since n is the same and $i = nv_0$ the emission current must be reduced by $\sqrt{m/M}$ to obtain the same space charge conditions, and thus the tube impedance or voltage-current ratio is increased by the factor $\sqrt{M/m}$. The mean velocity of emission from the cathode is given by

$$\frac{1}{2} mv_0^2 = \frac{3}{2} kT \quad . \quad . \quad . \quad . \quad . \quad (57)$$

where T is the absolute temperature and k is Boltzmann's constant. Thus, T need not be altered, and since the velocity distribution is given by

$$N(v) = Ae^{-\frac{mv^2}{2kT}} \quad . \quad . \quad . \quad . \quad . \quad . \quad (58)$$

this also remains unchanged.

Thus this analysis, as well as the wavelength formulæ (46) and (52), show that the use of positive ions of mass M instead of electrons of mass m would result in an increase in the Barkhausen-Kurz wavelength by a factor $\sqrt{M/m}$. The

relevant data for the more important alkali metals are given in the following table.

TABLE VI

Alkali element	At. Wt.	M/m	$\sqrt{M/m}$
Lithium . . .	7	13,200	115
Sodium . . .	23	43,300	208
Potassium . . .	39	73,300	270
Cæsium . . .	133	250,000	500

Hence the use of lithium ions would result in a wavelength factor of 115 and for cæsium ions a factor of 500; and thus if the electronic oscillation wavelength was, for example, 1 metre (frequency 300 Mc/s), the wavelength with lithium would be 115 metres (2·61 Mc/s), and with cæsium 500 metres (600 kc/s). It will be evident that this renders the determination of the tube properties much easier as far as frequency is concerned.

Sources of Positive Ions. Although the thermionic properties of cathodes emitting electrons are well known, those dealing with the emission of positive ions are not so well known and thus they will be briefly dealt with. The emission of positive ions by hot metals and by heated salts has been described by O. W. Richardson (47), and more recent work on this problem has been dealt with by A. L. Reimann (46), who gives a summary of the experimental work. It has been shown by I. Langmuir and K. H. Kingdom (32) that copious emission of positive ions is obtained when a tungsten filament is heated to redness in the vapour of one of the alkali metals. It is suggested that this phenomenon is due to the fact that the electron affinity of tungsten (work function) is 4·54 volts, while the ionising potential of cæsium, for example, is 3·87 volts, and thus heating of the tungsten causes ionisation. For positive ion emission it is necessary that the filament be above a certain critical temperature, below which the alkali condenses on the tungsten to form a complex emitting surface with a much lower work function. Now under these conditions no ions are emitted, but on the other hand, the

electron emission enormously increases. This source of ions is convenient, especially for cæsium due to its low work function.

Some information on positive ion sources is given by A. M. Tyndall (54), who finds glass sources suitable for metals like lithium and the other alkali metals. In the case of cæsium a mixture is made in the proportions Cs_2O . Al_2O_3 . $2SiO_2$ and this is heated in a graphite crucible until a glass bead is formed. This is then ground up and reheated and the grinding repeated. A paste is then made with distilled water, and this is painted on the tungsten filament, which can be in the form of a small spiral.

For the heavier metals a convenient and constant source has been given by C. H. Kunsman (30, 31), and H. A. Barton, G. F. Harnwell and C. H. Kunsman (3), in which a mixture of 95% iron oxide, 4% Al_2O_3 and 1% alkali salt is ground together. It is then heated dull red and reground, and then heated orange red and again reground. After reduction by heating in hydrogen a paint is made with xylol, which is then applied to the tungsten filament. Other positive ion emitters are described by J. P. Blewett and E. J. Jones (5), and J. Koch (29).

High Vacuum Technique. For the experiments the vapour method for producing positive ions was employed, since this is particularly suitable for the production of cæsium ions, due to their low ionisation potential. There were two triodes available, the first being a normal type AT40, with cylindrical electrodes, and the second, a specially constructed tube with planar movable electrodes. This is similar to one described by R. A. Chipman (6), and the details are given in Fig. 29*b*. To reduce surface leakage the tube was of double-ended construction, the anode being supported from the glass pinch at one end while filament and grid were supported from the other pinch. The filament consisted of a tungsten strip about 3 mm. wide, coplanar with a guard plate or ring surrounding it but separated by a small gap so that the electrostatic field was practically normal to the emitting surface. The grid and anode were mounted as shown, so that they could be moved relatively to each other and to the cathode by gently tapping the tube. The envelope was made of pyrex glass so that it

could be baked out at a high temperature, and the pyrex pinches with tungsten seals were joined to the cylindrical envelope.

Before the insertion of the cæsium the glass walls of both

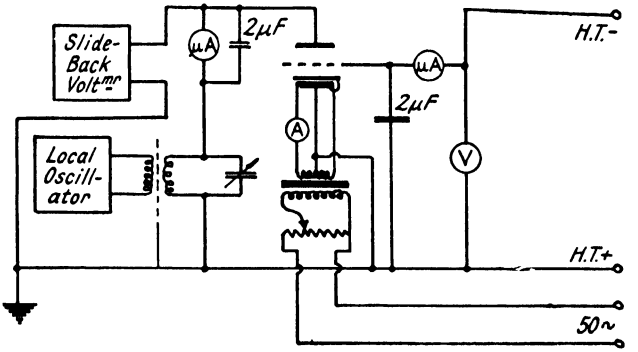

FIG. 29a. Circuit for resonance rectification.

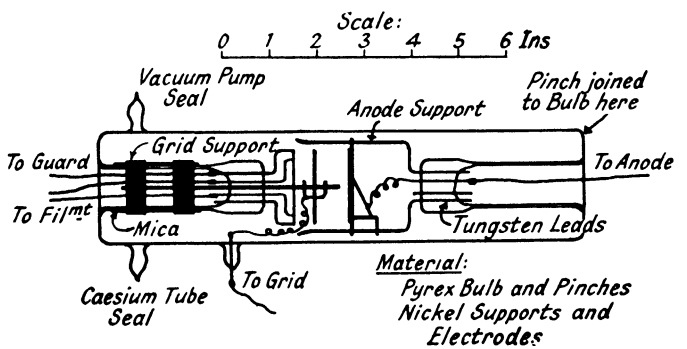

FIG. 29b. Construction of planar triode.

these triodes were degassed by heating for three hours in an oven constructed of sheet asbestos sides and an electric heating element, and maintained at a temperature of 500° C., which is about 50° C. below the softening point of pyrex. At the same time, a high vacuum was maintained by a mercury diffusion pump with a liquid air trap and suitable backing pump. In some experiments a solid carbon dioxide trap was used,

and the final traces of water vapour were removed by a phosphorus pentoxide filter, but it was found that the degree of vacuum obtained was not so good, and after a time oxidation of the cæsium in the tube took place. After this period of baking the triode was allowed to cool slowly for an hour and then the electrodes and supports were heated to cherry red for about a minute by means of an eddy current heating generator and coil. The former was of the Poulsen arc pattern, the carbon arc being run in a coal-gas atmosphere, and the power input was about 10 kw. While this was satisfactory for the cylindrical triode, it was difficult to heat the planar electrodes sufficiently and electron bombardment was also found unsatisfactory due to the size of the electrodes.

The cæsium was placed in the triode by a method similar to that described by J. Strong (51). The alkali metal in the form of its azide was contained at the end of a zig-zag side piece sealed into the glass walls, and this was then put in the triode by alternately distilling the metal and sealing off the portions of the zig-zag side piece, the resulting nitrogen being, of course, pumped away as soon as it was found. The last distillation resulted in a clear film of metallic cæsium on the glass walls, and when the pressure had fallen to about 10^{-6} mm., as shown by the mercury in the McLeod gauge sticking, the triode was sealed off from the pump.

Although the positive ion emission is independent of the filament temperature, provided this is above a certain critical value, it does depend on the vapour pressure of the cæsium, and thus comparatively large currents could be obtained by keeping the tube warm, a convenient method being immersion in a bath of transformer oil kept at a steady temperature by heating coils controlled by a thermostat. Leakage effects were further minimised by placing small heating coils of 26 S.W.G. nichrome wire, dissipating a few watts, inside the glass pinch supports, thus driving the cæsium on to the cooler bulb.

Resonance Rectification. E. W. B. Gill and R. H. Donaldson (18) have shown that by applying a high-frequency potential from an independent source to the anode of the triode, anode current is found to flow at certain grid potentials

which are related to the wavelength of operation. This has also been used by R. A. Chipman (7) for measurements on triode electronic oscillations and in the first instance this measuring technique was followed with the positive ion tubes.

The circuit used is shown in Fig. 26*a*, and in the anode lead a normal coil and condenser were placed, which were adjusted so that they behaved as an inductance, and a radio-frequency voltage was induced from a nearby separate generator of conventional type. A sensitive microammeter was included in this circuit and the potential of the anode was approximately that of the filament centre point. The induced voltage was measured with a slide-back voltmeter, care being taken to keep the connections reasonably short. The grid was kept at a large negative potential by means of a normal rectifier unit with an adjustable voltage control and the grid current was measured with a microammeter.

Cylindrical Triode. Some resonance rectification curves which give the relation between anode current and grid potential are shown in Fig. 30 for a fixed frequency of 750 kc/s and an emission of 22·7 μA, while the anode potential was that of the positive end of the filament or about 0·5 volts positive with respect to the centre point. These curves were taken for different voltage amplitudes and it will be seen that while anode current flows only over a certain range of grid potential the value of the latter does not appear to be critical. It was not convenient to use a fixed grid potential and vary the frequency of the applied signal, but it is obvious that curves of similar shape would be obtained and that these would be much broader than the resonance curves associated with selective tuned circuits.

Some experiments were made to determine the changes due to small variations in anode potential, and the results of Fig. 31 show that the optimum grid potential falls slowly as the anode is made more positive with respect to the filament centre point. The maximum value of anode current rises as the potential is made negative. These changes have been referred to by L. F. Dytrt (12) for electron oscillators. It should be pointed out that these values of anode current are the observed increases when the voltage amplitude is applied

since there is generally a small current always present due to leakage, electron emission, etc.

Planar Triode. Similar measurements were made on the

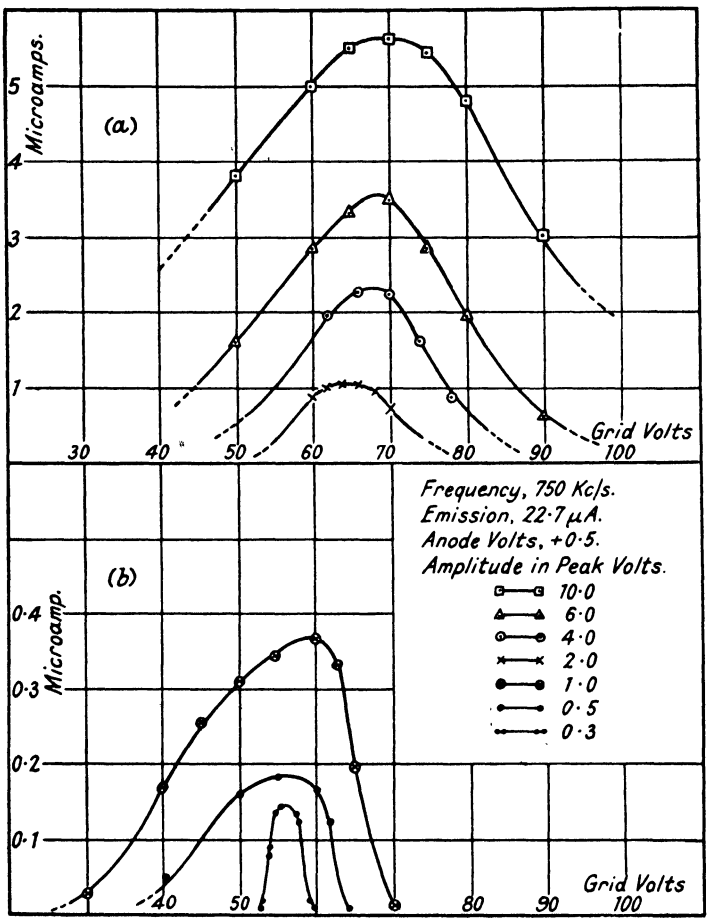

FIG. 30. Resonance rectification curves—cylindrical triode.

plane electrode positive ion tube and the resonance rectification curves are given in Fig. 32 for different frequencies and three different values of electrode spacing. It will be seen that the 800 kc/s curve at the largest spacing shows a subsidiary resonance effect. These were noted in several experiments

and their presence with ordinary electronic oscillations has been pointed out by several workers. From the formulæ quoted earlier for the wavelength it is evident that the value of $\lambda^2 E_g$ should tend to be constant and that if the square of

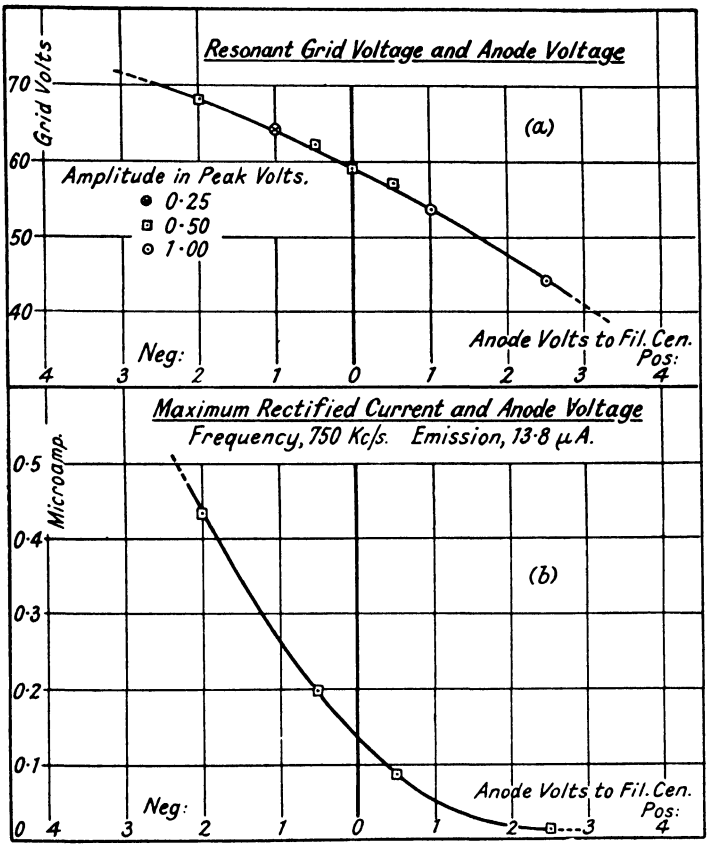

FIG. 31. Effect of anode voltage changes.

the frequency is plotted against optimum grid potential, a linear relation should result. Fig. 33 gives this relation for four different spacings and it will be seen that the curves are all convex upwards. At the same time they do not approximate to the theoretical values given in the simple formula for plane electrodes. Fig. 33 also shows the grid current,

which represents the positive ion emission, after correcting for leakage, etc., as a function of grid potential. These resemble normal emission curves except that the saturation is not well

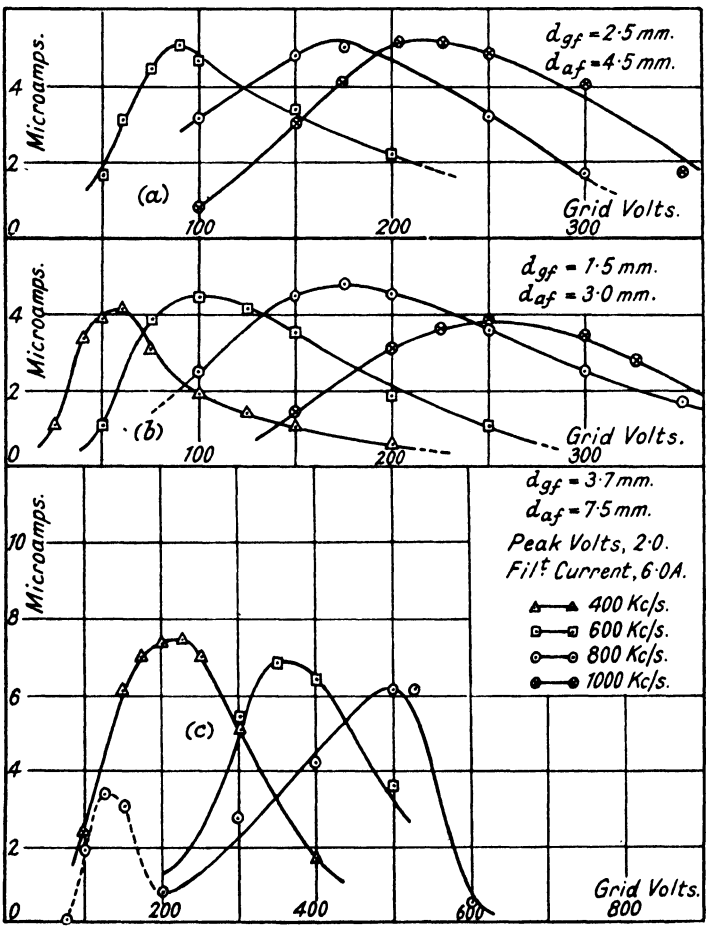

FIG. 32. Resonance rectification curves—planar triode.

marked. Most of the experimental points occur when the tube is space-charge limited, and it would be expected that the transit time under such circumstances would not be that given by methods neglecting space charge. In fact, the dis-

crepancies in the frequency relation mentioned above could be qualitatively explained by the fact that space charge can be shown to increase the transit time.

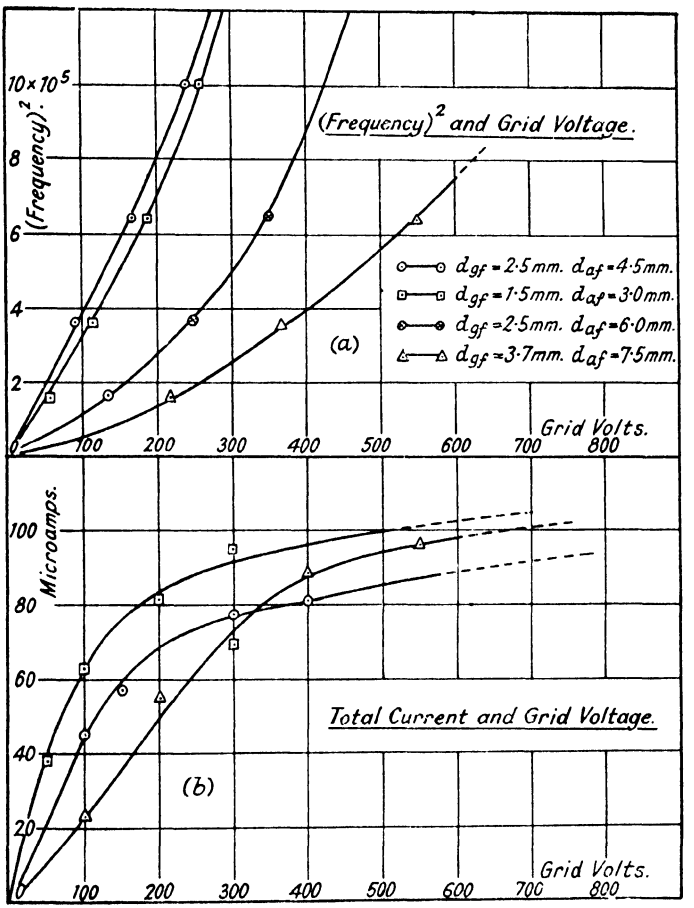

FIG. 33. Changes due to grid voltage.

General Conclusions. It will have been noted that the emission currents obtained are comparatively small and also that due to the long transit time of these massive ions, space-charge limitation occurs also when the current is small. Thus it is expected that the tube resistance would be of a very

high order and this is confirmed by the currents observed in the resonance rectification experiments which lead, even in the most favourable circumstances, to resistance values of the order 1 megohm. Sustained oscillations of small amplitude have been detected with the cylindrical electrode tube as described by W. S. Elliott and J. A. Ratcliffe (13), in the case when the anode circuit impedance was zero, thus proving conclusively for the first time that true Barkhausen-Kurz oscillations can take place without tuned circuits. However, from the point of view of determining the tube properties, such high impedances are difficult to measure. Thus, while reliable radio-frequency measurements on thermionic tubes can be made at frequencies up to about 100 Mc/s, it would seem that artificial lengthening of the transit time rather increases the difficulty of measurement of the tube properties. This view is confirmed when the experiments on the magnetron are described, and since in this case lengthening of the transit time can be accomplished without the complication and practical difficulties of producing positive ions, more detailed measurements are made. That these will be of value is shown by the fact that experiments of E. W. B. Gill (17) and J. S. McPetrie (38), as well as theory, indicate that the oscillations produced by positive grid triodes and magnetrons have much in common.

BIBLIOGRAPHY

1. ALFVEN, H. "The Barkhausen-Kurz Generator." *Phil. Mag.*, 1935, **19**, 419.
2. BARKHAUSEN, H. and KURZ, K. "The Shortest Waves Producible by Means of Vacuum Tubes." *Phys. Z.*, 1920, **21**, 1.
3. BARTON, H. A., HARNWELL, G. F. and KUNSMAN, C. H. "Positive Ion Emitters." *Phys. Rev.*, 1926, **27**, 739.
4. BENHAM, W. E. "A Contribution to Tube and Amplifier Theory." *Proc. Inst. Rad. Eng.*, 1938, **26**, 1093.
5. BLEWETT, J. P. and JONES, E. J. "Filament Sources of Positive Ions." *Phys. Rev.*, 1936, **50**, 464.
6. CHIPMAN, R. A. "The Electron Oscillation Characteristics of an Experimental Plane-electrode Triode." *Proc. Phys. Soc.*, 1935, **47**, 1042.
7. CHIPMAN, R. A. "Ultra High Frequency Resonances in the Positive Grid Triode." *Proc. Phys. Soc.*, 1939, **51**, 566.
8. CLAVIER, H. G. "Production and Utilization of Micro-rays." *Elec. Comm.*, 1933, **12**, 3.

9. CLAVIER, H. G. "The Influence of Transit Times of Electrons in Vacuum Tubes." *L'Onde Élec.*, 1937, **16**, 145.
10. COCKBURN, R. "Determination of the Fundamental Types of Electron Oscillations in a Triode Valve." *Proc. Phys. Soc.*, 1937, **49**, 38.
11. COPIN, H. "Action of a Magnetic Field on the Electrons of Oscillating Triodes." *Rev. Gén. d'Élec.*, 1939, **46**, 568.
12. DYTRT, L. F. "Barkhausen-Kurz Oscillator Operation with Positive Plate Potentials." *Proc. Inst. Rad. Eng.*, 1935, **23**, 241.
13. ELLIOTT, W. S. and RATCLIFFE, J. A. "Barkhausen-Kurz Oscillations with Positive Ions." *Nature*, 1940, **145**, 265.
14. FAY, C. E. and SAMUEL, A. L. "Vacuum Tubes for Generating Frequencies above One Hundred Megacycles." *Proc. Inst. Rad. Eng.*, 1935, **23**, 199.
15. GILL, E. W. B. "Electrical Oscillations of Very Short Wavelength." *Phil. Mag.*, 1931, **12**, 843.
16. GILL, E. W. B. "The Theory of Ultra Short Wave Generators." *Phil. Mag.*, 1934, **18**, 832.
17. GILL, E. W. B. "A Short Wave Generator." *Phil. Mag.*, 1939, **28**, 203.
18. GILL, E. W. B. and DONALDSON, R. H. *Phil. Mag.*, 1933, **15**, 1177.
19. GILL, E. W. B. and MORRELL, J. H. "Short Electric Waves obtained by Valves." *Phil. Mag.*, 1922, **44**, 161.
20. GILL, E. W. B. and MORRELL, J. H. "Short Electric Waves obtained by the Use of Secondary Emission." *Phil. Mag.*, 1925, **49**, 369.
21. HAMBURGER, F. "Electron Oscillations with a Triple Grid Tube." *Proc. Inst. Rad. Eng.*, 1934, **22**, 79.
22. HERSHBERGER, W. D. "Modes of Oscillation in Barkhausen-Kurz Tubes." *Proc. Inst. Rad. Eng.*, 1936, **24**, 964.
23. HOLLMANN, H. E. "The Mechanism of Electron Oscillations in a Triode." *Proc. Inst. Rad. Eng.*, 1929, **17**, 229.
24. HOLLMANN, H. E. "The Generation of Ultra Short Waves by Thermionic Valves." *Z. f. Hochf. Tech.*, 1930, **35**, 21 and 76.
25. HOLLMANN, H. E. "The Retarding Field Tube as a Detector for any Carrier Frequency." *Proc. Inst. Rad. Eng.*, 1934, **22**, 630.
26. HOLLMANN, H. E. "Ultra Short Wave Technique" (2 Vols.), 1937.
27. JONESCU, T. V. "A New Micro Wave Generator." *Comptes Rendus*, 1937, **204**, 1411.
28. KOCKEL, B. and MROWKA, B. "On the Theory of the Barkhausen Valve." *Z. f. Tech. Phys.*, 1938, **2**, 42.
29. KOCH, J. "Positive Ion Emitters." *Z. f. Phys.*, 1936, **100**, 669.
30. KUNSMAN, C. H. "Positive ion Emitters." *Science*, 1925, **62**, 269.
31. KUNSMAN, C. H. "Positive Ion Emitters." *J. Franklin Inst.*, 1927, **203**, 635.
32. LANGMUIR, I. and KINGDOM, K. H. "Thermionic Effects caused by Vapours of Alkali Metals." *Proc. Roy. Soc.*, 1925, **107**, 61.
33. MATSUDAIRA, K. "Ultra High Frequency Oscillations of Diodes and Triodes." *Electrot. J. Tokyo*, 1939, **3**, 19.

34. McPetrie, J. S. "A Graphical Method for Determining the Transit Time of Electrons in Triodes under Conditions of Space Charge Limitation." *Phil. Mag.*, 1933, **16**, 284.
35. McPetrie, J. S. "The Determination of the Inter-electrode Times of Transit of Electrons in Triode Valves with Positive Grid Potentials." *Phil. Mag.*, 1933, **16**, 544.
36. McPetrie, J. S. "Experiments with Inverted Diodes having Various Filament Cathodes." *Phil. Mag.*, 1935, **19**, 501.
37. McPetrie, J. S. "A Diode for Ultra High Frequency Oscillations." *Wireless Eng.*, 1934, **11**, 118.
38. McPetrie, J. S. "Electronic Oscillations in Positive Grid Triodes and Resonance Oscillations in Magnetron Generators." *J. Inst. Elec. Eng.*, 1937, **80**, 84.
39. Megaw, E. C. S. "Electronic Oscillations." *J. Inst. Elec. Eng.*, 1933, **72**, 313.
40. Moore, W. H. "Electron Oscillations without Tuned Circuits." *Proc. Inst. Rad. Eng.*, 1934, **22**, 1021.
41. Müller, J. "The Spiral Grid Electron Oscillator." *Ann. Phys.*, 1935, **21**, 611.
42. Müller, J. "Electron Oscillations in High Vacua." *Hochf. Tech. u. Elek. akus.*, 1933, **41**, 156.
43. Nakamura, S. "Electronic Oscillations produced by a Thermionic Tube with Plane Electrodes operated in Push Pull." *Nippon Elec. Comm. Eng.*, 1938, **10**, 134.
44. Pfetscher, O. and Müller, J. "Barkhausen-Kurz Oscillators." *Hochf. Tech. u. Elek. akus.*, 1935, **45**, 1.
45. Ratcliffe, J. A. and Kownacki, S. "A Method of Investigating Electron Inertia Effects." *Nature*, 1938, **141**, 1009.
46. Reimann, A. L. "Thermionic Emission," 1934.
47. Richardson, O. W. "Emission of Electricity from Hot Bodies." 1921.
48. Rostagni, A. "Barkhausen-Kurz Oscillators." *Atti. R. Accad. Torino.*, 1931, **66**, 124.
49. Rostagni, A. "The Theory of Barkhausen-Kurz Electron Oscillators." *Radio and Televisione*, 1939, **3**, 28.
50. Scheibe, A. "The Generation of Ultra-short Waves with Hot-Cathode Tubes." *Ann. Phys.*, 1924, **73**, 54.
51. Strong, J. "Procedures in Experimental Physics." 1937.
52. Thompson, B. J. and Zottu, P. D. "An Electron Oscillator with Plane Electrodes." *Proc. Inst. Rad. Eng.*, 1935.
53. Tonks, L. "Electronic Oscillations." *Phys. Rev.*, 1927.
54. Tyndall, A. M. "Mobility of Positive Ions." 1938.
55. Ullrich, E. H. and McPherson, W. L. "Micro-ray Communication. *J. Inst. Elec. Eng.*, 1936, **78**, 629.
56. Lüdi, F. "The Theory of Transit-time Oscillations." *Helvet. Phys. Acta*, 1940. **13**, 77.
57. Nakamura, R. "Characteristics of Electron Oscillations and Their Input Resistance." *Electrot. J. Tokyo*, 1940, **4**, 180.
58. Hoffmann, F. "Retarding-field Valves with a Magnetic Field." *Hochf. Tech. u. Elek. akus.*, 1940, **56**, 137.

CHAPTER IV

THE MAGNETRON—PART ONE

(*a*) CUT-OFF CHARACTERISTIC

Introduction. The motion of charged particles in combined electric and magnetic fields has long been known, and the consideration in the case of the diode by A. W. Hull (29) led to the introduction of the magnetron. This is essentially a thermionic tube placed in a magnetic field so that the lines of force are approximately normal to the electric field between the electrodes. Although the electrodes can be plane, in practice they are invariably cylindrical, the cathode being in the form of a fine filament, while the anode may be in the form of one or more segments. As the magnetic field is gradually increased, a value is reached when the travelling charged particles move in such curved paths that they just miss the anode, and at this point the anode current rapidly decreases (see Fig. 34*b*). This value is termed the critical field and the corresponding potential difference between the electrodes is the critical voltage. In addition to this current "cut-off," various other phenomena are observed at the critical condition, particularly when the tube is acting as a generator. Although the technical use of the magnetron lies in its use as a generator of very high frequency electric energy, it is instructive in the first instance to examine in detail its properties under static and low frequency conditions.

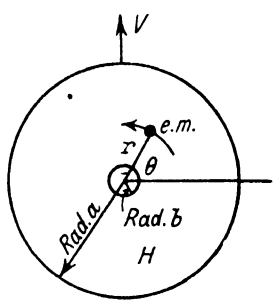

FIG. 34*a*. Analysis of cylindrical magnetron.

Simple Theory, In Fig. 34*a*, if r,θ are the co-ordinates of the travelling charged particle and e,m its charge and mass respec-

tively, then the tangential equation of motion, with H the magnetic field and V the steady anode potential, is

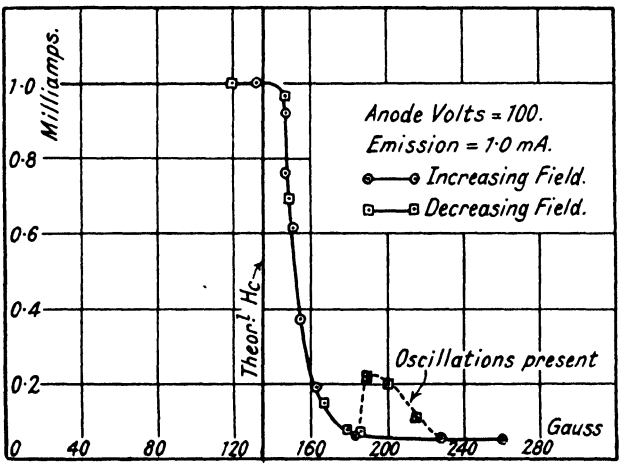

FIG. 34*b*. Current cut-off in the magnetron.

$$r\frac{d^2\theta}{dt^2} + 2\frac{dr}{dt}\cdot\frac{d\theta}{dt} = \frac{eH}{mc}\cdot\frac{dr}{dt} \quad . \quad . \quad . \quad . \quad (59)$$

which reduces to

$$\frac{1}{r}\cdot\frac{d}{dt}\left(r^2\frac{d\theta}{dt}\right) = \frac{eH}{mc}\cdot\frac{dr}{dt} \quad . \quad . \quad . \quad . \quad (60)$$

Integration of (60) gives, assuming the particle leaves the cathode at zero time and that the cathode radius is b,

$$\frac{d\theta}{dt} = \frac{eH}{2mc}\left(1 - \frac{b^2}{r^2}\right) \quad . \quad . \quad . \quad . \quad . \quad (61)$$

Now at the turning point the radial velocity is zero, and hence, neglecting the initial velocity of emission,

$$\frac{m}{2}\left(r\frac{d\theta}{dt}\right)^2 = eV \quad . \quad . \quad . \quad . \quad . \quad (62)$$

and thus if the particle just grazes the anode of radius a

$$V = \frac{eH^2a^2}{8mc^2}\left(1 - \frac{b^2}{a^2}\right)^2 = \frac{eH^2a^2}{8mc^2} \quad . \quad . \quad . \quad (63)$$

when $b \ll a$. It is obvious from this derivation that the "cut-off" magnetic field strength is independent of the voltage distribution between the electrodes, and hence (63) is true whether space charge is present or not. Similarly in the planar magnetron it can be shown that the cut-off field is given by

$$V = \frac{eH^2d^2}{2mc^2} \quad . \quad . \quad . \quad . \quad . \quad . \quad (64)$$

where d is the interelectrode distance.

The transit time in the planar magnetron at the cut-off condition is given by simple theory, see equation (74), as

$$T = \frac{\pi mc}{eH} \quad . \quad . \quad . \quad . \quad . \quad . \quad (65)$$

when the emission is vanishingly small. This time is increased when space charge is present and when this is sufficient to reduce the cathode field to zero W. E. Benham (5) shows that the transit time is doubled. With cylindrical electrodes the analysis is not easy, but it is possible to arrive at a graphical solution, which shows that as the cathode radius tends to zero the transit time tends to the value given above for planar electrodes, and that when the cathode radius is finite the transit time slightly exceeds this value.

Many experiments were carried out on the magnetron and other forms of diodes to examine the above relations, and some of these have already been described by the author elsewhere (27). The circuit used is shown in Fig. 35a, the filament,

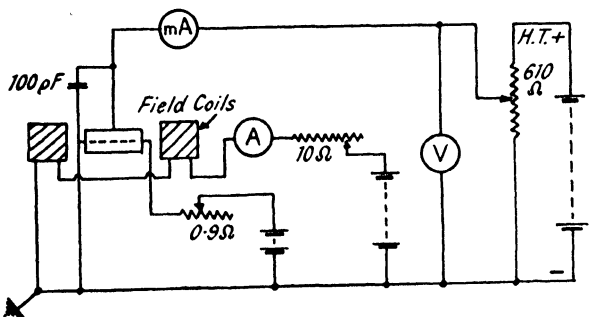

Fig. 35a. Circuit for cut-off measurements on diodes.

anode and field coils being supplied by batteries and the currents controlled by rheostats. The measuring instruments were of Cambridge Unipivot pattern fitted with appropriate shunts or series resistances. The magnetic field was sometimes obtained with an air-cored solenoid, but more often with an iron-cored electromagnet.

Solenoid Details. The details of the solenoid are shown in Fig. 35*b*, and this was specially designed and constructed to give as uniform a field as possible over the volume occupied by the electrodes. It consists of a paxolin tube, 3 in. diameter and 12 in. long, wound with 1,375 turns of 22 S.W.G. D.C.C. copper wire disposed in five layers. The special long diode used with this solenoid had an anode 8 cm. long and 1 cm. diameter, and this was mounted vertically as shown with the aid of two plumb lines and the centering screws in the upper support. With the tilting screw set to zero the solenoid was so arranged on the base that it, too, was absolutely vertical. Calculation involving the use of spherical harmonics shows that H_r, the radial component of field at a small distance r from the axis of a solenoid of length $2l$ and radius R, and at a small distance x from the middle point of the length, is related to H_0, the field on the axis at the middle point, by the equation

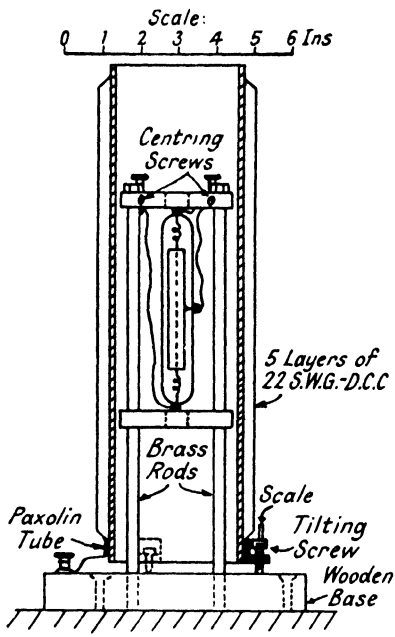

FIG. 35*b*. Construction of air cored solenoid.

$$\frac{H_r}{H_0} \simeq \frac{3}{2}\cdot\frac{x}{l}\cdot\frac{r}{R}\,\frac{R^3}{l^3}\left(1+\frac{10}{3}\frac{x^2}{l^2}-\frac{13}{4}\frac{R^2}{l^2}\right) \quad . \quad . \quad (66)$$

We are mostly concerned with the radial component of field

at the extreme ends of the anode and at the anode radius ; here

$$\frac{x}{l} \simeq \frac{1}{4}, \frac{r}{R} = \frac{1}{10}, \text{ and } \frac{R}{l} = 3 \quad . \quad . \quad . \quad . \quad (67)$$

and hence it follows that in the worst case H_r/H_0 is of the order of 1·25 parts in 10^3, and with the fields employed the transverse magnetic field was in fact less than the horizontal component of the earth's field. The solenoid could be tilted through a small angle relative to the electrode axis to investi-

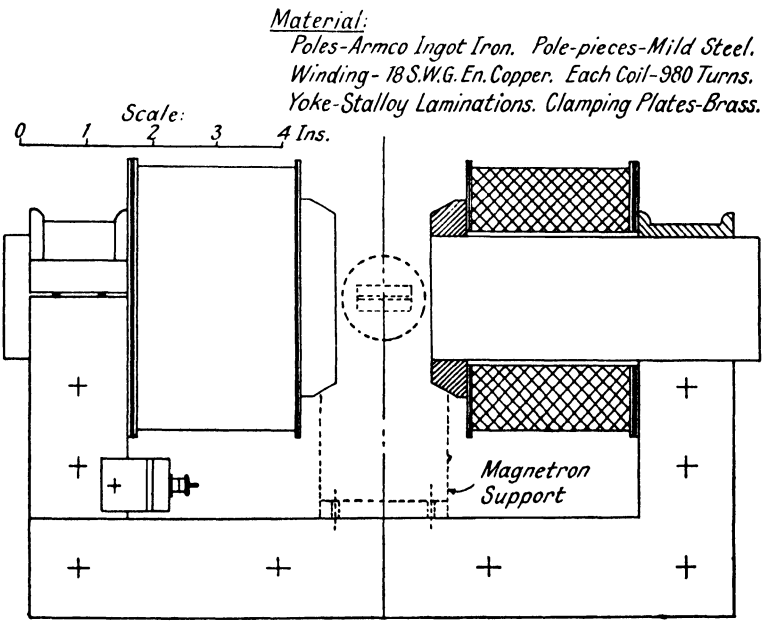

FIG. 36. Construction of electromagnet.

gate the effects of tilting on the cut-off curve. In operation the heating of the winding imposed an upper limit, of about 100 gauss, on the longitudinal field strength.

Electro Magnet Details. For measurements when much higher field strengths were necessary an iron-cored electromagnet was constructed. In the experiments the magnetic field was determined from the magnetising current by means of a previous calibration with a search coil and Grassot fluxmeter.

The details of the magnet in final form are shown in Fig. 36, from which it will be seen that the magnetic circuit consists of a laminated Stalloy yoke and special Armco soft iron poles. The magnetron was mounted horizontally so that the electrode structure is in the centre of the air gap, and the base-holder was arranged so that the tube could be rotated about its axis

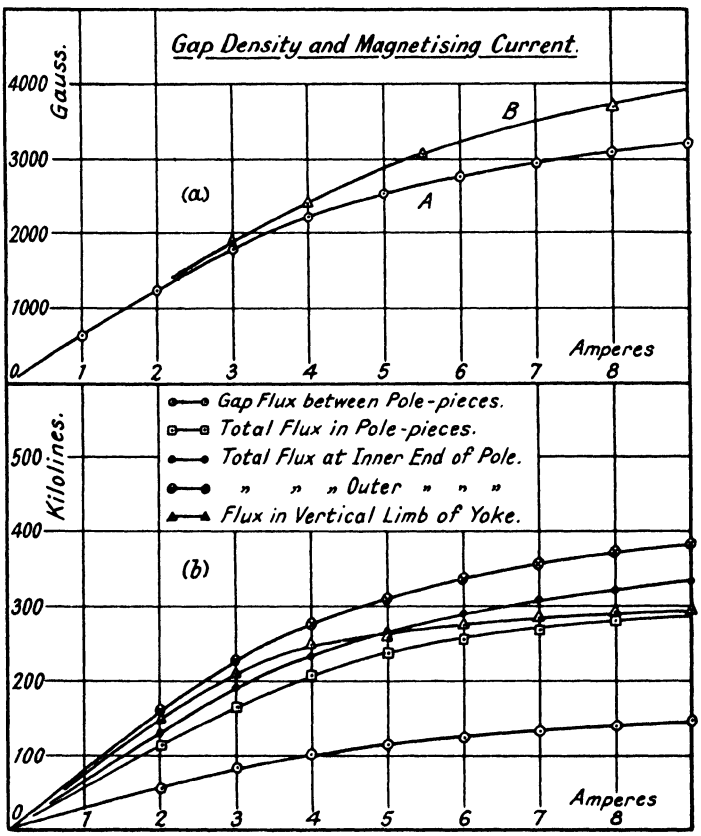

FIG. 37. Magnetisation curves of electromagnet.

for 25° on either side of its neutral position. The coils of enamelled wire are wound on brass formers, paper interleaving being inserted between alternate layers. The yoke and poles are held by cast-brass side pieces and clamps, while the annealed

mild steel pole pieces were shrunk on the poles, provision being made for adjusting the length and diameter of the air gap if required at some future time.

Fig. 37*a*, Curve A, gives the gap density in terms of magnetis-

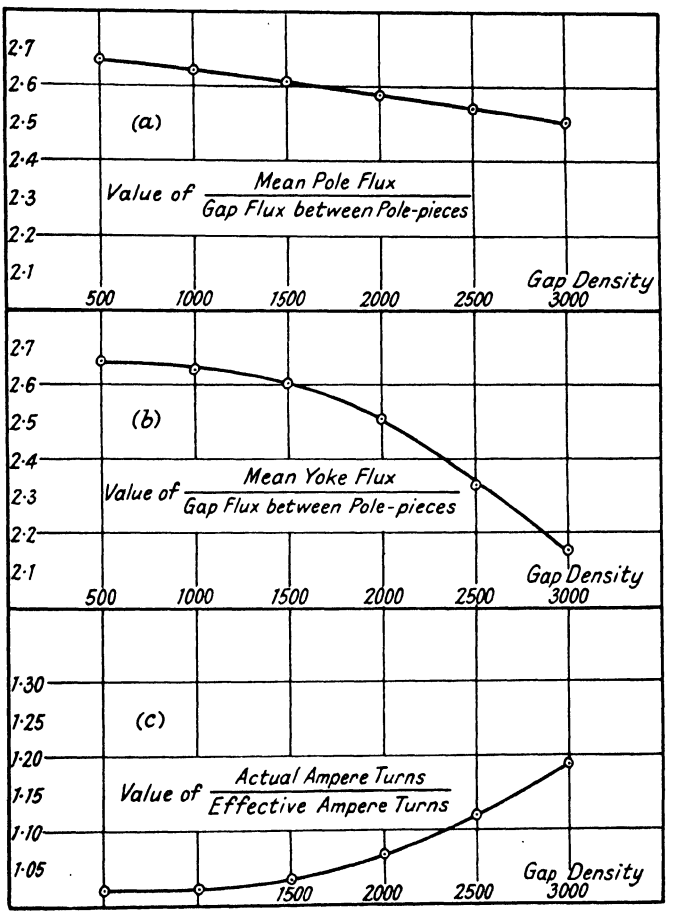

FIG. 38. Design data curves for electromagnet.

ing current, and, provided the coils are always energised in the same direction, the error due to hysteresis does not at any point exceed 5 gauss. Although the field between the pole pieces is found to be very uniform, with such a long gap, there

is considerable leakage, and unless this is allowed for in the design serious saturation of the iron circuit will occur. Fig. 37*b* shows the total flux in various parts of the magnetic circuit. Fig. 38*a* gives the mean pole flux and Fig. 38*b* the mean yoke flux in terms of the gap flux directly between the pole pieces, thus enabling the iron circuit to be designed for any required gap density. It will be observed from these factors that only one-third to one-half of the flux is effective ; if the diameter of the pole pieces is reduced the flux leakage is increased, so that the gap density is not increased appreciably. There is also a small coil leakage factor shown in Fig. 38*c*, since the required ampere turns were found to be slightly greater than the calculated value. The magnet gives a field of 2,000 gauss with a coil temperature rise of 40° C. and 2,500 gauss with a rise of 80° C., while higher fields can be obtained for shorter periods. With both coils in series the ohmic resistance when cold is 7·1 Ω, and thus a field of 500 gauss can be obtained with an energy of only 4·6 watts. Although these data refer to this one magnet, the above design data is found to hold good for similar shapes, but different sizes. Curve B in Fig. 37*a* gives the density for a very large magnet which was used later, which had a cast iron magnetic yoke, 3 by 4 in., and two coils with 2,000 turns each. The magnet was used with a 3-in. air gap and the height overall was about 20 in. and the weight over 1 cwt.

Cut-off Curves. Equation (63) shows that for a given value of H the anode current I_a should be independent of V until this falls below the calculated value, when the anode current should cease completely and abruptly ; alternatively, for a given value of V the anode current should cease when H is increased to a value above that given by (63). A typical curve showing the effect of varying the magnetic field is given in Fig. 34*b*. On taking this curve with decreasing magnetic field feeble oscillations were found at the point marked, although in all the cut-off experiments the anode was connected to the filament by a small condenser of 100 $\mu\mu$F. A typical experimental relation of I_a and V is shown in Fig. 43*a* (curve A). It will be seen that, although I_a decreases very rapidly near the value $V = 200$, yet the transition portion of the curve is

rounded for a considerable range of voltages, both near the top and the bottom of the curve.

The rounded portion near the top will be termed the " knee " of the curve and that near the bottom as the " foot." Experience shows that curves such as those above are very sensitive to the angle between the magnetic field and the electrode axis. There is no apparent reason for such anomalous behaviour and thus the various possible causes will be discussed in detail. Possible causes of the knee and foot are (*a*) emission velocity of electrons ; (*b*) magnetic field not parallel to the axis ; (*c*) the cathode not an equipotential cylinder ; (*d*) cathode eccentric and/or not parallel to the axis of the anode ; (*e*) presence of space charge ; (*f*) fringing of electric field at the ends of the electrodes ; (*g*) high-frequency oscillations of small amplitude.

Initial Electron Velocities. If the electrons leave the cathode in any direction with initial energy eV_0, and with a radial component of velocity u, it is easy to show that equation (63) becomes

$$\left\{\frac{2e}{m}(V + V_0)\right\}^{\frac{1}{2}} = \frac{Hea}{2mc}\left(1 - \frac{b^2}{a^2}\right) + \frac{bu}{a} \quad . \quad . \quad (68)$$

In practice the most probable value of V_0 will be of the order of 0·1 volt, whereas V may be several hundred volts. Thus it seems clear that the effect of V_0 and u should always be small and that their effect on the knee and foot should become progressively less as V increases, which is contrary to experience. Thus it is considered that initial velocities do not play a dominant part in the formation of the foot.

Tilt of Magnetic Field. Up to now we have considered the magnetic field to have an axial direction, but it is necessary to examine the effect of small inclinations as, in practice, stray fields, which may, of course, be of various directions, are present. In addition, deliberate inclination of the main field can cause, under certain circumstances, a marked increase in output or other pronounced effects when the tube is generating high-frequency oscillations. Experiment shows that a slight inclination of the magnetic field to the electrode axis has a very marked effect on the shape of the cut-off curve. Before introducing the experimental curves it is helpful to study

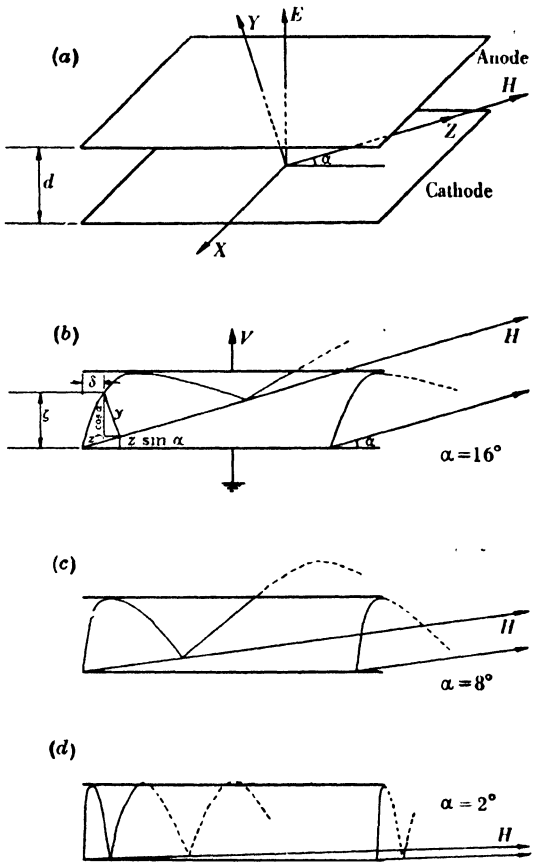

FIG. 39. Electron-paths in the planar magnetron.

analytically the electron paths in such circumstances. The analytical work is much simplified if attention is restricted to a planar system of electrodes, and doubtless the solution so obtained will differ only in degree and not in kind from that for a cylindrical system. Thus, let the uniform magnetic field H be inclined at an angle $\frac{1}{2}\pi - \alpha$ to the uniform electric field E, and let rectangular co-ordinate axes be taken as shown in Fig. 39*a* with the Z-axis directed along H. Then the equations of motion are

$$m\frac{d^2z}{dt^2} = Ee \sin \alpha . \quad . \quad . \quad . \quad . \quad . \quad . \quad (69)$$

$$m\frac{d^2y}{dt^2} = Ee\cos\alpha - \frac{He}{c}\frac{dx}{dt} \quad . \quad . \quad . \quad . \quad (70)$$

$$m\frac{d^2x}{dt^2} = \frac{He}{c}\cdot\frac{dy}{dt} \quad . \quad . \quad . \quad . \quad . \quad . \quad . \quad . \quad (71)$$

Equations (69–71) show that the motion in the XY plane is undisturbed by the motion in the YZ plane. Hence the motion in the XY plane is a cycloid if the initial velocity is zero and the motion along the Z-axis is given by

$$z = \frac{Ee}{2m}t^2\sin\alpha \quad . \quad . \quad . \quad . \quad . \quad . \quad . \quad (72)$$

If this motion is considered in relation to Fig. 39*a* it will be understood that any electron which leaves the " cathode " plane must ultimately reach the anode plane, though it may have performed many hops in the process and it will reach the anode plane at a point very far removed from its point of departure from the cathode plane. Hence if the electrode planes were infinite in extent no value of the magnetic field could cause any reduction of anode current unless α were zero, when complete cut-off would occur for a definite value of H. Thus it may be inferred that the comparatively sharp cut-off curves, such as are shown in Fig. 43*a*, obtainable in practice from diode tubes, are possible only because the electrode system has a finite length ; and it would seem likely that the larger the electrode system the greater will be the sensitivity to tilt.

The distance which the particle has moved in the direction of E is a maximum when

$$\frac{dy}{dt}\cos\alpha + \frac{dz}{dt}\sin\alpha = 0 \quad . \quad . \quad . \quad . \quad (73)$$

so that $$\frac{c}{H}\cos^2\alpha\sin\frac{eHt}{mc} + \frac{et}{m}\sin^2\alpha = 0,$$

i.e. $$\sin pt + pt\tan^2\alpha = 0, \text{ where } p = \frac{eH}{mc} \quad . \quad . \quad (74)$$

If α is zero, $\sin pt = 0$ and the transit time $t = \frac{\pi mc}{eH}$. In time t the electron has moved a distance ζ in the direction of E such that

$$\zeta = \frac{eE}{mp^2}\cos^2\alpha\left(1 - \cos pt + \frac{p^2t^2}{2}\tan^2\alpha\right)$$

$$= \frac{eE}{mp^2} \cos^2 \alpha \left(1 - \cos pt + \frac{\sin^2 pt}{2 \tan^2 \alpha}\right)$$

when t satisfies (74).

Let V_0 be the potential for a given value of H at which the electron just grazes the anode when $\alpha = 0$, and V the potential at any maximum value of ζ. Then

$$\frac{\zeta}{d} = \frac{V}{2V_0} \cos^2 \alpha \left(1 - \cos pt + \frac{\sin^2 pt}{2 \tan^2 \alpha}\right) \quad . \quad . \quad (75)$$

During the time taken to reach a maximum excursion in the direction of E the electron has advanced parallel to the electrodes (see Fig. 39*b*) a distance

$$\delta = z \cos \alpha = \frac{Ee}{4m} t^2 \sin 2\alpha$$

$$= \frac{Ee}{4m} \frac{\sin^2 pt}{p^2} \frac{\sin 2\alpha}{\tan^4 \alpha},$$

from (74). Hence $$\frac{\delta}{d} = \frac{V}{8V_0} \frac{\sin 2\alpha}{\tan^4 \alpha} \sin^2 pt \quad . \quad . \quad . \quad . \quad . \quad (76)$$

Now let $pt = n(\pi + \beta)$, where n is odd; then (75) and (76) become

$$\frac{\zeta}{d} = \frac{V}{2V_0} \cos^2 \alpha \left(1 + \cos n\beta + \frac{\sin^2 n\beta}{2 \tan^2 \alpha}\right) \quad . \quad . \quad (77)$$

and $$\frac{\delta}{d} = \frac{V}{8V_0} \frac{\sin 2\alpha}{\tan^4 \alpha} \sin^2 n\beta \quad . \quad . \quad . \quad . \quad (78)$$

If $n\beta$ is small, it follows from (74) that

$$n\beta \doteqdot \frac{\pi \tan^2 \alpha}{1 - \tan^2 \alpha}$$

$$\doteqdot \pi\alpha^2 \quad . \quad . \quad . \quad . \quad . \quad . \quad . \quad . \quad (79)$$

provided that $\alpha \ll 1$. Expansion of (77) gives

$$\frac{\zeta}{d} = \frac{V}{V_0} \cos^2 \alpha \left\{1 + \frac{n^2\beta^2(1 - \tan^2 \alpha)}{4 \tan^2 \alpha} + \frac{n^4\beta^4(\tan^4 \alpha - 4)}{48 \tan^2 \alpha} + \ldots\right\}$$

$$= \frac{V}{V_0} \cos^2 \alpha \left\{1 + \frac{\pi^2 \tan^2 \alpha}{4(1 - \tan^2 \alpha)} - \frac{\pi^4 \tan^6 \alpha}{12(1 - \tan^2 \alpha)^4} + \ldots\right\}$$

$$\doteqdot \frac{V}{V_0} \cos^2 \alpha \left(1 + \frac{\pi^2\alpha^2}{4} - \frac{\pi^4\alpha^6}{12}\right) \quad . \quad . \quad . \quad . \quad . \quad . \quad . \quad (80)$$

Similarly, $$\frac{\delta}{d} \doteqdot \frac{V}{V_0}\frac{\pi\alpha}{4}\left(1 - \frac{4\alpha^2}{3} - \frac{\pi^2\alpha^4}{3}\right) \quad . \quad . \quad . \quad . \quad (81)$$

If $V/V_0 = 1$, it follows from (77) or (80) that the electron will miss the anode at the first excursion. It will, however, reach the anode at the first excursion if

$$\frac{V}{V_0} = \frac{1 + \tan^2\alpha}{1 + \frac{1}{4}\pi^2\tan^2\alpha} \doteqdot 1 - \frac{\pi^2 - 4}{4}\tan^2\alpha$$

$$\doteqdot 1 - 1{\cdot}45\,\alpha^2 \quad . \quad . \quad . \quad (82)$$

Equation (80) is valid only when $n\beta$ is small, and this will not be the case if the electron reaches the anode only after several hops. To find the time on the journey it will then be necessary to solve (75) for $\zeta/d = 1$. Thus, if we put $V/V_0 = k$, the equation for t is

$$\cos pt = \frac{\tan^2\alpha}{2}p^2t^2 - \left\{\frac{2(1 + \tan^2\alpha)}{k} - 1\right\}. \quad . \quad (83)$$

This can be solved graphically for assigned values of α, k and p by plotting $\cos pt$ as ordinate against p^2t^2 as abscissa and noting the intersection of this curve with the line

$$Y = \frac{\tan^2\alpha}{2}X - \left\{\frac{2(1+\tan^2\alpha)}{k} - 1\right\}.$$

An example of this construction is shown in Fig. 40. After the value of pt which satisfies (83) has been found in this way, δ/d can be found by substitution in (76).

If the electrode planes have a finite extension, it follows that some electrons will not have reached the anode before they have passed beyond its bounding edge ; thereafter they would be lost to the system and would proceed in a circular helix whose axis is the direction of H. Only those electrons will reach the anode which leave the cathode at a distance from one bounding edge given by (76).

It is now possible to plot a " cut-off " curve for planar electrodes whose width in the direction of progress of the electrons is any assigned multiple of the distance between cathode and anode. Thus, for example, suppose that the width is 2·0 cm. and the distance 0·5 cm., these values being chosen because they are analogous to the dimensions of the

Marconi-Osram CW10 magnetron which has a cylindrical anode 1·0 cm. diameter and 2·0 cm. long. The path of an electron emitted from one edge of the cathode, when α has

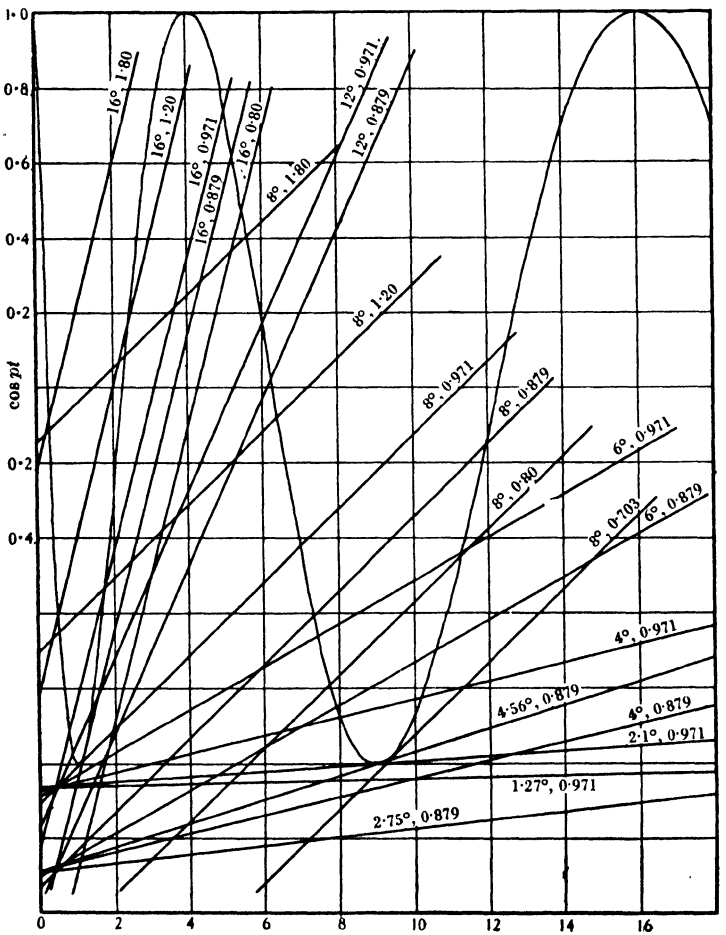

FIG. 40. Showing cos pt and p^2t^2. Lines represent $Y = \frac{\tan^2\alpha}{2} X - \left\{\frac{2(1 + \tan^2\alpha) - 1}{k}\right\}$ for various values of α and k as marked.

various values between 2 and 16°, is shown in Figs. 39*b–d*. The trajectories of this figure illustrate clearly the mechanism of the effect under discussion. Also it will be clear from this

figure that, even if H exceeds the critical value for $\alpha = 0$, there is yet a possibility that some electrons will reach the anode after several hops, though the majority will pass beyond the electrode system. Deduced curves of " cut-off " (relating I_a with V, with H constant) for the chosen electrodes are shown in Fig. 41*a* : the three curves in this figure relate respectively to $\alpha = 0$, 8 and 16^0. It will be seen that when α is not zero, (*a*) the presence of H reduces the current even though V is high above the critical value ; (*b*) the precipice on the current curve is approached by a rounded knee ; (*c*) the precipice occurs at a voltage which depends on α ; (*d*) there is a marked foot to the " cut-off " curve and the current may be considerable even when V is much less than the critical value. Comparison of Fig. 41*a* with Figs. 42*a*, *b* shows that a slight inclination of the field may be an important factor in producing the knee and foot of the " cut-off " curve.

Fig. 41*b* shows the calculated relation between α and I_a for a constant value of H and for $V/V_0 = 1{\cdot}0$, $0{\cdot}971$ and $0{\cdot}879$: these curves should be compared with those in Figs. 44. It should be noted that this analysis for planar electrodes has assumed a constant potential gradient between the plates and is therefore valid only for vanishingly small currents, since it ignores the field of the electrons in transit. It is well known that when α is zero the critical relationship is independent of the field distribution, but this does not hold when α is not zero.

The corresponding analysis for cylindrical electrodes is very complex, because the effective value of α varies from point to point of the path, and also the path depends on the angular co-ordinate of the point of departure of the electron from the cathode. Electrons will necessarily perform a complicated helical path progressing along the electrode axis but at an angle to it, so that any path will ultimately reach the anode if the system is long enough, and complete cut-off cannot occur. The theory of the cylindrical magnetron with inclined magnetic field has been examined by N. Carrara (15), who gives deduced curves showing the current distribution at different portions of the anode surface. This is a practical problem since a disadvantage of the magnetron is that the

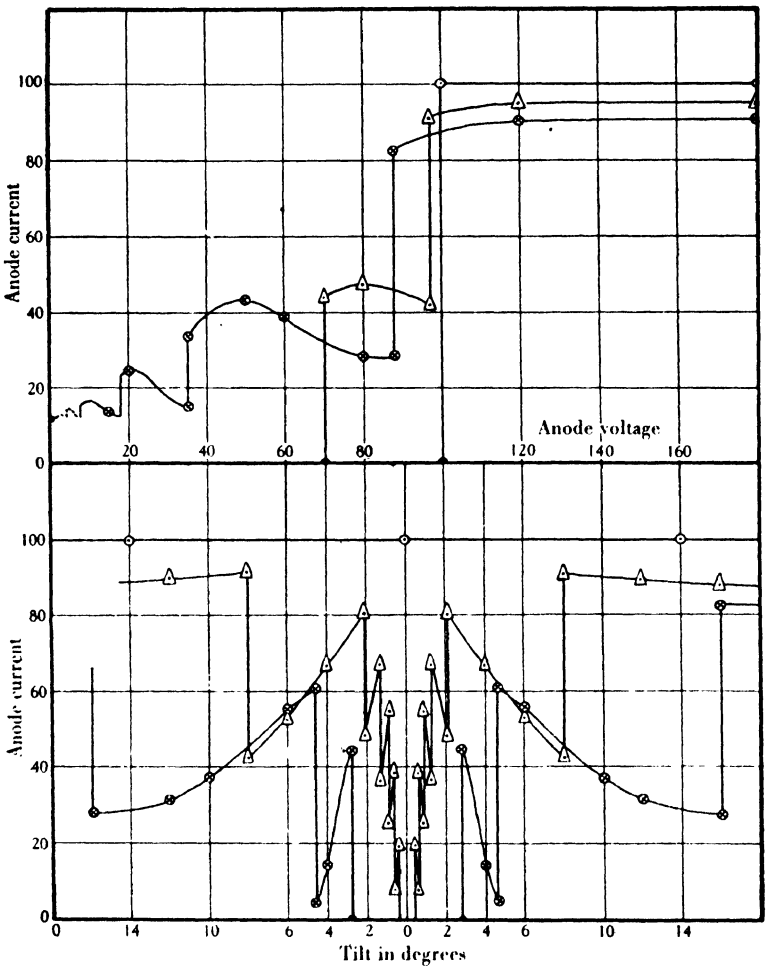

FIG. 41. Calculated cut-off curves.

(*a*) (Upper half) Calculated cut-off curve for planar magnetron with constant magnetic field.

Tilt zero ⊙
Tilt 8° △
Tilt 16° ⊗

(*b*) (Lower half) Calculated tilt curve for planar magnetron with constant magnetic field.

$V/V_0 = 1$ ○
$V/V_0 = 0{\cdot}971$ △
$V/V_0 = 0{\cdot}879$ ⊗

heating of the anode may tend to be non-uniform, thus limiting the dissipation power of this electrode.

Voltage Drop along the Filament. If α is zero and H is constant, then the anode current will start to decrease when the potential between the anode and the positive end of the filament is reduced to the critical value depending on H, a and b. For further decrease of V the anode current would fall at a constant rate and become zero when V had been reduced by an amount V_f. Thus voltage drop along the filament will certainly cause a uniform slope in the " cut-off " curve, but apparently will not tend to cause a knee or a foot to the curve. In these circumstances the cut-off curve would extend over a range V_f whatever the magnitude of H employed. Dr. E. B. Moullin has kindly furnished the writer with " cut-off " curves relating I_a and V (H constant) in which V was measured respectively from the negative end of the filament, from the positive end of the filament, and from a point at the potential of the mid-point of its length. These three curves were identical in shape and the two outside members of the family could be superposed on the middle member by moving either along the voltage axis by an amount equal to half the voltage drop along the filament. Dr. Moullin also used a rotary commutator to measure the anode current at instants when the heating current was zero and he found that the cut-off curve then obtained was identical in shape, within the limit of experimental error, with that obtained when no commutator was used. Also he found that when the anode voltage was measured with respect to a point at the potential of the mid-point of the filament, the cut-off curve relevant to A.C. heating was indistinguishable from that obtained with D.C. heating. Thus it seems certain that the voltage drop along the filament plays only a second-order *rôle* in the shape of the " cut-off " curve.

Eccentricity of Electrodes. Although the field between two eccentric cylinders obeys a comparatively simple law, it is very difficult to deduce the motion of an electron in such a field, more especially because the path must depend on the point of departure from the cathode. Since the electric field between the cylinders is that of two line charges which are inverse points for both circular cross-sections, it is clear that for a

small eccentricity the field must be very nearly that resulting from the superposition of a radial field and a small uniform transverse field (due to the image line charge at the distant inverse point). Thus the problem must have some resemblance to that of the split anode magnetron and we may hazard the suggestion that, if cut-off does not occur, current tends to arrive at points in the anode which are more distant than others from the cathode. Also it seems possible that some electrons may miss a small cathode at their first approach to it and thus there would be a tendency for successive orbits to be spirals in a plane perpendicular to the axis ; for this reason it would be desirable to make observations with a valve in which the eccentricity could be varied.

Though the filament of short diodes appears to be remarkably concentric and parallel to the anode axis, yet in fact the two axes can scarcely be parallel ; it follows that, in any experiment in which the magnetic field is tilted, the field must at different stages be parallel first to one and then to the other axis. This may account for the slight dissymmetry sometimes found in the curves relating α and I_a. It seems not unlikely that small imperfections of construction will have an effect similar to that due to a small angle of tilt, as discussed above for planar electrodes.

To examine these effects experimentally cut-off curves of anode current and field strength were taken with the two anode segments at different potentials. These curves are shown in Fig. 44*b* ; it will be seen that, considering the increase of current caused by these large potential differences, it is unlikely that any small eccentricity which may be present could lead to the currents forming the foot discussed above.

Effect of Space Charge. In the absence of eccentricity, angle of tilt, etc., the critical condition for a given magnetic field depends only on the anode potential and not on the distribution of field, and thus should be independent of the magnitude of I_a. On the other hand, if the emission suffices to produce space-charge limitation, increasing the magnetic field will cause a gradual decrease of I_a until complete cut-off occurs at H_c.

To examine this effect we will assume that the electrodes

are cylindrical and that the magnetic field is parallel to the electrode axis. The radius of the cathode will be taken very small compared with that of the anode. It is assumed that the space charge is at least sufficient to reduce the field at the cathode to zero, the radius of the potential barrier is also small, and that the electrons leave this with zero velocity.

The electric force in this case is not constant throughout the inter-electrode space. If ϕ is the potential at any point in the system, then the equations of motion become

$$\frac{d^2r}{dt^2} - r\left(\frac{d\theta}{dt}\right)^2 = \frac{e}{mc} \cdot \frac{d\phi}{dr} - \frac{eH}{mc} \cdot r \cdot \frac{d\theta}{dt} \quad . \quad . \quad (84)$$

$$\frac{1}{r} \cdot \frac{dt}{d}\left(r^2 \frac{d\theta}{dt}\right) = \frac{eH}{mc} \cdot \frac{dr}{dt} \quad . \quad . \quad . \quad . \quad (85)$$

By integrating equation (85) and assuming the particle leaves the barrier at zero time, we have

$$\frac{d\theta}{dt} = \frac{eH}{2mc}\left(1 - \frac{r_0^2}{r^2}\right) = \frac{eH}{2mc} \quad . \quad . \quad . \quad . \quad (86)$$

when the radius r_0 of the barrier is taken to be negligibly small.

By inserting (86) in (84), multiplying each side by $\frac{dr}{dt} \cdot dt$ and integrating, we obtain, assuming ϕ is zero at the barrier,

$$\left(\frac{dr}{dt}\right)^2 + \frac{e^2H^2}{4m^2c^2} r^2 = \frac{2e\phi_r}{mc} \quad . \quad . \quad . \quad . \quad (87)$$

where ϕ_r is the potential at radius r.

At the critical condition when the particle just grazes the anode the radial velocity is zero, and if V_c is the potential of the anode we have from (87)

$$V_c = \frac{H_c^2 e a^2}{8mc} \quad . \quad . \quad . \quad . \quad . \quad . \quad . \quad (88)$$

which is identical with the value previously obtained (equation 63) with space charge absent.

We now wish to determine the relation between anode current and voltage at the critical condition and also the time of transit from the barrier to the anode.

If ρ is the density of charge per unit volume, then Poisson's equation becomes, in cylindrical co-ordinates,

$$\frac{1}{r}\frac{d}{dr}\left(r\frac{d\phi}{dr}\right) = 4\pi\rho \quad . \quad . \quad . \quad . \quad . \quad (89)$$

and if I is the current per unit length of the cathode

$$I = 2\pi r\rho\frac{dr}{dt} \quad . \quad . \quad . \quad . \quad . \quad . \quad (90)$$

Combination of (89) and (90) leads to

$$\frac{d}{dt}\left(r\frac{d\phi}{dr}\right) = 4\pi r\rho\frac{dr}{dt} = 2I \quad . \quad . \quad . \quad . \quad (91)$$

This, on integration, and taking $r = 0$ at $t = 0$, gives

$$r\frac{d\phi}{dr} = 2It \quad . \quad . \quad . \quad . \quad . \quad (92)$$

When (86) and (92) are inserted in (84) we have

$$\frac{d^2r}{dt^2} + \frac{e^2H^2}{4m^2c^2}r - \frac{2eI}{mc}\frac{t}{r} = 0 \quad . \quad . \quad . \quad . \quad (93)$$

It is not possible to integrate this equation in order to determine the electron paths. The procedure followed by A. W. Hull (29) and S. J. Braude (11) is to obtain an approximate solution by assuming that the space-charge forces are unaffected by the magnetic field and inserting in equation (93) the relation

$$r = \sqrt{\frac{8eI}{3mc}}\, t^{3/2} \quad . \quad . \quad . \quad . \quad . \quad (94)$$

given by I. Langmuir (33).

On integration and taking $\frac{dr}{dt}$ as zero at the turning-point in the orbit, the transit time is given as

$$T = \frac{\sqrt{15mc}}{He} \quad . \quad . \quad . \quad . \quad . \quad . \quad (95)$$

which is 23% more than the value previously obtained (equation 74) with space-charge forces negligible.

A solution of this equation has also been given by F. B. Pidduck (40), who transforms (93) and expands it in a power

series. This leads to a value of the transit time to the turning point of

$$T = \frac{5{\cdot}038mc}{He} \quad . \quad . \quad . \quad . \quad . \quad . \quad . \quad (96)$$

which is 60% more than the value for zero space charge. The conditions obtaining in the magnetron under space charge limitation have also been examined by E. B. Moullin (39). It is shown by consideration of the planar magnetron that if the magnetic field is just less than the critical value, then the electric field at the cathode is always positive provided the filament emission is less than $9/4\pi = 0{\cdot}716$ of the space charge limited current appropriate to the anode potential employed. If the magnetic field equals or exceeds the critical value the anode current will cease, and all electrons will return to the cathode. In such circumstances the force at the cathode will be zero when the emission current is half that given above, and further increase of magnetic field will cause a contraction in the diameter of the electron cloud. It is then shown that when the field at the cathode is zero then the distance between the cathode and boundary of the cloud tends to half the distance it would be if the emission were very small. A similar relation is obtained in the cylindrical case by examination of the result obtained by F. B. Pidduck (40) that the radius of the cloud is given by $15{,}400I^{\frac{1}{2}}/H^{3/2}$, where I is the emission current in electromagnetic units. With a very fine filament a potential barrier cannot be formed at cut-off unless the emission current exceeds 0·04 of the space charge limited current. Thus it is concluded that space charge cannot produce a foot on the cut-off curve, and in fact it would seem to decrease the possibility of an electron reaching the anode, and that as the magnetic field is continually increased the effect of space charge should become progressively more negligible.

In practice, both the foot and the position of the precipice do depend on the emission and this is illustrated by Fig. 42*a*, which shows the cut-off curves on a Marconi CW10 magnetron for five different emission currents covering a range of 100,000 to 1. It will be noticed that for comparatively large emissions the anode current for a given voltage is independent of the current evaporated from the filament, and in the figure this

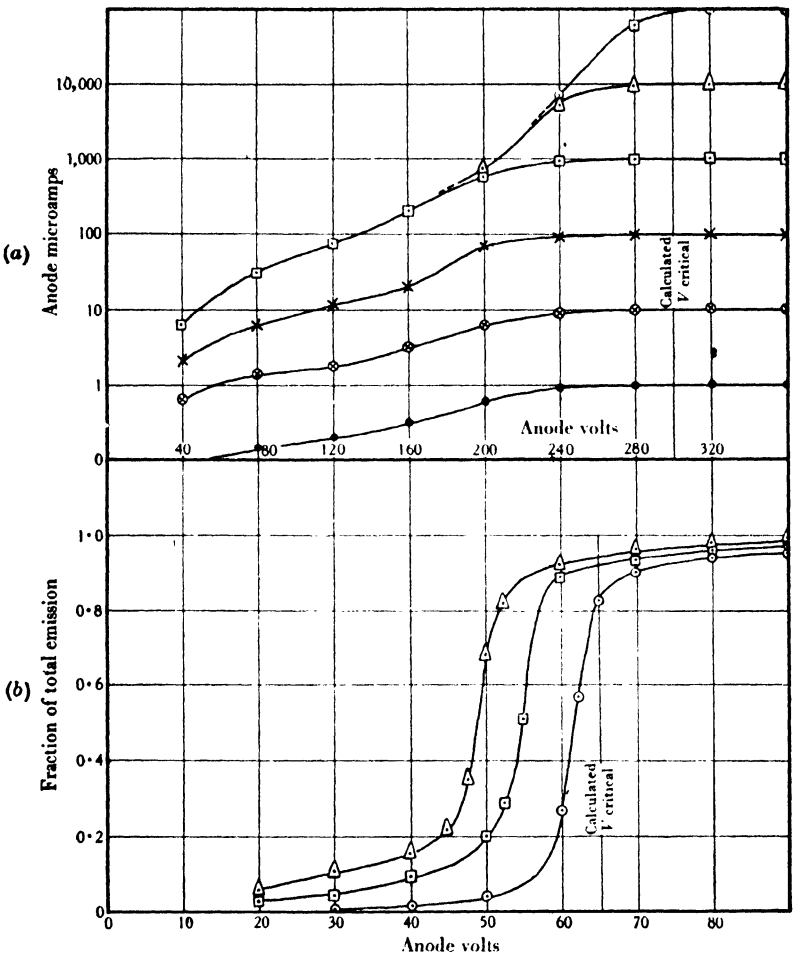

FIG. 42. Cut-off curves for magnetron CW10.

(*a*) (Upper half) Cut-off curves for magnetron CW10. Magnetic field 230 gauss.

Filament emission 100 mA ⊙
Filament emission 10 mA △
Filament emission 1 mA ⊡
Filament emission 100 μA ×
Filament emission 10μA ⊗
Filament emission 1 μA ●

(*b*) (Lower half) Cut-off curves for special long diode. Magnetic field 108 gauss.

Filament emission 10 mA ⊙
Filament emission 1 mA ⊡
Filament emission 100 μA △

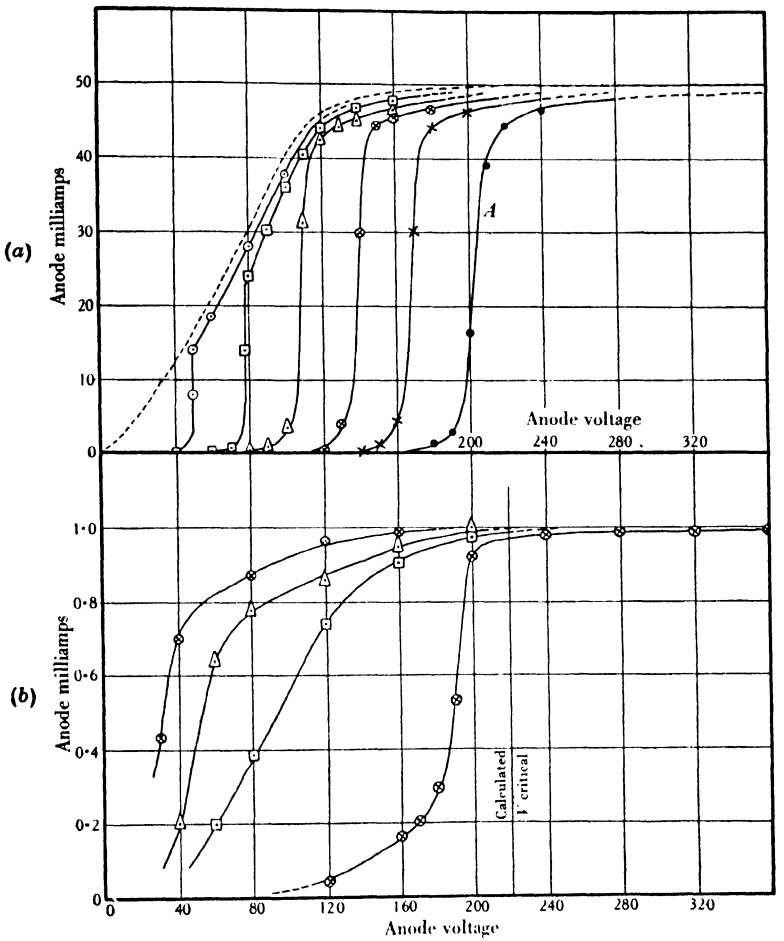

FIG. 43. Cut-off curves for the magnetron.

(*a*) (Upper half) Cut-off curves for magnetron CW10.
Filament emission 50 mA
Magnetic field
Dotted line zero, 77 gauss ⊙,
106 gauss ⊡, 124 gauss △,
144 gauss ⊗, 160 gauss ×,
183 gauss ●

(*b*) (Lower half) Cut-off curves for magnetron CW10.
Filament emission 1 mA
Magnetic field 200 gauss
Angle of tilt, zero ○
Angle of tilt, 4° ⊡
Angle of tilt, 8° △
Angle of tilt, 12° ⊗

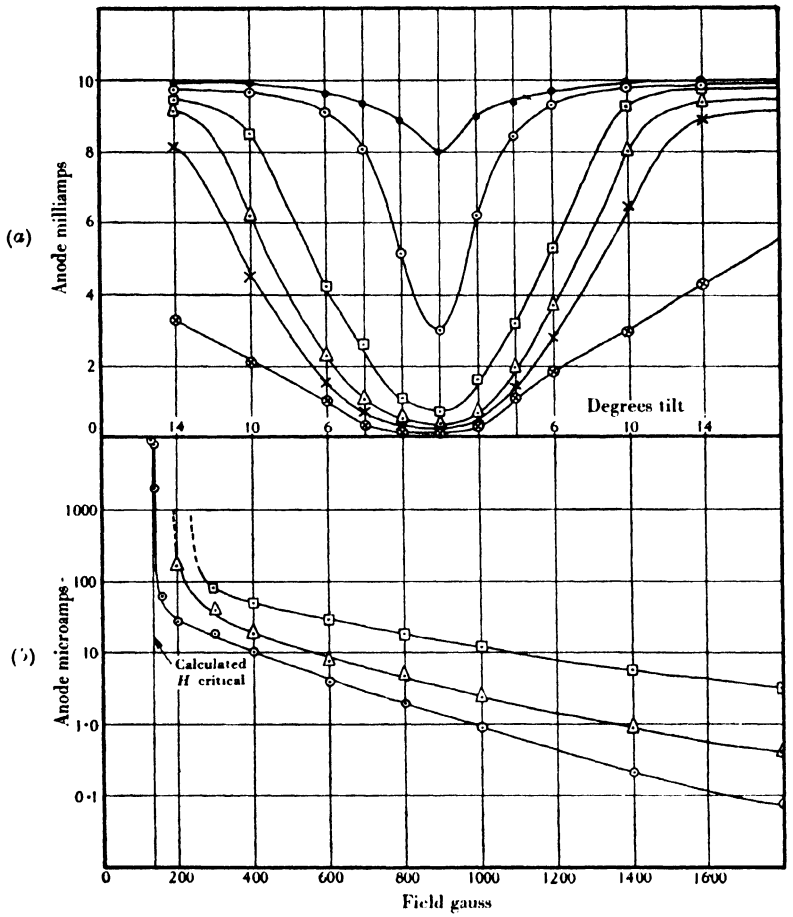

FIG. 44.

(*a*) (Upper half) Tilt curves for magnetron CW10.
Magnetic field 200 gauss
Filament emission 10 mA
Anode voltage 202 ●
Anode voltage 195 ⊙
Anode voltage 180 ⊡
Anode voltage 160 △
Anode voltage 120 ×
Anode voltage 80 ⊗

(*b*) (Lower half) Cut-off curves for magnetron CW10.
Mean anode voltage 100
Filament emission 10 mA
Angle of tilt, zero
Potential between segments, zero ⊙
Potential between segments, 20 volts △
Potential between segments, 40 volts ⊡

holds over a range of 100 to 1. When the emission is only a few microamperes the cut-off curve has a foot very reminiscent of Fig. 41*a*. Undulations on the foot have often been attributed to the undetected presence of electronic oscillations, but every precaution was taken, by the use of condenser shunts, etc., to inhibit such oscillations in the circuit used.

Fig. 43*a* is instructive in showing the effect of a magnetic field greater than the critical value on an anode current which is space-charge limited, while Fig. 44*a* shows a curve of I_a as a function of α for an emission of 10 mA. Comparison of curves, such as those of Figs. 42*a* and 44*a*, taken with different filament emissions suggests that the presence of space charge tends to reduce dissymmetry due to small imperfections of concentricity and alignment, an effect which is perhaps inherently probable.

It should be noted that if from Fig. 43*a* we plot the square of the magnetic field against the anode voltage at a selected current on the steep portion of the curves (say when I_a has fallen to 15 mA), we obtain a practically linear relation, although the line does not pass through the origin. For the tube used, a and b were respectively 5 and 0·065 mm., and the slope of this line yields a value of e/m, which is too small by about 1% but is correct within the limits of experimental error.

Field Fringing. The effect of fringing may be examined either by the use of guard-ring extensions to the anode or by comparing the cut-off curves obtained from long and from short diodes. Some experiments were made on two special diodes, the anodes of which consisted of a central cylinder about 1 cm. long with two guard-rings on either side and separated from it by narrow gaps. The diameter of the anode and rings was about 6 mm., but it was observed that the axes of the anode and rings were not parallel in these two diodes type E585, Nos. 2 and 4. Thus application of the magnetic field causes a longitudinal motion of the electrons and the anode current may increase at cut-off. Hence, although the results follow the previous curves, the experiments were not conclusive in deciding to what extent the fringing of the electric field modifies the cut-off curves. Fig. 45 gives the curves for these diodes, and it will be seen that the cut-off is

very indefinite. Fig. 46 shows the variation of anode current as the electrode axis is tilted with respect to the magnetic field.

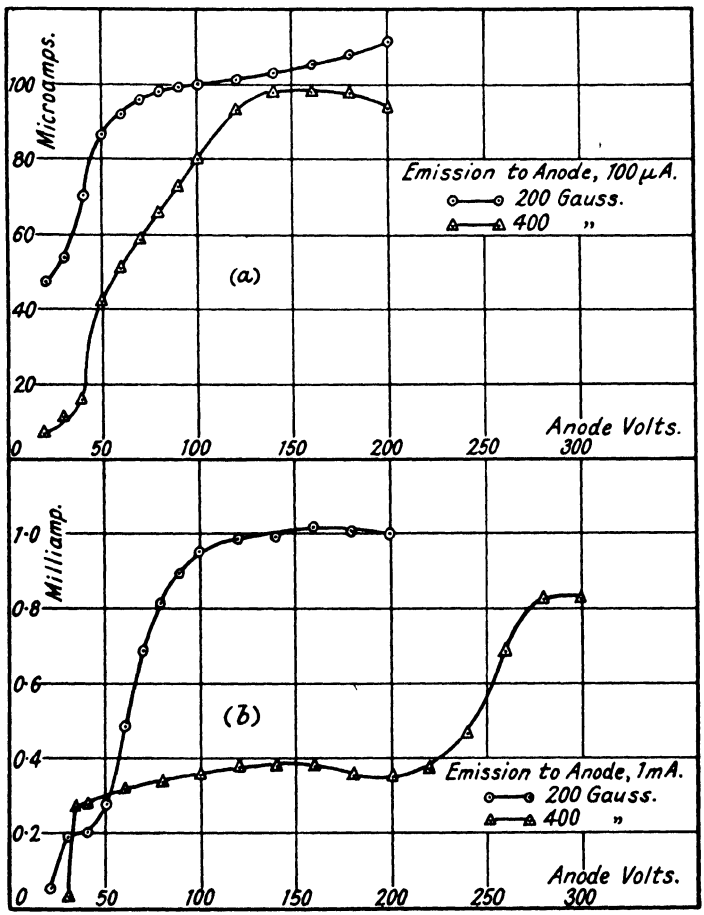

FIG. 45. Cut-off curves for guard-ring diode.

Accordingly measurements were made on the special long diode previously described. The tungsten filament of this tube was kept in tension by a molybdenum spring and appeared to be both concentric and coaxial with the anode to a considerable degree of accuracy, while special care was taken

with such a long electrode to ensure that the magnetic field had no radial component of appreciable magnitude at any point of the length.* The cut-off curves obtained are shown in

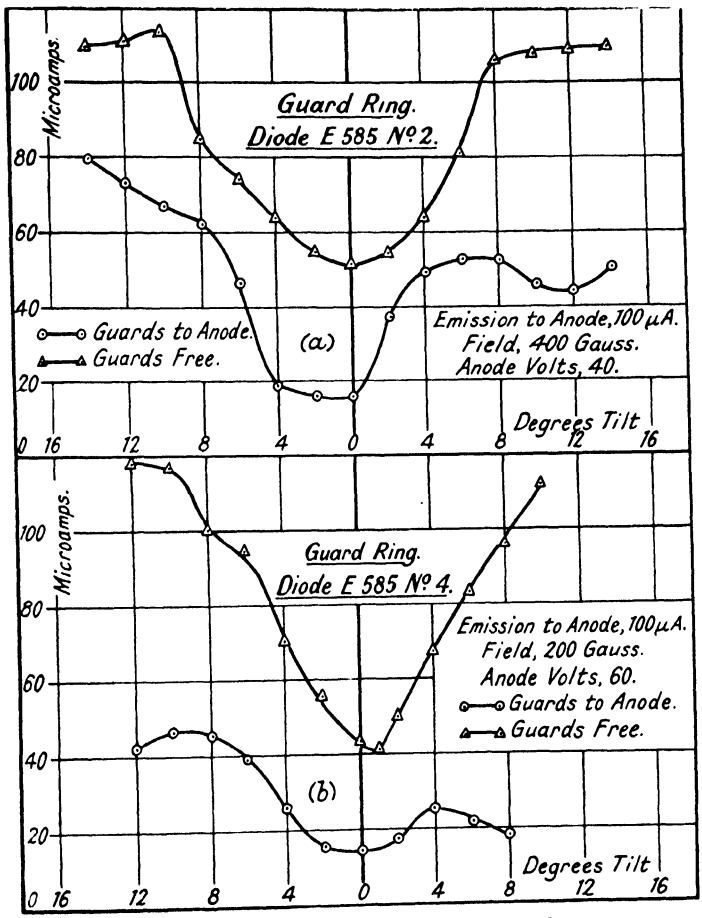

FIG. 46. Tilt curves for guard-ring diode.

Fig. 42*b* and do not approach the ideal more closely than those of Fig. 43*a*. It is therefore concluded that the fringing of electric field at the ends of the anode has no important effect on the cut-off curve. It was found that tilting the tube by $\pm$ 1° in three different planes by a three-point support did not

* See page 87 equation (67).

affect the cut-off curve in any part by a detectable amount. Hence it is thought that the curves of Fig. 42*b* probably approach the ideal as closely as can be obtained with any practical apparatus.

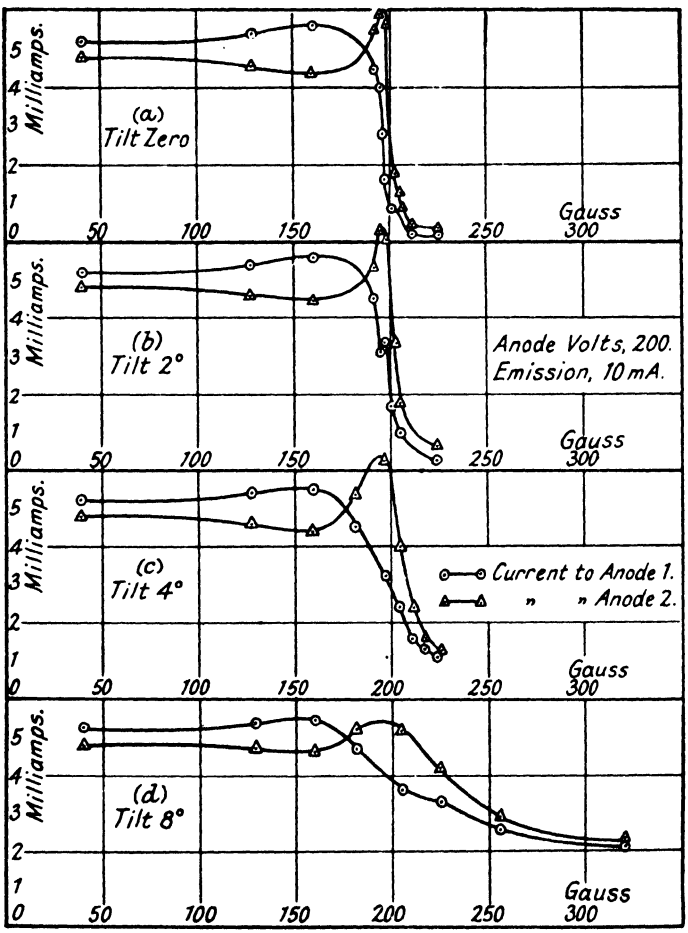

FIG. 47. Split-anode magnetron cut-off curves.

The anode of the magnetron type CW10 was in the form of two segments, and in most of the above experiments these were joined together and kept at the same potential. As a further possible test of the effect of small imperfections of

construction the current was measured, in the cut-off region, for each half anode. Fig. 47 shows these cut-off curves for each segment, which were held at the same potential, for four different angles of tilt of magnetic field. At fields well removed from the cut-off value the curves for either segment do not differ appreciably, but it will be noticed how sensitive, near the cut-off field, the anode current is to minute imperfections in electrode geometry, such as anode diameter, etc.

Random Electron Motion. If electrons are emitted from an equipotential cathode with initial energy eV and without a component of velocity along the filament, they will traverse a circular path of diameter a such that

$$V = \frac{eH^2}{8mc^2} a^2 \quad . \quad . \quad . \quad . \quad . \quad . \quad . \quad (97)$$

the anode being at cathode potential. In such circumstances the curve relating anode current and magnetic field may be expected to reveal the velocity distribution of the electrons. If H is expressed in terms of V, the curve may well be expected to coincide with that relating anode current to the negative potential of the anode in the absence of magnetic field (retarding field characteristic). However, experiment shows that these are not the same, and, for example, the filament temperature of the long diode was adjusted to give an emission current of 100 μA, the filament drop being about 4 volts. A curve was then obtained relating the anode current to the negative potential of the anode, reckoned with respect to the potential of the mid-point of the filament. Then, with the anode at the potential of the mid-point of the filament, a curve was obtained relating the anode current to the magnitude of the axial magnetic field, which was expressed in terms of equivalent volts by equation (97). The results of these two experiments are shown below :—

TABLE VII

I_a in μA . .	60	42	26	11	5	2	1
$-V_a$ in volts .	0	0·5	1	1·5	2	2·5	3
Volt equiv. of H .	0	0·70	1·4	2·8	6·2	11·5	15

This table shows that the presence of the magnetic field appears to increase enormously the proportion of high velocity electrons. Thus a negative potential of 3 volts suffices to reduce the anode current to one-sixtieth of its value when the anode potential is zero. But to reduce the current to the same fraction when the anode potential is zero requires a magnetic field corresponding to an emission energy of 15 volts. It does not seem possible for the electrons to gain energy from the magnetic field directly, and it may be that the effect is due to some high-frequency oscillation within the tube which discloses itself only in this way. Presumably this effect is associated with the persistent tail of the cut-off curves, and such a gain of electron energy would account for the well-known effect, discussed by I. M. Wigdortschik (45) and others, of additional heating of the filament by the returning electrons when the magnetron is operated near the cut-off condition at high anode potentials. It has also been shown by E. G. Linder (34, 35) that in certain circumstances the electrons may have greater energy than can be accounted for simply by the electric potentials and initial velocities. In the cut-off condition in the magnetron, and also under certain circumstances in retarding field tubes, a fraction of the orbital energy of an electron is converted into energy of random motion, and thus the electron will not, in general, return to the cathode surface. If it is assumed that a mean amount of energy of V electron volts per electron is changed from the orbital to the random type, then electrons will be able to travel towards the cathode only up to a limiting distance at which the potential is V. At this equipotential cylindrical surface the electrons retain their random motion which is Maxwellian in nature and thus a virtual cathode is formed. The theory is supported by experimental results obtained by probe measurements, and the various possible causes for this interchange of energy or " scattering " are considered. Such causes are scattering by gas molecules, collisions between electrons and electron oscillations of a plasma nature.

Conclusions. Although no definite conclusion has been reached on the cause for these discrepancies in the cut-off curve, it has been shown that the anode current cut-off is

sharp, and moreover occurs very nearly at the field given by theory only when the emission is large. When the emission current is small the divergence from theory is large, and in view of the thorough treatment of this problem it seems unlikely that this is due to merely geometric and static causes alone. When the high-frequency properties of the magnetron are considered later it will be further evident that dynamic effects in the cut-off region, even in the absence of external circuits, cannot be entirely excluded.

(*b*) DYNATRON RÉGIME

Negative Resistance Properties. Some curves relating to the split-anode magnetron have already been given, but when the potential of either segment is varied about a mean value in the presence of a magnetic field greater than the cut-off value the current flowing to the segments is typified by Fig. 48 for three different values of magnetic field (including zero). These curves show the remarkable property that the current flowing to the segment which is instantaneously at the lower potential is, within limits, greater than that to the higher potential segment. Thus to a small alternating voltage the magnetron behaves as a negative resistance, and when the magnetic field is greater (smaller standing current) this negative resistance obtains over a larger voltage amplitude. When the potential difference between the segments is large, then the higher potential segment takes more current, and thus at a certain voltage amplitude the magnetron resistance changes from negative to (through infinity) positive values. While the above curves were taken with magnetic fields only slightly exceeding the cut-off value, Fig. 49 illustrates the results with a field strength nearly twenty times this value; and although the current values are minute the magnetron still exhibits negative resistance properties, but the resistance is of the order of megohms, compared with the value of about 1 kilohm near the cut-off condition.

When a thermionic tube has the properties of a negative resistance it is capable, when connected to a tuned circuit of sufficient dynamic resistance, of maintaining continuous

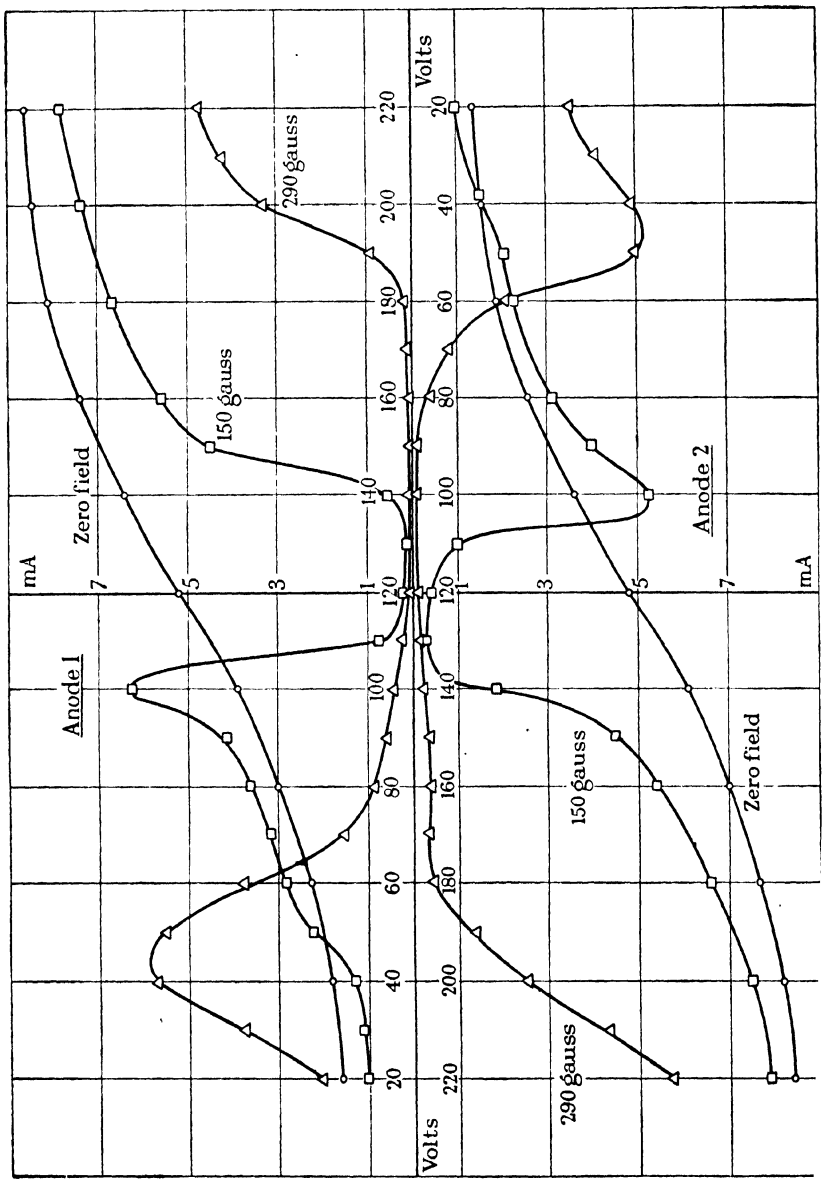

FIG. 48. Static curves of magnetron. Filament emission 10 mA.

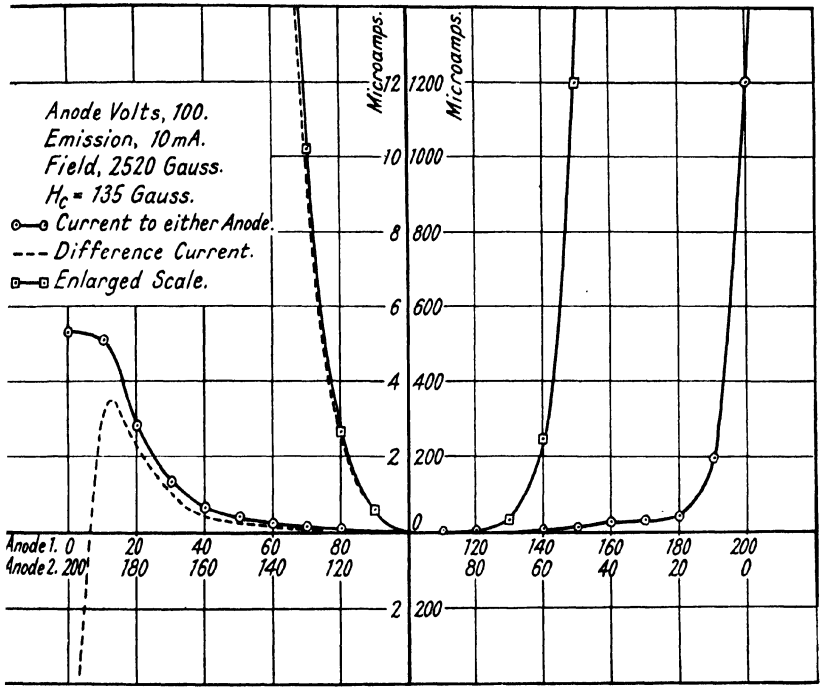

FIG. 49. Static curves at intense magnetic field strengths.

oscillations. The split-anode magnetron is no exception to this and from similarity with the negative resistance triode and tetrode this mode of oscillation is termed "dynatron," and in general the analysis of dynatron tubes, Poulsen arc generators, etc., can be applied directly to it. Thus if the 3,000 $\mu\mu$F condenser shown in Fig. 60 were charged and then connected across the 300 μH coil, the subsequent oscillation would cause the potential of the two segments to fluctuate, in antiphase with one another, about the mean potential provided by the high tension supply. In the absence of the magnetic field of the magnetron, the tube would increase the damping of the oscillation; if, however, the current flowing to the cathode from each segment tends to decrease with rising potential, then the tube will decrease the damping or even make it negative. For magnetic fields exceeding the cut-off

value, anode current tends to flow only on the peaks of the voltage cycle, and thus in this respect the split-anode magnetron is similar to the Class C amplifier or oscillator tubes, previously considered, operating in push-pull. There does not appear to be a complete explanation for the existence of these properties, but it is probably due in some measure to the distortion of the electrostatic field by the potential difference between the segments, as has been suggested by E. W. B. Gill and K. G. Britton (18) and H. Zuhrt (47).

It will be convenient to consider here the radius of the electron cloud under static conditions when $H \gg H_c$. If the cloud radius is r and the emission is assumed small, so that

$$\frac{V_r}{V} = \frac{\log r/b}{\log a/b} \quad . \quad . \quad . \quad . \quad . \quad . \quad (98)$$

then

$$\frac{r}{a} = \frac{H_c}{H} \frac{[1 - b^2/a^2]}{[1 - b^2/r^2]} \sqrt{\left(\frac{\log r/b}{\log a/b}\right)} \quad . \quad . \quad . \quad (99)$$

and for the magnetron CW10 we have the values shown in the following table :—

TABLE VIII

H/H_c .	1·0	1·8	4·0	7·0	12·8	27·2	36·3	58·8	∞
a/r .	1	2	5	10	20	50	60	70	77
r/b .	77	38·5	15·4	7·7	3·85	1·54	1·28	1·10	1·00
$I_a(\mu A)$	10^4	25	5·0	1·1	0·1	0·003	—	—	—

The last line gives for reference the measured anode current when both segments were at 100 volts with a filament emission of 10 mA. Thus at the high magnetic fields of Fig. 49 the electron orbits are not far removed from the cathode. It has been shown by E. B. Moullin (39) that with a finite emission the radius of the cloud is less and that if the space charge is sufficient to cause the field at the cathode to become zero, then the cloud radius tends to one-half the above values. The effect of magnetic field tilt has been shown previously to (*a*) tend to reduce space charge by causing electrons to move longitudinally and finally leave the inter-electrode space, and (*b*) incline the axis of the cylindrical cloud and bring it closer

to the anode to an extent depending on the angle of tilt and the length of the electrodes.

With the split anode magnetron, when the resultant current i flowing through the coil (the difference of the currents flowing to either anode) is plotted against an angular base θ, then the fundamental component can be determined from Fourier analysis by taking twice the mean value of $i \sin \theta$. Since the voltage amplitude is known, this gives directly the fundamental component of negative resistance. From the above static characteristics it is evident that there is a maximum value of power output given by the ratio (voltage amplitude)^2/resistance occurring at an optimum magnetic field which is generally about twice the cut-off value. Fig. 50 shows the cycle of

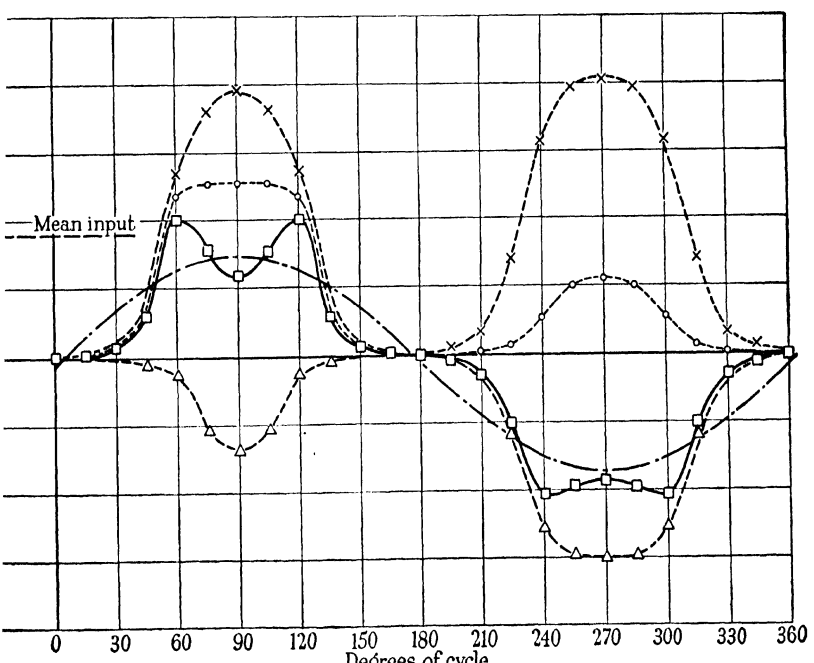

FIG. 50. Cycle of currents deduced from Fig. 48.

Anode 1 ⊙ - - - - - ⊙
Anode 2 △ - - - - - △
Output ($A_1 - A_2$) □ ——— □
D.C. input ($A_1 + A_2$) × - - - - ×

Output (fundamental) —— · ——
Total a.c. voltage 110 (r.m.s.).
Field strength, 290 gauss.

currents under a given set of operating conditions, the full line curve representing the power component of current in the tuned circuit. Since the anode current is sensibly cut off when the tube is not oscillating, it is clear that the battery supplies power by virtue of the rectified current which results from the oscillation, and this is shown on the same diagram. It has been shown by E. C. S. Megaw (36) how the magnetron properties in this régime can be calculated by this method of Fourier analysis.

When the period of the fluctuating inter-segment potential is large compared with the transit time of the electrons the magnetron in this régime can be considered as a symmetrical two-terminal impedance (apart from necessary connections to the filament and high tension supplies) with zero phase angle. In the absence of magnetic field the transit time is given approximately by

$$T = \frac{2{\cdot}5}{100} \cdot \frac{d_{cm}}{\sqrt{V_{\text{volts}}}} \mu\text{secs.} \quad . \quad . \quad . \quad (100)$$

and the critical field increases this by a factor of about four. Thus if $v = 100$, $d = 0{\cdot}5$, T is of the order 1/200 microsec., and provided the frequency is less than, say, 10 Mc/s the effects of transit time can be neglected. Hence some measurements were made on the properties of the split-anode magnetron in the dynatron régime, and for these the mains frequency of 50 c/s was chosen as being the most convenient.

It will be understood that the amplitude of oscillation which can be maintained in a circuit must have that value for which the fundamental component of resistance of the tube is equal and opposite to the dynamic resistance of the circuit. Hence a low-frequency measurement of this fundamental component will enable the performance of the magnetron at any frequency appreciably less than the inverse of the transit time of the electrons to be predicted.

Measurements at Low Frequency. The fundamental component of resistance can be measured at power frequencies by a dynamometer; for if the complex anode current passes through the suspended coil, and the field, due to the fixed coils, alternates simple-harmonically at the fundamental frequency

of the anode current, the resulting couple is due only to that fundamental component. A fuller description of this method as applied to normal tubes has been given by D. A. Bell (2) and E. B. Moullin (38), while the results obtained with magnetrons have been described by the author elsewhere (26).

The circuit diagram of the measuring system is shown in

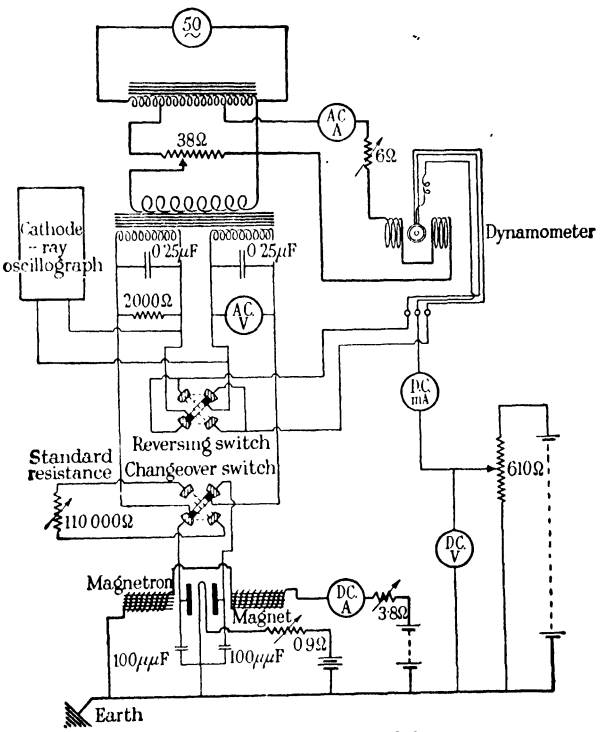

FIG. 51. Diagram of connections used for measurement of magnetron impedance.

Fig. 51. The H.T. supply was connected to the centre tap in the suspended coil, and the suspension strips were used to connect the two ends of the coil, through identical windings of a transformer, to the anodes. The moving coil had an inductance of 18 μH and a resistance of 60 Ω, and the fixed coils had an inductance of 12 μH; thus the respective reactances were small compared with the resistances in series with them. The dynamometer, complete with deflection coils,

was mounted in a wooden case with glass front and rear panels and the coil deflection was observed by means of a small mirror and the usual lamp and scale. The voltage amplitude was applied to the segments by means of a double secondary transformer of the normal silicon iron laminated core type with the coils of D.C.C. copper wire wound on ebonite formers. Care was taken to see that no unintentional wave-form distortion took place due to magnetic saturation, even at the highest voltages employed.

A 3-in. diameter gas-focussed cathode ray oscillograph, complete with built-in amplifier, time base, high tension supply, etc., was also connected to the circuit. Apart from making observations on the current wave-form of the magnetron, this instrument was used for detecting the undesired presence of high-frequency oscillations which revealed themselves as a sudden broadening of the wave-form trace usually on the nearly vertical sides where the magnetron resistance is extremely low.

The negative resistance of the tube at any assigned amplitude was determined by matching the observed deflection with that which resulted when the tube was replaced by a standard known non-inductive resistance. The deflections were given the same sense by reversing the leads to the moving coil. The

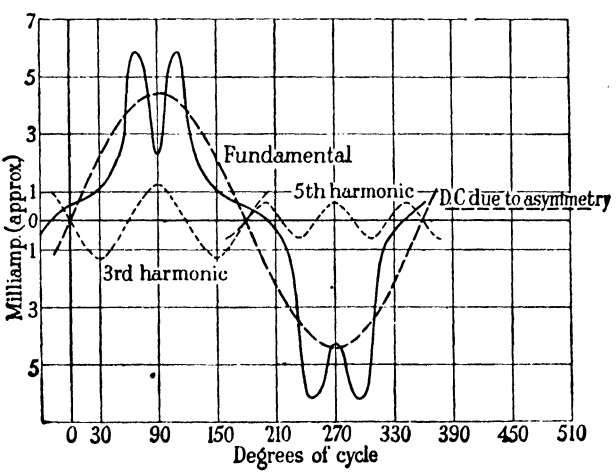

FIG. 52. Wave-form of magnetron, deduced from oscillogram.

sensitivity was such that resistances up to 0·25 MΩ could be measured with applied potentials of the order of 100 volts (r.m.s.). The accuracy of the method was verified by making a Fourier analysis of oscillograms of the anode current. An example taken under conditions differing only slightly from those stated in Fig. 51 is given in Fig 52, the resistance value measured as above being almost identical with the value revealed by analysis.

To examine whether the experimental results are sensitive to small changes in anode voltage the test corresponding to that recorded in Fig. 52 was performed with a peaked wave-form of voltage containing third and fifth harmonic components of approximately 5% and 3% respectively. This was obtained from the output of an electrical generator with a small number of slots per pole, and the oscillograph was used as a means of estimating the harmonic components. It was found that such change in wave-form resulted in the output being decreased by 11% from 409 to 363 mW. Since Fourier analysis of the curve of anode current in Fig. 52 reveals a ratio of $I_3/I_1 = 0{\cdot}28$ and $I_5/I_1 = 0{\cdot}14$, then, as shown in p. 11, for any reasonable magnification Q of the anode circuit no harmonic component of voltage is as great as 1%. Thus it is clear that the method described is sensibly correct even when the oscillatory circuit has a magnification much lower than would be tolerated in practice.

Voltage Amplitude. The relations between the fundamental component of negative resistance and the r.m.s. value of the sinusoidal fluctuations of anode potential are shown in Fig. 50*a*. The resistance is high for small amplitudes and reaches a minimum when the amplitude increases, and finally again becomes large and ultimately positive. If the dynamic resistance of the tuned circuit is less than this minimum value then oscillation will not be maintained. Since the resistance is high for small amplitudes, it is only possible to start the oscillation by temporarily increasing the circuit resistance or reducing the magnetic field. For any circuit resistance higher than the minimum it is seen that two amplitudes are possible, the smaller one being unstable.

Power Output. Ignoring the very small power dissipated

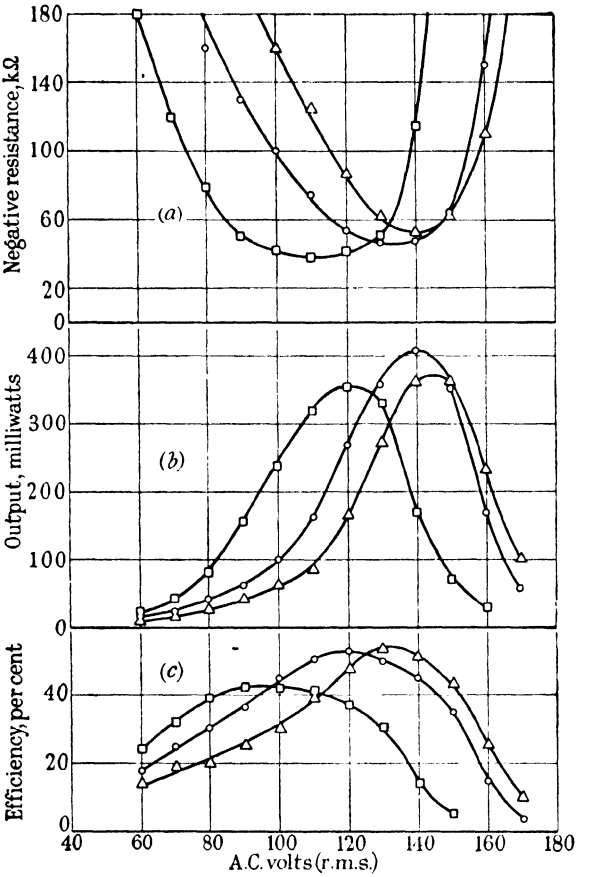

FIG. 53. Variation with voltage amplitude.

Anode voltage	120
Filament emission	50 mA
Field 220 gauss	□——□
Field 290 gauss	○——○
Field 345 gauss	△——△

in the circuit by the higher harmonic components of current, the output would be V^2/R, where R is the negative resistance appropriate to the amplitude V. Fig. 53*b* shows this output and the curves rise to a maximum which occurs very near to the value of V giving minimum resistance. In practice this optimum resistance value would be obtained by two tapping

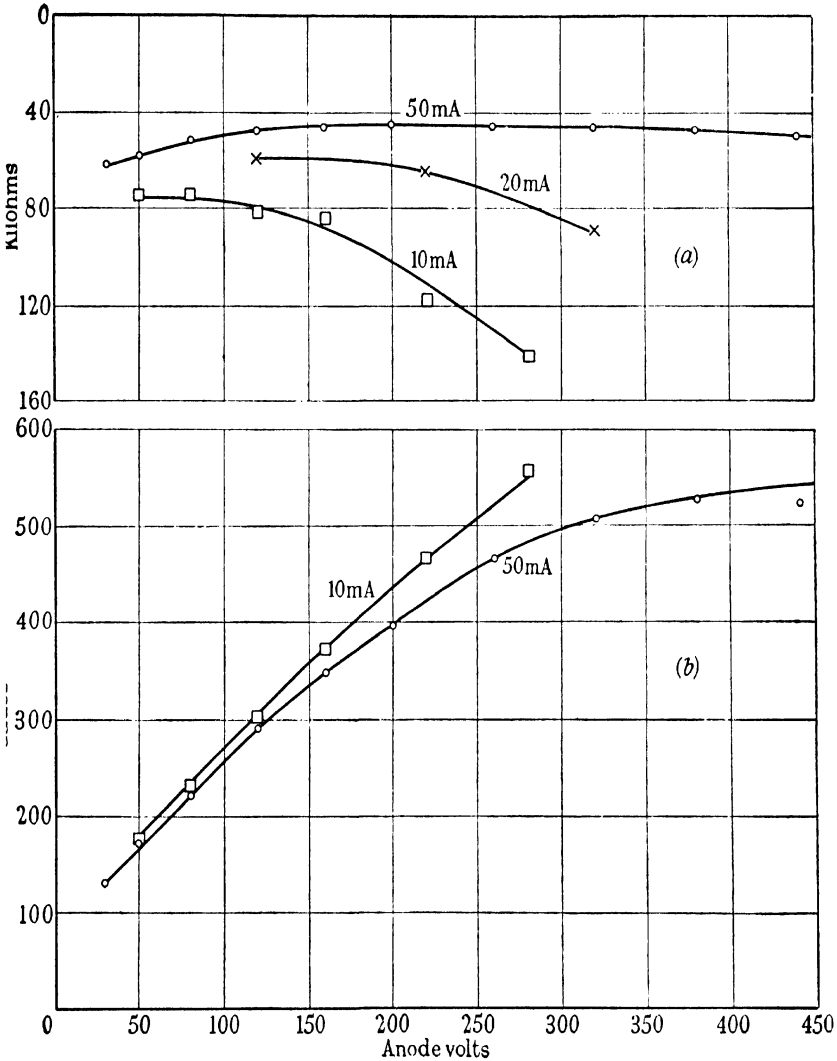

FIG. 54. Variation with anode voltage.

(*a*) Variation of optimum load impedance with anode voltage.
Total filament emission 10 mA □——□
Total filament emission 50 mA ○——○
Total filament emission 20 mA ×——×
(*b*) Variation of optimum field strength with anode voltage.
Total filament emission 10 mA □——□
Total filament emission 50 mA ○——○

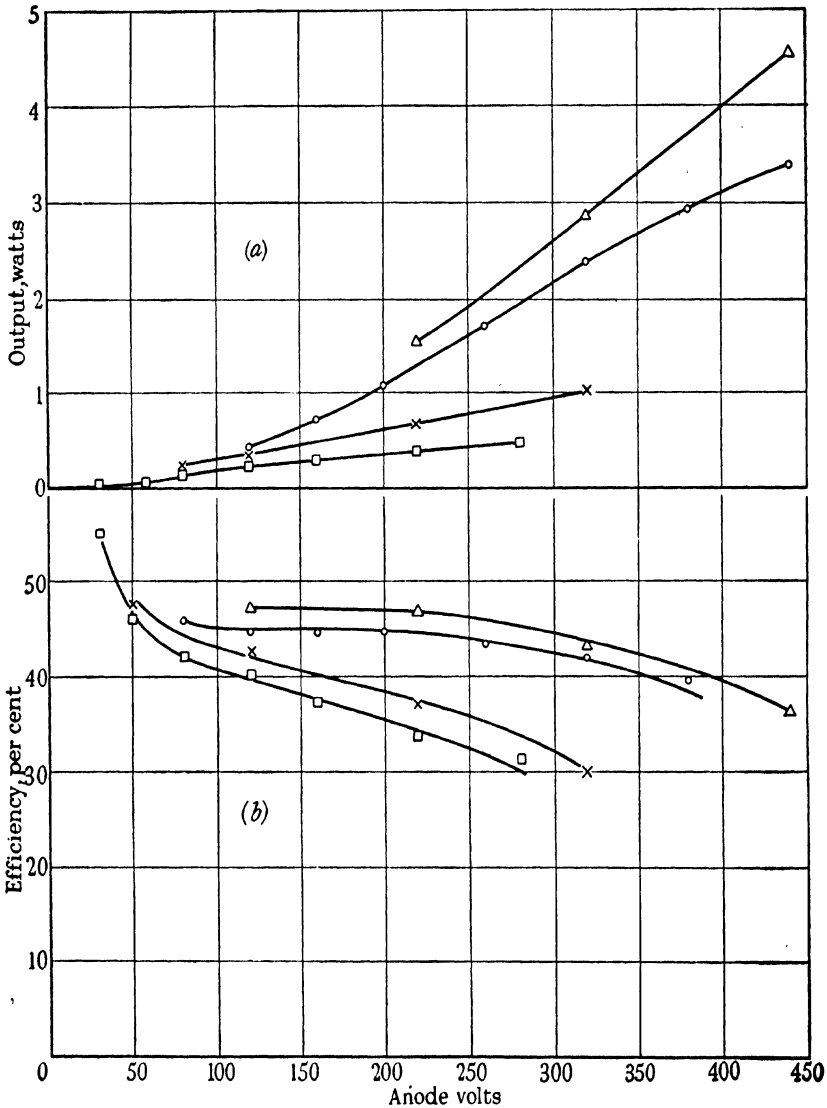

FIG. 55. Output and efficiency with anode voltage.

(*a*) Variation of maximum output with anode voltage.
(*b*) Variation of efficiency at maximum output with anode voltage.

Total emission 80 mA △——△
Total emission 50 mA ○——○
Total emission 20 mA ×——×
Total emission 10 mA □——□

points on the coil. Measurement of the rectified anode current enables the efficiency to be calculated, and this is shown in Fig. 53*c*. Comparison of these sets of curves shows that the amplitude for maximum efficiency is nearly that for maximum output and that there is a best value for the magnetic field, which in general is about twice the critical field. These optimum conditions are examined below.

Fig. 54*a* shows the manner in which the load resistance for maximum output is related to the voltage of the high-tension supply for different filament emissions. The field strength for maximum output increases in a nearly parabolic manner with anode voltage as shown in Fig. 54*b*, the effect of filament emission being small.

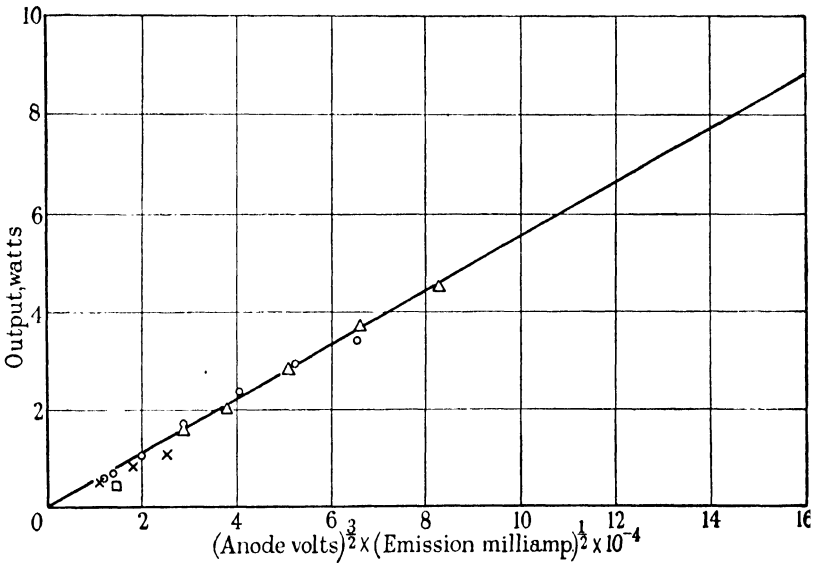

FIG. 56. Variation of output with anode voltage and filament emission of magnetron.

Emission 80 mA △ Emission 50 mA ○
Emission 20 mA × Emission 10 mA □

Figs. 55*a* and *b* show the relation between maximum output and efficiency respectively with supply voltage, and it will be seen that it is important to have as large a filament emission as possible. It was not possible to use supply voltages up to

the maximum for this particular magnetron (or tube) (1,000 volts), but Fig. 56 gives a relation between output and supply voltage and filament emission which can be used as a guide. It is seen that this relation is best given by the equation

$$W_{\text{watts}} = 0{\cdot}55 \times 10^{-4} \times V_{\text{volts}}^{3/2} \times I_{\text{mA.}}^{1/2} \quad . \quad . \quad (101)$$

Tilt of Magnetic Field. The previous experiments were made with the direction of the uniform field coincident with the axis of the electrodes. Fig. 57*a* shows the effect on the output of inclining the electrode axis to the field. The upper and lower curves relate to a constant field strength, and show the relation between maximum output and angle of tilt; it may be seen that in these conditions the output may be increased or decreased by tilting the electrodes. These changes, however, are not due to adjustment of the axial component of the field strength as such (thus $\cos 6^\circ = 0{\cdot}9945$), but are related to pronounced changes in the foot of the cut-off curve. The middle curve of Fig. 57*a* relates to a test in which the field strength was adjusted to give maximum output at various angles of tilt. Fig. 57*b* shows the corresponding curve of efficiency in the three conditions of test used in Fig. 57*a*. The efficiency is small at large angles of tilt, because then the current cannot be cut off by the field in the static state. Examination of the wave-form of current showed that the harmonic content in certain cases was reduced slightly by tilting the field; this is probably associated with the small rise of efficiency and output.

Anode Modulation. The behaviour of the tube under conditions of anode modulation for use as a radio telephone transmitter is given in Fig. 58 for different constant values of magnetic field and circuit impedance. On the rising portion of the curve only a certain depth of modulation can be used without causing the oscillations to cease, but the linearity is good. The falling portion enables nearly full modulation to be obtained, but the linearity is not good, the efficiency is poor due to the employment of high anode voltage at a comparatively low field strength, and, as will be seen below, considerable frequency modulation is present.

Frequency Stability. In the absence of changes, due to temperature, etc., in the values of the circuit parameters the

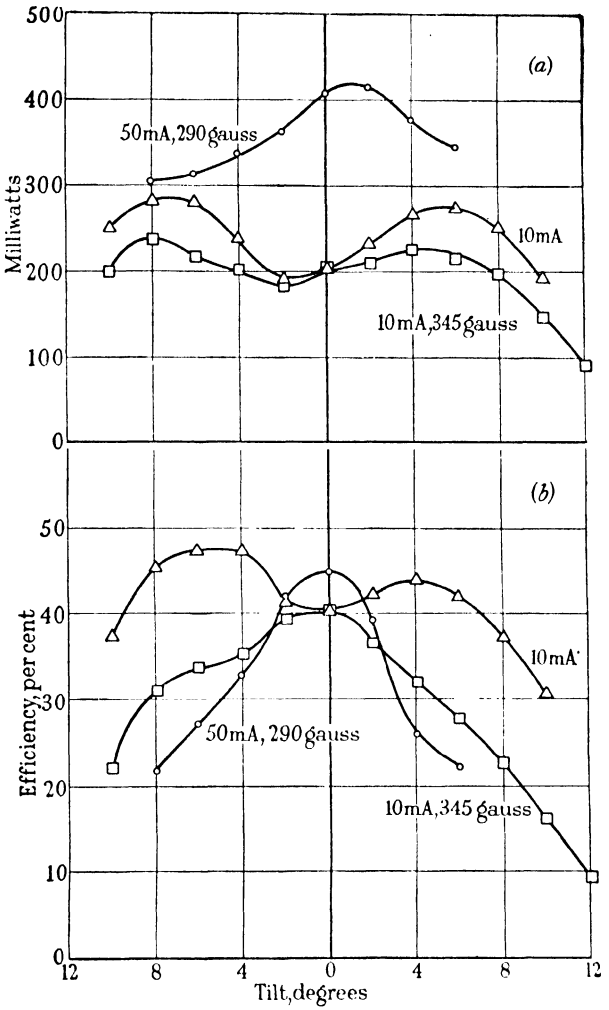

FIG. 57. Effect of tilt of magnetic field.

(*a*) Variation of power output with tilt of field, at constant anode voltage (120) and saturation emission.
(*b*) Variation of efficiency with tilt of field, at constant anode voltage (120) and saturation emission.

With constant field and optimum load impedance ○——○
With constant field and optimum load impedance □——□
With optimum field and optimum load impedance △——△

frequency stability depends mainly on the harmonic content of the anode current, and the analysis given for the dynatron by E. B. Moullin (37) can be applied to the magnetron directly.

The frequency stability of the magnetron in this régime was

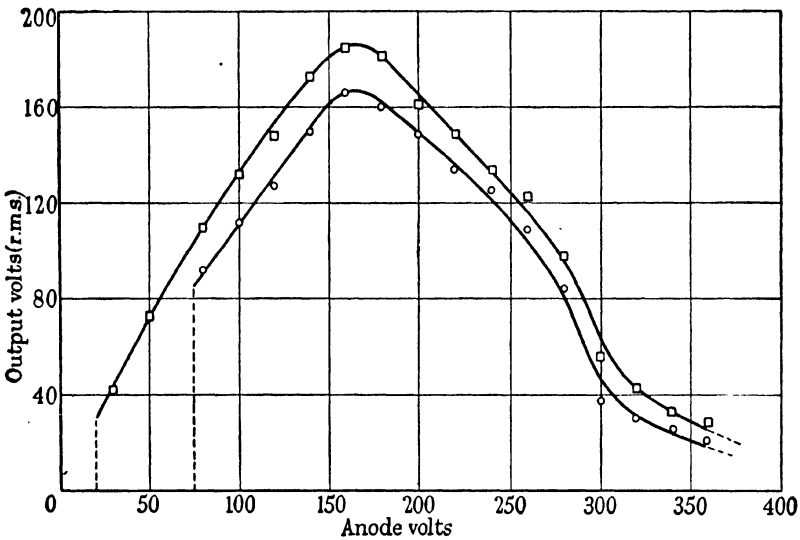

FIG. 58. Variation of output voltage with anode voltage.
Field strength 230 gauss
Filament emission 50 mA
Load impedance 50kΩ ○——○
Load impedance 200kΩ □——□

determined at a low radio frequency when acting as a self-contained generator, the practical details of which are given below. The frequency was compared with that of a suitable source of standard frequency by means of a normal radio receiver which emitted a beat note corresponding to the frequency difference. The tuned circuit of the magnetron included a small calibrated condenser which had a range of variation of about 10 $\mu\mu$F, and this was adjusted so that the beat note was equal to the steady frequency (about 1,000 c/s) given by a separate audio-frequency generator, this being accomplished by detecting the second beat note with a pair of headphones and the receiver loud speaker. Since the

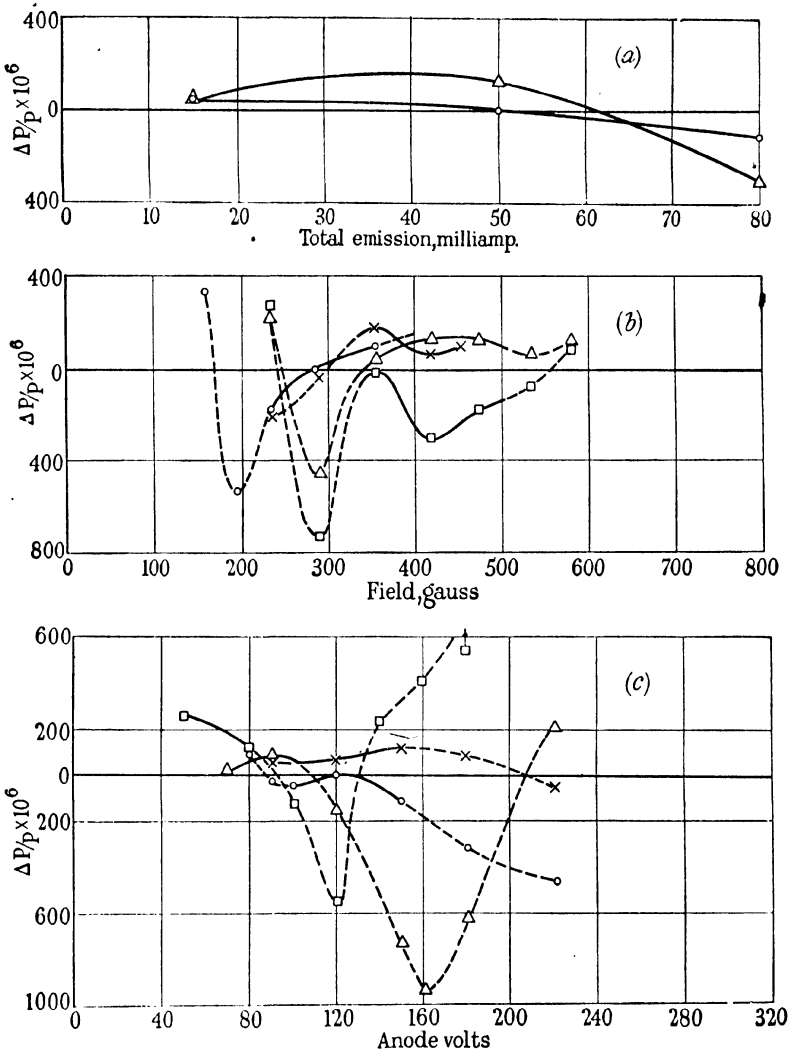

FIG. 59. Variation of frequency with operating conditions. Mean frequency 200 kc./sec.; load impedance 63 kΩ.

(*a*) 220 volts, 420 gauss △——△
120 volts, 290 gauss ○——○

(*b*) 120 volts, 50 mA ○——○
220 volts, 50 mA △——△
220 volts, 15 mA ×——×
220 volts, 80 mA □——□

(*c*) 235 gauss, 50 mA △——△
290 gauss, 15 mA ×——×
290 gauss, 50 mA ○——○
195 gauss, 50 mA □——□

T.T.

total tuning capacitance is known, simple calculation enables the change in generated radio frequency for a given change in fine tuning capacitance, consequent upon changes in the external operating conditions, to be ascertained.

Some measurements are given in Figs. 59*a*, *b* and *c*, the latter being of importance in showing the variation in carrier frequency under anode modulation. Provided the tube is operated near its best conditions, the frequency changes as shown by the full lines are small, but become large when the conditions are such that the output is small and the current wave-form very distorted. Comparison with Fig. 58 shows that the value of anode voltage for maximum output corresponds to the position of minimum frequency.

Radio Frequency Measurements. As a further check on the validity of the method of predicting the performance in terms of the fundamental component of negative resistance appro-

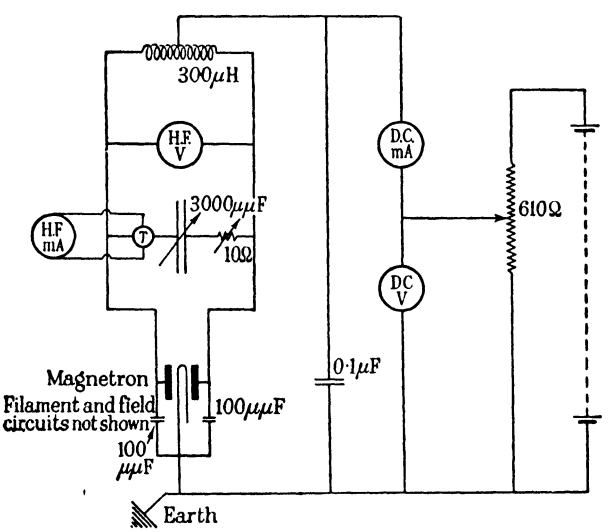

FIG. 60. Diagram of connections for radio-frequency measurements.

priate to a sinusoidal fluctuation of anode voltage, the output was measured when the system was acting as a self-contained generator.

A frequency of about 200 kc/s was chosen because it was convenient for measurement, far removed from the conditions of tests at 50 c/s and also from the region of resonance oscillations. The circuit diagram is drawn in Fig. 60, which also shows the values of the various circuit components. It was necessary to connect the two anodes to the cathode by condensers of 100 $\mu\mu$F capacitance as shown to prevent short-wave oscillations. The high-frequency resistance of the coil and condenser (when connected to the cold magnetron) was measured in the frequency range 170 to 290 kc/s ; in this range the magnification Q was constant to within $\pm$ 2% and had a mean value of 166. The current through the condenser was measured by a thermal ammeter or deduced from the reading of an electrostatic voltmeter when the resistance of the thermal ammeter (1·02 ohms) was objectionable. The load impedance was varied by means of a 10-ohm calibrated resistance box valid at 200 kc/s.

Measurements of output were made in a variety of operating conditions, shown collected in the two following tables. The seventh and eighth columns of Table IX show respectively the output in milliwatts measured when oscillating at 200 kc/s and predicted from the tests at 50 c/s, such as are recorded in Figs. 53, 54, etc., and the agreement is satisfactory. In Table X the ammeter and series resistance was removed and then the circuit had a dynamic resistance of 63 kΩ. The output voltage was measured for various supply voltages and the measured and predicted values are shown for comparison in the sixth and

TABLE IX

Anode Volts	Field Gauss	Saturation Emn. mA.	Angle of Tilt	Series Res. in Ohms	R.F. Current in mA.	Output in mW.	Value at 50 ~	Discrepancy %
220	230	50	0	6·19	286	508	526	+3·5
160	,,	,,	0	5·20	333	580	605	+4·3
140	,,	,,	0	4·20	307	398	438	+10
120	,,	,,	0	3·22	294	342	337	−1·4
,,	290	,,	+5°	4·20	250	264	290	+10
,,	255	,,	0	3·22	303	296	282	−4·7
,,	,,	80	0	3·22	307	304	310	+2·0

seventh columns of Table X ; here the agreement is usually closer than 1% and well within the accuracy of measurement. The figures in the last two columns of Table X show for com-

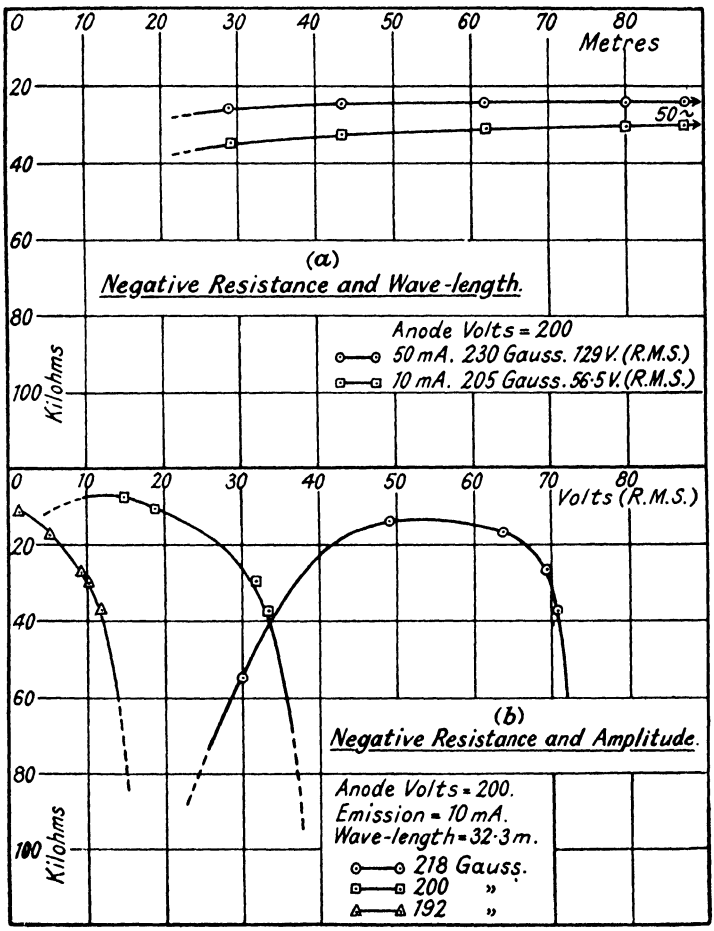

FIG. 61. Dynatron régime at high frequencies.

parison the measured and predicted input ; here again the agreement is satisfactory. Thus these measurements perhaps suffice to establish the validity of the method of prediction.

The radio-frequency measurements mentioned above were

TABLE X

Anode Volts	Field Gauss	Saturation Emn. mA.	Angle of Tilt	Dyn. Res. in Ohms	R.F. Volts	Volts at 50 ~	D.C. Input mA.	Input mA at 50 ~
220	345	50	0	63,000	246	244	—	—
200	,,	,,	0	,,	233	232	—	—
180	,,	,,	0	,,	216	214	—	—
160	,,	,,	0	,,	198	204	—	—
140	,,	,,	0	,,	174	176	—	—
120	,,	,,	0	,,	150	152	6·50	7·02
100	,,	,,	0	,,	125	123	—	—
120	290	,,	0	,,	150	149	8·20	8·35
120	220	,,	0	,,	135	134	9·40	9·50

at such a low frequency that electron transit time effects played a negligible part. Some measurements were made, by a method described later, of the tube resistance at much higher frequencies, and it will be seen from Fig. 61*a* that this is practically independent of frequency, but that when this reaches about 5 Mc/s (60 metres) the resistance rises. The resistance as a function of amplitude is shown in Fig. 61*b*, and it will be seen that this is similar to that found at 50 c/s. This modification in tube resistance at high frequencies is undoubtedly due to the same cause—electron inertia—that has been commented on previously in the case of normal type valves. Thus, although the magnetron can act as a generator in this régime at much higher frequencies, it experiences a falling off in power output.

BIBLIOGRAPHY

1. AWENDER, H., THOMA, A. and TOMBS, D. M. "The Paths of the Electron in the Magnetron." *Zeit. f. Phys.*, 1935, **97**, 202.
2. BELL, D. A. "Investigation of Valve Performance by an Electrodynamometer Method." *J. Inst. Elec. Eng.*, 1935, **76**, 415.
3. BELLUSTIN, S. V. "Motion of Electrons in Electric and Magnetic Fields with Space Charge." *Phys. Z. Sowjet*, 1936, **10**, 251.
4. BELLUSTIN, S. V. "Study of a Whole Anode Magnetron Neglecting the Space Charge." *J. Tech. Phys.*, 1939, **13**, 1188.
5. BENHAM, W. E. "Electronic Theory and the Magnetron Oscillator." *Proc. Phys. Soc.*, 1935, **47**, 1.
6. BETHENOD, J. "Variation of Space Current in a Magnetron under the Action of the Magnetic Field." *Comptes Rendus*, 1939, **209**, 832.

7. BOVSHEVEROV, V. M. "Characteristic Curves of the Split Anode Magnetron." *Tech. Phys. U.S.S.R.*, 1935, **2**, 567.
8. BRAUDE, S. J. "On the Cut-off in the Plane Magnetron with Space Charge." *Phys. Z. Sowjet.*, 1935, **7**, 565.
9. BRAUDE, S. J. "Motion of Electrons in Electric and Magnetic Fields." *Phys. Z. Sowjet.*, 1935, **8**, 584.
10. BRAUDE, S. J. "On the Wavelength of the Electronic Oscillations in the Plane Magnetron." *Phys. Z. Sowjet.*, 1935, **8**, 667.
11. BRAUDE, S. J. "Motion of Electrons in Electric and Magnetic Fields with Space Charge." *Phys. Z. Sowjet.*, 1937, **12**, 1.
12. BRENEV, I. V. "Construction of the Static Characteristics of a Split Anode Magnetron." *J. Tech. Phys.*, 1936, **6**, 302.
13. BRENEV, I. V. "An Investigation of the Magnetron on the Basis of its Static Characteristics." *J. Tech. Phys.*, 1936, **6**, 677.
14. CARRARA, N. "The Magnetron as a Negative Resistance." *Alta Freq.*, 1935, **4**, 20.
15. CARRARA, N. "The Inclined Field Magnetron." *Alta Freq.*, 1935, **4**, 314.
16. DOSSE, J. "Graphical Determination of Electron Paths in a Magnetic Field." *Z. f. Tech. Phys.*, 1936, **17**, 315.
17. ENGBERT, W. "Potential Distribution in the Magnetron." *Hochf. Tech. u. Elek. akus.*, 1938, **51**, 44.
18. GILL, E. W. B. and BRITTON, K. G. "The Action of the Split Anode Magnetron." *J. Inst. Elec. Eng.*, 1936, **78**, 461.
19. GRECHOWA, M. T. "Path Curves of the Electron in the Split Anode Magnetron." *Tech. Phys. U.S.S.R.*, 1935, **2**, 560.
20. GRECHOWA, M. T. "Investigation of the Electron Path Curves in the Magnetron." *Tech. Phys. U.S.S.R.*, 1936, **3**, 633.
21. GROSZKOWSKI, J. and RYZKO, S. "The Distribution of Electrostatic Field in Split Anode Magnetrons." *Hochf. Tech. u. Elek. akus*, 1936, **47**, 55.
22. GRÜNBERG, G. and LULASCHKOV, W. "On the Theory of the Split Anode Magnetron." *Tech. Phys. U.S.S.R.*, 1935, **2**, 482.
23. GRÜNBERG, G. and WOLKENSTEIN. "The Influence of a Magnetic Field on Electron Motion between Coaxial Cylinders." *Tech. Phys. U.S.S.R.*, 1937, **4**, 179.
24. HARA, G. "Relation between Virtual Cathode and Potential Distribution in Magnetrons." *Electrot. J. Tokyo*, 1939, **3**, 72.
25. HARR, O. "Current Distribution over the Anode Surface of the Two Split Magnetron." *T. F. T.*, 1938, **27**, 167.
26. HARVEY, A. F. "Output and Efficiency of the Split Anode Magnetron Oscillating in the Dynatron Régime." *J. Inst. Elec. Eng.*, 1939, **84**, 683.
27. HARVEY, A. F. "The Cut-off Characteristic of the Single Anode Magnetron." *Proc. Camb. Phil. Soc.*, 1939, **35**, 637.
28. HOLLMANN, H. E. "The Magnetron as a Negative Resistance." *Ann. Phys.*, 1931, **8**, 956.
29. HULL, A. W. "The Effect of a Uniform Magnetic Field on the Motion of Electrons between Coaxial Cylinders." *Phys. Rev.*, 1921, **18**, 13.
30. KATZMAN, Y. A. and RUBINA, T. F. "The Static Characteristics of a Split Anode Magnetron." *J. Tech. Phys.*, 1939, **9**, 499.

31. KILGORE, G. R. "Magnetron Oscillators for Frequencies from 300–600 Mc/s." *Proc. Inst. Rad. Eng.*, 1936, **24**, 1140.
32. LÄMMCHEN, K. "The Static Negative Characteristic of the Habann Valve." *Hochf. Tech. u. Elek. akus.*, 1938, **51**, 60.
33. LANGMUIR, I. "The Effect of Space Charge and Residual Gases on Thermionic Currents." *Phys. Rev.*, 1913, **2**, 450.
34. LINDER, E. G. "Excess Energy Electrons and Electron Motion in High Vacuum Tubes." *Proc. Inst. Rad. Eng.*, 1938, **26**, 346.
35. LINDER, E. G. "Effect of High Energy Electron Random Motion on the Magnetron Cut-off Curve." *J. Appl. Phys.*, 1938, **9**, 331.
36. MEGAW, E. C. S. "An Investigation of the Magnetron Short Wave Oscillator." *J. Inst. Elec. Eng.*, 1933, **72**, 326.
37. MOULLIN, E. B. "Effect of Curvature of the Characteristic on the Frequency of the Dynatron Generator." *J. Inst. Elec. Eng.*, 1933, **73**, 186.
38. MOULLIN, E. B. "The Response of a Valve Generator to a Modulating Voltage." *Wireless Eng.*, 1938, **15**, 371.
39. MOULLIN, E. B. "Considerations of the Effect of Space Charge on the Magnetron." *Proc. Camb. Phil. Soc.*, 1940, **36**, 94.
40. PIDDUCK, F. B. "Notes on the Theory of the Magnetron." *Q. Journ. Math.*, 1936, **7**, 201 *et seq.*
41. RANZI, I. "Phenomenon of Negative Resistance in a Diode subjected to a Magnetic Field." *Nuovo Cim.*, 1929, **6**, 249, 310.
42. RANZI, I. "Negative Resistance in a Diode subjected to a Magnetic Field." *Lincei Rend.*, 1929, **9**, 652.
43. SPIWAK, G. V. and ZREBNY, P. E. "On the Magnetron Cut-off Curve." *Comptes Rendus de l'U.R.S.S.*, 1939, **24**, 237.
44. TONKS, L. "Motion of Electrons in Crossed Electric and Magnetic Fields with Space Charge." *Phys. Z. Sowjet.*, 1935, **8**, 572.
45. WIGDORTSCHIK, I. M. "Investigation of the Additional Heating of the Filament in a Magnetron." *Phys. Z. Sowjet*, 1936, **10**, 634.
46. WIGDORTSCHIK, I. M. "Velocity Distribution of Electrons under the Influence of a Magnetic Field." *Phys. Z. Sowjet.*, 1936, **10**, 245.
47. ZUHRT, H. "The Static Characteristics of the Split Anode Magnetron." *Hochf. Tech. u. Elek. akus.*, 1936, **48**, 91.
48. OMOTO, Y., and MORIATA, K. "Electrostatic Field and Capacitance of a Split Anode Magnetron." *Electrot. J. Tokyo*, 1940, **4**, 147.
49. BELLUSTIN, S. V. "On the Static Theory of the Magnetron." *J. Exp. and Theor. Phys.*, 1940, **10**, 190 and 455.
50. ROSE, A. "Mechanical Model for Electron Motion in a Magnetic Field." *J. Appl. Phys.*, 1940, **11**, 711.
51. CHANG, HSU and CHAFFEE, E. L. "Characteristics of the Negative Resistance Magnetron." *Proc. Inst. Rad. Eng.*, 1940, **28**, 519.
52. BRILLOUIN, L. "Theory of the Magnetron." *Phys. Rev.*, 1941, **60**, 385.
53. BRAUDE, S. J. "Effect of Magnetic Field on the Space Charge in Diodes." *J. Tech. Phys.*, 1940, **10**, 217.

CHAPTER V

THE MAGNETRON—PART TWO

(*a*) RESONANCE RÉGIME

Introduction. The properties of the magnetron in this régime appear to have been first examined, both theoretically and experimentally, by K. Posthumous (98), who considers the general case of a split-anode magnetron with k pairs of segments, and it is found that for fields greater than the cut-off value a type of oscillation can occur in which the wavelength is proportional to the field strength. For any given conditions there is a sharply defined maximum frequency given by

$$\omega = \frac{2Vk10^8}{a^2H} \quad . \quad . \quad . \quad . \quad . \quad (102)$$

where ω is the pulsatance, V the mean anode voltage, H the field strength, and a the anode radius.

Thus for any given magnetron the wavelength λ is given by the relation

$$\frac{\lambda V}{H} = \text{constant} \quad . \quad . \quad . \quad . \quad . \quad (103)$$

and it is this fact that the wavelength of oscillation depends only partly on the constants of the external circuit, which clearly distinguishes the resonance type oscillations from the dynatron type. If the external circuit is in the form of a very long Lecher wire system, then the wavelengths of the oscillation obtained are given approximately by the above formulæ. The magnetron exhibits these properties of the resonance régime from wavelengths of the order of 10 cm. up to indefinitely long wavelengths, and is capable of giving as a generator with high efficiency the largest obtainable power outputs at ultra-short wavelengths. It is pointed out by E. W. B. Gill and K. G. Britton (20), and it is shown experimentally, that for any

given wavelength there are optimum values of anode voltage and magnetic field. A suggested theory is outlined based on multiple orbits of the electrons, a small deflection being given each time they pass the gap between the segments, and this is confirmed by experiments on tubes with different radii and number of segments. Thus in the cylindrical magnetron it can be assumed that most of the potential drop occurs near the filament, and a small residue may be supposed to be spread across the space to the anodes. In this case the electron motion is practically circular, but if, in the two-segment tube for example, the anodes are at a potential $V \pm V_1 \sin \omega t$, then an electron passing one of the gaps will be deflected towards the segment which is at a lower potential. If the electron collides with the anode, then there exists a simple type of negative resistance which, as we saw in Chapter IV, leads to dynatron oscillations. If, however, the electron is not deflected sufficiently to collide with the anode, it precesses around the tube, suffering further deflections at each gap, provided the frequency of the fluctuating segment potential is correct. In this manner an amplified form of negative resistance occurs, and thus an electron, whose time for describing an orbit is very short, is able to maintain an oscillation of much greater periodic time. Support for this electron precession theory is given by some photographs shown by G. R. Kilgore (55), who used a magnetron with a small amount of residual gas present, so that the electron motion produced ionisation, thus making their paths visible.

Some measurements on the properties of the magnetron in this régime have also been made by J. S. McPetrie (66), and in order that these could be made at reasonably long wavelengths low anode voltages and intense magnetic fields were employed. The impedance of the tube was measured by an adaptation of P. Willan's method. Thus if the capacitance of a resonant circuit, which is inductively coupled to the coil of a thermionic tube oscillator, is varied, then the frequency of the oscillator changes in the neighbourhood of the resonant condition. If Z is the dynamic resistance of the resonant circuit, then this is given by $Z = \dfrac{1}{\pi f \Delta C}$, where ΔC is the

difference in capacitance of the coupled circuit corresponding to the points of maximum and minimum oscillator frequencies and f is the undisturbed oscillator frequency. If these frequency changes are observed with the aid of a separate beat oscillator, then the magnetron impedance can be determined by noting the resistance and reactance changes when it is connected directly across the resonant circuit. Measurements were made which showed the distinction between negative resistance in the dynatron and resonance régimes, and in the case of the latter it was shown that in the range of oscillations the resistance was negative and that the impedance had a reactive component which made the magnetron equivalent to a small capacitance. It was deduced from these capacitance changes that a resonant condition existed within the tube and that oscillations did not occur without the simultaneous appearance of this resonance. This resonance was found to have the features associated usually with a series electrical circuit, but with the component impedances consisting of a negative resistance, negative inductance, and negative capacitance. It is also shown that there is much similarity between these resonance oscillations and the electronic oscillations found in retarding-field tubes, which were discussed in Chapter III.

Thus it was found that electronic oscillations in positive grid triodes occurred in the neighbourhood of resonance, where the tube capacitance decreases from positive values at wavelengths less than that corresponding to resonance, to zero near resonance, and then to increasing negative values as the wavelength is further increased. The magnetron experiments indicated that the oscillations occurring at fields greater than the " critical " value were also associated with a tube resonance of the same type, since the capacitance variation about the resonant wavelength was exactly the same as that obtained with a special split-anode triode when used as an electronic oscillator. Maximum amplitude was obtained, with both " resonance " oscillations in magnetrons and electronic oscillations in triodes, in the neighbourhood of the maximum tube capacitance. The beat frequency between a triode electronic oscillator and, say, a harmonic of a retro-active oscillator was found to be more of the nature of a hiss than of a pure note.

When this was repeated with a split-anode magnetron it was found that near the critical field the beat frequency was relatively pure, but on increasing the field to the condition for resonance oscillations the beat frequency was very similar to that observed with the triode.

The similarity between the type of resonance, the poor wave-form, and the operating conditions for the resonance oscillations and the triode electric oscillations indicate that these two types of oscillations are actually of the same form. It was suggested that these oscillations are due to the finite transit time of the electrons giving rise to a negative resistance and reactance. If an alternating e.m.f. is applied between the cathode and anode of a diode then alternating current will flow across the tube. If the displacement current due to the inherent diode capacitance is neglected then as the frequency is raised the convection current will lag on the anode potential due to electron inertia. When the lag is between $\pi/2$ and $3\pi/2$ the tube is equivalent to an inductance or capacitance in series with a negative resistance, there being an apparent resonance as the reactance changes sign at $\pi/2$ lag.

An account of the split-anode magnetron in the resonance régime (under the term dynatron) at ultra-short wavelengths has been given by E. C. S. Megaw (70), who shows that the power output and efficiency increase and the impedance decreases as the wavelength continually decreases to its lower limit. It is suggested that these effects are due to negative resistance modified by changes due to the transit time of the electrons. Due to the practical importance of these oscillations a large portion of the recent literature on magnetrons at ultra-short wavelengths has been devoted to resonance oscillations. In addition to the use (incorrectly) of the term dynatron, these resonance oscillations are discussed under a variety of names. Since they were first described by K. Posthumous (98), they are often called after his name, while since E. Habann (33) was the first to obtain negative resistance from a cylindrical magnetron with two segments, the split-anode magnetron operating in this régime is often referred to as a Habann tube, especially on the Continent. In Japan, where much work has been done on magnetron generators, the

resonance oscillations are generally referred to as B-type. Although the magnetron in this régime has been examined in conjunction with external circuits to form a self-contained ultra-high-frequency generator, there is little information on the properties of the tube alone. The author, however, has made some measurements, some of which have been described elsewhere (37), as discussed below.

Description of Experiments. For the determination of the properties of the magnetron in this régime the circuit shown in Fig. 62 was used, the voltage amplitude being supplied by a separate electrostatically screened radio-frequency generator. The amount of coupling was varied by adjusting the distance

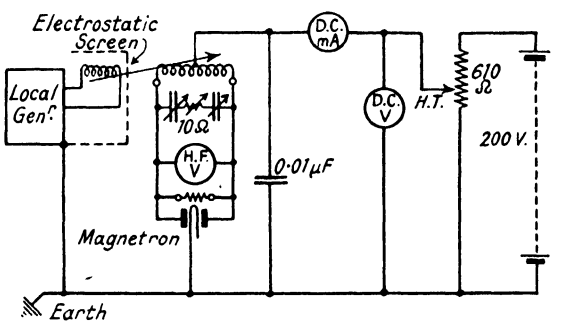

FIG. 62. Circuit for impedance measurements.

between the generator coil and the coil of the measuring set, and in order that the induced voltages could be reasonably large without too tight a coupling the separate generator used in the experiments was another magnetron, and thus it was possible to obtain the required power over a large range of frequency.

The method of measuring the magnetron impedance was to connect the anode segments to an external impedance consisting of a symmetrical double-rotor condenser (capacitance of each half variable between 30 and 200 $\mu\mu$F) and a coil (inductance between 0·9 and 18 μH), the centre point of which was kept at a steady positive potential.

Since the split-anode magnetron is a symmetrical thermionic tube, the tuning condenser must be a double rotor unit. It

consisted, as shown in Fig. 63*a*, of two units mounted in different compartments which are screened from each other and externally by thin tinned sheet iron. The screens are

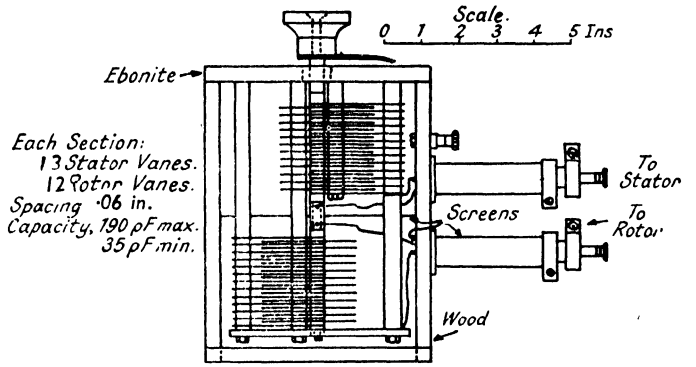

FIG. 63*a*. Double rotor condenser for magnetron.

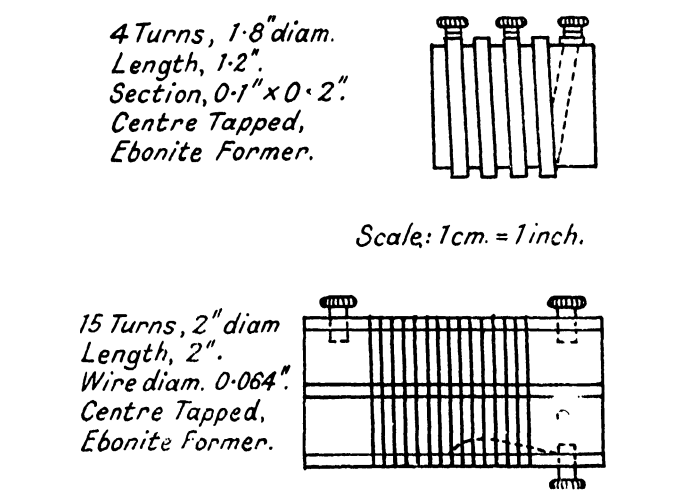

FIG. 63*b*. Centre-tapped short-wave coils.

continued up to the rotor and stator terminals, which are arranged so that the main body of the condenser is well removed from the coil.

Two typical coils are shown in Fig. 63*b*, and it will be seen that the centre points are brought out to a separate terminal.

At the longer wavelengths an absorption type wavemeter, consisting of a variable condenser and interchangeable coils, was used, and this had been calibrated by means of a variable frequency oscillator and a broadcast receiver. For the shorter wavelengths the wavemeter shown in Fig. 64*a* was constructed

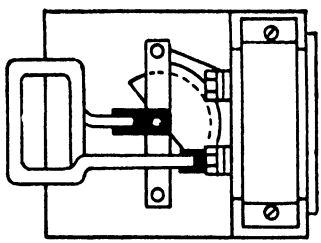

Coil, 2 Turns, 1·5" × 1·0".
Conductor Section, 0·1" × 0·2"
Condenser, 50 μμF max.
Meter, Weston 500 mA Thermal.
Scale: 1 cm. = 1 inch.

FIG. 64*a*. Absorption wavemeter. Range 2·5–11 metres.

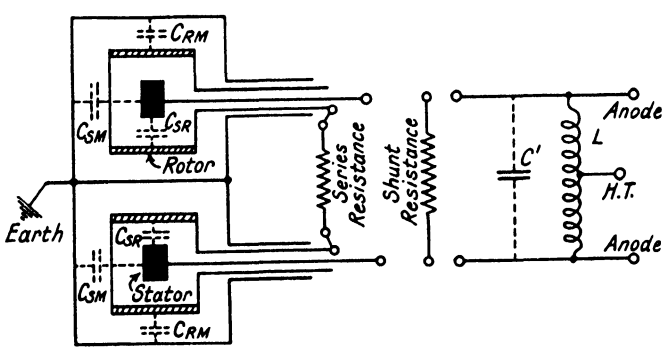

FIG. 64*b*. Diagrammatic sketch of load circuit.

from a two-turn coil connected to a 50 μμF variable condenser. A Weston type thermal ammeter connected in series with the coil and condenser was used as an indicator of resonance and approximate strength of oscillation. The large value of tuning

capacitance enabled the wavelength range to be comparatively large. This instrument was calibrated from a pair of Lecher parallel wires about 8 metres long which were excited in different modes by connection to the magnetron.

In the impedance measurements a variable series resistance was used which consisted of a rotary stud switch, and each element, of value approximately 1 ohm, was a short length of 40 S.W.G. Eureka wire, so that skin and proximity effects were negligible at the frequencies concerned. From Fig. 64*b* it will be seen that only a portion of the radio-frequency current

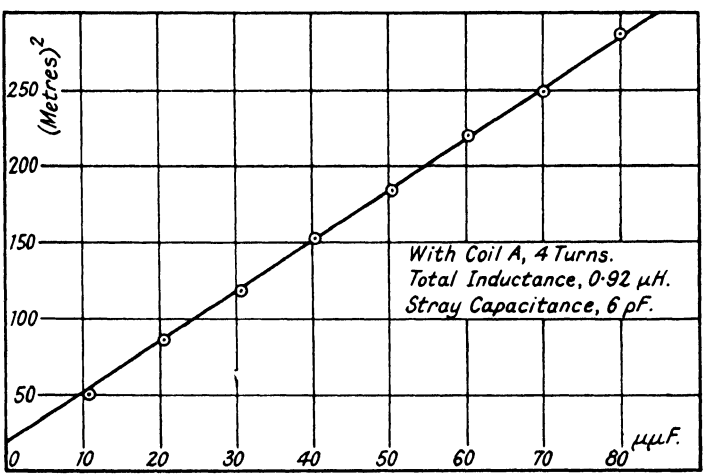

FIG. 65. Wavelength calibration of tuned circuit.

passes through this resistance, and thus to correct for this the effective resistance was taken as the observed value multiplied by $(\frac{1}{2}C_{SR}/\frac{1}{2}C_{SR} + \frac{1}{2}C_{SM} + C')^2$, where C' is the capacitance of the magnetron, voltmeter and coil. In order that the resistance of the condenser, variable resistance box, and the connections should be as low as possible, the wiring was of thick copper conductor of minimum length. The condenser was calibrated for wavelength by adjusting the circuit to resonance with the local generator and then measuring the wavelength by means of the calibrated wavemeter. A curve of wavelength and tuning capacitance is given in Fig. 65 for the four-turn inductance coil.

The dynamic resistance of the coil and condenser circuit, when connected to the magnetron with its filament cold, was determined as a function of wavelength. This was made by the distuning method or by connecting metallised resistors in parallel with the coil, or by inserting small series resistances, as described above, in the lead connecting the two halves of the condenser. Suitable corrections were made as described in Chapter II for the inevitable distributed inductances and capacitances of the circuit and the agreement of the three methods was then very good.

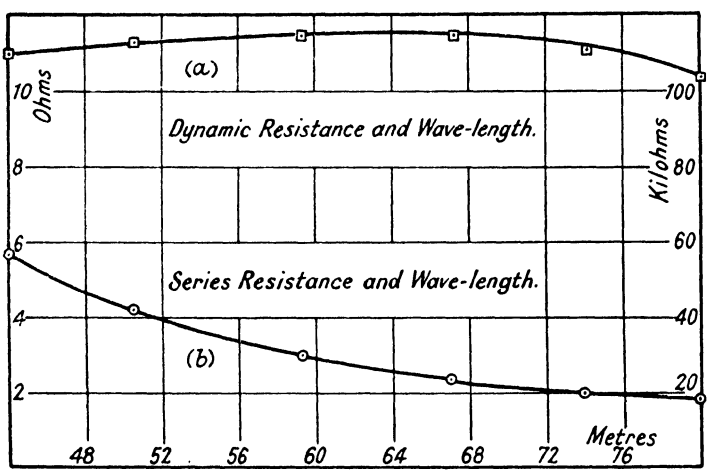

FIG. 66. High-frequency resistance of coil.

The dynamic resistance and equivalent series resistance of the complete circuit are given in Fig. 66 for the twelve-turn coil used at the longer wavelengths. Attempts were made to estimate the circuit resistance from S. Butterworth's formula. Thus for a coil of fifteen turns of $d = 0{\cdot}064$ in. diameter copper wire spaced $D = 0{\cdot}14$ in. and diameter $2a = 5{\cdot}0$ cm. and length $b = 5{\cdot}0$ cm. we will take a working frequency of 10 Mc/s. Then the parameter $Z \equiv \sqrt{\frac{4\pi p a^2}{\rho}}$, in which p is the pulsatance and ρ the conductivity of the metal, has the value 55 and hence

$$F(Z) \equiv \frac{\sqrt{2Z} - 3}{4} = 18{\cdot}7 \quad . \quad . \quad . \quad . \quad (104)$$

$$G(Z) \equiv \frac{\sqrt{2Z} - 1}{8} = 9{\cdot}7 \quad . \quad . \quad . \quad . \quad (105)$$

For a short coil with a given number of turns the radio-frequency resistance R_n is given in terms of the D.C. resistance R_o by

$$\frac{R_n}{R_o} = 1 + \left(1 + \tfrac{1}{8}\omega_n \frac{d^4}{D^4}\right)F(Z) + \mu_p \frac{d^2}{D^2}\left(1 + \tfrac{1}{2}v_n\phi_1 \frac{d^2}{D^2}\right)G(Z) \quad (106)$$

where ω_n, μ_p, v_n, ϕ_1 are tabulated by S. Butterworth.† Inserting these values in (106)

$$\frac{R_n}{R_o} = 1 + 19{\cdot}2 + 11{\cdot}9 = 32{\cdot}1 \quad . \quad . \quad . \quad (107)$$

and since $R_o = 0{\cdot}0083 \times 2{\cdot}5 = 0{\cdot}021\ \Omega$, $R_n = 0{\cdot}67\ \Omega$. It can be shown that the radiation resistance given by, where S is the area of the coil,

$$R_r = \frac{16\pi^4 S^2}{3\lambda^4 c} = \frac{16\pi^4 c S^2}{3\lambda^4 10^9}\ \Omega. \quad . \quad . \quad . \quad (108)$$

is negligible, and since the measured value of series resistance was $2{\cdot}0\ \Omega$ there is a considerable discrepancy. Some of this difference is due to the damping of the diode voltmeter and the losses in the variable condenser, but the larger part cannot be accounted for, and is thus due to leakage and dielectric losses of the circuit components.

The voltage amplitude was measured by a pair of small diodes and the circuit of the voltmeter is shown in Fig. 67*b*. The voltmeter was connected across the magnetron segment leads, and it has the advantage that the damping resistance (about $1\ \text{M}\Omega$) and input capacitance (about $1{\cdot}8\ \mu\mu\text{F}$) were distributed equally across the two halves of the coil. With the magnetron the voltages applied to each diode were similar, but in arrangements where this would not be the case the total voltage could be measured by using a separate series resistance for each diode. The diodes used were type V24, and in use the grid was connected to the anode, while the range of applied potentials was from 5–100 volts (r.m.s.) at frequencies

† Or see E. B. Moullin (75).

from 3 to 50 Mc/s. The filaments of each diode took 0·75 amp. at 5 volts, and since they were of pure tungsten the effect of initial electron velocities was noticeable. A Unipivot having a full scale deflection of 24 μA was used as an indicator. The components were so chosen in value as to keep the errors,

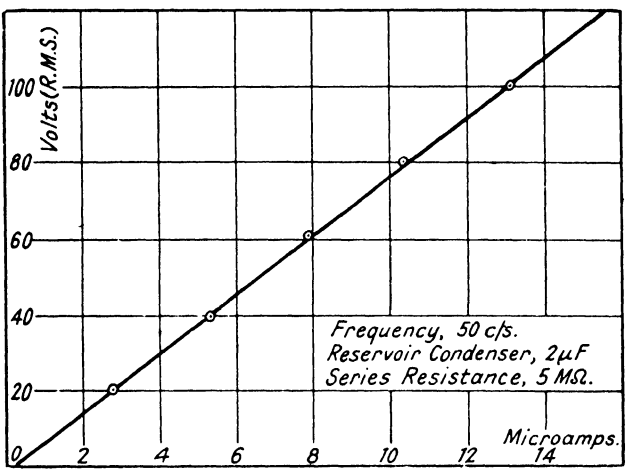

FIG. 67*a*. Push-pull diode peak voltmeter calibration curve.

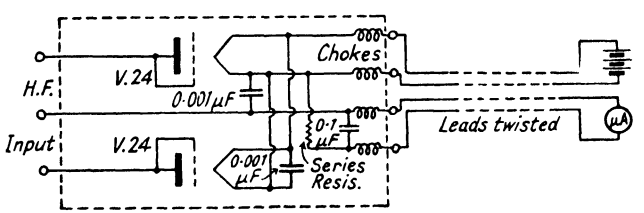

FIG. 67*b*. Diode voltmeter circuit.

discussed generally in the second chapter, to a minimum. The voltmeter was calibrated at 50 c/s and the curve is shown in Fig. 67*a*, this being assumed valid over the range of frequencies employed.

Method of Measurement. Much care was devoted to a choice of a suitable method of measuring the absolute tube resistance. Since the magnetron in this régime is equivalent to a complex non-linear impedance, the distuning method (capacitance or

frequency variation) or methods similar to that due to P. W. Willans could not be employed. Finally, two methods were used according as the tube resistance was less than or greater than the dynamic resistance of the external circuit. In the first, the tube and circuit together acted as a generator whose output voltage at various wavelengths was maintained at any assigned and constant value by placing an appropriate resistor in parallel with the coil ; and since the circuit had already been calibrated its dynamic resistance was known at any wavelength when shunted by the known resistor. As the circuit power factor was not large the fluctuations of anode potential are very nearly simple harmonic, and thus the fundamental component of negative resistance of the magnetron at any wavelength and amplitude is equal to the known dynamic resistance. In the second method a voltage of the desired magnitude was induced from a separate electrostatically screened generator, self-oscillation of the magnetron being prevented by inserting sufficient resistance in the circuit. Then the filament of the magnetron was lit and the voltage amplitude brought back to its initial value by placing a suitable resistor in parallel with the coil, the circuit being retuned by slight adjustment of the condenser. The resistance necessary to do this is equal to the negative parallel resistance of the magnetron.

To reduce the uncertainties of measurement and the confusion which arises due to the different régimes in the magnetron associated with very short wavelengths, most measurements were made at comparatively long wavelengths. This necessitated the use of very strong magnetic fields, and values up to 3,500 gauss were provided by an iron-cored air-gap electromagnet of conventional form but of design appropriate to such intense fields. This has been described in Chapter IV.

Wavelength and Anode Voltage. The negative resistance in the resonance régime is shown in Fig. 68 as a function of wavelength for three values of H.* The value of E (r.m.s. voltage amplitude) chosen was such that the potential fluctuations of each anode were about V†/10. It will be seen that the value of $-R$ (negative resistance) increases with λ (wavelength) in a comparatively gradual manner so long as λ is

* Magnetic field strength. † Mean positive anode potential.

greater than a certain value depending on H, and that when λ is less than this value $-R$ increases much more rapidly ; in either case $-R$ tends to the value given by the static characteristics, this being too high to be shown on the diagram. The minimum values of $-R$ lie on a line of unit slope (shown dotted), but it will be observed that for any given condition the value of λ is not critical and the magnetron would function well as a generator over a considerable range of wavelength if connected to a circuit of sufficiently high dynamic resistance.

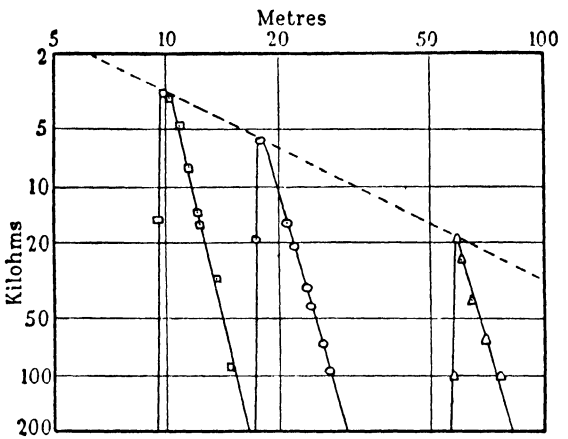

FIG. 68. Variation of negative resistance with wavelength.
Anode voltage, 100 volts
Filament emission, 10 mA
Amplitude, 13·6 volts (r.m.s.)
Field strength 320 gauss —□——□—
Field strength 560 gauss —○——○—
Field strength 1,790 gauss —△——△—

It is generally accepted that resonance oscillations are found only when λ (in cm.), V and H have values given by $\lambda V/H = K$, where K is a constant depending on the diameter and number of segments of the anode, but the results given show that negative resistance occurs over a considerable range of K. It will be convenient to use K as defined in discussing the experimental results, and thus for the conditions of Fig. 68 negative resistance occurs when K lies between 160 and 800. Measurements on the positions of minimum negative resistance give

$K = 266$ when $E/V = 0{\cdot}45$, $K = 325$ when $E/V = 0{\cdot}136$ (as in Fig. 68), and $K = 405$ when $E/V = 0{\cdot}026$.

The above curves were repeated for other anode voltages between 50 and 200 volts, and the values of $-R$ obtained were almost identical with those given above provided E/V was kept the same and H was altered with V so that K remained the same. Similar curves can be obtained when V is varied (instead of λ), but it is useful in this case to consider a fixed

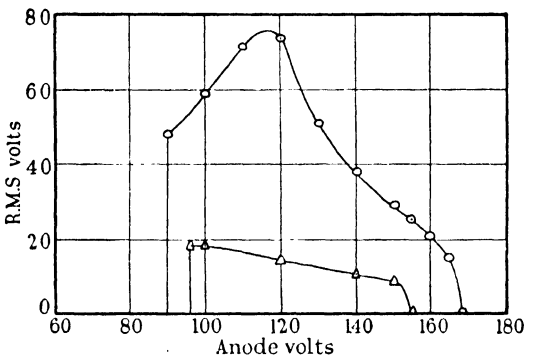

FIG. 69. Variation of voltage amplitude with anode voltage.
Field strength, 2,215 gauss
Filament emission, 10 mA
Wavelength, 61·8 m.
Negative resistance 115 kΩ —○——○—
Negative resistance 24·8 kΩ —△——△—

resistance and examine the changes in amplitude. Modulation characteristics for two values of $-R$ are given in Fig. 69.

Magnetic Field and Voltage Amplitude. These " resonance " curves can also be derived when H is varied as in Fig. 70 for seven different wavelengths. From these it will be seen that the minimum value of $-R$ is proportional to λ as indicated by the upper dotted line. For a given value of λ there is only a restricted range of H in which the tube exhibits marked negative resistance ; nevertheless, it is likely that the proportionate increase of $-R$ is not attributable to the increase of λ *per se*, but to the effect of going further along the curved foot of the cut-off curve with the subsequent contraction of the electron cloud. As this value of H is proportional to V,

while H_c varies as $\sqrt{V}$, the operating point moves along the curved foot as V (or H) is made larger.

Since negative resistance is not found for $H < H_c$ the figure shows that for any value of V there is a minimum wavelength.

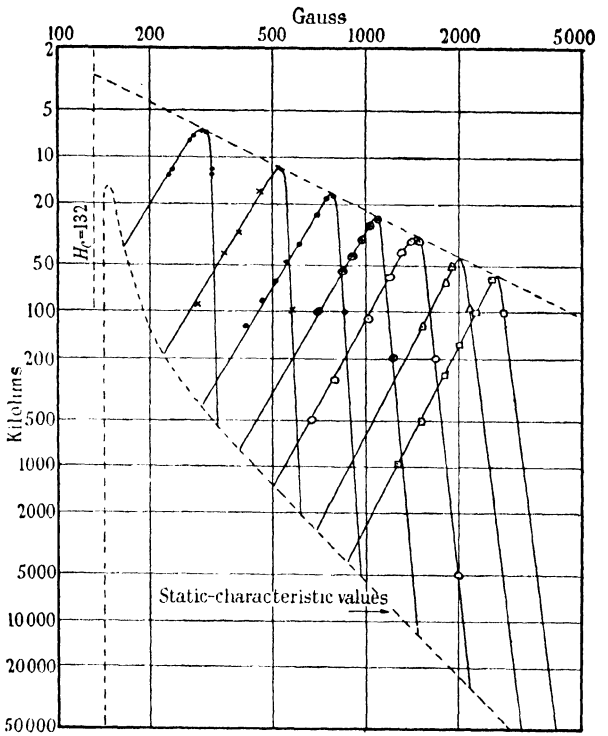

FIG. 70. Variation of negative resistance with field strength at various different wavelengths.

Anode voltage, 100 volts
Filament emission, 10 mA
Amplitude, 29 volts (r.m.s.)
Wavelength 9·27 m. —●●—●●—
Wavelength 14·7 m. —×—×—×—
Wavelength 23·2 m. —●—●—
Wavelength 33·1 m. —⊗—⊗—
Wavelength 43·3 m. —⊙—⊙—
Wavelength 61·8 m. —△—△—
Wavelength 80·3 m. —⊡—⊡—

The positions of minimum resistance are seen to be given by $K = \lambda V/H = 300$, and as $H_c = \sqrt{(181\ V)}$ the corresponding minimum wavelengths are given by $\lambda H_c = 54{,}000$. Thus the minimum wavelength decreases as H_c (and hence V) increases. It will be seen later that a similar relation obtains for the

wavelength of the electronic oscillations, but the value of the constant is then about 11,000. Provided sufficient field strength is available there appears to be no maximum wavelength to the resonance régime, and negative resistance (but of a very high value) would be found at indefinitely long (but not infinite) wavelengths. Accordingly the fact that self-oscillation is not encountered at long wavelengths is not due to any restriction by the properties of the magnetron, but is due to the lack of adequate circuits and the difficulty of providing the necessary intense fields.

Measurements show that the result of repeating the curves of Fig. 70 with other amplitudes is that $-R$ tends to increase with E, and since the tube impedance is given by the vector sum of the parallel impedances of the dynatron and resonance régimes the importance of carrying out these measurements at sufficiently long wavelengths will be realised. At very short wavelengths all types of magnetron oscillations occur near the critical field, and much of the confusion into which the study of the magnetron has fallen is due to this fact. At relatively long wavelengths no electronic oscillations are possible and the resonance oscillations occur at magnetic field intensities such that, as shown above, simple negative resistance effects are negligible.

The curves in Fig. 71*a* show the relation between the fundamental component of negative resistance and the voltage amplitude, for three fields ranging from 11·3 to 16·8 H_c. It will be seen that the negative resistance is proportional to the amplitude so long as this is greater than a lower limit (which increases with field strength), and it should be understood that the almost vertical rise in negative resistance is a real effect. Since the relations result in straight lines directed to the origin it is evident that the fundamental component of anode current is constant whatever the voltage between the segments. It has recently been shown theoretically by G. Hara (34) that in this régime the magnetron tends to have constant-current properties.

On the other hand, the mean anode current, as in Fig. 71*b*, increases with voltage amplitude in a linear manner, and it should be noticed that it may be much less than the funda-

mental component ; thus when $H = 1{,}950$ the latter is always 0·61 mA (r.m.s.), whereas the input current can have any value (within limits) greater than 0·13 mA. A wave-form consistent with these results is difficult to conceive, and it is likely that

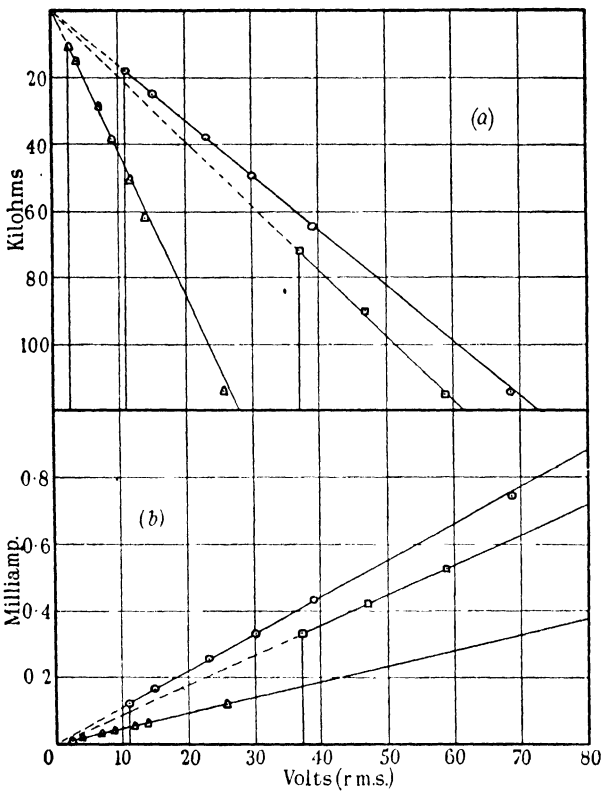

FIG. 71.

(*a*) Variation of negative resistance with voltage amplitude.
(*b*) Variation of input current (d.c.) with voltage amplitude.

Anode voltage, 100 volts
Filament emission, 10 mA
Wavelength, 61·8 m.

Field 1,525 gauss —△——△—
Field 1,950 gauss —⊙——⊙—
Field 2,260 gauss —⊡——⊡—

the fluctuating component of anode current is not caused by the conduction effects familiar in normal tubes. It is observed that the tube resistance does not decrease indefinitely as the amplitude and field strength are reduced, but tends to a

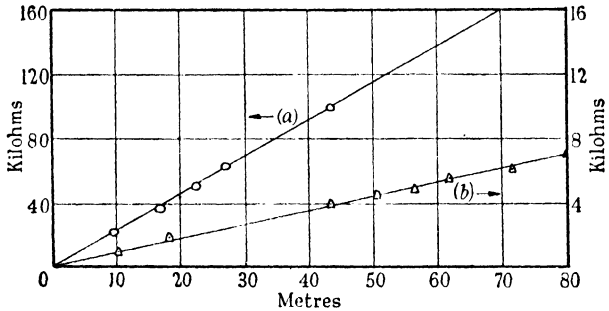

FIG. 72.

(*a*) Variation of optimum load resistance with wavelength.
Anode voltage, 200 volts
Field strength, optimum
Filament emission, 10 mA

(*b*) Variation of minimum negative resistance with wavelength.
Anode voltage, 100 volts
Field strength, optimum
Filament emission, 10 mA

minimum. Fig. 72 shows that the relation between these minimum resistances and wavelength is linear and results in a value of K of 282.

Filament Emission and Angle of Tilt. The previous results have been obtained with I_e (total filament emission) large enough to make the tube resistance sensibly independent of it. Fig. 73*a* shows how $-R$ decreases, as I_e increases, to a blunt minimum and then slowly increases for large values of I_e. It is also found that λ varies with I_e, and by measuring the minimum value of λ (which is well defined, as Fig. 68 shows) for given conditions the results of Fig. 73*b* were obtained. It will be seen that the wavelength for a given amplitude and field increases as I_e decreases, which is the opposite to what would be expected if this " resonant " wavelength were directly related to the electron transit time.

Fig. 74*a* shows how I_a (mean anode current) and the power E^2/R (the input to a load resistance R) vary with emission, the measurements being taken with a constant value of resistance. It will be seen that I_a and E^2/R reach maximum values when I_e is near the optimum value. A point of interest is that I_a is normally only slightly less than I_e, and thus the input current to the tube must be nearly constant over the cycle, and that its wave-form must be sensibly rectangular; it is probable that most of the current flows alternately to either

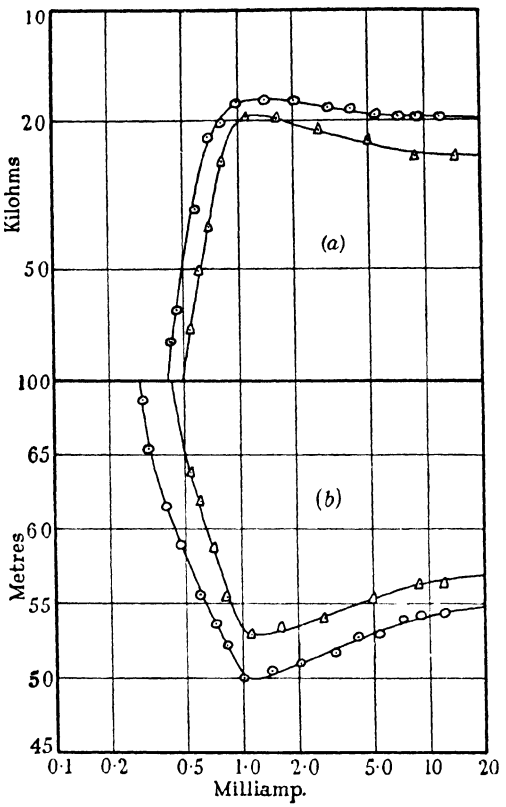

FIG. 73.

(*a*) Variation of negative resistance with filament emission.
(*b*) Variation of wavelength (minimum) with filament emission.
Anode voltage, 100 volts
Field strength, 1,790 gauss
Amplitude, 13·6 volts (r.m.s.)
Tilt zero ——⊙——⊙—
Tilt 4° —△——△—

anode segment during the half-cycle when it is at the lower potential. Attempts to verify this directly by observing the wave-form of the input feed current by an oscillograph or by determining the Fourier components (if any) by suitable tuned circuits have been only partly successful. When this is considered with the effect of voltage amplitude and the small radius of the electron cloud it seems that the electron motion

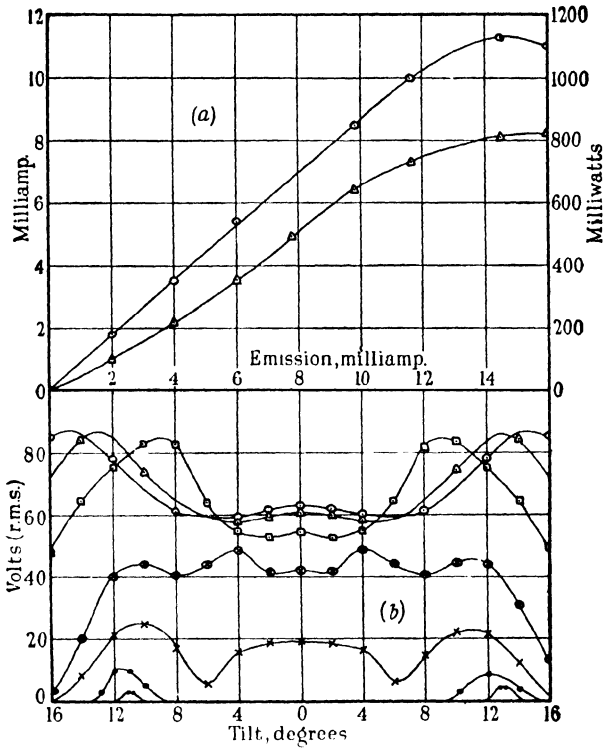

FIG. 74.

(*a*) Variation of input current and of power with filament emission.
Anode voltage, 200 volts
Wavelength, 9·27 m.
Field strength, optimum
Resistance, 18·6 kΩ
Tilt, zero
Input current —⊙——⊙—
Power —△——△—

(*b*) Variation of amplitude with angle of tilt.
Anode voltage, 100 volts
Wavelength, 61·8 m.
Field strength, optimum
Resistance, 115 kΩ
Emission 10 mA —⊙——⊙—
Emission 0·1 mA —●●—●●—
Emission 5 mA —△——△—
Emission 2 mA —⊡——⊡—
Emission 1 mA —⊕——⊕—
Emission 0·5 mA —×——×—
Emission 0·2 mA —●——●—

induces a constant radio-frequency current in the anode circuit while the input current assumes a value directly related to the power E^2/R. It should be emphasised that the optimum values of I_e, particularly at the longer wavelengths, are only a very small fraction of the normal space-charge-limited current appropriate to the steady anode potentials, and thus there

appears to be some condition in the tube which tends to increase the space charge.

It will have been seen that the changes due to increasing α (angle of tilt of field) are similar to those due to decreasing the emission, a result in agreement with one of the known effects on space charge. Small tilts are found not to cause appreciable changes in the tube properties (*i.e.*, zero tilt is always a maximum or minimum point), but when α is large the effects are complex, as shown in Fig. 74*b*, where the voltage amplitude, for a convenient value of resistance, was measured as a function of tilt. It will be seen that at zero tilt the amplitude rapidly decreases with emission when this is less than about 5 mA, and if I_e is less than about 0·25 mA there is no amplitude for which $R = -115\,\text{k}\Omega$. The humps near $\alpha = 12°$ show that tilt can decrease the negative resistance in certain cases, and this effect is related to the electron-cloud radius, since when this is large (as when H and hence λ are small) tilt causes no improvement. This agrees with theory since when the cloud radius is small, tilt causes the ends to approach more closely to the anode, without, however, causing the electrons to collide—as happens when the cloud is originally just within the anode sheath. It was further noticed that the optimum value of H decreases as α increases, and it is of interest to point out how apparent dissymmetry in the valve is much reduced as the emission increases—a fact not unique to the results of Fig. 74*b*, as we saw in Chapter IV.

Reactance and Phase Angle. It has been shown by J. S. McPetrie (67) and A. Giacomini (19) that in the resonance régime the impedance of the magnetron has a reactive component, and this was measured in terms of the difference of the necessary tuning capacitance with the magnetron filament cold and hot. The apparent resistance and capacitance are shown as a function of wavelength in Fig. 75, from which it will be seen that the magnetron operation in general causes an apparent decrease of electrode capacitance. The corresponding curves of reactance and phase angle are also shown ; it will be seen that the latter changes from near 90° lead to near 90° lag, and this is because $-R$ tends to infinity more rapidly than C (change in capacitance) tends to zero. Measure-

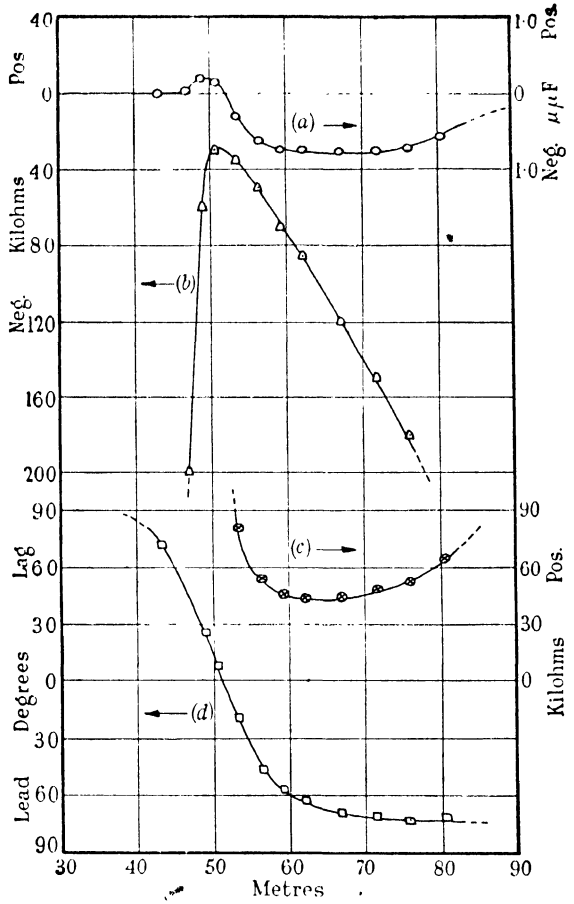

FIG. 75. Variation of (*a*) change in tube capacitance, (*b*) negative resistance, (*c*) reactance, and (*d*) phase angle, with wavelength.

Anode voltage, 100 volts
Filament emission, 10 mA
Field strength, 1,790 gauss
Amplitude, 13·6 volts (r.m.s.)

Capacitance —○——○—
Resistance —△——△—
Reactance —⊕——⊕—
Phase angle —⊡——⊡—

ments show that C varies inversely as the amplitude, and hence the phase angle is independent of amplitude. The phase angle is also independent of wavelength provided this is accompanied by proportionate changes of field strength. Since $-R$ has been shown to vary as λ, it follows that C is sensibly independent of wavelength, its greatest value being

of the order 1 $\mu\mu$F in this tube. Fig. 76 shows these reactance changes against field strength, and, as is to be expected, the relations are similar, although in an opposite sense, to those with wavelength. At both low and high values of magnetic

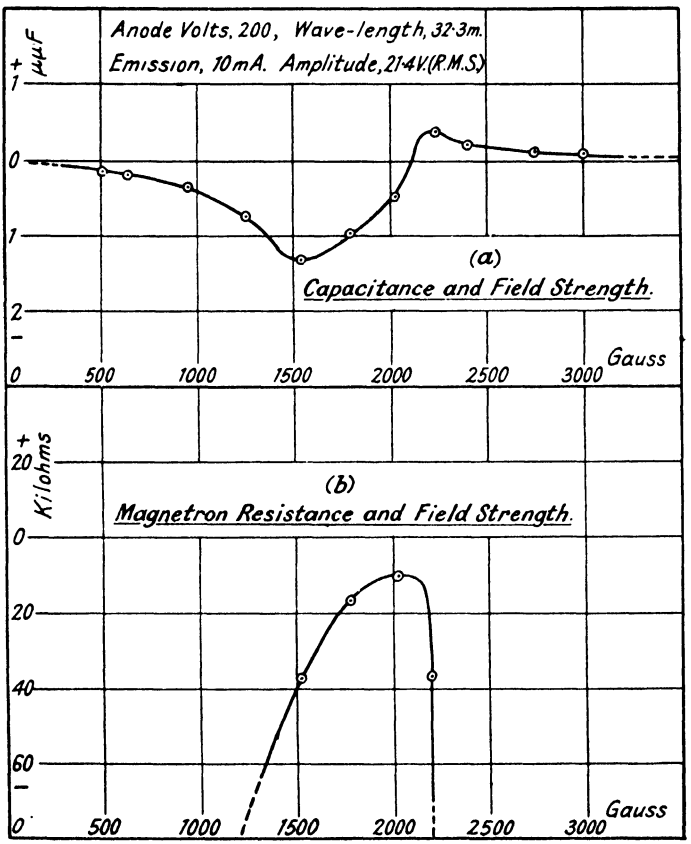

FIG. 76. Variation of resistance and capacitance with field strength.

field the tube capacitance is practically equal to its geometric capacitance, and thus it appears that it is not possible to visualise the magnetron as a series resonant circuit, as suggested by J. S. McPetrie (66). Evidently something in the nature of a complex filter network would be necessary to explain the rapid resistance and reactance changes.

Generation of Oscillations. For any assigned load resistance the power output can be calculated when the amplitude is known, and this output is found to reach a maximum as the field strength is increased. This maximum output is shown as a function of load resistance in Fig. 77*a* for five wavelengths, and it will be seen that each rises to a blunt maximum. The optimum value of field does not, however, change much over a wide range of load resistance. Determination of I_a makes it possible to calculate the efficiency at maximum output, and this is found to be of the order of 40%–60% and is sensibly independent of wavelength. It may be deduced from Fig. 71

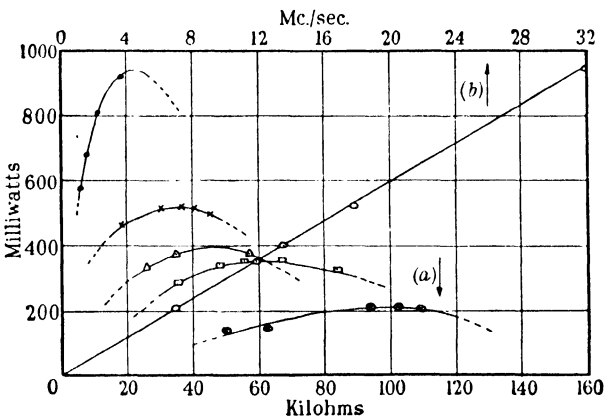

FIG. 77.

(*a*) Variation of power with load resistance at various different frequencies.
(*b*) Variation of maximum power with frequency.

Anode voltage, 200 volts
Filament emission, 10 mA
32·2 Mc./s., 9·27 m. —●——●—
17·8 Mc./s., 16·85 m. —×——×—
13·4 Mc./s., 22·35 m. —△——△—
11·2 Mc./s., 26·75 m. —⊡——⊡—
6·9 Mc./s., 43·30 m. —⊙——⊙—
Maximum power —⊙——⊙—

that the efficiency in general is nearly independent of amplitude and resistance, but it is found to vary with anode voltage and filament emission. The maximum output is shown as a function of frequency in Fig. 77*b*, and results in a linear relation. The optimum load decreases linearly with wavelength as in Fig. 72. The magnetic field at maximum output is shown in Fig. 78*a* as a function of wavelength and in Fig. 78*b*

as a function of anode voltage, and these linear relations result in a value of K that differs little from a mean of 292.

When generating oscillations in this régime under conditions where the input is large the magnetron shows the well-known

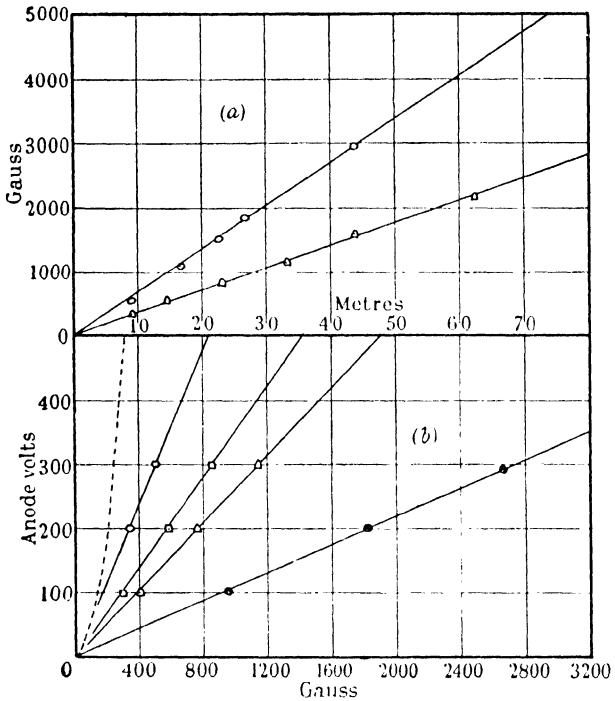

FIG. 78.

(*a*) Variation of field strength for maximum power and for minimum wavelength, with wavelength.
Anode voltage, 200 volts — Maximum power —⊙——⊙—
Anode voltage, 100 volts — Minimum wavelength—△——△—
(*b*) Variation of anode voltage with field strength, for maximum power.
Cut-off condition – – – – – – Wavelength 8·0 m. —⊡——⊡—
Wavelength 4·8 m. —○——○— Wavelength 11·0 m. —△——△—
Wavelength 26·8 m. —⊕——⊕—

phenomenon of additional heating of the filament. In these conditions of maximum output a sudden decrease of load is liable to cause an increase in the oscillatory voltage with excessive anode heating or electron bombardment of the filament which may lead to instability of the tube with disastrous

results. To prevent the anode current rising to a dangerous value a series resistance is sometimes inserted in the high-tension lead. L. H. Ford (14) has described a magnetron oscillator with a compound field winding on the electromagnet and a differential connection, in which the anode current opposes the main magnetising current, is used in conjunction with a series resistance. This arrangement has the advantage that changes in anode current result in $\lambda V/H$ still remaining constant and removal of the load leads to a drop in anode current without cessation of the oscillations. The causes for filament bombardment will be discussed in the next section.

The relation between power (E^2/R) and I_e shown in Fig. 74*a* indicates that modulation by control of the space current (as by means of a suitable control grid) is possible provided the current is below the optimum value but the linearity is not good and the mean output would be low. Fig. 69 shows that anode modulation is possible, both when the amplitude increases with V and when it decreases. In the former case the modulation depth is limited (and sometimes zero), and if this limit is exceeded a hysteresis effect occurs which at the longer wavelengths is sufficient to prevent the oscillations from building up again without circuit readjustment. Similar results would be expected from field strength modulation, but it has been shown that if H and V are altered in the same ratio then the amplitude for a given resistance alters similarly : thus nearly full and linear modulation is possible in this manner, although with normal iron-cored electro-magnets some trouble would probably be experienced with the higher audio-frequencies in speech modulation. It is apparent from Fig. 71*a* that linear modulation is also possible by variation of the load resistance by a suitable modulating system, but the depth is restricted to an extent depending on the field.

Consideration of Fig. 71*a* shows that self-oscillation is not possible when the load resistance is less than a certain minimum value which depends on H, but if a voltage of sufficient magnitude is applied the tube exhibits negative resistance at the wavelength of the applied potential. Thus the effective value of the load resistance to the source of fluctuating potential is reduced, resulting in amplification. For example, if the load

resistance is made 60 kΩ with $H = 2{,}260$, then for an amplitude of 40 volts (r.m.s.) the negative resistance is 78 kΩ, making the effective load resistance 260 kΩ. The driving power is 6·1 mW and the output is 26·7 mW, resulting in a power amplification of 6·5 dB. The linear relation between negative resistance and amplitude shows that the tube would amplify a wave with a depth of modulation depending on the field strength, but the modulation wave would be distorted and, since the driving power varies during the cycle, it would be necessary for this stage to have a low internal resistance to avoid further distortion.

Fig. 71*a* also suggests that, for any given conditions, knowledge of the voltage amplitude, when the tube and a given circuit act as a generator, determines the dynamic resistance of the circuit; and as a result of the linear relation between resistance and wavelength in the magnetron it is possible to calibrate it at long wavelengths and measure circuit resistances at much shorter wavelengths. Although the curves shown apply to symmetrical circuits, similar ones could be derived for the case in which the tube is operated in an unsymmetrical manner.

The split-anode magnetron has been the subject of much development, mainly with the intention of providing, in this régime of oscillation, large power outputs at very high frequencies. Although the frequency of operation can generally be very high, since electron inertia effects are put to advantage, from the point of view of power output the magnetron has some of the disadvantages of normal type thermionic tubes, one being that the high-frequency output is collected at the same electrode as the D.C. supply input. Thus large oscillatory voltages and currents necessitate still larger D.C. voltages and currents with consequent high power dissipation. The power output is thus limited by a compromise between small electrodes giving high frequency of operation and large electrodes giving greater heat dissipation—a condition which has already been discussed with regard to normal tubes.

It is an advantage in favour of the magnetron that under some conditions, as shown above, the radio-frequency current may much exceed the mean input feed current. High output

and efficiency are obtained from the special magnetron described by H. Gutton and S. Berline (30), which has twelve anode segments, while special beam magnetrons have been described by K. Okabe (81–92), S. Uda (110–115), and others. In a water-cooled electron-beam magnetron described by K. Okabe (88) the central filament is surrounded by the water-cooled cylindrical anode, this electrode merely serving to accelerate the electrons in travelling from the cathode. The oscillation electrodes are placed at either end of the anode in a plane at right angles to the filament, and can be two or four in number. The external oscillatory circuit is connected to these end electrodes and the electron motion induces currents thus maintaining oscillation. Very high efficiencies are obtained and a small radiation-cooled sectionalised magnetron operating

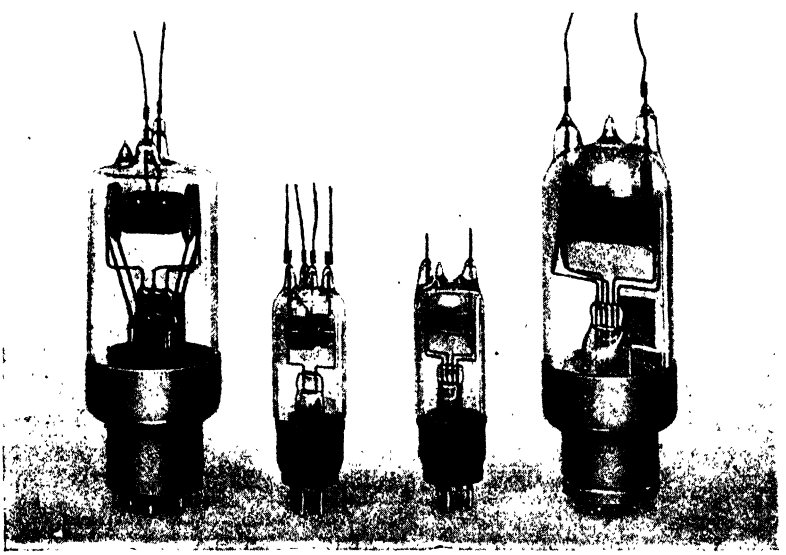

(*a*) (*b*) (*c*) (*d*)

FIG. 79. Typical magnetron tubes.

(*a*) Experimental tube ; 10 W. output at 25–30 cm.
(*b*) Type E.639.
(*c*) Type CW.11.
(*d*) Type E.465.

on these principles has successfully produced a useful output of 100 to 200 watts at wavelengths between 50 and 80 cm. Other types of resonance oscillators are described by F. W. Gundlach (25, 26), A. Haelbig (32), and others, and as with normal triodes and pentodes, increased heat dissipation can be obtained by water cooling the anode.

Fig. 79 illustrates some typical magnetron tubes of Marconi-Osram manufacture. Type E.639 is a four-segment tube which can be connected to give either four- or two-segment

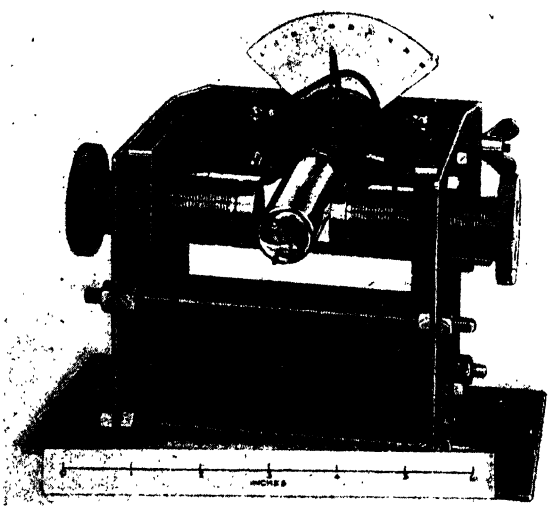

FIG. 80. Experimental adjustable permanent magnet.

operation to give alternative wavelength ranges of 0·5 to 1·5 metres (output 20–40 watts) and 1·5 to 5·0 metres (output 20–50 watts). The anode voltage is 1,000–1,500 volts and the dissipation is 60 watts. The magnetic field required is 500–1,500 gauss for a gap length of 1½ in. Type 465 is intended for electro-medical use with a wavelength range of 2–8 metres. A further magnetron is the E821, with a dissipation of 150 watts, and with the four-segment connection an output of 160 watts at 1 metre and 33 watts at 50 cm. can be obtained, while the E880, with a dissipation of 50 watts, can give an output of

28 watts at 50 cm. with an efficiency of 37%. Equation (102) shows that, in general, higher frequencies can be obtained by the use of more than one pair of anode segments, although in practice the number of segments rarely exceeds four. In this case alternative connections of the segments are possible to give different frequency ranges.

G. R. Kilgore (55) describes a magnetron in which the whole oscillatory circuit is inside the glass bulb and since the conductors were of large cross section and of good thermal conductivity the heat dissipation can be raised by a factor of about twenty over a normal tube. One such generator had an anode dissipation of 200 watts, giving an output of 50 watts at 550 Mc/s with an efficiency of 30%. Shielding electrodes were used to reduce the electron bombardment of the glass walls opposite the anode ends due to the focussing effect of the magnetic field. A further tube was described in which the anode was water cooled, an internal circuit again being used. This tube could dissipate more than 500 watts and would give a power of 100 watts at a frequency of 600 Mc/s with an efficiency of about 25%.

A disadvantage of the magnetron as a generator from the radio communication point of view is that its frequency stability is not very good, and although it is probably no worse as a self-oscillator than the normal triode and better than the Barkhausen oscillator, it is very difficult to drive the magnetron from a more stable source. Frequency variations due to magnetic field fluctuations can be greatly reduced by the use of a permanent magnet which is satisfactory and convenient provided the wavelength and anode voltage do not require frequent alteration. Fig. 80 shows an experimental adjustable permanent magnet made for this purpose by the General Electric Co. Ltd. The frequency stability of the magnetron in the dynatron régime shows that in the neighbourhood of the best operating conditions the stability is of the order 200 parts in 10^6. Small variations in tube resistance due to changes in the operating conditions have an effect on the generated frequency, but the curves of Fig. 68 suggest that the behaviour of the magnetron in the resonance régime in respect of frequency stability should be the same as that

for any " dynatron type " generator. Frequency changes due to small variations in the tube reactance can be reduced by the use of circuits with a small L/C ratio and low values of dynamic resistance, but these conditions are not conducive to good circuit stability.

To overcome modulation difficulties J. Groszkowski and S. Ryzko (24) constructed a tube with a conical anode so that the variations of output with anode potential V would be linear as would be expected from the cut-off formula, where r_a is the anode radius

$$H_c = \frac{6{\cdot}72}{r_a}\sqrt{V} \quad . \quad . \quad . \quad . \quad . \quad . \quad (109)$$

The experiments showed, however, no improvement and it was concluded that space charge distorts the field so that the total cathode emission is always collected by the anode. They showed, however, that it is possible to obtain deep and distortionless modulation by varying the potential of a supplementary electrode which took the form of a cylindrical spiral placed like a grid between the cathode and anode. The oscillation wavelength was 180 cm. and the modulating grid resistance was 50kΩ.

(*b*) ELECTRONIC RÉGIME

Introduction. It is well known that the magnetron has negative resistance properties at wavelengths which are such that the periodic time is closely related to the electron transit time. The properties in this régime, usually known as that of electronic oscillations, are practically independent of external conditions and relate to wavelengths usually less than 15 cm. Although the efficiency and power output are low, these oscillations include the shortest continuous waves that can be generated. The electronic oscillations in the magnetron constituted its first use as a generator of very high frequency power, and they are, in general, found in the neighbourhood of the critical field. The frequency is usually higher than the fundamental resonant frequency of the smallest external circuit which can be attached to the tube and the external circuit, generally in the form of Lecher wires, must be adjusted in length so that an overtone resonance occurs. Since experi-

ment shows that λH is generally nearly a constant of about 11,000 (where λ is in centimetres and H in gauss), and as this agrees closely with the value given by a wave with a period equal to the approximately calculated electron transit time, it has been generally assumed that this type of oscillation is directly related to the orbital motion of the electrons.

The production of electronic oscillations by means of the magnetron was first carried out by A. Žáček (116), who found oscillations in the neighbourhood of the critical field with an optimum wavelength given by λH = constant. K. Okabe (78) produced electronic (or A-type) oscillations down to 25 cm. wavelength with cylindrical diodes and the measured wavelengths agreed with the values calculated on the hypothesis that the oscillation period is equal to twice the time of transit of an electron from cathode to anode. It was found that an improvement could be obtained if a split-anode construction was adopted. It has been noted by A. A. Slutzkin and D. S. Steinberg (103), and later by G. R. Kilgore (54), that for these electronic oscillations the angle between the magnetic lines of force and the electrode axis is of importance, and is not, in general, zero. This tilt of magnetic field has been examined by H. E. Hollmann (44), both theoretically and experimentally. It is possible to give a plausible explanation of the hypothesis that the period of the electronic oscillations is equal to the time taken by an electron to travel from cathode to anode and back. In this case, electrons leaving the cathode during the positive half cycle arrive at the anode when its potential is in the negative half cycle and electrons leaving during the negative half cycle will fail to reach the anode. Thus both anode current and the space charge will be greatest during the negative half cycle and oscillations will tend to be maintained.

The time of transit of the electrons in the magnetron has been discussed in Chapter IV, and K. Okabe (78) obtained an approximate general solution with zero space charge and negligible cathode radius leading to $T = \frac{\pi m}{He}$ and $\lambda H = 10{,}650$, although more accurate graphical methods lead to a value of the constant slightly greater than this. E. C. S. Megaw (68) has described experiments on electronic oscillations in mag-

netrons and good agreement with these theoretical results were obtained with variations of filament emission, angle of tilt, anode voltage, etc. It was suggested that the tilt of magnetic field was necessary to obtain optimum space charge conditions, and this has also been suggested by G. R. Kilgore (54).

Description of Experiments. It is difficult to make accurate measurements on the magnetron properties in this régime of oscillation since the frequency is very high. Although it may be feasible to reduce this by using positive ions, as described for the Barkhausen-Kurz oscillator, examination of the cut-off relationship shows that even for very low anode voltages the field strengths required would be exceedingly large, those for cæsium ions being greater than 20,000 gauss. The disadvantage due to the increase of impedance because of the smaller positive ion current would not be serious, since with electrons this is of a very low order. Since the cut-off field varies inversely as the anode radius, the wavelength of the electronic oscillations would increase directly with increase of radius, but to obtain oscillations at, say, 3 metres would require diameters of the order of 6 cm., and apart from difficulties due to tube construction it would not be easy to get uniform fields over such a large area and length of gap. Thus, in either case the limitations are mainly due to those of available field strength—the condition also commented on in the case of resonance oscillations. As a result of this, the measurements in the first instance were made to find the relations between frequency and power output with the various operating conditions with the view to the understanding of the mechanism of these oscillations.

Since the tube properties are practically independent of the external impedance, the magnetron can be operated as a self-excited generator and the wavelength of the external oscillation carefully measured. The circuit used was a pair of parallel wires several wavelengths long (λ about 30 cm.), and in addition this served as an indication of the wavelength of oscillation. The wires were of 16 S.W.G. bare copper freely supported at either end as shown in Fig. 81*a*, while a sliding bridge in the form of a metal screen 15 cm. square was used for shorting

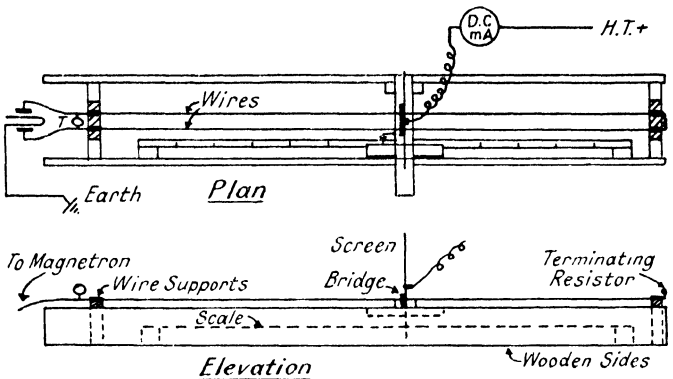

FIG. 81*a*. Lecher wire apparatus.

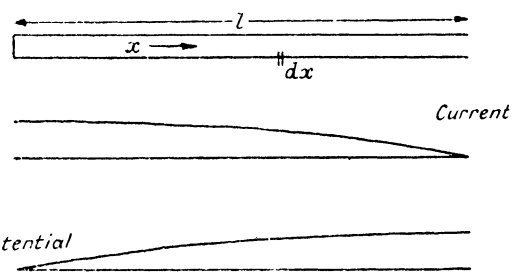

FIG. 81*b*. Distribution of potential and current along a quarter wave line.

the wires and leading in the high-tension input, and the idle portion of the line was terminated by a suitable resistor. The position of this bridge was indicated by a pointer moving over a graduated scale, and care was taken to keep the length of the circuit, on which the wavelength was measured, freely supported and well away from neighbouring objects. The voltage and current distribution along such a system are well known, and that for a quarter wave line is given in Fig. 81*b*. If V_0 and i_0 are the maximum values of voltage and current respectively, then the standing wave system is given by

$$V = V_0 \sin \omega t \sin \frac{\pi x}{2l} \quad . \quad . \quad . \quad . \quad (110)$$

$$i = i_0 \cos \omega t \cos \frac{\pi x}{2l} \quad . \quad . \quad . \quad . \quad (111)$$

where ω is the pulsatance and x the distance along the line. Providing the frequency is sufficiently high the velocity of propagation along the wires is that of light, and thus the wavelength measured along the wires is the same as that in free space. The impedance at any point is given by

$$Z = Z_0 \tan \omega t \tan \frac{\pi x}{2l} \quad . \quad . \quad . \quad . \quad (112)$$

where Z_0 is the characteristic impedance given by

$$Z_0 = \sqrt{L/C} \quad . \quad . \quad . \quad . \quad . \quad (113)$$

where L and C are the inductance and capacitance respectively per unit length. If D is the distance apart and R the radius of the wires, then

$$L = 0{\cdot}00924 \, (\log_{10} D/R + 0{\cdot}1085) \, \mu\text{H/cm.} \quad . \quad (114)$$

$$C = \frac{0{\cdot}1333}{\log_{10}\{D/2R + (D^2/4R^2 - 1)^{1/2}\}} \, \mu\mu\text{F/cm.} \quad . \quad (115)$$

Thus if $D = 1{\cdot}4$ cm., $R = 0{\cdot}09$ cm., then $L = 0{\cdot}012$, $C = 0{\cdot}112$ and $Z_0 = 327\ \Omega$, and if $D = 3{\cdot}0$ cm., $R = 0{\cdot}09$ cm., then $L = 0{\cdot}015$, $C = 0{\cdot}088$ and $Z_0 = 415\ \Omega$. Some information on other types of circuits, such as coaxial lines and wave guides, will be given in Chapter VI.

The amplitude of oscillation was usually indicated by a thermocouple and millivoltmeter placed near the magnetron, the position being adjusted for maximum millivoltmeter reading. In operation the shorting bridge is a point of minimum potential and thus the " maximum " positions should repeat themselves every half wavelength as the bridge is moved along. In practice the mean value of several half wavelengths was taken, and for λ about 30 cm. the readings could be repeated to about 2 mm.

Filament Emission and Angle of Tilt. As the resistance in the electronic régime is particularly sensitive to changes in magnetic field the latter was accurately determined by using an electromagnet with a stalloy yoke so that hysteresis was reduced to a minimum, and by careful calibration with a flux-meter. The presence of undesired long wavelength oscillations, inherent to the form of circuit adopted, was eliminated by suitable adjustment of emission and tilt.

It is known that the amplitude depends considerably on the angle of tilt, and it was found that the optimum tilt varied with the filament emission in the manner shown in Fig. 82*a* for a given set of operating conditions. Thus for vanishingly small emissions the optimum tilt appears to be zero, although

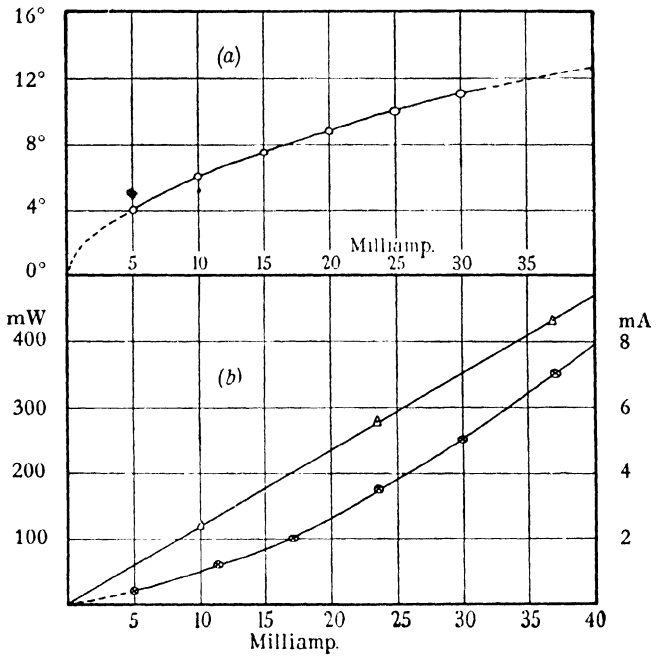

FIG. 82.

(*a*) Variation of optimum angle of tilt with filament emission.
(*b*) Variation of anode-current increase and of equivalent filament heating with anode current.

Anode voltage, 700 volts	Optimum tilt	—○——○—
Field strength, 405 gauss	Anode-current increase	—⊕——⊕—
Wavelength, 30 cm.	Filament heating	—△——△—

the tube resistance would then be very high. Thus tilt is necessary to reduce the space charge caused by the larger emissions, an effect which is in agreement with theory. It is likely that the advantage of slight tilt is the reduction in resistance previously discussed, although the fact that the magnetic field only just exceeds the cut-off value means that a

large number of electrons collide with the anode, resulting in low efficiency. The amplitude increases to a maximum with emission and tilt and then falls for larger currents. Thus there appears to be some mechanism in the tube, as noted for the resonance oscillations, which increases the normal space charge, since saturation should not occur until the emission is of the order of several amperes with the high anode-voltages employed.

The determination of the tube resistance itself is difficult owing to the very short wavelengths and the finite size of electrodes, which make the tube equivalent to a small uncertain length of line. It was found that the amplitude indication was little affected by changing the line impedance from 250 to 500 ohms and that in order to obtain maximum brightness of a load lamp whose steady current resistance was 10 ohms it was necessary to place it near a voltage antinode. Since the power outputs were of the order of 1 watt and the voltage amplitude appeared to be only a few volts it would seem that the resistance has a very low value (in the neighbourhood of 20 ohms) at this wavelength. Extrapolation of the resistance values found at the longer wavelengths in the resonance régime would indicate such a resistance, and it is probable that the magnetron resistance is always low near the cut-off condition. This would be explained by the fact that the electrons at the outer portion of their orbits pass very close to the segment gaps and experience the maximum force due to any potential differences.

Wavelength and Magnetic Field. It has been shown that negative resistance in the electronic régime exists at wavelengths such that λH is a constant of about 11,000, and, moreover, that this value appears to be closely related to the transit time of the electrons. The values of this product were measured under different conditions, and the variation of λH with H is shown in Fig. 83 to be sensibly linear, the required field strengths being slightly greater than the cut-off value. Fig. 84 shows that λH increases with the emission but tends to a minimum when this becomes small. The corresponding curves of tilt (also shown) result in an effect to be expected from Fig. 82*a*.

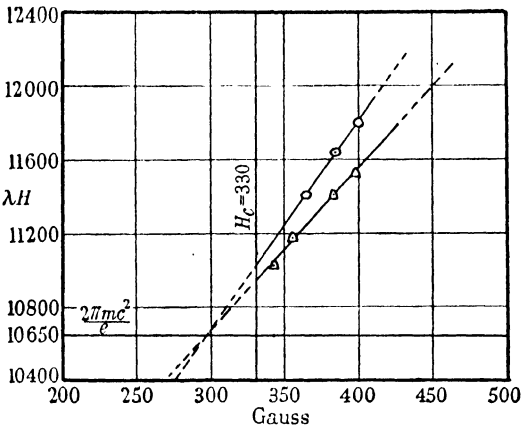

FIG. 83. Variation of λH (in cm. gauss) with field strength.
Anode voltage, 600 volts.
Emission 27 mA, tilt 9·5° —○——○—
Emission 14 mA, tilt 8·0° —△——△—

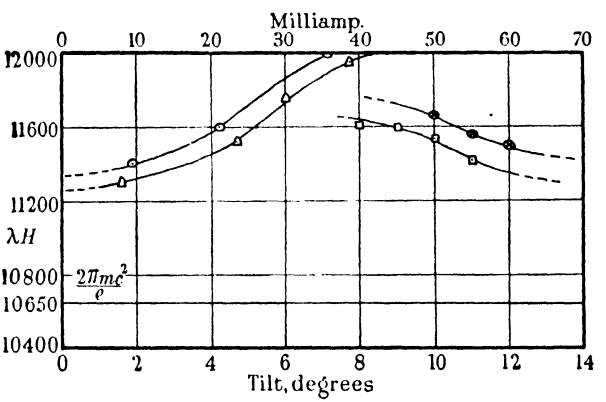

FIG. 84. Variation of λH (in cm. gauss) with filament emission and with angle of tilt.
Field strength, 384 gauss.
Anode voltage 600 volts, tilt 8° —⊙——○—
Anode voltage 600 volts, tilt 10° —△——△—
Anode voltage 600 volts, emission 21 mA —⊡——⊡—
Anode voltage 630 volts, emission 36 mA —⊕——⊕—

It will be observed that the minimum values to which λH tends are generally within the range 11,000–11,400, the lower values relating to conditions in which the space charge would

be expected to be less. It is known that if the magnetic field is such that the electrons just miss the anode, then when the cathode radius is made zero the electron transit-time tends to the value

$$T = \frac{2\pi mc}{He} \quad . \quad . \quad . \quad . \quad . \quad . \quad . \quad (116)$$

for vanishingly small emissions, and to the first order this time is not changed by small angles of tilt. A wave with this periodic time gives $\lambda H = 10{,}650$, and for the cathode radius of the valve used graphical integration of A. W. Hull's equations gives a value of λH about 15% greater. F. B. Pidduck shows that the effect of space charge in the cylindrical (and in the planar) magnetron is to increase the electron transit-time, and while the observed changes in λH can be qualitatively explained by changes in space charge it seems that the observed value is less than would be expected from theory. It is not possible to arrive at any definite conclusion since the oscillations generally occur at fields exceeding the cut-off value, and with small alternating voltages between the segments it is difficult to estimate the transit-time under such conditions.

Intermediate Régimes. From the above results it is possible to calculate the values of $\lambda V/H$ over the range of negative resistance. In particular, the value for maximum output varies only slightly and has a mean of 44 which is about 0·15 of the value of 292 for maximum output of resonance oscillations. This suggests that there may be other régimes of negative resistance with intermediate relations, and some of these have been found. The resistances of the magnetron in these minor régimes tend to be high since oscillations are found only at comparatively high anode voltages, and in some cases large angles of tilt and critical values of filament emission are necessary. Some typical results are given in Table XI below.

The value of $\lambda H/10{,}650$ is usually known as the " order of oscillation," and is taken as unity for the normal electronic oscillation. The first four results show that oscillation can take place when, as in the electronic régime, λH tends to be constant, although the order of oscillation is very high. All

TABLE XI

λ	V	H	α	I_e	$\lambda V/H$	$\lambda V/(44H)$	λH	$\lambda H/10{,}650$	$-R$
cm.	volts	gauss	degrees	mA					kΩ
370	200	1,120	17	6	66	1·5	415,000	38·9	
370	300	1,140	3·5	2	97	2·2	420,000	39·4	
370	400	1,120	17	6	132	3·0	415,000	38·9	Approx. 20
370	500	1,100	8	5	168	3·8	407,000	38·2	
370	300	371	0	1·5	297	6·8	137,000	12·8	
370	300	640	8	15	173	3·9	237,000	22·2	
370	300	1,680	16	20	66	1·5	620,000	58·2	

the results show that intermediate values of $\lambda V/H$ are possible, but the fact that the optimum tilts and emissions are different makes it difficult to come to any definite conclusion regarding the relation between them. No extensive measurements were made of the properties of the tube under these conditions, but it was noted that they tended to be those associated with the resonance oscillations as well as the electronic type. It is important that these minor oscillations show properties similar to those of the other two régimes, since it points to a similarity between the latter. Thus many of the tube properties determined at longer wavelengths could be applied, at least qualitatively, to the electronic régime of negative resistance, and it is possible that they could be applied in part to electronic oscillations occurring in thermionic tubes in general.

These oscillations have also been found and described by J. S. McPetrie (67), who has made a comprehensive study with single anode, two-segment and four-segment magnetrons. It was found that oscillations could be produced with single-anode tubes at magnetic field intensities much greater than the critical value and with various values of λH. When λ was plotted against H the experimental points lay closely to a series of parallel lines given, for constant anode voltage, by

$$\frac{\lambda}{H} = \frac{\text{const}}{n} : n = 1, 2, 3, \text{ etc.}$$

the constant being 283 for the tube under test. Sometimes two or three frequencies would be obtained with one value of magnetic field, but it was possible to separate these by suitable adjustment of the filament emission. A point of considerable

interest is that, although no normal electronic oscillation could be detected complying with the condition $\lambda H = 11{,}000$ near the critical field, the line $n = 7$ cuts the line $\lambda H = 11{,}000$ at the critical field. With other anode voltages the positions of the parallel lines altered in such a way that for a given wavelength the ratio of anode voltage to magnetic field intensity remained constant. The slope of the lines was such that for each line λ/H = constant, so that as H for a given wavelength λ is proportional to the anode voltage, $\lambda V/H$ = constant. The values of this constant for a series of anode voltages are given in the following table for a magnetron with an anode diameter of 1·0 cm.: they correspond to the lines having respectively the maximum and minimum observed values of $\lambda V/H$.

TABLE XII

Anode voltage.	λ in cms.	Magnetic field, gauss.	λV/H
300	590	560	315
,,	140	1,040	40
360	500	640	280
,,	98	840	42
480	480	820	280
,,	145	1,580	44
600	580	1,120	310
,,	115	1,600	43

The average maximum and minimum values of $\lambda V/H$ from this table are respectively 296 and 42. The ratio of these two numbers is about 7, showing that for a given magnetic field there was a ratio of 7 in the range of wavelengths of the oscillations obtainable. Similar results were observed with two- and four-segment tubes, and in general it was found that $\lambda V/H$ for electronic oscillations increases with wavelength, becoming the same as that for resonance oscillations at a common wavelength. In addition it was found that if i is the static anode current corresponding to the field H, then the experimental results for both two- and four-segment tubes gave a relation

$$\lambda^2 i = \text{constant}$$

which is similar to that given in Chapter III for the *G-M* oscillations in retarding field tubes.

Additional Filament Heating. As with resonance oscillations, additional filament heating occurs, which is revealed by the anode current exceeding the value for H zero. Since I_a is only

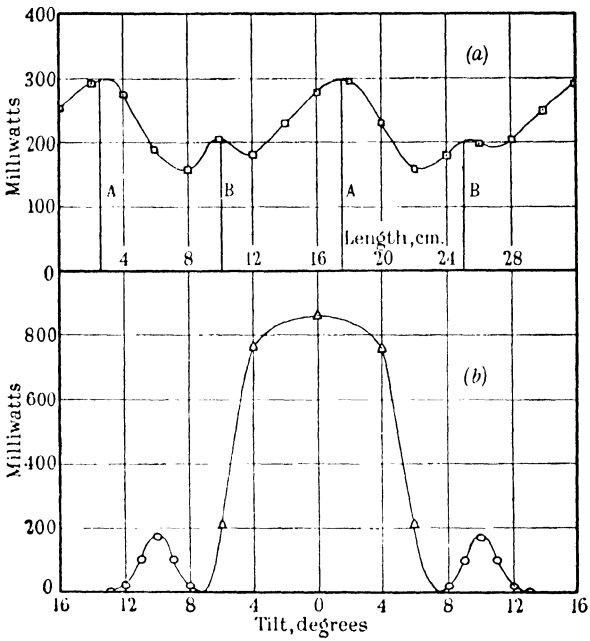

FIG. 85.

(*a*) Variation of filament heating with change in length of externa circuit.
(*b*) Variation of filament heating with angle of tilt.
Anode voltage, 700 volts.
Field strength, 381 gauss.
Filament emission, 35 mA.
" A " represents minimum external output.
" B " represents maximum external output.
Wavelength 30 cm., tilt 10° —⊡——⊡—
Wavelength 30 cm. —⊙——⊙—
Wavelength 350 cm. —△——△—

slightly less than I_e any observed increase in I_a is due mainly to an increase of emission. Fig. 82*b* shows this increase and the equivalent filament heating power (derived from the emission characteristic, Fig. 1) as a function of anode current for a constant anode voltage. This effect increases with the

input to the tube, and since the output falls appreciably for large emissions it is evident that this effect can occur when there is no external evidence of oscillation.

The filament was heated from a sensibly constant-current source and the changes in battery filament heating due to resistance variations were determined by a potentiometer and millivoltmeter. After the equivalent heating has been corrected for this some energy remains, namely that imparted to the filament during operation and which must come from the anode supply. Moreover, the filament-resistance changes obtained from the characteristics given in Fig. 1 correspond to those which would occur if the increased anode current were entirely due to an increase in filament emission ; and thus in this case any effects due to secondary emission, positive ion current, or other causes are negligible.

This energy is expressed in Fig. 85*a* as a function of changes in length of the external circuit. It will be noted that this effect is greater when the external output is a minimum (and actually nearly zero), and suggests that the mechanism causing this heating would be present with the anode segments short-circuited. The rises in anode current in this experiment were of the order shown in Fig. 82*b*. Fig. 85*b* shows this heating energy as a function of angle of tilt, and some results for the larger resonance régime heating are also included. It would seem that this heating is due to the electrons returning to the filament with higher velocities than those with which they left, since it has been previously demonstrated in Chapter IV that it is possible for the electrons in the course of their orbits to have greater velocities than those given by simple calculation. It is uncertain, however, whether it is a necessary condition that oscillation shall be present.

This additional heating of the filament has been investigated by O. Pfetscher and W. Puhlmann (94), who conclude that it is due to bombardment of the filament by returning electrons which acquire increased energy by virtue of their oscillations, while A. P. Maidanov (65) considers that it is due to ionic bombardment as the heating varies with the residual gas pressure and its atomic weight, and states that observable effects are noted at pressures as low as 10^{-6} mm.

Single Anode Oscillations. Although the type of magnetron used for generating these electronic oscillations is the normal one with the anode in two segments, it is possible, as mentioned earlier, to generate these with the single-anode magnetron, but as the power output and efficiency are even less than that for the split-anode magnetron these oscillations are not of much practical importance. Since they are of possible theoretical interest, the properties of the single-anode magnetron were briefly examined. This was done by connecting together the two anode leads and joining them to the end of one of the parallel wires while the end of the other wire was joined through a 0·001 μF condenser to the filament terminal. The power output was so small that with the thermocouple in the best position the millivoltmeter deflection amounted to only a few divisions. The wavelength readings obtained are given in the following table :—

TABLE XIII

Wavelength in cm.	Field in Gauss	Anode Volts	Emission mA.	Tilt in Degrees	λH	$\frac{\lambda V}{H}$
30·5	406	700	23	7·5	12,370	52·6
26·5	436	700	23	9·0	11,560	42·5

It will be seen that the values of λH and $\frac{\lambda V}{H}$ are generally similar to those for the split-anode magnetron. In addition, small deflections of the millivoltmeter were observed at other positions of the bridge, and it is probable that these weak intermediate oscillations were similar to those found in the case of the split-anode magnetron, although the single-anode tube has not been found to generate resonance oscillations. It is stated by K. Okabe (87) that oscillations were observed at magnetic fields greater than the critical value, but most workers have confined themselves to the main oscillation occurring about $\lambda H = 11{,}000$.

Generation of Oscillations. As a generator in the electronic régime the split-anode magnetron is capable of producing extremely short wavelengths, but the power output and

efficiency are very low. For shorter wavelengths the electrodes must be made small with consequent reduction in dissipation and power output. The variation of output with frequency for a given tube is similar to that of the Barkhausen-Kurz oscillator. The optimum anode voltages and filament emissions increase with frequency, and thus there is a fairly sharply defined minimum frequency set by the allowable anode dissipation. As with normal tubes, water cooling of the anode can be employed, particularly if this is of the single (non-slit) type.

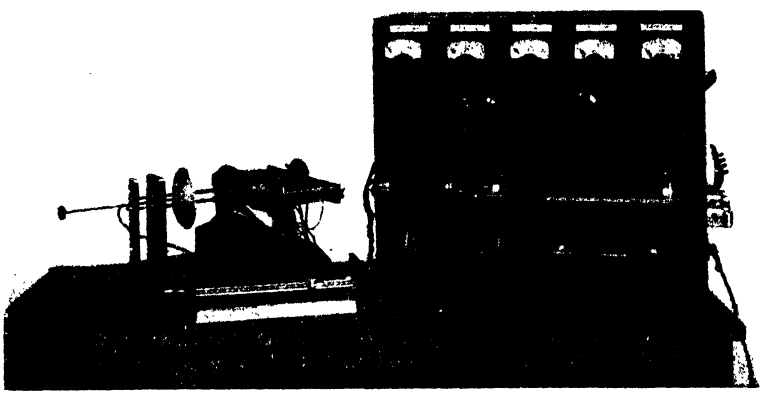

FIG. 86. Magnetron oscillator with power supply unit and absorption wavemeter. The oscillator parallel wire system shown is for λ = 20–35 cm. and is interchangeable with other systems for longer wavelengths.

Fig. 86 shows a complete electronic oscillator made by the General Electric Co. Ltd. It incorporates a type CW10 magnetron, which is similar to that on which most of the above measurements have been made. The anode voltage is 1,000–1,200 volts and the dissipation 50 watts and the normal wavelength range is 20–35 cm.

E. G. Linder (62) has described a magnetron capable of generating wavelengths of about a few centimetres in which the external circuit is inside the glass envelope, although this of course restricts the possible range of oscillation. Improved

output and efficiency is obtained when end plates, held at a suitable high potential, are used instead of the more usual tilted magnetic field. This particular tube has proved very reliable and stable in operation and at a frequency of 3,000 Mc/s an output of 2·5 watts was obtained at an efficiency of 12%. The tantalum anodes were 8 mm. in length, 4 mm. in diameter, and separated by a slit 0·5 mm. wide. The end plates were held about 0·5 mm. from the anode ends and the best operating potential was about half that of the anode. A later type is described (63) in which the anode itself forms the resonant circuit, and this tube gives an output of 20 watts on 9 cm. with an efficiency of 20%. The output was determined by means of tungsten filaments connected directly to the anode segments inside the envelope, and instability due to filament bombardment was avoided by arranging that anode current increases caused a decrease of filament heating current. The optimum values of load resistance were found to be of the order of 20–50 Ω, this being found by estimating the skin effect in the load filaments.

Other magnetrons capable of generating electronic oscillations have been described by H. Richter (99), K. Okabe (92), and A. A. Slutzkin (104–106).

Although the klystron, to be described later, has some advantages over the magnetron as an ultra-short wave generator, the latter is capable of excellent performance as a self-contained generator, both in the resonance and electronic régimes, due to its low internal resistance and large radio-frequency current output. Its use in radio communication as a transmitter appears to be limited, since modulation of the carrier output is difficult and unsatisfactory, and, unlike the triode or pentode, it cannot be easily driven as a power amplifier from a more stable source of frequency.

Although many direct properties of the magnetron have been measured and compared with the known theory, no complete explanation of its mechanism of operation has been found. In this respect an increased knowledge of the behaviour of the electrons in their orbits from the theoretical point of view, particularly under dynamic conditions, would be desirable. There appears to be experimental evidence which

strongly suggests that these régimes are not entirely distinct, and that the magnetron properties may differ in them only because of the varying effects due to electron motion or allied phenomena.

BIBLIOGRAPHY

1. AHRENS, E. "Water-cooled Four Slit Magnetron for Decimetre Waves." *Hochf. Tech. u. Elek. akus.*, 1937, **50**, 181.
2. AWENDER, H. "Experiments on Generation of Extremely Short Wavelengths with Magnetic Field Valves." *Funktech. Monat.*, 1937, **3**, 347.
3. AWENDER, H. "The Properties and Use of the Magnetic Field Valves." *Funktech. Monat.*, 1938, **4**, 173, 201.
4. BERGER, H. "Fundamentals of the Magnetron Valve." *Funktech. Monat.*, 1938, **4**, 97.
5. BIGUENET, O. and PIERRET, E. "On the Ultra Short Waves obtained with a Magnetron." *J. Phys. et Rad.*, 1935, **6**, 67.
6. BIGUENET, O. and PIERRET, E. "On the Anomalous Increase of Anode Current in Magnetrons." *J. Phys. et Rad.*, 1936, **7**, 33.
7. BOGGIO, T. "New Integration of Equations of Electron motion in Superposed Electric and Magnetic Fields." *Comptes Rendus.*, 1938, **207**, 134.
8. BOVSHEVEROV, V. M. and GRECHOWA, M. T. "Magnetrons for Decimetre Waves." *J. Tech. Phys.*, 1935, **5**, 69.
9. DEHLINGER, W. "Ultra High Frequency Oscillation of the Magnetostatic Vacuum Tube." *Physics*, 1932, **2**, 432.
10. ELDER, F. R. "The Magnetron Amplifier and Power Oscillator." *Proc. Inst. Rad. Eng.*, 1925, **13**, 159.
11. ERARD, J. and PIERRET, E. "Influence of Magnetic Field Tilt on the Oscillations in a Magnetron." *J. Phys. Rad.*, 1938, **9**, 54.
12. FASSI, G. and SALOM, G. "The Magnetron as a Generator of Micro Waves." *Alta Freq.*, 1934, **3**, 396.
13. FISCHER and LÜDI. "The Posthumous Oscillations in the Magnetron." *Bull. Assoc. Suisse Elec.*, 1937, **28**, 277.
14. FORD, L. H. "A Magnetron Oscillator with a Compound Field Winding." *J. Inst. Elec. Eng.*, 1940, **86**, 293.
15. FRITZ, K. "Production of Oscillations with the Habann Valve." *Hochf. Tech. u. Elek. akus.*, 1935, **46**, 16.
16. FRITZ, K. "Theory of Transit Time Oscillations of the Magnetron." *Telefunken Zeit.*, 1936, **17**, 31.
17. FRITZ, K. "Generator Circuit using a Magnetron." *Hochf. Tech. u. Elek. akus.*, 1937, **49**, 105.
18. FRITZ, K. "Energy Balance of the Electrons in Magnetic Field Valves." *Telefunken Zeit*, 1937 **18**, 37.
19. GIACOMINI, A. "Anomalous Dispersion in the Magnetron." *La Ricerca Scient.*, 1934, **1**, 650.
20. GILL, E. W. B. and BRITTON, K. G. "The Action of the Split Anode Magnetron." *J. Inst. Elec. Eng*, 1936, **78**, 461.
21. GOTO, K. and NISHIMURA, S. "Series Modulation of Split Anode Magnetron Oscillators." *Electrot. J. Tokyo.*, 1938, **2**, 133.

22. GROOS, O. "The Magnetic Field Valve Emitter." *E. N. T.*, 1937, **14**, 325.
23. GROOS, O. "Production of Dwarf Waves with Magnetron Emitters." *Hochf. Tech. u. Elek. akus.*, 1939, **51**, 37.
24. GROSZKOWSKI, J. and RYZKO, S. "A New Method of Modulating the Magnetron Oscillator." *Proc. Inst. Rad. Eng.*, 1936, **24**, 771.
25. GUNDLACH, F. W. "Recent Investigations on Decimetre Wave Magnetron Transmitters." *Hochf. Tech. u. Elek. akus.*, 1936, **48**, 201.
26. GUNDLACH, F. W. "The Habann Valve as a Generator of Decimetre Waves." *E.T.Z.*, 1937, **58**, 653.
27. GUNDLACH, F. W. "The Multi Wave Properties of Habann Generators." *T.F.T.*, 1938, **27**, 177.
28. GUNDLACH, F. W. "The Behaviour of the Habann Valve as a Negative Resistance." *E.N.T.*, 1938, **15**, 183.
29. GUNDLACH, F. W. "Modulation of Magnetron Emitters by Amplitude Limitation." *Hochf. Tech. u. Elek. akus.*, 1939, **53**, 10.
30. GUTTON, H. and BERLINE, S. "Research on Magnetrons for Ultra Short Waves." *Bull. de la S.F.R.*, 1938, **12**, 30.
31. HAELBIG, A. "A Magnetron free from Back Heating." *Z. f. Tech. Phys.*, 1937, **18**, 247.
32. HAELBIG, A. "A Grid-controlled Magnetic Field Valve." *Hochf. Tech. u. Elek. akus.*, 1937, **50**, 96.
33. HABANN, E. "The Split Anode Magnetron." *Z. f. Hochfreq.*, 1924, **24**, 115.
34. HARA, G. "The Magnetron as a Constant Current Oscillator." *Electrot. J. Tokyo*, 1939, **4**, 214.
35. HARA, G. "Internal Capacity and Resistance of Magnetrons." *Electrot. J. Tokyo*, 1940, **4**, 24.
36. HARA, G. and MITO, S. "Wavelength of Electron Oscillations in the Magnetron." *Electrot. J. Tokyo*, 1939, **3**, 23.
37. HARVEY, A. F. "The Impedance of the Magnetron in Different Regions of the Frequency Spectrum." *J. Inst. Elec. Eng.*, 1940, **86**, 297.
38. HELLER, G. "The Magnetron as a Generator of Ultra Short Waves." *Philips Tech. Rev.*, 1939, **4**, 189.
39. HERRIGER, F. and HÜLSTER, F. "The Oscillations of Magnetic Field Valves." *Telefunken Rohre.*, 1936, **7**, 71 and 221.
40. HERRIGER, F. and HÜLSTER, F. "Oscillations Valves in with Magnetic Fields." *Hochf. Tech. u. Elek. akus.*, 1937, **49**, 123.
41. HISHIDA, M. "Theory of Asymmetrically Split Magnetrons." *Electrot. J. Tokyo*, 1939, **3**, 144.
42. HOLLMANN, H. E. "The Behaviour of the Electron Oscillator in a Magnetic Field." *E.N.T.*, 1929, **6**, 377.
43. HOLLMANN, H. E. "The Generation of Ultra Short Waves by Thermionic Valves." *Z. f. Hochf. Tech.*, 1930, **35**, 21 and 76.
44. HOLLMANN, H. E. "The Magnetron as a Negative Resistance." *Ann. Phys.*, 1931, **8**, 956.
45. HOLLMANN, H. E. "Arrangement for Push-Pull Modulation of Split Anode Magnetrons." *Hochf. Tech. u. Elek. akus.*, 1937, **49**, 105.

46. HOLLMANN, H. E. "Survey of New Magnetic Field Valves." *Funktech. Monat.*, 1938, **3**, 75.
47. HULL, A. W. "The Effect of a Uniform Magnetic Field on the Motion of Electrons between Co-axial Cylinders." *Phys. Rev.*, 1921, **18**, 13.
48. HÜLSTER, F. "Cathode Overheating in the Magnetic Field Valve." *Telefunken Rohre.*, 1938, **14**, 217.
49. ILJINSKI, V. and LUKOSHKOV, V. "The Formation of Negative Resistance in the Split Anode Magnetron." *J. Tech. Phys.*, 1938, **8**, 1996.
50. ITO, Y. "Contribution to the Theory of the Two Slit Magnetron in the C Region." *Rep. Rad. Res. Japan.*, 1937, **7**, 159.
51. ITO, Y. and KATSURAI, S. "The Three Slit Magnetron and Three Phase Oscillations." *Nippon Elec. Comm. Eng.*, 1937, **1**, 467.
52. KATSURAI, S. "Generation of Three Phase Oscillations by a Three Slit Magnetron." *Electrot. J. Tokyo*, 1937, **1**, 152.
53. KATSURAI, S. "Theory of the Split Anode Magnetron Oscillator." *Nippon Elec. Comm. Eng.*, 1937, **1**, 129.
54. KILGORE, G. R. "Magnetostatic Oscillators for Generation of Ultra Short Waves." *Proc. Inst. Rad. Eng.*, 1932, **20**, 1741.
55. KILGORE, G. R. "Magnetron Oscillators for Generation of Frequencies from 300–600 Mc/s." *Proc. Inst. Rad. Eng.*, 1936, **24**, 1140.
56. KILGORE, G. R. "The Magnetron as a High Frequency Generator." *J. Appl. Phys.*, 1937, **8**, 666.
57. KOHLER, H. W. "Measurement of Output of Magnetrons using Thermocouples." *Proc. Inst. Rad. Eng.*, 1937, **25**, 1381.
58. LÄMMCHEN, K. "Differentiation of the Various Types of Oscillation in a Habann Valve." *Hochf. Tech. u. Elek. akus.*, 1938, **51**, 87.
59. LÄMMCHEN, K. and LERBS, A. "First Order Transit Time Oscillations in Magnetrons." *Hochf. Tech. u. Elek. akus.*, 1938, **52**, 186.
60. LÄMMCHEN, K. and MÜLLER, L. "Sinusoidal Oscillations in the Habann Valve." *E.N.T.*, 1939, **16**, 37.
61. LINDER, E. G. "Improved Magnetron Oscillator." *Phys. Rev.*, 1934, **45**, 656.
62. LINDER, E. G. "Description of the End Plate Magnetron." *Proc. Inst. Rad. Eng.*, 1936, **24**, 633.
63. LINDER, E. G. "The Anode Tank Circuit Magnetron." *Proc. Inst. Rad. Eng.*, 1939, **27**, 732.
64. MAIDANOV, A. P. "Graphite Anodes in Split Anode Magnetrons." *J. Tech. Phys.*, 1935, **3**, 1563.
65. MAIDANOV, A. P. "Influence of Gas Pressure on the Energy and Efficiency of Magnetron Oscillators." *Phys. Z. Sowjet.*, 1936, **10**, 718.
66. MCPETRIE, J. S. "Electronic Oscillations in Triodes and Resonance Oscillations in Magnetrons." *J. Inst. Elec. Eng.*, 1937, **80**, 84.
67. MCPETRIE, J. S. "Experimental Investigation of Resonance and Electronic Oscillations in Magnetrons." *J. Inst. Elec. Eng.*, 1940, **86**, 283.

68. MEGAW, E. C. S. "An Investigation of the Magnetron Short Wave Oscillator.," *J. Inst. Elec. Eng.*, 1933, **72**, 326.
69. MEGAW, E. C. S. "A Magnetron Oscillator for Ultra Short Wavelengths." *Wireless Eng.*, 1933, **10**, 197.
70. MEGAW, E. C. S. "Magnetron Valves for Ultra Short Wavelengths." *G. E. C. J.*, 1936, **7**, 94.
71. MORITA, K. "Obliquely Split Magnetron." *Nippon Elec. Comm. Eng.*, 1937, **1**, 477.
72. MÖLLER, H. G. "Electron Paths and Mechanism of Excitation of Oscillations in Split Anode Magnetrons." *Hochf. Tech. u. Elek. akus.*, 1936, **47**, 115.
73. MÖLLER, H. G. "Theory of the Mechanism of Oscillations in the Split Anode Magnetron." *Hochf. Tech. u. Elek. akus.*, 1936, **48**, 133.
74. MÖLLER, H. G. "Measurement of the Electron Ring Current in the Magnetron." *Hochf. Tech. u. Elek. akus.*, 1936, **48**, 141.
75. MOULLIN, E. B. "Radio Frequency Measurements," 1931.
76. MULLER, F. "Theory of the Magnetron Valve Transmitter with Split Anode." *Tech. Phys. U.S.S.R.*, 1935, **1**, 509 and 529.
77. OHTAKA, S. "A B-type Parallel Wire Oscillator." *Electrot. J. Tokyo.* 1938, **2**, 70.
78. OKABE, K. "The Short Wave Limit of Magnetron Oscillators." *Proc. Inst. Rad. Eng.*, 1929, **17**, 652.
79. OKABE, K. "Magnetron Oscillations of a New Type." *Proc. Inst. Rad. Eng.*, 1930, **18**, 1748.
80. OKABE, K. "Production of Ultra Short Waves with Double Anode Magnetrons." *Rep. Rad. Res. Japan*, 1935, **5**, 69.
81. OKABE, K. "A New Electron Oscillator." *Rep. Rad. Res. Japan*, 1936, **6**, 69.
82. OKABE, K. "Electron Beam Magnetron." *Electrot. J. Tokyo*, 1937, **1**, 30.
83. OKABE, K. "Mechanism of Type B Magnetron Oscillations." *Electrot. J. Tokyo*, 1937, **1**, 69.
84. OKABE, K. "Split Anode Magnetron of Special Type." *Electrot. J. Tokyo*, 1937, **1**, 213.
85. OKABE, K. "Mechanism of Split Anode Magnetron Oscillators." *Nippon Elec. Comm. Eng.*, 1937, **1**, 530.
86. OKABE, K. "The Virtual Cathode in the Magnetron." *Rep. Rad. Res. Japan*, 1938, **8**, 21.
87. OKABE, K. "Obtaining Dwarf Waves with Multi Split Anode Magnetrons." *Rep. Rad. Res. Japan*, 1938, **8**, 27.
88. OKABE, K. "Electron Beam Magnetrons and Type B Magnetron Oscillations." *Proc. Inst. Rad. Eng.*, 1939, **27**, 24.
89. OKABE, K. and OWAKI, K. "A New Electron Oscillator." *Nippon Elec. Comm. Eng.*, 1937, **1**, 461.
90. OKABE, K. and OWAKI, K. "Production of Dwarf Waves by the Osaka Tube." *Nippon Elec. Comm. Eng.*, 1938, **2**, 212.
91. OKABE, K. and OWAKI, K. "A Sectionalised Magnetron." *Electrot J. Tokyo*, 1938, **2**, 257.
92. OKABE, K. "Magnetron Oscillations of Ultra Short Wavelengths and Electron Oscillations in General." 1938, 57 pp.

93. OWAKI, K. "Specially Sectionalised Magnetron Tube." *Nippon Elec. Comm. Eng.*, 1939, **16**, 631.
94. PFETSCHER, O. and PUHLMANN, W. "High Power Habann Generator for Micro Waves." *Hochf. Tech. u. Elek. akus.*, 1936, **47**, 105.
95. PIDDUCK, F. B. "Treatise on Electricity," 1924.
96. PONTE, M. "The Use of Magnetic Fields for the Production of Ultra Short Waves." *J. Phys. Rad.*, 1932, **3**, 183.
97. PONTE, M. "The Use of Magnetic Fields for the Production of Ultra Short Waves." *L'Onde Elec.*, 1934, **13**, 493.
98. POSTHUMOUS, K. "Oscillations in a Split Anode Magnetron." *Wireless Eng.*, 1935, **12**, 126.
99. RICHTER, H. "Production of cm. and mm. Waves in Magnetrons." *Hochf. Tech. u. Elek. akus.*, 1938, **51**, 10.
100. ROSEN, L. "Characteristics of a Split Anode Magnetron as a Function of Slot Angle." *Rev. Scient. Instr.*, 1938, **9**, 372.
101. RUNGE, W. "The Generation of Oscillations with the Magnetron." *Telefunken Z.*, 1934, **15**, 5.
102. SCHWAYENBACH, H. A. "Space Charges and Oscillations in Magnetron Triodes." *Helv. Phys. Acta*, 1935, **9**. 565.
103. SLUTZKIN, A. A. and STEINBERG, D. S. "Production of Short Wave Undamped Oscillations by the Use of a Magnetic Field." *Ann. Phys.*, 1929, **1**, 658.
104. SLUTZKIN, A. A. and LELJAKOV, P. P. "A Special Type of Magnetron Oscillation." *Phys. Ber.*, 1933, **14**, 1266.
105. SLUTZKIN, A. A. and OTHERS. "The Generation of Electromagnetic Waves below 50 cm. with Magnetrons." *Phys. Z. Sowjet.*, 1934, **6**, 150.
106. SLUTZKIN, A.A. and OTHERS. "Factors influencing the Output and Efficiency of Magnetrons." *Phys. Z. Sowjet.*, 1934, **5**. 887.
107. SSUSLOV, S. A. "The Occurrence of Oscillations in the Magnetron at Low Electric Field Strengths." *Phys. Z. Sowjet.*, 1936, **10**, 262.
108. UCHIDA, Y. "Modulation of Magnetron Oscillators with Auxiliary Electrodes." *Electrot. J. Tokyo*, 1937, **1**, 115.
109. UCHIDA, Y. and OTHERS. "Radiation-cooled Magnetron with Four Slit Anode." *Nippon Elec. Comm. Eng.*, 1939, **15**, 537 and *Electrot. J. Tokyo*, 1938, **2**, 290.
110. UDA, S. "Sentron—a New Tube for Ultra Short Waves." *Rep. Rad. Res. Japan*, 1938, **8**, 47.
111. UDA, S. "Valves for Ultra Short Waves—Sentrons." *J. Scient. Instr.*, 1939, **16**, 171.
112. UDA, S. and OTHERS. "On Sentrons—a New Tube for Ultra Short Waves." *Electrot. J. Tokyo*, 1937, **1**, 167 and *Nippon Elec. Comm. Eng.*, 1938, **10**, 171.
113. UDA, S. and ISHIDA, M. "'Sentron' Oscillations with Electron-coupled Secondary Circuit." *Electrot. J. Tokyo*, 1938, **2**, 95.
114. UDA, S. and OTHERS. "Ultra High Frequency Oscillations obtained by Sentrons." *Electrot. J. Tokyo*, 1938, **2**. 266 and 291.
115. ZÁČEK, A. *Zeit f. Hochf.*, 1928, **32**, 172.
116. OWAKI, K. "The Magnetron with a Bowl-type Resonator." *Electrot. J. Tokyo*, 1940, **4**. 188.

CHAPTER VI

MISCELLANEOUS TUBES AND CIRCUITS AT VERY HIGH FREQUENCIES

(*a*) THE KLYSTRON AND ALLIED TUBES

Power Outputs. At very high frequencies normal modulation of the electron stream has been previously shown to present considerable difficulties, due to the finite electron transit time between the cathode and control grid or electrode. Although this can be partially overcome by using high accelerating voltages and fields, it will be apparent that, apart from mere voltage difficulties and limitations, it would be difficult for any grid operating with reasonably high radio-frequency potentials to exercise complete control over the beam so as to modulate it. Thus attention has been directed to modulating systems which only alter the velocity of the electrons to a greater or less extent. Before describing these and other specialised thermionic tubes it will be instructive to compare the power outputs of different types and ratings of tubes in the high-frequency spectrum.

Fig. 87 gives the useful power output as a function of operating frequency (or wavelength) of examples of normal triodes, Barkhausen-Kurz generators, and magnetrons, some of which have been described in the preceding chapters. The 3B/250A is a triode with an anode dissipation of 25 watts at 300 volts, while the D156548 is a larger tube capable of dissipating 50 watts. Both tubes have thoriated tungsten filaments and are of double-ended construction, so that the effect of the anode grid capacitance can be reduced by connecting them at the mid-point of a half-wave transmission line. The 4304B (or its equivalents, DET12 and TY150) has a dissipation of 50 watts at 1,250 volts, while the smaller 4316A (or TY04 30) triode dissipates 30 watts. The electrode and lead arrangements of these latter triodes is of more or less normal construc-

tion although, if necessary, they can be used with parallel line external circuits. The RCA888 is a small water-cooled triode whose size has been reduced as much as possible consistent with the power desired. The pure tungsten filament takes

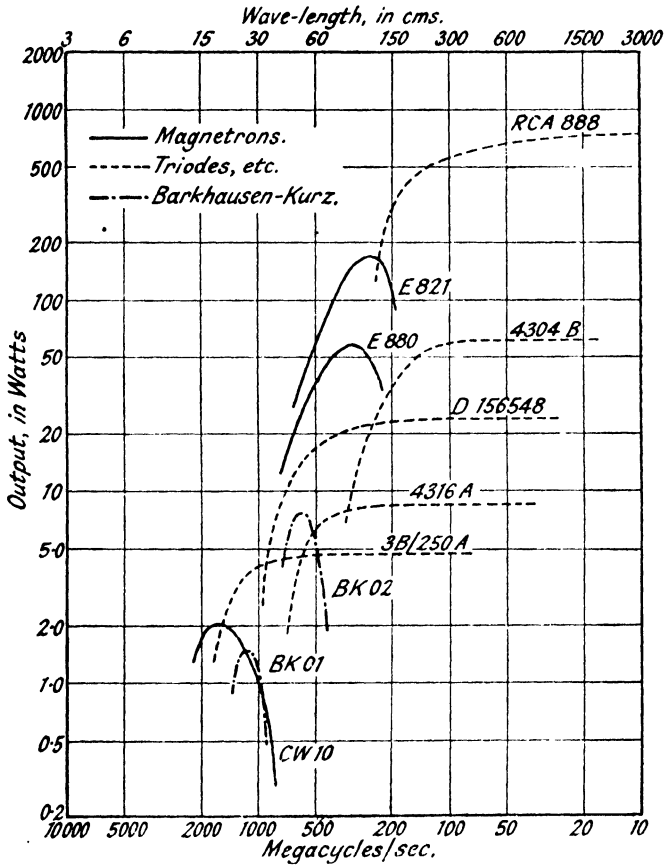

FIG. 87. Power outputs of different types of tubes.

24 amps. at 11 volts and the anode dissipation is 1,000 watts at 3,000 volts.

The retarding field tube denoted BK01 is of normal pattern, but the BK02 has the spiral grid construction described in Chapter III. The CW10 is a split-anode magnetron of 50 watts

dissipation at 2,000 volts, and it will be observed how the power outputs of these three electronic oscillators varies rapidly with frequency. The E880 is a four-segment tube of 50 watts dissipation with the segments cross-connected internally while another, the E821, employs special electrode materials, so that although the anode length and diameter are only 2·0 and 1·0 cm. respectively, it can dissipate 150 watts. This diagram will be found very helpful when comparison is needed between the performances of thermionic tubes of whatever type. At wavelengths over 10 metres there is, in general, little limitation on the tube output from the operating frequency point of view, and thus the obtainable powers tend to be limited by the available high tension and filament supplies and cooling facilities.

Velocity Modulation. This section is concerned with the properties of thermionic tubes which use velocity modulation of the electron stream as opposed to the emission density modulation used in normal tubes. This operation is found to have advantages at very high frequencies and, in the Klystron, types of electromagnetic resonators are used instead of tuned circuits, Lecher wires or concentric lines. In addition, the high-frequency energy is collected at separate electrodes while the beam finally impinges on an anode which can be at a comparatively low potential, thus increasing the power handling capacity of the tube. Thus before the actual Klystron is described it will be more instructive to examine these various points.

A simple allied example is the beam deflection tube, which in construction is similar to the normal cathode ray tube. The signal voltage is applied to the deflector plates and the anode is divided into two portions. Thus as the direction of the beam is altered so the current flowing to either anode is varied. The possibility of using these beam deflection tubes for ultra-short and decimetre wave amplification has been pointed out by F. M. Colebrooke (44) and H. E. Hollmann and A. Thoma (173). Since the deflection plates are at the same point along the beam, transit time damping is small, and initial calculation shows that this would be of the order of one-tenth the corresponding value in a grid-controlled tube of ordinary dimensions. U.

Tiberio (148) also considers these tubes and shows that in order to obtain a high value of mutual conductance a flat blade form of electron stream must be used, and to reduce phase differences between the electrons arriving at the anodes it was necessary to make the electron trajectories as parallel as possible. A difficulty is that secondary emission causes a supplementary random delay and even when suppressor grids were used this effect is serious. Such thin beams have also been considered by A. V. Haeff (57). G. Jobst (81) describes another allied tube which employs a shock excitation and frequency multiplication method whose principal feature is the compression of a large charge, arising from the cathode during a comparatively long discharge time, into electron bunches strongly compressed in time, through whose transit in the discharge space sharply defined current pulses are produced with a high harmonic content.

Although the name velocity modulation has long been familiar, as for example, in the television scanning system for cathode ray oscillographs described by L. H. Bedford and O. S. Puckle (16), its application to thermionic tubes is more recent, and among the first to mention or consider it were A. Arsenjewa-Heil and O. Heil (3), O. Heil (68), and E. Brüche and A. Recknagel (31). The latter point out that when a beam of moving electrons is acted upon by a rapidly changing field, the electrons tend to collect in groups, and these in passing through the electrodes may have different phase relations. These out-of-phase groups may be " focussed " or brought into phase by an accelerating field. If the amplitude and frequency of this latter high-frequency field are chosen properly with respect to the velocity of the electron groups and their spacing, it is possible to slow up the first electrons in each group, allow the central electrons of the group to proceed at their original velocity, and to accelerate the last electrons in the group. At the focal point the electron group becomes a plane of electrons and the charge density is extremely high ; thus if a collector is placed there the induced current due to the arrival of the focussed group is correspondingly large. In this way transit time effects in the tube itself may be minimised to any desired degree by employing beams of high speed

electrons which pass through fields of comparatively restricted volume. Whereas this earlier work was restricted, in that the input and output regions were interconnected, the more recent devices are often constructed so as to isolate the input and output portions of the structures.

In velocity modulated tubes considerable use is made of the technique of electron optics, and a good account of the general principles of this is given by L. M. Myers (106). A. V. Haeff (57) and L. P. Smith and P. L. Hartman (133) describe the properties of electron beams and the divergence and focussing of dense beams of ions and electrons. The travelling particles in the beam set up a space charge which tends to produce divergence, and thus magnetic or other focussing is necessary. In the case of ions the maximum currents possible are comparatively small, as pointed out in Chapter III. The potential distribution

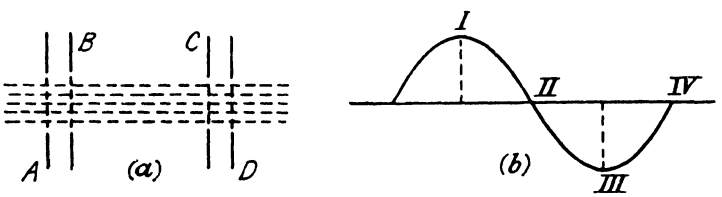

FIG. 88. Illustration of velocity modulation.

and maximum current in long-focussed electron beams is worked out so that design data can be obtained for practical tube structures in which considerable space charge is present. The motion of the electrons under the combined actions of electric and magnetic fields is analysed to determine the minimum permissible value of magnetic field so that the results of the analysis can be utilised as a good approximation to the actual state of affairs. J. R. Pierce (111) gives a theoretical analysis of the maximum current density in electron beam devices in which point focus or line focus concentrating systems are employed.

The general principle of velocity modulation as applied to thermionic tubes may be summarised from the account by W. C. Hahn and G. F. Metcalf (62). In Fig. 88*a* A–D represent four plane parallel grids, of which A and D are at a fixed, while B and C are at a mean, high steady potential. The latter are

further joined together and subjected to a radio-frequency potential. An electron stream from a suitable cathode passes through these grids, and since the steady potential can be made quite high while the grids A–B and C–D are close together, any effects due to electron transit time can be made negligible even at very high frequencies. When the potential of the signal source or grids is positive with respect to the mean potential, the first pair of grids acts to accelerate the electron beam, whereas the second pair of grids acts to decelerate the beam. Between the two sets of grids there is no field, since the grids B and C adjacent to this region are connected together. The effect of the signal voltage is, therefore, to produce alternate accelerations and decelerations as the polarity of the signal changes and the phase of the velocity change is always opposite in the two sets of grids. Now if Fig. 88*b* represents the alternating voltage, then any electrons passing through A–B at the instant I acquire an increased velocity, while those at II are slowed up. This process is repeated at C–D, and if these are spaced from A–B so that the transit time is any multiple of the half period the effect is doubled. Thus in general there is a modulation equivalent to twice the peak radio-frequency potential, and since this is half a period out of phase with the potential the input is that of a pure capacitance. In the arrangement of O. Heil (68) the applied potential is made a further half cycle out of phase with the current, thus causing the input to be that of a negative resistance and giving the tube the ability to generate self-sustained oscillations. In the normal arrangement the grids B and C collect no radio-frequency power and the input impedance is therefore very high.

There are several methods of utilising this velocity modulated stream of electrons, and generally these are such that the beam is converted into a convection modulated one. Thus if the beam is deflected by electric or magnetic fields some of the electrons can be discriminated according to their velocities and collected. Alternatively, a retarding field can be used and the faster electrons collected while the slower ones are turned back. More often the beam is allowed to drift freely for a certain distance, during which the faster electrons overtake

the slower ones, and the beam is then converted into one of a variable space charge density. These changes can be best understood by first considering an electron which passes the centre of the high-frequency field just as that field is changing from opposing to helping electrons. At the second set of grids this electron has practically the same speed as at the first grid, but another electron which passed the centre of the field a few electrical degrees earlier has had its speed reduced, and another, passing a few degrees later, is going faster. Now, if there is enough field-free space beyond the last grid, these differences in speed cause the electrons ahead and behind the one of unchanged speed to draw nearer to it. Another electron of unchanged speed, a half-cycle earlier or later, has its neighbours draw away from it. Consequently at a suitable distance from the grids the stream contains bunches of electrons denser than the stream leaving the grids and separated by regions less dense. The problem of the transfer of power to or from an electron beam by an oscillating circuit has also been examined theoretically by E. V. Condon (45) for the case where space charge effects can be neglected.

The Drift Tube. In the design of the Klystron much care must be devoted to the conditions obtaining in this drifting electron beam. It will be apparent that this " bunching " of charges will be opposed by space charge forces, although the mean space charge density will have no effect. W. C. Hahn (59) considers this effect and treats the beam as a dispersive dielectric, along which the high-frequency waves travel. He considers an infinitely long cylindrical beam and the superimposed alternating motion is assumed to be of small amplitude. A steady longitudinal magnetic field is taken to be present, and this in fact is used in practice to prevent divergence of the beam. Maxwell's equations in cylindrical co-ordinates are used, and after complex mathematical analysis suitable design data is arrived at. Information bearing on this problem has been given by L. Tonks and I. Langmuir (152) and D. L. Webster (156). In general these " de-bunching " forces due to space charge are found to limit the gain in amplifiers and to be a serious factor in oscillators of high power working on long wavelengths. In a further analysis W. C. Hahn (60) gives a

method for calculating the amplitude of the waves in the cylindrical electron beam produced by a sinusoidal radio-frequency voltage across a gap in the outer perfectly conducting boundary. The energy of the beam with space charge and the effect of finite gap lengths are examined and an expression derived for the transconductance of two gaps along the length of the beam.

The conditions in the drift tube have been examined by D. M. Tombs (150). If the velocity of the electrons entering the buncher is equivalent to a voltage V_b and $V \sin \omega t$ is the alternating potential across the grids producing the velocity modulation, then the electrons leaving have velocities given by

$$u = \sqrt{V_b + V \sin \omega t} = \sqrt{V_b(1 + m \sin \omega t)} \quad . \quad (117)$$

where m is the depth of modulation given by V/V_b and ω is the pulsatance. Now if u_0 is the velocity of the electrons with no modulation, then

$$u/u_0 = \sqrt{1 + m \sin \omega t} \quad . \quad . \quad . \quad . \quad (118)$$

An analysis is then given of the electron density down the beam in the drift tube at successive instants of time by graphical methods. Empirical formulæ are derived for the positions of maximum density and phase displacement. The inherent difficulty of an actual Klystron apparatus is pointed out, in that the radio-frequency currents remain on the inside of the resonators producing the field between the inner surface of the grids. Thus electrons passing through will emerge at battery velocity and unmodulated whatever radio-frequency potentials are present, so that the effect in any practical apparatus must involve transit time. In the analysis it is possible to derive an equivalent generator of, in general, a non-sinusoidal voltage, which would make the electrons enter the drift tube with the same velocities as they would acquire allowing for transit time. The curves given present a clear physical picture of the changes in velocity modulated beams. The method and some of the results obtained have been criticised by R. Komfner (91) and C. Strachey (145), particularly regarding the depth of modulation.

S. Ramo (112) has examined the propagation of waves down

the beam for the most important case, that of a magnetically focussed electron beam. As mentioned above, in a velocity modulated tube a small increment of velocity added at the modulating grids is propagated along the beam and makes a useful disturbance at the receiving grids. The existence of two space charge waves is postulated with different phases between their respective velocity V_z and conduction current ψ_z modulations. One wave travels slightly slower than the beam, and is represented by

$$V_{zs} = V_s \sin(\omega t - \gamma_s z - \alpha_s) \quad . \quad . \quad . \quad (119)$$

$$\psi_{zs} = gV_s \sin(\omega t - \gamma_s z - \alpha_s) \quad . \quad . \quad . \quad (120)$$

and the other slightly faster than the beam given by

$$V_{zf} = V_f \sin(\omega t - \gamma_f z - \alpha_f) \quad . \quad . \quad . \quad (121)$$

$$\psi_{zf} = gV_f \sin(\omega t - \gamma_f z - \alpha_f - \pi) \quad . \quad . \quad (122)$$

where γ_0 is the propagation constant of the beam so that approximately

$$\gamma_s = \gamma_0(1 + \delta), \gamma_f = \gamma_0(1 - \delta) \quad . \quad . \quad (123)$$

and α is an arbitrary phase constant and g is a constant depending on the tube parameters called the wave transconductance.

At the modulating grid the conduction current modulations are equal and opposite in phase, while the velocity modulations are equal and in phase. If l is the length of the drift tube, then the waves at the receiving grids are represented by

$$V_{zs} = V_s \sin[\omega t - \gamma_0(1 + \delta)l] \quad . \quad . \quad . \quad (124)$$

$$V_{zf} = V_s \sin[\omega t - \gamma_0(1 - \delta)l] \quad . \quad . \quad . \quad (125)$$

$$\psi_{zs} = gV_s \sin[\omega t - \gamma_0(1 + \delta)l] \quad . \quad . \quad (126)$$

$$\psi_{zf} = gV_s \sin[\omega t - \gamma_0(1 - \delta)l] \quad . \quad . \quad (127)$$

Thus the total conduction current modulation is

$$[\psi_{zf} + \psi_{zs}] = 2gV_s \sin(\gamma_0 \delta l) \sin\left(\omega t - \gamma_0 l - \frac{\pi}{2}\right) . \quad (128)$$

This shows that there are certain optimum drift tube lengths for which the ratio of conduction current modulation at the output to velocity modulation at the input is a maximum. These occur when $\gamma_0 \delta l$ is equal to odd multiples of $\pi/2$. The phase of the wave transconductance is such that the output

current lags the input voltage by $(-\gamma_0 l - \pi/2)$, and for a grid or tube of length $\pi/2$ it is such that the tube impedance is that of a negative resistance. Maxwell's equations are then applied and the conditions of propagation of these waves are determined. There are a number of different kinds of waves which fulfil the conditions for propagation, and these are termed zero rank and high rank. The characteristics of these waves are described. If it is assumed that the drift tube diameter is $\frac{1}{2}$ in., the electron beam diameter is $\frac{1}{4}$ in., beam current is 10 mA, drift tube steady voltage 1,500, frequency 1,000 Mc/s, then g in the ideal case is 48×10^{-6} micromhos. The optimum drift tube length is given by

$$l_0 = \frac{\pi}{2\gamma_0\delta} = \frac{\pi}{2\gamma_0 . 0{\cdot}03} = 19{\cdot}2 \text{ cm.} \quad . \quad . \quad (129)$$

These axial waves have also been examined by S. Ramo (114) for the case when there is no magnetic focussing field. It is shown that at certain discrete frequencies (above a certain cut-off frequency) space charge waves are possible which still possess only the axial components of velocity and conduction current modulation. In general, the waves are such that the electrons have radial and azimuthal velocities and they can be divided into E and H type according to the field configurations.

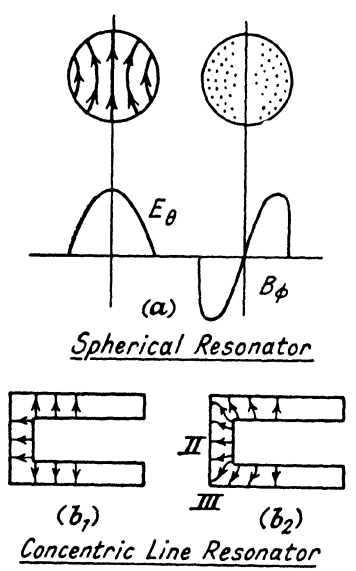

FIG. 89. Types of electromagnetic resonators.

The Rhumbatron. It has already been mentioned that special resonators are used for energy storage and these are termed "Rhumbatrons" (Greek for rhythmic oscillation). The simplest resonator is the sphere considered by W. W. Hansen (63) and shown in Fig. 89*a*. The lines of electric and magnetic force are shown together with their values across

the cross-section of the sphere. The volume is bounded by a material of high conductivity and is capable of resonating at certain wavelengths. Solution of the field equations consistent with the special boundary conditions yields for a sphere of radius a, a fundamental wavelength given by $\lambda = 2{\cdot}28a$, and this is related to $\sqrt{LC}$, where L and C are the effective inductance and capacitance respectively. The characteristic impedance is defined as $\sqrt{L/C}$, and for the sphere this is $2{\cdot}66c$, where c is the velocity of light. If ρ is the resistivity, the depth of penetration δ is $\sqrt{\frac{\rho}{2\pi\omega}}$, where ω is the pulsatance. The equivalent shunt resistance defined by L/CR becomes $10^4\lambda/\delta$. The factor Q which is $2\pi \times \frac{\text{Total Energy}}{\text{Loss per cycle}}$ is defined as $\sqrt{\frac{L}{CR^2}} = 0{\cdot}318\frac{\lambda}{\delta}$, where R is the radio-frequency resistance. Since there is no radiation or dielectric material, this resistance is very small, and thus Q may be of the order of 1,000 and the impedance of the order of megohms. Thus it will be realised that these resonators are very efficient at very high frequencies, although it would be expected that their advantages would not be so apparent with a comparatively low impedance tube like the magnetron previously described. Other forms of resonators considered by W. W. Hansen (63) are cylindrical and square prisms, the prolate spheroid, which is considered the most efficient, and (47) the closed concentric line shown in Fig. 89*b*. If the field distribution is assumed to be as in (b_1), then it can be considered as a concentric line terminated by a capacitance, but the wavelength can be calculated more accurately by taking the correct distribution of (b_2) and choosing a function in region III, satisfying the boundary conditions and solving this by a series.

F. Borgnis (22) works out the theory for the fundamental oscillations of a cylindrical cavity of arbitrary cross-section, the cases of circular, rectangular and elliptical cross-sections being worked out numerically. The quantities calculated include the natural wavelengths, attenuation, equivalent attenuation resistance, dynamic capacitance and self-induct-

ance, and the wave impedance. The natural oscillations of electrical cavity resonators have also been examined by W. L. Barrow and W. W. Mieher (14), who consider the coaxial and hollow-pipe types. If the centre conductor of a perfect coaxial resonator is slowly withdrawn, a hybrid type results that continuously alters form until, when the conductor is completely removed, it becomes a perfect cylindrical resonator. The resonance phenomena of coaxial and cylindrical resonators may be described completely in terms of the standing waves caused by multiple reflections of travelling waves of the various types that exist on coaxial and hollow-pipe transmission lines

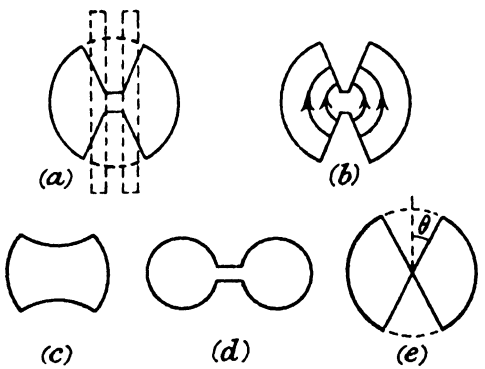

FIG. 90. Resonators suitable for velocity modulated tubes.

respectively. A number of resonant modes are possible and the first ten resonant frequencies for each resonator are tabulated, and these were confirmed by experiments. For use with amplitude or velocity modulated electron beams, the closed ends of the resonator would be replaced by grids and the changes due to this are examined, although effects due to the electron stream itself were not included in the measurements.

In operation the electrons must traverse the region of radio-frequency potential in a time small compared with the wave period, and thus before being suitable for use in Klystrons the above resonators must be modified. Thus W. W. Hansen and R. D. Richtmyer (65) consider the resonators shown in Fig. 90, in which it will be seen that the maximum radio-frequency

potential occurs across a small space through which the electrons can move in a minimum time. Calculations are made, as before, for the values of λ, $\sqrt{\frac{L}{C}}$ and $\sqrt{\frac{L}{CR^2}}$, and changes in these quantities, due to alteration in the dimensions, shapes and angles of the various resonators are shown. For example, the resonator of (*e*) has an optimum angle θ_0 which gives an impedance of 2·66 MΩ at a wavelength of 10 cm. Also R. D. Richtmyer (121) has shown that suitably shaped objects of dielectric material can function as electrical resonators, but even when constructed of quartz the dielectric losses are likely to be serious and make these resonators inferior to the metal ones, except perhaps at the very highest frequencies. The resonators are in the form of wave guides, to be considered later, and arranged so that the outlet is in communication with the inlet end. The resonant modes of a dielectric sphere are also examined.

The stream of electrons of variable space charge density which comes from the drift tube is capable of exciting these Rhumbatrons. This may be done by making holes or grids in two of the opposing walls adjacent to the region of high electric field strength, and passing through these grids and this field the periodically changing stream of electrons, the charges being so timed that more electrons pass when the field is such as to take energy from them than when the field is reversed. The reason why a sphere, for example, is not a suitable shape of Rhumbatron is that its wavelength is only about 1·14 times its diameter, and so even if an electron had a speed equal to that of light, it would never get through the sphere before the field reversed. For best operation the path of the electron in the resonator must not be much longer than $\beta\lambda/2$, where $\beta = v/c$ and v = electron velocity, and it seems best to have the path still shorter. In the operation of these resonators no use is made of high-frequency lead wires, nor is there any solid dielectric, and it should be specially noted that there is no external radiation field. If the electron stream is sent through the Rhumbatron, and this is oscillating in the proper phase to retard the electrons in the bunches, then a portion of the D.C.

power of the cathode rays is converted into high-frequency electrical energy.

Special Power Amplifiers. The first complete arrangement that will be described is the power amplifier of A. V. Haeff (56), which is capable of giving high powers at very high frequencies, although in this case convection current modulation is obtained directly by means of a grid acting in the normal manner and not through the medium of velocity modulation as in the true Klystron. This grid is excited externally, as, for example, by a magnetron giving about 10 watts power, and the electrons then travel under the influence of accelerating electrodes, shown in

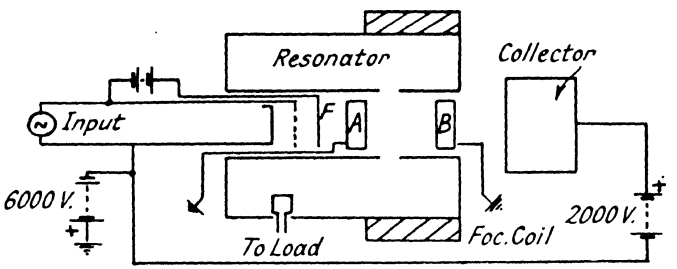

FIG. 91. Special power amplifier.

Fig. 91 as A and B across a gap in an enclosed resonant circuit. A focussing magnetic field is used as well as a focussing electrode *F*. The cathode and grid are at a high negative potential (6,000 volts), while the resonator, etc., are earthed. When the modulation frequency is equal to that of the resonator a high radio-frequency voltage is induced across the gap and energy is supplied to the resonator by the electron beam. Since there is no external radiation there is no trouble due to feed back to the input circuit. Finally the electrons impinge on the collector (or anode) which is at a comparatively low voltage (2,000 volts), so that dissipation losses are also low.

In this amplifier electron transit time effects are minimised by utilising electrons of high velocity, and this is accomplished without increased dissipation and loss in efficiency by separating the functions of the output electrode and of the current-collecting electrode and by making use of electron focussing. The high frequency losses due to circulating currents are

minimised by using current-carrying electrodes of large periphery. The energy of the electromagnetic field within the space between the inner and outer conductors of the resonator is transferred to the useful load by means of a coupling loop. A typical development tube gave 110 watts at 450 Mc/s with an efficiency of 35%. The current to the accelerating electrodes was less than 100 μA.

A similar tube, the RCA825, has been described by A. V. Haeff and L. S. Nergaard (41) and (164), which will transmit at ultra-high frequencies a wide band of frequencies. The figure of merit of a tube for wide band service is defined as the transconductance divided by the geometric mean of the input and output capacitances. A high figure of merit can be obtained by reducing the grid cathode spacing to a minimum because of the fact that the input capacitance increases in inverse proportion to the first power of grid-cathode spacing, while the transconductance increases as the second power of the spacing. In order to obtain sharp cut-off characteristics and to make full use of the cathode area, the turns per inch of the grid must be increased in proportion to the reduction in the grid-cathode spacing, and because the grid-wire diameter cannot be reduced indefinitely for mechanical reasons, the μ of the control grid will be high. To obtain sufficient current at negative control grid potentials an intense accelerating field must be used which normally necessitates the accelerating electrode being close to the control grid, thus increasing its capacitance, or the use of very high voltages. In the inductive output amplifier the latter can be employed without the corresponding high dissipation, and thus the high-frequency electrodes can be of small size with a small output capacitance. In the actual tube a system of magnetic lenses is used for focussing together with a suppressor electrode which prevents secondary electrons, which leave the low potential collector electrode from arriving at the high-frequency electrodes, where they would absorb useful energy. The latter is assisted in its action slightly by the space charge, which is, of course, present at this point. With an accelerating potential of 3,000 volts and a beam current of 40 mA the transconductance was 6 mA/volt, the input capacitance being 6 $\mu\mu$F and the output 2 $\mu\mu$F. At a

frequency of 500 Mc/s a power output of 10 watts has been obtained with a gain of 10dB when the tube operates into a circuit loaded to give a 10 Mc/s band width. The efficiency was 25%, and at lower power levels, when Class A operation is used, a power gain of 13dB can be obtained.

The Klystron. The arrangement of R. H. Varian and S. F. Varian (153), termed the Klystron (Greek for waves breaking on a beach), is shown in Fig. 92. The plane oxide cathode *A* emits electrons and space charge effects are counteracted by the

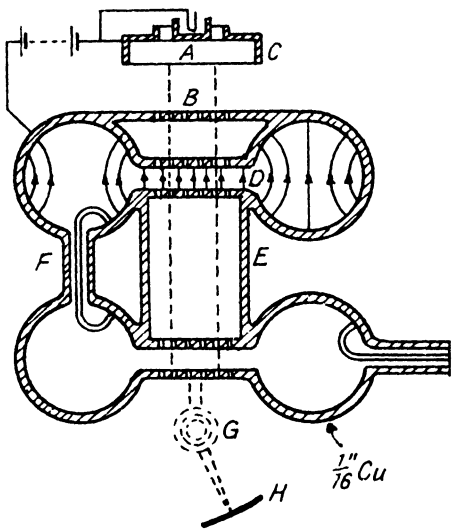

FIG. 92. Construction of the Klystron.

electrode *C*. They are then accelerated and pass through the grid *B* which straightens them into a beam, after which they pass through the two grids *D* of the resonator or Rhumbatron, where velocity modulation takes place. These grids must have high electrical conductivity to avoid spoiling the resonators ; they must have high heat conductivity to dissipate the energy derived from the electrons striking them ; and they should have as little projected area as possible to keep the number of electrons intercepted at a minimum. To satisfy these requirements the grids are made of honeycomb form by drilling sheets of copper $\frac{1}{16}$ in. thick. The "lattice constant"

of the grid is determined by the requirement that the radio-frequency field along the electron path should usually change from zero to full value in a distance short compared with that travelled by an electron in one half-cycle.

This first Rhumbatron is termed the "buncher," since after the electrons pass along the field free drift tube E they collect in bunches of different charge density. Thence they enter the second Rhumbatron or "catcher," which is excited, the oscillation energy coming from the source of steady high potential. The distance between the two grids is usually less than the distance travelled by an electron, moving with velocity βc, in one half-cycle. For the buncher this would be $\beta\lambda/2$; but in the catcher some of the electrons are slowed nearly to rest, so that $\beta\lambda/4$ is a closer approximation. In practice the latter spacing is used for both, so that the Rhumbatrons can be made nearly identical, so as to simplify tuning. Smaller grid spacings can be used, but with some impairment of the shunt impedance. The two Rhumbatrons are connected, mainly for mechanical reasons, by the tube E, whose length is determined by a compromise between the following opposing considerations. First, the shorter the tube the less distance the electrons have in which to bunch, with the result that for best bunching they must be given a larger spread in velocity. This, on the other hand, tends to reduce the efficiency because (a) more power is required to drive the buncher as its voltage is increased, and (b) since no electrons should be thrown back in the catcher, only the slowest ones can be stopped, and so a larger spread in velocities means more loss of energy, due to incomplete stoppage of the faster electrons. On the other hand, a large bunching distance increases the difficulty of getting a large fraction of the beam into the catcher. In practice the compromise chosen is not critical, and the apparatus works well over a large range of distance.

When the buncher is driven by some independent source of power, such as an antenna receiving a signal, the Klystron behaves as an amplifier, while if a grid and anode (not shown) are placed at the outlet of the catcher it behaves as a detector, since it can be arranged that the current alters with input signal strength. When some of the output energy is fed back to the

input by means of the loop circuit F the Klystron becomes a self maintained oscillator. The phase of the feed back voltage is adjusted by varying the mean speed of the electrons through the Klystron. A simple oscillation detector consists of a magnetic field G, which rotates the electron path according to

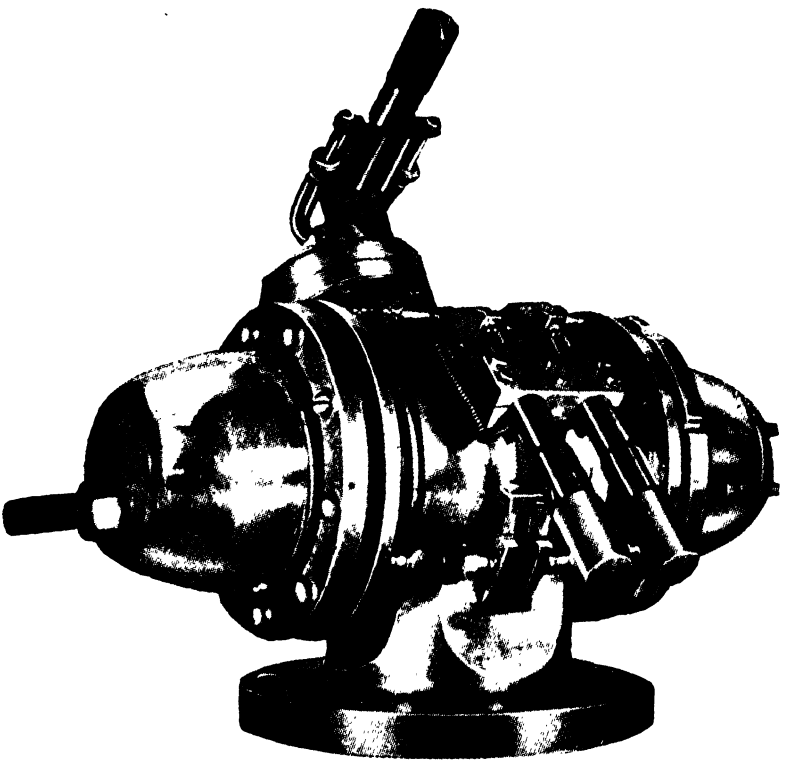

FIG. 93. Klystron high-frequency oscillator at 10 cm. wavelength.

its velocity, and thus when oscillations start the spot at the fluorescent screen H lengthens into a line. Due to the very low decrement of the Rhumbatrons, careful tuning is necessary, and this can be done by slightly distorting their shape with a screw adjustment. An illustration of the complete arrangement is given in Fig. 93.

The power absorbed in the buncher is considered by D. L.

Webster (156), who concludes that this is small compared with the purely ohmic losses. The power in the catcher is also calculated, and it is shown that ideally 58% of the D.C. input energy can be converted into radio-frequency power. It is possible to arrange matters so that the wave-form of the buncher is peaked, and thus a higher frequency can be obtained by operating the catcher on one of the harmonics. The radio-frequency power can be taken to a suitable load by either inductive coupling with a loop as shown in Fig. 92 or electrostatically by means of an insulated electrode.

The energy supply has one terminal connected to the cathode parts *A* and *C* and the other to the assembly of Rhumbatrons, grids, etc. Choice of a suitable voltage is governed by the following considerations. As the voltage is raised, at constant power, the needed current decreases and the needed shunt impedance increases. On the other hand, as the voltage is decreased, troubles with spreading of the beam by space charge increase. Clearly the proper voltage depends on the power output desired and other factors, but in general the conditions are not critical, and, for example, it is possible to use many different voltages, from 300 to 4,000, on a single Klystron oscillator.

(*b*) WAVE GUIDES AND HORN RADIATORS.

Introduction. To complete this survey it is instructive to describe briefly the operation of wave guides, since apart from their extending use in the transmission of power at high frequencies the principle is of use in the design and construction of generators and other apparatus at these frequencies. It has already been shown in Chapter II that the electrode capacitances and lead inductances of thermionic tubes form a considerable portion of the tuned circuit, and if transmission lines are used then the electrode capacitance makes the tube equivalent to a certain length of line. Thus as the operational frequency increases it becomes necessary to consider the tube as an inherent portion of the tuned circuit and the design of its electrodes and their arrangement must be such as to facilitate this.

Before considering electromagnetic wave guides proper, a brief description of the properties of transmission lines will be given. The parallel wire line has been briefly considered in earlier chapters, and a comprehensive account of parallel and concentric lines is given by F. E. Terman (147). The general relations are

$$E_s = E_r \cosh px + I_r Z_o \sinh px \quad . \quad . \quad (130)$$

$$I_s = I \cosh px + \frac{E_r}{Z_o} \sinh px \quad . \quad . \quad (131)$$

$$Z_s = E_s/I_s \quad . \quad . \quad . \quad . \quad . \quad . \quad . \quad . \quad (132)$$

where E_r and I_r, E_s and I_s are the voltages and currents at the receiving and sending ends respectively. The propagation constant is $p = \alpha + j\beta$, where α is the attenuation and β the wavelength constant. At high radio-frequencies $\alpha = \frac{R}{2}\sqrt{\frac{C}{L}} = \frac{R}{2Z_0}$ and $\beta = 2\pi/\lambda$, where λ is the wavelength. A short-circuited transmission line of less than a quarter wavelength acts as a high-quality low-loss inductive reactance, while an open-circuited line of less than a quarter wavelength acts as a low-loss capacitance reactance. If the latter is required to pass direct current (high-frequency choke), then a short-circuited line between a quarter and half wavelength long can be used. P. H. Smith (134) expresses the impedance at any point along the line in terms of the characteristic impedance Z_0 and the distance in wavelengths; thus, for a loss-less line,

$$Z_s/Z_0 = \frac{Z_r/Z_o + j \tan 2\pi x/\lambda}{1 + j(Z_r/Z_0) \tan 2\pi x/\lambda} \quad . \quad . \quad . \quad (133)$$

A chart is given from which the resistance and reactance at any point along the line can be read off. The changes of line resistance due to proximity effect and radiation have been considered by L. E. Reukema (120), who finds that the selectivity factor Q then decreases as the frequency increases for both parallel-wire and concentric lines. Optimum values of Q and Z_o are obtained by calculation, and these are found to occur with different line dimensions and to be of a much lower order than when radiation and proximity effects are neglected.

Thus a parallel line of 0·5 in. conductors spaced 0·68 in. between axes gives a Q of 2,655 at 300 Mc/s, whereas the more accurate figure is only 423, while the optimum Q of 771 is obtained with conductors 0·10 in. diameter spaced 0·32 in.

L. S. Nergaard and B. Salzberg (109) show theoretically that the imaginary part of the characteristic impedance cannot be neglected even at the highest frequencies. It is shown that the highest tuned impedance of a low-loss transmission line, either short-circuited or open-circuited at one end and tuned by a variable capacitator of negligible losses at the other end, is obtained when the line is operated at self-resonance so that its length is practically an integral number of quarter wavelengths. This is of practical importance, since the elementary tuned circuit usually consists of a capacitance shunted by a line, and this is adjusted to maximum absolute impedance by altering either the capacitance or line length. The theory was verified by experiments made on a parallel line with conductor diameters 0·375 in. spaced 0·75 in. apart. One end was shorted by a movable bar, while the other was terminated by a mica condenser. The impedance was determined by noting the change in line length necessary to reduce the voltage across the line to 0·707 of its resonant value. If $\Delta\theta$ is this change, θ_r the electrical line length at resonance and Z_0 the real part of the characteristic impedance, the resonant impedance is given by

$$\frac{r}{Z_0} = \frac{\sin^2 \theta_r}{\Delta\theta} \quad . \quad . \quad . \quad . \quad . \quad . \quad . \quad (134)$$

With both copper and steel rods, maximum impedances occurred at multiples of 90°, which is contradictory to theory which neglects the imaginary part of Z_0. True wave guides will now be considered in which there is no return conductor.

Types of Guides. The propagation of electromagnetic waves through the inside of conducting tubes or pipes was first examined by Lord Rayleigh (116), and he showed that for a given diameter of guide there are critical frequencies below which the waves are rapidly attenuated and above which they are freely transmitted. The most idealised conditions of an infinitely long non-conducting cylinder of arbitrary dielectric constant embedded in a perfectly conducting material were

assumed. The results of other early work on wave guides are given by P. Debye and D. Hondros (47), H. Zahn (159) and O. Schriever (128), who considered dielectric guides. Transmission phenomena associated with a non-conducting dielectric cylinder, are referred to as dielectric wire waves, and they are not the same as hollow-pipe waves, since they have different field configurations and obey different laws. More recently G. C. Southworth (139) has examined dielectric guides and carried out experiments on their propagation at high frequencies. If the wire is of dielectric material without a metal enclosure, then some of the wave power is transmitted through the surrounding space. For high dielectric constants and frequencies far above cut-off the power is propagated largely inside the guide. The effectiveness of the dielectric guide depends on its dielectric constant ϵ and ceases when this is the same as that of the surrounding medium. Further work on propagation along dielectric wires has been given by A. Klemt (88), A. G. Clavier (40), E. Kašpar (85), and others.

However, it is the hollow metal tube which has become prominent, due to its practical application to radio communication. It has been found experimentally that waves can be transmitted inside a metal tube, but the frequency required is very high. The necessity for this has been simply illustrated by G. W. O. Howe (76). In an electromagnetic wave the magnetic field strength H is equal to the electric field strength E in air or to $\sqrt{\epsilon}E$ in a dielectric. Now consider a disc of radius r normal to E, then the MM.F around the disc is $\pi r^2 \epsilon \frac{dE}{dt} \cdot \frac{1}{c}$. This is equal to $2\pi r H$, and thus we have

$$\pi r^2 \epsilon \omega E = H \cdot 2\pi r \cdot 3 \cdot 10^{10} = \sqrt{\epsilon} E \cdot 2\pi r \cdot 3 \cdot 10^{10} \qquad (135)$$

making $\omega = \frac{6 \cdot 10^{10}}{r\sqrt{\epsilon}}$, and thus the minimum frequency is roughly given by $f = 10^{10}/r\sqrt{\epsilon} = 2{,}000$ Mc/s for an air pipe of 10 cm. internal diameter.

Types of Transmitted Waves. G. C. Southworth (139, 140) shows that four main types of waves can be propagated along hollow conducting tubes, and the field configurations of these longitudinal and transverse waves are shown in Figs. 94 and 95

respectively. The first two waves E_{01} and E_{11} are designated electric, since there is a component of electric force along the guide. These waves bear some similarity to those on a single or double wire coaxial cable respectively, but the usual central core can be considered as replaced by an air core carrying longitudinal displacement currents, and it is the rapid reversal of these which produces the magneto motive

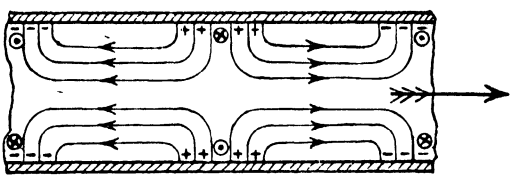

(*a*). E_{01} Wave. The crosses and dots in circles indicate the direction of the concentric magnetic field. The curves represent the electric field.

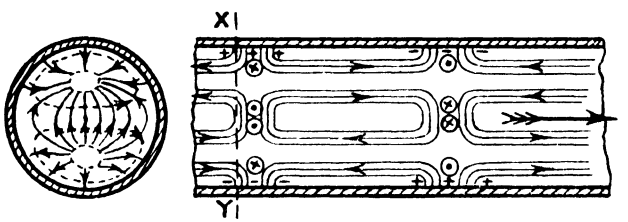

(*b*). E_{11} Wave. The crosses and dots in circles indicate the direction of the magnetic field. The curves represent the electric field. In the section through XY in the direction of the arrow the dotted curves represent the magnetic field.

FIG. 94. Field configurations of the transverse magnetic waves.

forces corresponding to the concentric magnetic field. The other two types of waves, H_{01} and H_{11}, are termed magnetic, since there is a component of magnetic force along the guide. The electric field is concentric, producing circular displacement currents. No electric lines of force end on the sheath in the H_{01} wave and the attenuation decreases continuously as the frequency increases indefinitely. The H_{11} wave has longitudinal magnetic and lateral electric fields, but the magnetic flux, instead of flowing along the centre core, flows along the upper

part of the tube, sweeping across and returning along the bottom of the tube.

J. R. Carson, S. P. Mead and S. A. Schelkunoff (38) and W. L. Barrow and L. J. Chu (8) also discuss the different types of waves. Any hollow pipe having both a longitudinal and a transverse component of electric field, but only a transverse

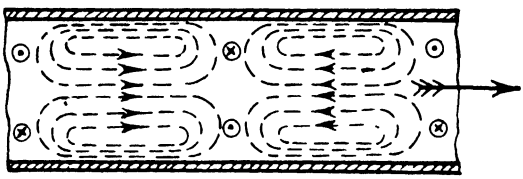

(*a*). H_{01} Wave. The dotted curves represent the magnetic field. The crosses and dots in circles indicate the direction of the concentric electric field.

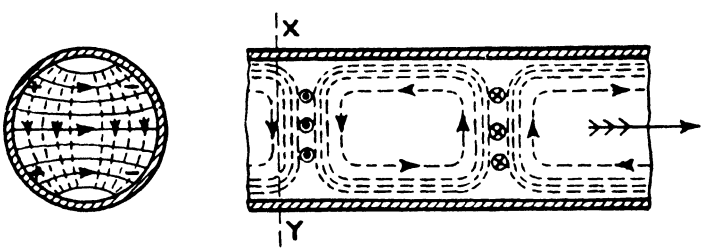

(*b*). H_{11} Wave. The crosses and dots in circles indicate the direction of the electric field. The dotted curves represent the magnetic field. In the section through XY in the direction of the arrow the dotted curves represent the magnetic field.

FIG. 95. Field configurations of the transverse electric waves.

component of magnetic field is called an *E* wave, while a wave having both a longitudinal and a transverse component of magnetic field, but only a transverse component of electric field, is called an *H* wave.

Theory of Propagation. The theory of the propagation of hyper (very high) frequencies along hollow metal tubes has been given more recently by G. C. Southworth (139), who confirms the earlier work. The cut-off wavelengths are such that the circumference of the guide in wavelengths is equal to the roots

of certain Bessel functions which result from the solution of Maxwell's field equations in cylindrical co-ordinates. The characteristic impedance is obtained by integrating the Poynting vector over the tube cross section and dividing by the square of the effective current. This is zero at cut-off and rises to asymptotic values as the frequency increases, except for the H_{01} wave. For maximum power the guide is terminated by a film of resistive material transverse to the guide followed by a reflector, or, alternatively, by a resonant chamber containing some dissipative material. The best matching is when standing waves in the guide are eliminated. By using reflectors resonant effects may be produced, giving rise to frequency selectivity. Discontinuities in guides cause

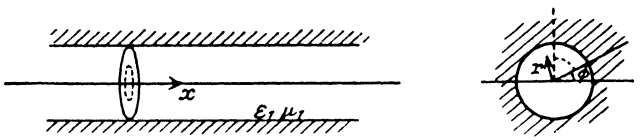

FIG. 96. Hollow metal tube acting as a wave guide.

radiation, and this can be increased by opening the tube out into a horn, which also helps to terminate the line.

The transmission of electromagnetic energy at very high frequencies through the inside of hollow tubes has also been considered by W. L. Barrow (6). The geometrical configuration is shown in Fig. 96, where an infinitely long hollow cylinder is assumed to be cut out of a homogeneous conductor of otherwise infinite extent. The space inside the cylinder is assumed to be a non-conductor of dielectric constant ϵ_1 and permeability μ_1, while the conductor has conductivity σ_2 and permeability μ_2. It is assumed that the wave is propagated along the guide in the x direction and that the wave is of the E_{01} type. From Maxwell's equations

$$\text{curl } H = \sigma_2 E + \frac{\partial \epsilon_1 E}{\partial t} \quad . \quad . \quad . \quad . \quad (136)$$

$$\text{curl } E = -\partial \frac{\mu_1 H}{\partial t} \quad . \quad . \quad . \quad . \quad (137)$$

and by the insertion of the proper boundary conditions, an

equation for E_x can be obtained. When the tube material is perfectly conducting there is no attenuation, and if the frequency is below a limiting value the propagation constant is imaginary. This " cut-off " frequency, below which no propagation takes place, is given by, where a is the radius,

$$f_c = \frac{y_0}{2\pi\sqrt{\mu_1\epsilon_1}} \cdot \frac{1}{a} \quad . \quad . \quad . \quad . \quad . \quad . \quad (138)$$

where $y_0 = 2{\cdot}4048$ is the first root of the Bessel equation $J_0(x) = 0$. We also have

$$E = Ee^{-hx+i\omega t} \quad . \quad . \quad . \quad . \quad . \quad (139)$$

$$H = He^{-hx+i\omega t} \quad . \quad . \quad . \quad . \quad . \quad (140)$$

where $h = \alpha + i\beta$ is the propagation constant, α being the attenuation and β the phase constant. The wavelength in the guide is given by

$$\lambda_g = \frac{2\pi}{\beta} = \frac{2\pi}{\sqrt{\omega^2\mu_1\epsilon_1 - \left(\frac{y_0}{a}\right)^2}} \quad . \quad . \quad . \quad (141)$$

and the phase velocity is

$$v_p = \frac{\omega}{\beta} = \frac{\omega}{\sqrt{\omega^2\mu_1\epsilon_1 - (y_0/a)^2}} \quad . \quad . \quad . \quad (142)$$

while the group velocity is

$$v_g = \frac{1}{\partial\beta/\partial\omega} = \frac{\sqrt{\omega^2\mu_1\epsilon_1 - (y_0/a)^2}}{\omega\mu_1\epsilon_1} \quad . \quad . \quad (143)$$

In an air-filled tube these equations give $f_c = 1{\cdot}148 \times \frac{10^{10}}{a}$, $\lambda_c = 2{\cdot}615a$, while the wavelength inside the guide is $\lambda_g = \frac{2\pi}{\sqrt{(\omega/c)^2 - (y_0/a)^2}}$.

In the engineering treatment of transmission lines, the characteristic impedance is generally an indispensable quantity. The absence of a second parallel metal conductor makes this conception somewhat artificial in the hollow tube system. The displacement current inside the pipe assumes the *rôle* of the return conductor, and hence a quantity Z_0 is defined, called the characteristic impedance, which relates the strength

of the longitudinal current along the pipe to the transverse electromotive force between the guide axis and wall. The characteristic impedance given by Voltage/Current is defined by

$$Z = \frac{\int_0^a E_r\,dr}{\oint_{r=a} H\phi\,d\phi} = \frac{\beta/\omega}{2\pi y_0 \epsilon_1 J_1(y_0)} = \frac{1{\cdot}44 \times 10^{12}\beta}{\omega} \quad . \quad (144)$$

and this is zero at the cut-off frequency f_c, but rises to 48 Ω as the frequency increases indefinitely.

It is also possible to have transversely polarised H_{11} waves and now $\lambda_c = 3{\cdot}41a$, $\beta = \sqrt{\left(\frac{\omega}{c}\right)^2 - \left(\frac{1{\cdot}841}{a}\right)^2}$, $\lambda_g = \frac{a}{\sqrt{\left(\frac{a}{\lambda}\right)^2 - {\cdot}086}}$.

J. Saphores and L. Brillouin (124) give a description of hollow-tube waves, and the following table for the various critical wavelengths for a circular guide containing only air ($\epsilon = 1$), in terms of the diameter D.

TABLE XIV

Types of waves	E_{01}	E_{11}	E_{21}	H_{01}	H_{11}	H_{21}
Critical wavelengths	1·31D	0·82D	0·61D	0·82D	1·71D	1·05D

For the comparatively favourable case of the H_{11} wave a tube of diameter 2 cm. requires wavelengths less than 3·5 cm. Since the critical frequency is proportional to $1/\sqrt{\epsilon}$, the possibility is indicated of considerably reducing the critical frequencies by filling the tube with a material of high dielectric constant, but it is evident that the usefulness of this resource will probably be considerably limited by high losses in the dielectric at very high frequencies, and also by considerations of cost.

Attenuation. In the earlier theory of wave guides dissipation was neglected, and this appears to have been first treated by J. R. Carson, S. P. Mead, and S. A. Schelkunoff (38), who assume a sheath of high conductivity surrounding a good

dielectric. It is confirmed that there can exist the fundamental E and H waves, and in addition, geometric harmonics. Contrary to the case of the normal coaxial conductor, in the hollow guide there must exist an axial component of electric or magnetic intensity. If $K = K_R + iK_I$ is the characteristic impedance, then it may be shown $K = \overline{W} + 2i\omega\ (\overline{T} - \overline{U})$, where $\overline{W}$ is the mean power, $\overline{T}$ the mean magnetic and $\overline{U}$ the mean stored electric energy for unit current. Now we can calculate this quantity for, say, unit axial current for the E_{01} wave and call it the characteristic impedance. Also if Q is the mean dissipation per unit length, then the attenuation $\alpha = \overline{Q}/2\overline{W}$. The transmission through unshielded dielectric guides is also considered. W. L. Barrow (6) has examined the attenuation of the longitudinal waves in hollow metal guides. When the conductivity is good but not perfect there is slight attenuation of the waves, and for this to be a minimum $\lambda/a = 1{\cdot}5$, where λ is the wavelength in free space. For copper tubes this minimum attenuation for the longitudinal wave is $170a^{-3/2}$ dB/mile, and thus for $a = 20$ cm., $\lambda = 30$ cm., it is 2 dB/mile. The corresponding value for lead is 6·5 dB and for iron 45 dB. The attenuation does not exceed the minimum by more than 10%, provided $1 < \frac{\lambda}{a} < 2$. This subject has also been considered by G. C. Southworth (139). Examination of the attenuation of these waves in metal tubes of finite conductivity shows that the H_{01} wave has the unique property of decreasing attenuation as the propagation frequency is indefinitely increased. This unique wave is only found in guides of circular cross section, and such properties have not been found in any other transmission system. The attenuation of all four waves is infinite at the respective cut-off frequencies and falls as the frequency increases. All except H_{01} fall to a minimum and then slowly increase. The attenuation for the H_{11} wave was measured in a 6-in. copper tube 1,250 ft. long, and good agreement with the results derived by theory was obtained.

Practical Details. The preceding discussion has shown how the theory of the propagation of electromagnetic waves in hollow conducting tubes can be developed from Maxwell's

equations. The application of these guides and particularly the terminal devices does not yield easily to theory, and thus some experimental details will be given. In the experiments of G. C. Southworth (139) the velocity of propagation was measured with water contained in tubes about 6 in. diameter and 3 ft. long, the frequency being about 100–300 Mc/s. With the shielded tube the phase velocity approaches infinity as the frequency nears cut-off. Some of the apparatus described consists of a resonant chamber of variable length which can be

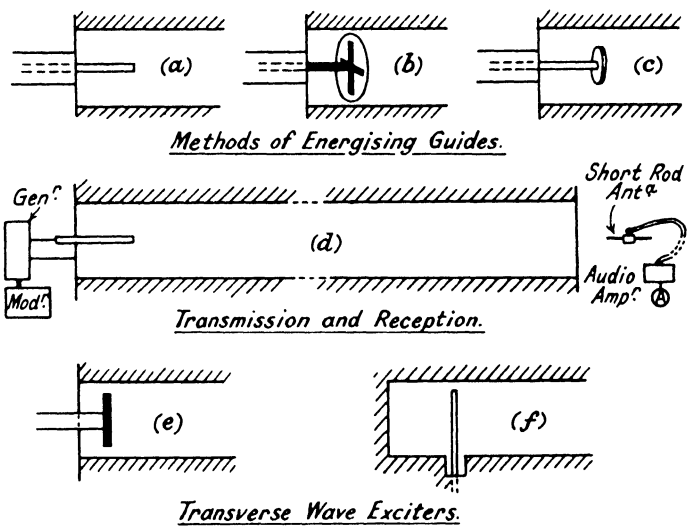

FIG. 97. Methods of energising waves guides. (*a*)–(*d*) for *E* waves, (*e*) and (*f*) for *H* waves.

used as a wavemeter—the dimensions being about 5 in. diameter, 2 ft. long for 15–20 cm. waves. For generating H_{11} waves, say, a magnetron or Barkhausen generator is arranged inside the tube, the leads being connected to opposite sides of the tube and a reflector on one side was used. A similar arrangement can be used for a receiver. As an indicator a small dipole and crystal detector can be used.

A terminal device at the sending end must take high-frequency energy from a pair of conductors and cause this energy to be propagated down the tube. Except for questions of insulation and of impedance of the biconductor system,

terminal devices for the sending and for the receiving ends may be identical, because any device that will radiate waves of the hollow-tube type will be equally effective in picking them up.

The hollow-pipe transmission system differs radically from conventional systems in regard to the configuration of the field about the conductor. In the hollow-pipe system several distinct kinds of waves are possible, and consequently the terminal device may be designed to excite waves of the desired type, and generally both sending and receiving terminals should transmit and receive waves of a single type only.

The simplest and one of the most effective terminals comprises a length of coaxial rod, the one in Fig. 97*a* having a coaxial feed, and arranged for longitudinal waves. Because of the symmetry of its electromagnetic field, the coaxial rod terminal is well suited to excite or intercept hollow-tube waves. The waves travel faster in the hollow tube than they do in the coaxial terminal, and the field can be considered to be distorted to allow the formation of closed loops in the electric field that break away from the coaxial rod terminal and propagate themselves down the hollow tube. A better energy transfer is obtained by matching the impedances of the tube and rod. Fig. 97*b* shows a terminal with radial wires to concentrate the radial current and allow reflections from the back face to be given the proper phase to reinforce the forward radiation. Fig. 97*c* shows a coaxial rod with a metal disc on its end, and, as with the other terminal devices, matching is possible. Some of the experiments carried out by W. L. Barrow (6) were done with the aid of a galvanised iron tube 44 cm. diameter and 460 cm. long, and a Barkhausen-Kurz oscillator was used which gave wavelengths down to 38 cm. The cut-off frequency was about 500 Mc/s ($\lambda_c = 60$ cm.), and no transmission along the tube was observed above this wavelength. Signals, etc., could be received at ten times the distance than without the guide. Either a crystal detector or an acorn tube with short rods as antennæ proved to be a satisfactory probe for the field measurements and an amplifier, a copper-oxide meter, and headphones completed the receiver as shown in Fig. 97*d*.

It has already been mentioned that other kinds of waves

are possible and for the transverse waves the terminations required are different and parastic rods may be placed in the guide and a reflector behind the driving rod, as shown in Figs. 97*e* and *f*. The rod length may be $\frac{\lambda}{2}$, and by using vertically and horizontally polarised waves three separate communication channels can be obtained. The free end of the guide causes radiation, which is more or less directive, but better matching and more direct radiation can be obtained by flaring the guide into a horn. Transverse waves are well suited for beam purposes and the directivity in general depends on $\frac{\lambda}{a}$ as well as on the type of wave.

Various Shapes of Guides. The hollow pipe of rectangular cross-section has been discussed theoretically by Lord Rayleigh (116) and L. Brillouin (27) and by S. A. Schelkunoff (125) to some extent, for actual finitely conducting pipes. The theory has also been derived by W. L. Barrow and L. J. Chu (8) for the transmission of electromagnetic waves in hollow conducting pipes of rectangular cross-section in the case of perfectly conducting and imperfectly conducting materials. From similarity with the waves in cylindrical tubes, type $E_{n,m}$ and $H_{n,m}$ waves are defined according to the field configurations within the tube and the various classes of terminating devices are described. The basic principle in the construction of these is that a conducting rod, or rods, carrying current of the proper frequency is disposed inside the tube so as to coincide with a line of electric intensity of the field pattern for the desired wave, consideration being given to the phase of the currents when two or more rods are employed. The H_{01} wave has outstanding characteristics in that it has the simplest configuration of all hollow-pipe waves, possessing only the one transverse component of electric intensity, and it has the lowest critical frequency as well as the smallest attenuation. In a rectangular pipe, H. Reidel (118) shows that no wave has been found whose attenuation decreases indefinitely as the frequency is increased. It is possible to resolve the rectangular guide waves to an equivalent form in which the wave appears

as a superposition of two sets of ordinary plane waves that are multiply reflected back and forth between the side walls of the pipe. W. L. Barrow and L. J. Chu (8) use this resolution to calculate the attenuation in imperfectly conducting guides and various curves are given for alternative guide dimensions, and some experimental results are given using a 2 by 3 in. guide at a wavelength of 12·5 cm.

L. J. Chu (39) considers the propagation of waves in guides of elliptical cross-section. It has been found that a certain instability of the H_{01} wave in cylindrical tubes seems to take place, due to the unavoidable departure of the shape of the cross-section of realisable pipes from that of an exact circle. Theory shows that if a circular guide becomes only slightly elliptical the curve of attenuation *versus* frequency for the H_{01} wave will assume the general form typical of hollow-pipe waves. Therefore the attenuation will go through a minimum value and eventually increase with increasing frequency. The propagation along elliptical guides has also been examined by L. Brillouin (27), who shows that the E_{01} and H_{01} waves are stable in that their propagation is not affected by slight deformations of a circular tube. Waves such as E_{11}, for example, split into two components of different velocities, and thus, due to phase changes, the wave will become elliptically polarised. A. W. Melloh (101) makes some measurements with damped electromagnetic waves down to 4·5 cm. wavelength by the use of a comparatively simple spark generator. Transverse waves were generated and several experiments were made on tubes deformed to an approximately elliptical shape, the effect of deformation on the wave propagation in the pipe being a matter of engineering concern. The wavelengths in the guide were measured when it was excited along its maximum and then its minimum diameters and good agreement with theory was obtained. It was also shown that grids or filters consisting of, say, eleven wires of 19 gauge copper wire mounted parallel to one diameter, prevent the propagation of certain waves while allowing others to pass freely.

S. Sonada, S. Morimoto, and M. Ito (138), consider the propagation of waves along curved guides as it may happen in practice that a perfectly straight installation cannot be

obtained. H. Buchholz (35) also considers curved wave guides and shows that transverse waves may become elliptically polarised, due to the different velocities of the component waves into which they split. Only small changes in the propagation constants for longitudinal waves take place, so that their travel is for all practical purposes unaffected for small curvatures. R. D. Richtmyer (121) shows that the attenuation of a dielectric wave guide which goes around a corner is always finite, but approaches zero (neglecting dielectric losses, etc.) more or less exponentially as the radius of bending is made large compared to the wavelength, and can therefore very easily be made negligible.

Horn Radiators. In order to match properly the hollow pipe to the external space and to produce more directive

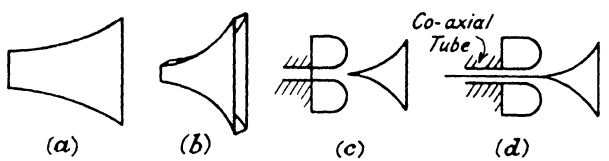

FIG. 98. Types of electromagnetic horn radiators.

patterns, W. L. Barrow (6) has suggested that the pipe can be flared into a horn-shaped radiator. The analogy of this kind of radiator to an acoustic horn is indeed close. However, the throat of an acoustic horn is usually much smaller than the wavelength, while the throat of the hollow-tube horn is comparable to it. Figs. 98*a* and *b* show simple flared types of circular and of rectangular cross-section respectively. Fig. 98*c* shows an interesting type for longitudinal waves that produces a uniform radiation concentrated in a plane perpendicular to the axis of the tube. Thus Figs. 98*c* and *d* are adaptable to broadcast radiation with longitudinal waves and Figs. 98*a* and *b* to beam radiation with transverse waves. The application of horn radiators is not confined to the hollow-tube system, for they may be fed by a coaxial or other lines, and this application is shown in Fig. 98*d*.

The design of these radiating electromagnetic horns has been examined by W. L. Barrow and L. J. Chu (7, 9). The

material may be metal in the form of iron sheet or copper cemented on plywood, but screen or semi-open structure may be employed and the horn opening protected by thin material. These horns may be excited by the hollow conductors described previously or directly by an oscillator in the throat. The *H* (transverse) waves are the best for a single lobe beam. There is an optimum dimension for the throat width to prevent radiation of high order waves. The power gain of the horn varies with the flare angle and is proportional to the aperture width expressed in wavelengths. It can be of the order of 20 dB for horns of, say, width 20λ. In addition, the field distributions inside the horn and in the radiated waves are examined.

W. L. Barrow and F. D. Lewis (11) also deal with the radiation of electromagnetic waves at high frequencies from flared horns of metal, and particularly with the characteristics of the sectoral horn whose cross-section is rectangular and whose sides flare in one direction only. Some experiments are described in which the total angle of flare ϕ_0 of the horn could be varied to examine the effect of changes on the radiated field pattern. For $\phi_0 = 10$ degrees the radiated energy is formed into a rather broad beam along the principal axis, and there is an irregular back radiation. As ϕ_0 is made larger, the beam becomes sharper up to a value of $\phi_0 =$ between 40 and 60 degrees. As the flare angle is made even greater, the beam becomes distorted by the appearance of secondary lobes, which push out into the principal lobe. At 40 to 60 degrees the sharp beam with the practical absence of secondary lobes in the forward half plane contrasts markedly with the presence of two or more such lobes of objectionably large amplitude in the patterns of conventional arrays of half-wave antennæ and of parabolic reflectors. In addition, by simple adjustment, the horn can be made to radiate wavelengths over a range of 2 to 1. For a given wavelength, the beam angle can be made smaller and the power gain larger by increasing the length, and thus the aperture, of the horn.

W. L. Barrow and F. M. Greene (10) have examined the rectangular hollow-pipe radiator. This shape has the advantage that it is a configuration ideally adapted to the production of strictly linear radio beams. In the experiments described the

H_{01} transverse wave was generally used and the radiation pattern was measured experimentally by an oscillator feeding into a pipe 15 cm. × 50 cm. in 8 ft. length sections arranged outside in a field. The oscillator was a type 316A triode operating on a wavelength of 40 — 125 cm., while the field strength measuring set was mounted on a trolley which could be pushed around a 100-ft. radius circle, there being no advan-

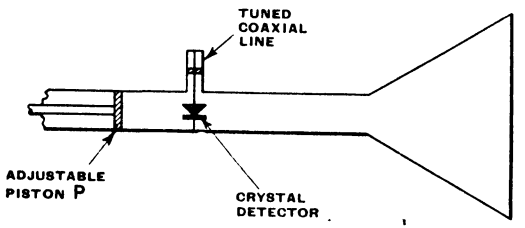

FIG. 99. Horn and receiver for 10 cm. waves.

tage in employing greater distances. Various radiation patterns are measured and given for lengths of pipe of 4·78 and 2·39 metres. A certain amount of backward radiation was observed, and by rotating the pipe axially through 90° the vertical radiation pattern could be measured. It is possible to use waves of different polarisations and the mouth of the

pipe can be fitted with a grid of parallel wires to select or discriminate against them.

Some experiments on metal horns as receivers have been made by G. C. Southworth and A. P. King (142), using a wavelength between 10 and 15 cm., the distance between transmitter and receiver being 30 to 100 times the wavelength. A diagrammatic illustration of the receiver has been given by G. W. O. Howe (77), and is shown in Fig. 99 together with a photograph of the complete horn and receiver. The resonance of the cavity is adjusted by the metal piston P, which must make good contact with the walls. The side tube constitutes a concentric transmission line, the length of which can be adjusted by a sliding piston on a central conductor. In this central conductor is a silicon-crystal rectifier actuating a microammeter or a potentiometer. This rectifier consists of a piece of silicon about 1 mm. diameter and 1 mm. long, let into the end of a small screw, and a contact wire of tungsten or phosphor bronze about 10 mils diameter and 2 mm. long. The horn was constructed of 22 gauge galvanised iron riveted and soldered at the joints. Power gains of 22 dB were obtained with the horns over a non-directional receiver.

Multiunit electromagnetic horns have been considered by W. L. Barrow and C. Shulman (13), who point out the advantages of flexibility of operation, electrical steerability, and relatively small length compared to the length of single horns of equivalent effectiveness. In the inter-connection of multiunit arrays and their successful operation, the mutual impedance between elements is of considerable importance. The mutual impedance between adjacent parallel horns whose mouth aperture is several wavelengths or more is substantially zero, even though their adjacent edges make actual contact, and thus horns may be treated as pure self-impedances from the standpoint of inter-connection in circuits. Some experiments were made on a wavelength of 8·3 cm., using a stabilised magnetron transmitter. By changing the phase of the entering waves it is possible to steer a directed beam with one of these multiple unit steerable horns, and similarly very sharp indications can be obtained as a direction finder in azimuth and elevation.

BIBLIOGRAPHY

1. ADAMS, N. I. and PAGE, L. "Electromagnetic Waves in Conducting Tubes." Phys. Rev., 1937, **52**, 647.
2. ALLERDING, A., DÄLLENBACH, W. and KLEINSTEUBER, W. "The Resotank, a New Generator for Micro Waves." *Hochf. Tech. u. Elek. akus.*, 1938, **51**, 96.
3. ARSENJEWA-HEIL, A. and HEIL, O. "A New Method of Producing Short Undamped Waves of Great Intensity." *Z. f. Phys.*, 1935, **95**, 752.
4. ASAI, S. "Tentative Proposition on the Mechanism of Electronic Oscillations." *Electrot. J. Tokyo*, 1941, **5**, 59.
5. AWENDER, H. and LANGE, O. "The Propagation of Decimetre and Centimetre Waves along Single Metallic and Dielectric Wires." *Funktech. Monat.*, 1938, **1**, 5, and **2**, 51.
6. BARROW, W. L. "Transmission of Electromagnetic Waves in Hollow Metal Tubes." *Proc. Inst. Rad. Eng.*, 1936, **24**, 1298.
7. BARROW, W. L. and CHU, L. J. "Electromagnetic Horn Design." *Elec. Eng.*, 1939, **58**, 333.
8. BARROW, W. L. and CHU, L. J. "Electromagnetic Waves in Hollow Metal Tubes of Rectangular Cross Section." *Proc. Inst. Rad. Eng.*, 1938, **26**, 1520.
9. BARROW, W. L. and CHU, L. J. "Theory of the Electromagnetic Horn." *Proc. Inst. Rad. Eng.*, 1939, **27**, 51.
10. BARROW, W. L. and GREENE, F. M. "Rectangular Hollow Pipe Radiators." *Proc. Inst. Rad. Eng.*, 1938, **26**, 1498.
11. BARROW, W. L. and LEWIS, F. D. "Sectoral Electromagnetic Horn." *Proc. Inst. Rad. Eng.*, 1939, **27**, 41.
12. BARROW, W. L., CHU, L. J. and JANSEN, J. J. "Biconical Electromagnetic Horns." *Proc. Inst. Rad. Eng.*, 1939, **27**, 769.
13. BARROW, W. L. and SHULMAN, C. "Multi-unit Electromagnetic Horns." *Proc. Inst. Rad. Eng.*, 1940, **28**, 130.
14. BARROW, W. L. and MIEHER, W. W. "Natural Oscillations of Electrical Cavity Resonators." *Proc. Inst. Rad. Eng.*, 1940, **28**, 184.
15. BARROW, W. L., and SCHAEVITZ, H. "Hollow Pipes of Relatively Small Dimensions." *Elec. Eng.*, 1941, **60**, 119.
16. BEDFORD, L. H. and PUCKLE, O. S. "A Velocity Modulation Television System." *J. Inst. Elec. Eng.*, 1934, **75**, 63.
17. BENHAM, W. E. "Phase Focussing in Velocity Modulated Beams." *Wireless Eng.*, 1940, **17**, 514.
18. BETHENOD, J. "The Electronic Valve with Velocity Modulation." *Comptes Rend.*, 1940, **210**, 103.
19. BLEWETT, J. P. and RAMO, S. "High-frequency Behaviour of a Space Charge Rotating in a Magnetic Field." *Phys. Rev.*, 1940, **57**, 635.
20. BLEWETT, J. P. and RAMO, S. "Propagation of Waves in a Space Charge rotating in a Magnetic Field." *J. Appl. Phys.*, 1941, **12**, 856.
21. BOONE, A. R. "The Development of the Klystron Micro Wave Generator and its Use for Blind Landing." *Scient. American*, 1940, **162**, 20.

22. BORGNIS, F. "The Fundamental Electrical Oscillations of Cylindrical Cavities." *Hochf. Tech. u. Elek. akus.*, 1939, **54**, 121.
23. BORGNIS, F. "Natural Electromagnetic Oscillations of Dielectric Spaces." *Ann. Phys.*, 1939, **35**, 359.
24. BORGNIS, F. "The Concentric Line as Resonator." *Hochf. Tech. u. Elek. akus.*, 1940, **56**, 47.
25. BORGNIS, F. "Electromagnetic Hollow Space Resonators in Short Wave Technique." *E. T. Z.*, 1940, **61**, 461.
26. BORGNIS, F. and LEDINIGG, E. "Phase-focussing of Electron Beams Travelling in a Straight Line." *Zeitschr. f. Tech. Phys.*, 1940, **21**, 256.
27. BRILLOUIN, L. "Propagation of Electro-magnetic Waves in a Tube." *Rév. Gen. de l'Elec.*, 1936, **40**, 227.
28. BRILLOUIN, L. "Propagation of Waves along Dielectric Cables." *Bull. Soc. des Elec.*, 1938, **8**, 899.
29. BRILLOUIN, L. "Hyper-frequency Waves and their Practical Use." *J. Franklin Inst.*, 1940, **229**, 709.
30. BRILLOUIN, L. and CLAVIER, M. "Propagation in Dielectric Cables and Circular Guide Cables." *Génie Civil.*, 1938, **113**, 504, 505.
31. BRÜCHE, E. and RECKNAGEL, A. "Phase Focussing of Electrons in Motion in Ultra High Frequency Fields." *Z. f. Phys.*, 1938, **108**, 459.
32. BUCHHOLZ, H. "The Quasi-optics of Ultra-short Wave Guides." *E.N.T.*, 1938, **15**, 297.
33. BUCHHOLZ, H. "Ultra Short Waves in Concentric Cables and Hollow Space Resonators." *Hochf. Tech. u. Elek. akus.*, 1939, **54**, 161.
34. BUCHHOLZ, H. "The Movement of Electromagnetic Waves in a Cone-shaped Horn." *Ann. Phys.*, 1940, **37**, 173.
35. BUCHHOLZ, H. "The Influence of the Curvature of Rectangular Hollow Conductors on the Phase Constant." *E.N.T.*, 1939, **16**, 73.
36. BUNIMOVICH, V. I. "An Oscillating System with Small Losses." *J. Tech. Phys.*, 1939, **9**, 984.
37. BUNIMOVITCH, V. I. "Use of Rectangular Resonators in Ultra High Frequency Technique." *J. Tech. Phys.*, 1940, **8**, 640.
38. CARSON, J. R., MEAD, S. P. and SCHELKUNOFF, S. A. "Hyper-frequency Wave Guides—Mathematical Theory." *Bell. Sys. Tech. J.*, 1936, **15**, 310.
39. CHU, L. J. "Electromagnetic Waves in Elliptic Hollow Pipes of Metal." *J. Appl. Phys.*, 1938, **9**, 583.
40. CLAVIER, A. G. "Theory of Cylindrical Dielectric Wave Guides and Coaxial Cables." *Bull. Soc. des Elec.*, 1938. **8**, 355.
41. CLAVIER, A. G. "Theoretical Relationships of Dielectric Guides and Coaxial Cables." *Elec. Comm.*, 1939, **17**, 276.
42. CLAVIER, A. G. and ALTOVSKY, V. "Experimental Research on the Propagation of Electromagnetic Waves in Cylindrical Guides." *Rev. Gen. de l'Elec.*, 1939, **45**, 697.
43. CLAVIER, A. G. and ALTOVSKY, V. "Experimental Researches on the Propagation of Electromagnetic Waves in Dielectric Guides." *Elec. Comm.*, 1940, **18**, 81.

44. COLEBROOKE, F. M. "Ultra Short and Decimetre Waves Valves and Deflection of a Focussed Beam." *Wireless Eng.*, 1938, **15,** 198.
45. CONDON, E. U. "Electronic Generation of Electromagnetic Oscillations." *J. Appl. Phys.*, 1940, **11,** 502.
46. CONDON, E. U. "Forced Oscillations in Cavity Resonators." *J. Appl. Phys.*, 1941, **12,** 129.
47. DEBYE, P. and HONDROS, O. "Electromagnetic Waves in Dielectric Wires." *Ann. Phys.*, 1920, **32,** 465.
48. DÖHLER, O. and LÜDERS, G. "Oscillation Regions of the Multislit Magnetrons." *Hochf. tech. u. Elek. akus.*, 1941, **58,** 73.
49. DÖRING, H., and MAYER, L. "Velocity Modulated Transit Time Valves." *E. T. Z.*, 1940, **61,** 685 and 713.
50. DROSTE, H. W. "Ultra High Frequency Transmission along Cylindrical Conductors and Non-conductors." *T.F.T.*, 1938, **27,** 199, 273, 310 and 337.
51. FERRARO, V. C. A., and FLINT, H. T. "Longitudinal Electromagnetic Waves between Parallel Plates." *Proc. Phys. Soc.*, 1941, **53,** 170.
52. FUCHS, W. H. J. and KOMPFNER, R. "Space Charge Effects in Velocity Modulated Beams." *Proc. Phys. Soc.*, 1942, **54,** 135.
53. GEIGER, M. "Current Flow Characteristics in Velocity Modulated Beams." *Phys. Berich.*, 1940, **21,** 710.
54. GEIGER, M. "Current Flow Characteristics in Velocity Modulated Valves." *Telefunk. Rohre*, 1939, **16,** 177.
55. GULYAEV, V. P. "The Theory of the Klystron." *J. Tech. Phys.*, 1941, **11,** 100.
56. HAEFF, A. V. "An Ultra High Frequency Power Amplifier of Novel Design." *Electronics*, 1939, **12,** 30.
57. HAEFF, A. V. "Space Charge Effects in Electron Beams." *Proc. Inst. Rad. Eng.*, 1939, **27,** 586.
58. HAEFF, A. V. and NERGAARD, L. S. "A Wide Band Inductive-output Amplifier." *Proc. Inst. Rad. Eng.*, 1940, **28,** 126.
59. HAHN, W. C. "Small Signal Theory of Velocity Modulated Electron Beams." *Gen. Elec. Rev.*, 1939, **42,** 258.
60. HAHN, W. C. "Wave Energy and Transconductance of Velocity Modulated Beams." *Gen. Elec. Rev.*, 1939, **42,** 497.
61. HAHN, W. C. "A New Method for the Calculation of Cavity Resonators." *J. Appl. Phys.*, 1941, **12,** 62.
62. HAHN, W. C. and METCALF, G. F. "Velocity Modulated Tubes." *Proc. Inst. Rad. Eng.*, 1939, **27,** 106.
63. HANSEN, W. W. "A Type of Electrical Resonator." *J. Appl. Phys.*, 1938, **9,** 654.
64. HANSEN, W. W. "On the Resonant Frequency of Closed Concentric Lines." *J. Appl. Phys.*, 1939, **10,** 38.
65. HANSEN, W. W. and RICHTMYER, R. D. "Resonators suitable for Klystron Oscillators." *J. Appl. Phys.*, 1939, **10,** 189.
66. HARA, G. and SOU, S. "Wave Guide Action of Parallel Conductors in Tubular Arrangement." *Electrot. J. Tokyo*, 1940, **4,** 233.
67. HARTIG, H. E. and MELLON, A. M. "The Transmission of Damped Electromagnetic Waves through Small Hollow Metal Tubes." *Phys. Rev.*, 1938, **54,** 646.

68. HEIL, O. "Velocity Modulated Valve." French Patent, **1936.**
69. HOLLMANN, H. E. "Spherical Tank Ultra High Frequency Oscillator." *Electronics*, 1938, **12,** 26.
70. HOLLMANN, H. E. "Ultra Short Wave Generator Valves." *Funktech. Monat.*, 1938, **10,** 319.
71. HOLLMANN, H. E. "New Transit-time Devices." *Funktech. Monat.*, 1940, **12,** 1.
72. HOLLMANN, H. E. and THOMA, A. "On the Theory of Drift Tubes." *Hochf. Tech. u. Elek. akus.*, 1940, **56,** 181.
73. HOLLMANN, H. E., and THOMA, A. "Beam Deflection Valves for Micro waves." *Hochf. tech. u. Elek. Akus.*, 1937, **49,** April, May.
74. HOLLMANN, H. E. "Ballistic Models of Velocity-modulated Transit-time Devices." *Hochf. Tech. u. Elek. akus.*, 1940, **55,** 73.
75. HOULDIN, J. E. "Wave Guides." *G. E. C. J.*, 1941, **11,** 172.
76. HOWE, G. W. O. "A New Type of Wave Transmission." *Wireless Eng.*, 1936, **13,** 291.
77. HOWE, G. W. O. "The Reception of Ultra Short Wavelengths by Metal Horns." *Wireless Eng.*, 1939, **16,** 109.
78. INAKATA, H. "General Consideration for Travelling Electromagnetic Fields produced in a long Hollow Pipe." *Nippon. Elec. Comm. Eng.*, 1941, **23,** 127.
79. IWAKATA, H. "The Wave Configurations of Travelling Electromagnetic Fields in a Long Hollow Cylinder." *Nippon. Elec. Comm. Eng.*, 1940, **19,** 178.
80. IWATAKA, I. "Hollow Metal Tubes and their Miscellaneous Constants." *Electrot. J. Tokyo*, 1941, **5,** 58.
81. JOBST, G. "Charges Moving Periodically in Electron Valves, particularly in Shock Excited Ultra Short Wave Oscillators." *Telefunken-Hausmittel.*, 1939, **20,** 84.
82. JONESCU, T. V. "A Short Wave Oscillator." *Comptes Rend.*, 1937, **204,** 1411.
83. JOUGET, M. "Natural Electromagnetic Oscillations of a Spherical Cavity." *Comptes Rend.*, 1939, **209,** 25 and 203.
84. KALININ, V. I. "The Theory of an Electron Beam Oscillator and Phase Focussing." *Electrosvyaz*, 1940, **9,** 46.
85. KAŠPAR, E. "Experimental Investigation of Electromagnetic Waves on Dielectric Wires." *Ann. Phys.*, 1938, **32,** 353.
86. KEMP, J. "Electromagnetic Waves in Metal Tubes of Rectangular Cross Section." *J. Inst. Elec. Eng.*, 1941, **88,** 213.
87. KLEINSTEUBER, W. "The Influence of Space Charge in Planar Retarding-field Tubes." *Hochf. Tech. u. Elek. akus.*, 1939, **53,** 199.
88. KLEMT, A. "Contribution to the Propagation of Electromagnetic Waves along Dielectric Wires." *Funktech. Monat.*, 1939, **4,** 122.
89. KOCKEL, B. "Theory of Velocity-modulated Tubes." *Zeitschr. f. tech. Phys.*, 1941, **22,** 77.
90. KOCKEL, B. and MAYER, L. "Velocity Modulated Electron Beams in Crossed Deflection Fields." *Jahrb. A.E.G.-Forschung.*, 1939, **6,** 72.
91. KOMFNER, R. "Velocity Modulated Beams." *Wireless Eng.*, 1940, **17,** 110.
92. KOMFNER, R. "Velocity Modulation." *Wireless Eng.*, 1940, **17,** 478.

93. KOMPFNER, R. "Transit-time Phenomena in Electronic Tubes." *Wireless Eng.*, 1942, **19**, 2.
94. KÖNIG, H. "Laws of Similitude of the Electromagnetic Field and Cavity Resonators." *Hochf. tech. u. Elek. akus.*, 1941, **58**, 174.
95. LAMONT, H. R. L. "Theory of Resonance in Micro-wave Transmission Lines with Discontinuous Dielectric." *Phil. Mag.*, 1940, **29**, 521.
96. LAMONT, H. R. L. "Use of the Wave Guide for Measurement of Micro-wave Dielectric Constants." *Phil. Mag.*, 1940, **30**, 1.
97. LLEWELLYN, F. B. and BOWEN, A. E. "Production of Ultra-high Frequency Oscillations by Means of Diodes." *Bell Sys. Tech. J.*, 1939, **18**, 280.
98. LÜDI, F. "The Ultra-short-wave Generator with Phase Focussing." *Helvet, Phys. Acta.*, 1940, **13**, 122.
99. LÜDI, F. "A New Type of Ultra-short-wave Generator with Phase Focussing." *Helvet. Phys. Acta*, 1940, **13**, 498.
100. MAYER, L. "Experimental Demonstration of Phase-focussing." *Z. f. Tech. Phys.*, 1939, **20**, 38.
101. MELLOH, A. W. "Damped Electromagnetic Waves in Hollow Metal Pipes." *Proc. Inst. Rad. Eng.*, 1940, **28**, 179.
102. MORIMOTO, S. "Research on Wave Guides and Electro-magnetic Horns." *Electrot. J. Tokyo*, 1940, **4**, 64.
103. MOULLIN, E. B. "Radiation Resistance of Surfaces of Revolution." *J. Inst. Elec. Eng.*, 1941, **88**, 50.
104. MÜLLER, J. "Investigation of Electromagnetic Hollow Spaces." *Hochf. Tech. u. Elek. akus.*, 1939, **54**, 157.
105. MÜLLER, J. J. and ROSTAS, E. "Transit Time Generator with only one Cavity." *Helv. Phys. Acta.*, 1940, **13**, 435.
106. MYERS, L. M. *Electron Optics*, 1937.
107. NEIMANN, M. S. "The Theory of Auto-oscillators." *Izvestiya Elek. Slab Toka.*, 1938, **5**, 7.
108. NEIMANN, M. S. "Convex Endovibrators." *Izvestiya Elek. Slab. Toka.*, 1939, **19**, 1, **10**, 21, and **11**, 24.
109. NERGAARD, L. S. and SALZBERG, B. "Resonant Impedance of Transmission Lines." *Proc. Inst. Rad. Eng.*, 1939, **27**, 579
110. PETRIE, D. P. R. "Effect of Space Charge on the Potential and Electron Paths of Electron Beams." *Elec. Comm.*, 1941, **20**, 100.
111. PIERCE, J. R. "Limiting Current Densities in Electron Beams." *J. Appl. Phys.*, 1939, **10**, 715.
112. RAMO, S. "The Electron-Wave Theory of Velocity Modulated Tubes." *Proc. Inst. Rad. Eng.*, 1939, **27**, 757.
113. RAMO, S. "Currents Induced by Electron Motion." *Proc. Inst. Rad. Eng.*, 1939, **27**, 584.
114. RAMO, S. "Space Charge and Field Waves in an Electron Beam." *Phys. Rev.*, 1939, **56**, 276.
115. RAMO, S. "Travelling Waves in Electron Beams." *Communications*. 1940, **20** and **24**.
116. RAYLEIGH, LORD. "On the Passage of Electric Waves through Tubes." *Phil. Mag.*, 1897, **43**, 125.
117. REBER, G. "Electric Resonance Chambers." *Communications*, 1938, **18**, 5 and 25.

118. REIDEL, H. "The Metallic Hollow Conductor as a Transmitter of Electromagnetic Waves." *Hochf. Tech. u. Elek. akus.*, 1939, **53**, 122.
119. REIDINGER, A. "Measurement of the Attenuation and Velocity of Waves in Metallic Tubes." *Hochf. tech. u. Elek. akus.*, 1941, **58**, 21.
120. REUKEMA, L. E. "Transmission Lines at very High Radio Frequencies." *Elec. Eng.*, 1937, **56**, 1002.
121. RICHTMYER, R. D. "Dielectric Resonators." *J. Appl. Phys.*, 1939, **10**, 391.
122. ROTHE, H. and KLEEN, W "The Importance of Electron Optics in the Technique of Amplifying Valves." *Z. f. Tech. Phys.*, 1936, **17**, 635.
123. RYTOV, S. M. "On the Attenuation of Electromagnetic Waves in Tubes." *J. Phys. U.S.S.R.*, 1940, **2**, 187.
124. SAPHORES, J. and BRILLOUIN, L. "General Properties of Dielectric Guides and Cables." *Elec. Comm.*, 1938, **16**, 346 and 350.
125. SCHELKUNOFF, S. A. "Transmission Theory of Plane Electromagnetic Waves." *Proc. Inst. Rad. Eng.*, 1937, **25**, 1457.
126. SCHELKUNOFF, S. A. "Electromagnetic Waves in Conducting Tubes." *Phys. Rev.*, 1937, **52**, 1078.
127. SCHELKUNOFF, S. A. "Note on Certain Guided Waves in Slightly Non-circular Tubes." *J. Appl. Phys.*, 1938, **9**, 484.
128. SCHRIEVER, O. "Electromagnetic Waves in Dielectric Conductors." *Ann. Phys.*, 1920, **63**, 645.
129. SCHRIEVER, O. "On the Use of Waves in Tubes as Transmission Channels." *Telefunken-Hausmittel.*, 1939, **20**, 55.
130. SCHRIEVER, O. "Physics and Technique of the Hollow Space Conductor." *E. T. Z.*, 1940, **61**, 749.
131. SEELIGER, R. "Theory of Electron Plasma Oscillations." *Zeitschr. J. Phys.*, 1942, **118**, 618.
132. SLEVOGT K. E. "Propagation of Decimetre Waves along a Dielectric Line." *Hochf. tech. u. Elek. akus.*, 1942, **59**, 1.
133. SMITH, L. P. and HARTMAN, P. L. "Formation and Maintenance of Electron and Ion Beams." *J. Appl. Phys.*, 1940, **11**, 220.
134. SMITH, P. H. "Transmission Line Calculator." *Electronics*, 1939, January, p. 29.
135. SONADA, S. "Research on Wave Guides and Electromagnetic Horns." *Electrot. J. Tokyo*, 1940, **4**, 35 and 41.
136. SONADA S. "Electromagnetic Waves Propagating through Metallic Tubes of Sectoral Section." *Electrot. J. Tokyo*, 1937, **1**, 214.
137. SONADA, S. "Research on Wave Guides and Electro-magnetic Horns." *Electrot. J. Tokyo*, 1940, **4**, 126.
138. SONADA, S., MORIMOTO, S. and ITO, M. "Transmission along Circularly Curved Wave Guides." *Electrot. J. Tokyo*, 1939, **3**, 215 ; and 1940, **4**, 47.
139. SOUTHWORTH, G. C. "Hyper frequency Wave Guides." *Bell. Sys. Tech. J.*, 1936, **15**, 284.
140. SOUTHWORTH, G. C. "Some Fundamental Experiments with Wave Guides." *Proc. Inst. Rad. Eng.*, 1937, **52**, 647.
141. SOUTHWORTH, G. C. "New Experimental Methods Applicable to Ultra Short Waves." *J. Appl. Phys.*, 1937, **8**, 660.

142. SOUTHWORTH, G. C. and KING, A. P. "Metal Horns as Directive Receivers of Ultra Short Waves." *Proc. Inst. Rad. Eng.*, 1939, **27**, 95.
143. SOUTHWORTH, G. C. "Wave Guides for Electrical Transmission." *Elec. Eng.*, 1938, **57**, 91.
144. SOUTHWORTH, G. C. "A Demonstration of Guided Waves." *Bell Lab. Record*, 1940, **18**, 194.
145. STRACHEY, C. "Velocity Modulated Beams." *Wireless Eng.*, 1940, **17**, 202.
146. STRATTON, J. A. "Electromagnetic Theory." 1941.
147. TERMAN, F. E. "Resonant Lines in Radio Circuits." *Elec. Eng.*, 1934, 54.
148. TIBERIO, U. "Deflection Valves for Ultra-short and Decimetre Waves." *Wireless Eng.*, 1938, **15**, 612.
149. TIBERIO, U. "A Beam Deflection Generator Tube for Micro Waves." *Alta Freq.*, 1935, **4**, 714.
150. TOMBS, D. M. "Velocity Modulated Beams." *Wireless Eng.*, 1940, **17**, 54.
151. TONKS, L. "A New Form of Electromagnetic Energy Equation when free Charged Particles are Present." *Phys. Rev.*, 1938, **54**, 863.
152. TONKS, L. and LANGMUIR, I. "Oscillations in Ionised Gases." *Phys. Rev.*, 1929, **33**, 195.
153. VARIAN, R. H. and VARIAN, S. F. "A High Frequency Amplifier and Oscillator." *J. Appl. Phys.*, 1939, **10**, 140 and 321.
154. VARIAN, R. H. and HANSEN, W. W. "New Radio Apparatus using 10 cm. Waves." *Sci. News Letter*, 1939, **35**, 89.
155. WATANABE, M. "A Note on Resonators and Wave Guides." *Electrot. J. Tokyo*, 1941, **5**, 7.
156. WEBSTER, D. L. "The De-buncher in Velocity Modulated Tubes." *J. Appl. Phys.*, 1939, **10**, 501.
157. WEBSTER, D. L. "The Theory of Klystron Generators." *J. Appl. Phys.*, 1939, **10**, 864.
158. WHEELOCK, N. "Velocity Modulation of Electron Beams." *Q. S. T.*, 1939, **23**, 37.
159. ZAHN, H. "Detection of Electromagnetic Waves in Dielectric Wires." *Ann. Phys.*, 1916, **49**, 907.
160. ———, —. "Klystron Ultra High Frequency Generator applied to Blind Landing Beams." *Interavia*, 1939, March, p. 2.
161. ———, —. "The Klystron Generator at 3,000 megacycles." *Electronics*, 1940, January, p. 25.
162. ——— "40 cm. Waves for Aviation." *Electronics*, 1939, November, p. 12.
163. ——— "Cathode Ray Amplifier Tubes." *Electronics*, 1939, April, p. 9.
164. ———, —. "The RCA825 Inductive-output Amplifier." *Q.S.T.*, 1940, **24**, 78.
165. ———, —. "Velocity-modulated Valves—Modern Trends in Tubes for U.H.F. Operation." *Wireless World*, 1941, **47**, 248.

INDEX